Impact du changement climatique et l'acidification des océans sur le cycle océanique de l'azote

Jorge Martinez-Rey

Université de Versailles Saint-Quentin-en-Yvelines

Laboratoire des Sciences du Climat et de l'Environnement - LSCE
École Doctorale des Sciences de l'Environnement - ED129

Thèse de Doctorat de
l'Université de Versailles Saint-Quentin-en-Yvelines

Discipline
Biogéochimie Marine et Climat

Impact of climate change and ocean acidification on the marine nitrogen cycle

Présentée par
Jorge Martínez-Rey

pour obtenir le grade de Docteur de
l'Université de Versailles Saint-Quentin-en-Yvelines

Soutenu le 6 de Fevrier, 2015

Jury

Dr. Sophie Bonnet, Institut Méditerranéen d´Océanologie, Marseille, France. Examinateur
Dr. Laurent Bopp, Laboratoire des Sciences du Climat et de l'Environnement, Gif-sur-Yvette, France. Directeur de thèse
Dr. Philippe Bousquet, Laboratoire des Sciences du Climat et de l'Environnement, Gif-sur-Yvette, France. Examinateur
Dr. Isabelle Dadou, Laboratoire d'Etudes en Géophysique et Océanographie Spatiales, Toulouse, France. Rapporteur
Dr. Marion Gehlen, Laboratoire des Sciences du Climat et de l'Environnement, Gif-sur-Yvette, France. Directeur de thèse
Dr. Nicolas Gruber, Eidgenoessische Technische Hochschule, Zürich, Switzerland. Invité
Dr. Parvadha Suntharalingam, University of East Anglia, United Kingdom. Rapporteur
Dr. Alessandro Tagliabue, University of Liverpool, Liverpool, United Kingdom. Invité

Numéro national d'enregistrement:

This project has been developed in the Biomac team
in the Laboratoire des Sciences du Climat et de l'Environnement in Gif-sur-Yvette, France,
and in part at the Environmental Physics department in the Institute of Biogeochemistry
and Pollutant Dynamics at ETH Zürich, Switzerland.

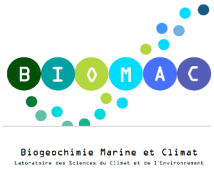

This project has been funded by the European Union
via the Greencycles II Project "Feedbacks in the Earth System",
European Community's Seventh Framework Programme (FP7 2007-2013)
under Grant 238366.

This work has not previously been accepted in substance for any degree and is not being concurrently submitted for any other degree. This dissertation is being submitted in partial fulfillment of the requirement of Ph. D. by the Université de Versailles - Saint Quentin en Yvelines.

This dissertation is the result of my own independent work and investigation, except where otherwise stated.
Other sources are acknowledged giving explicit references.
A bibliography is appended.

I hereby give consent for my dissertation, if accepted, to be made available for photocopying and for inter-library loan, and the title and summary to be made available to outside organizations.

Gif-sur-Yvette, France, 18th of November, 2014.

Acknowledgements

Thanks to Laurent Bopp,
for the opportunity of developing this work at LSCE,
for the confidence and continuous help throughout the project,
and for the positive, enthusiastic and practical perspective on every bit of work.

Thanks to Marion Gehlen,
for her guidance on the academic perspective,
for the frequent discussions and sharp ideas, particularly
for those saving my OceanSciences 2012 presentation in Salt Lake City.

Thanks to Alessandro Tagliabue,
for his permanent motivation, help and ideas,
for bringing the exciting ocean acidification proposal,
and for finding smart ways of how to fully exploit the technical towards the scientific realm.

Thanks to Niki Gruber,
for his voice from a different academic system,
for helping me to look carefully into details,
for leading me towards more complex scientific questions,
and for hosting me at ETH Zuerich.

Thanks to Christian Ethe,
for teaching me how to use PISCES,
from the very first to the very last steps,
and still today does.

Thanks to Elsa Cortijo and Philippe Bousquet,
for your essential support dealing with administration,
particularly with the delicate situation we faced at the end of this work.

Thanks to Parv Suntharalingam and to Erik Buitenhuis,
for the discussions, the monitoring
and for your help within the *Comite de These*.

Thanks to Dave Hutchins and Mike Beman,
for letting me participate in their research findings from a modelling perspective.

Thanks to Olivier Aumont
for his contributions and feedbacks on the ocean acidification part.

Thanks to Arnaud Caubel and Patrick Brockmann,
for all the support with the CMIP5 archives and data,
and for showing the path towards data visualization.

Thanks to the BIOMAC team,
Laure Resplandy, Stelly Lefort, Italo Massotti, Thomas Arsouze, Roland Seferian,
Veronique Mariotti, Julien Palmieri, Briac LeVu, James Orr, Sarah Tavernel, Priscilla LeMezzo,
Timothee Bourgeois, Jennifer Simeon, Mohamed Ayache and Didier Swingedouw.

Thanks to the LOCEAN department,
particularly to Vincent Echevin for his continuous
and helpful participation in the *Comite de These*.

Thans to the Environmental Physics department at ETH,
to Zouhair Lachkar, Damien Loher, Bianca Wagenbach, Dave Byrne, Kay Steinkamp,
Ivy Frenger, Olivier Eugster, Giuliana Turi, Ilaria Stenardo, Mark Payne, Matt Muennich,
Dominik Clement, Alex Haumann, Forough Fendereski, Yu Liu and Simon Yang,
for giving me a sense of belonging.

Thanks to Meike Vogt,
for being so enthusiastic and so helpful beyond the daily routines and frustrations,

Thanks to the Greencycles II network:
to Arnaud Heroult, Frans-Jan Parmentier, Matteo Willeit, Guillaume Villain, Daniela Dalmonech, Altug Ekici, Callum Berridge, Yanjiao Mi, Maria Martin Calvo, Catherine Morfopoulos, Alex, Alessandro Anav, Rozenn Kerbin, Aideen Foley, Jana Kolassa, Katherine Crichton, Miral Sha, Dominik Sperlich, Chao, Gerardo Lopez Saldaña, Ioannis Bistinas, Peter Landschuetzer, Beate Stawiarski. Lazslo Hunor, Wolfgang Cramer, Santi Sabate,
Soenke Zahle, Bethan Jones and Daniela Tomescu,
for such a wonderful journey.

Thanks to Andrew Friend
for making Greencycles II possible,
for leading, assembling and guiding to a good end the ship with all of us on board.

Thanks to Inga Hense,
for her help, support and comprehension when difficult decisions came in Hamburg.

Thanks to Jad Abumrad, Robert Krulwich and all the Radiolab team
for making every single podcast available for everyone,
for being there in the endless hours commuting to Saclay.

Thanks to the conception, inception and completion of the Bibliotheque National de France, whoever this applies to.
Places like these make cities and people better.

Thanks to the people contributing to ffffound, itsnicethat and typographicposters websites,
supporting graphic design, pushing the limits of layout and setting the trends into future data visualization.
A permanent source of inspiration.

Thanks to Alina Gainusa-Bogdan, Sauveur Belviso, Palmira Messina, Juliette Lathiere, Imen Braham and Raffaella Vuolo,
for blurring the boundary between the lab and the city.

Thanks to Charlotte Laufkoetter and Colleen O'Brien,
for all the fun and workshops together.

Thanks to Cristina Garea, Pepe, Philipp Riess, Claire Lochet, Jesenka Veledar, Lucia Marquez and Carles Casas,
for your support and friendship.

Thanks to Natasha MacBean, Annemiek Stegehuis, Tilla Roy, Jana Kolassa and Mehera Kidston,
for being such a good friends and for all the fun in Paris.

Thanks to Noela,
for putting me in this road, it took me places I would have never imagined.

Thanks to my family,
stronger than I am or I ever will,
bearing with distance and loneliness.

Résumé

Le cycle océanique de l'azote est à l'origine de deux rétro-actions climatiques au sein du système terre. D'une part, il participe au contrôle du réservoir d'azote fixé disponible au développement du phytoplancton et à la modulation de la pompe biologique, un des mécanismes de séquestration du carbone anthropique. D'autre part, le cycle de l'azote produit un gaz à effet de serre et destructuer d'ozone, le protoxyde d'azote (N_2O). L'évolution future du cycle de l'azote sous l'influence du rechauffement climatique, de la déoxygénation et de l'acidification des océans reste une question ouverte. Les processus tels que la fixation d'azote, la dénitrification et la production de protoxyde d'azote seront modifiés sous l'influence conjuguée des ces trois stresseurs. Ces interactions peuvent être évaluées grâce aux modèles globaux de biogéochimie marine. Nous utilisons NEMO-PISCES et l'ensemble des modèles CMIP5 pour projeter les modifications des taux de fixation d'azote, de nitrification, de production et des flux air-mer de N_2O à l'horizon de 2100 en réponse au scénario 'business-as-usual'. Les effets liés à l'action combinée du rechauffement climatique et de l'acidification des océans sur le réservoir d'azote fixé, la production primaire et la rétro-action sur le bilan radiatif sont également évalués dans cette thèse.

Abstract

The marine nitrogen cycle is responsible for two climate feedbacks in the Earth System. Firstly, it modulates the fixed nitrogen pool available for phytoplankton growth and hence it modulates in part the strength of the *biological pump*, one of the mechanisms contributing to the oceanic uptake of anthropogenic CO_2. Secondly, the nitrogen cycle produces a powerful greenhouse gas and ozone (O_3) depletion agent called nitrous oxide (N_2O). Future changes of the nitrogen cycle in response to global warming, ocean deoxygenation and ocean acidification are largely unknown. Processes such as N_2-fixation, nitrification, denitrification and N_2O production will experience changes under the simultaneous effect of these three stressors. Global ocean biogeochemical models allow us to study such interactions. Using NEMO-PISCES and the CMIP5 model ensemble we project changes in year 2100 under the business-as-usual high CO_2 emissions scenario in global scale N_2-fixation rates, nitrification rates, N_2O production and N_2O sea-to-air fluxes adding CO_2 sensitive functions into the model parameterizations. Second order effects due to the combination of global warming in tandem with ocean acidification on the fixed nitrogen pool, primary productivity and N_2O radiative forcing feedbacks are also evaluated in this thesis.

Contents

Chapter 1
Introduction

Chapter 2
Methods

Chapter 3
N-cycle in CMIP5 models

Chapter 6
Impact of ocean acidification on nitrification

Chapter 7
Conclusions and Perspectives

Chapter 8
References

Chapter 1

Introduction

1.1. Context

The nitrogen cycle (N-cycle) plays an pivotal role in the Earth's climate system. Nitrogen, together with other nutrients (mostly phosphorus (P) and iron (Fe) in the ocean, P and potassium (K) on land), is one of the limiting nutrients of the growth of plants, including marine phytoplankton in the ocean. Their metabolism requires a constant supply of bioavailable forms of nitrogen to grow. This mechanism links the N-cycle to the carbon cycle (C-cycle), which ultimately regulates terrestrial and oceanic carbon dioxide (CO_2) uptake from the atmosphere.

Land and ocean absorb substantial amounts of anthropogenic emissions of CO_2, thus reducing the anthropogenic greenhouse gas (GHG) effect and diminishing the potential impact of global warming. Net CO_2 uptake in land and ocean absorbs similar quantities of atmospheric CO_2, in the order of 1.0 to 3.2 PgC yr^{-1} over the last 2002-2011 time period (Ciais et al., 2013). They account to about half of the total anthropogenic CO_2 emissions, i.e., 8.3 PgC yr^{-1} over the last decade. In the ocean, whereas this net carbon sink is thought to be mainly driven by physical-chemical processes, phytoplankton growth is a key player in the oceanic carbon cycle. Phytoplankton production of organic matter leads to a vertical gradient of carbon in the ocean interior, a process known as the *biological pump*, contributing to the storage of anthropogenic CO_2. Figure 1 shows the coupling between the C-cycle and the N-cycle in land and ocean, with particular focus on the contributions and losses of different forms of nitrogen compounds into the nitrogen pool (Gruber and Galloway, 2008). Part of the strength of the *biological pump* relies on the sources and sinks of bioavailable nitrogen, and therefore on the intrinsic natural variability of the N-cycle. The pool of reactive (or *bioavailable*) nitrogen has been historically regulated by natural processes, shown in blue in Figure 1, such as N_2-fixation, nitrification and denitrification. These processes bond the atmospheric N-cycle with that from land and ocean. Over past timescales the natural variability of these processes has been suggested to drive the *biological pump*, with a direct impact on the climate system. In addition, two N-cycle processes (nitrification and denitrification) are responsible for the production of a powerful, long lived greenhouse gas and ozone (O_3) depletion agent called nitrous oxide (N_2O). The terrestrial and oceanic production of N_2O contributes directly to the atmospheric greenhouse gas budget, and therefore modulates in part the climate system.

Since the industrial revolution, and particularly since the development and extensive use of the Haber-Bosch process, fixing artificially atmospheric N_2 for its use as a fertilizer in the form of ammonium (NH_4^+), the natural N-cycle has been significantly altered. Human population growth and its associated industrial activity have released large amounts of nitrogen compounds to the atmosphere and have also increased the amount of fixed nitrogen in soils (Figure 1, in red). This additional supply of nitrogen compounds have increased the reactive nitrogen available via atmospheric nitrogen deposition in land and ocean surface. The massive use of fertilizers has also increased significantly the riverine nitrogen discharge directly into the ocean. The N-cycle has been altered indirectly by fossil fuel combustion and other industrial related activities that have increased the atmospheric concentration of CO_2, methane (CH_4) and N_2O, the so-called *greenhouse gases*. The increasing greenhouse gas concentration in the atmosphere has lead to phenomena such as global warming, ocean deoxygenation and ocean acidification (Gruber, 2011). These environmental forcings have a direct impact on many of the N-cycle processes and nitrogen compounds distribution.

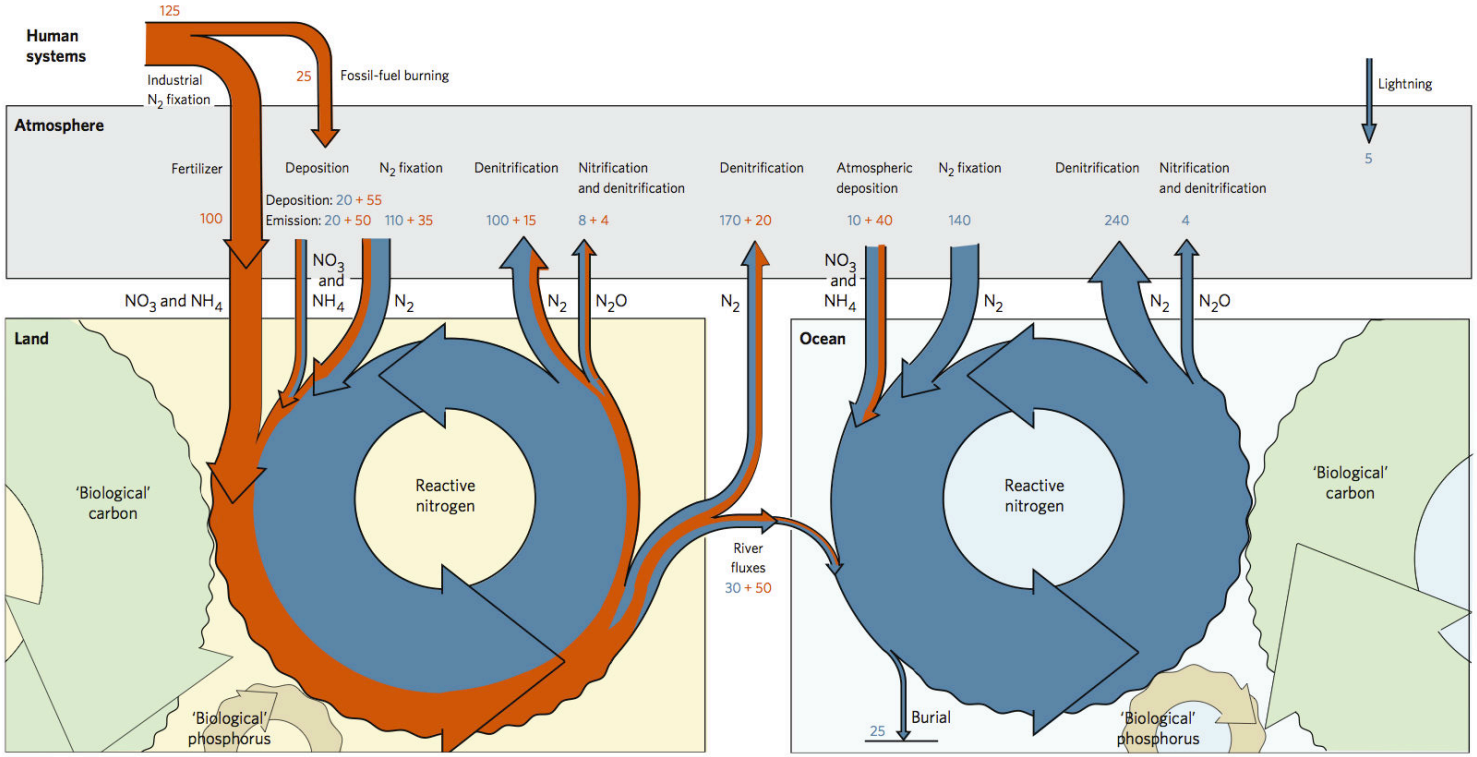

Figure 1: The coupling between the nitrogen cycle and the carbon cycle in the atmosphere, land and ocean. Natural N-cycle processes are shown in blue, while occurrence and relative magnitude of anthropogenic induced changes are shown in red. Inputs and losses of the reactive nitrogen pools in land and ocean are shown with arrows. The main natural inputs of nitrogen are atmospheric nitrogen deposition and N_2-fixation both in land and ocean. Natural losses of nitrogen occur via nitrification and denitrfication. Human perturbations of the N-cycle are via the extensive use of fertilisers, adding a significant amount of NO_3^- and NH_4^+ compounds in soils and eventually in river discharge to the ocean, and also with the production of atmospheric reactive compounds. (Gruber and Galloway, 2008).

Natural and anthropogenic perturbations of the N-cycle have been a matter of research over the last decades but their magnitude, effects and feedbacks in the climate system remain largely unknown, particularly in the ocean realm (Gruber and Galloway, 2008; Zehr and Ward, 2002). Many uncertainties exist concerning the current understanding of the N_2O formation processes in the ocean (Freing et al., 2012; Zamora et al., 2013), for instance, and the changes they might be subject to in future environmental conditions. Moreover, future oceanic forcings will certainly impact the regulating mechanisms of the bioavailable nitrogen pool, i.e., N_2-fixation, nitrification and denitrification, which in turn fuel the oceanic *biological pump*.

These questions can be addressed using Earth System Models (ESMs). ESMs are used to make future projections of changes in the N-cycle and, most important, to analyze the interactions among the N-cycle, the C-cycle, and the feedback within the marine stressors themselves. These models must be however evaluated in terms of their current capabilities to study present and future N-cycle processes, particularly when making future projections of oceanic N_2O sea-to-air emissions and analyzing changes in the fixed nitrogen pool.

1.2. The N-cycle at present

While the role of the marine N-cycle on a global scale is known from a biogeochemical and climate perspective, the understanding as today of the underlying mechanisms of N-cycle processes is not satisfactory (Gruber and Galloway, 2008; Zehr and Ward, 2002).

The oceanic N-cycle is a sequence of reduction and oxidation processes among nitrogen compounds in different oxidation states (Figure 2). The most abundant form of nitrogen in the ocean is dissolved dinitrogen (N_2). N_2 is reduced to ammonium (NH_4^+) as a product of N_2-fixation, a reduction process performed by a particular group of phytoplankton called *diazotrophs* in the surface layers of the ocean. NH_4^+ can be remineralized into ammonia (NH_3) and then oxidized back to N_2 via anaerobic ammonium oxidation (or *anammox*) (Thamdrup and Dalsgaard, 2002). Alternatively, NH_4^+ can also be oxidized via nitrification. Nitrification is a two-step bacterial process, turning NH_4^+ into NO_3^-, with a by product (N_2O) and an intermediate product, nitrite (NO_2), prior to complete the NO_3^- formation. The nitrogen cycle is closed back to N_2 by three reduction processes of NO_3^-. The first process is bacterial denitrification. Denitrifying bacteria respire NO_3^- when O_2 is completely exhausted. Denitrification turns NO_3^- into NO_2 and N_2O to produce N_2. The second process is *anammox*, producing NO_2 and eventually N_2. The last process is the dissimilatory nitrate reduction to ammonium, or DNRA, turning NO_3^- into NH_4^+.

The mechanisms and environmental conditions under which these processes occur are not yet fully understood. Processes such as N_2-fixation or nitrification have been a matter of study over the last decades, while other transformations such as anammox or DNRA are lacking a more accurate description and their relative importance in the N-cycle has been just hypothesized (Lam et al., 2009). The complexity of the nitrogen cycle relies not only on the many unknowns regarding occurrence and environmental controls, but also on the spatial coupling or decoupling of many of its processes, the uneven distribution of the nitrogen compounds in the ocean and the feedbacks between the processes that might self regulate the nitrogen content in the ocean over long timescales.

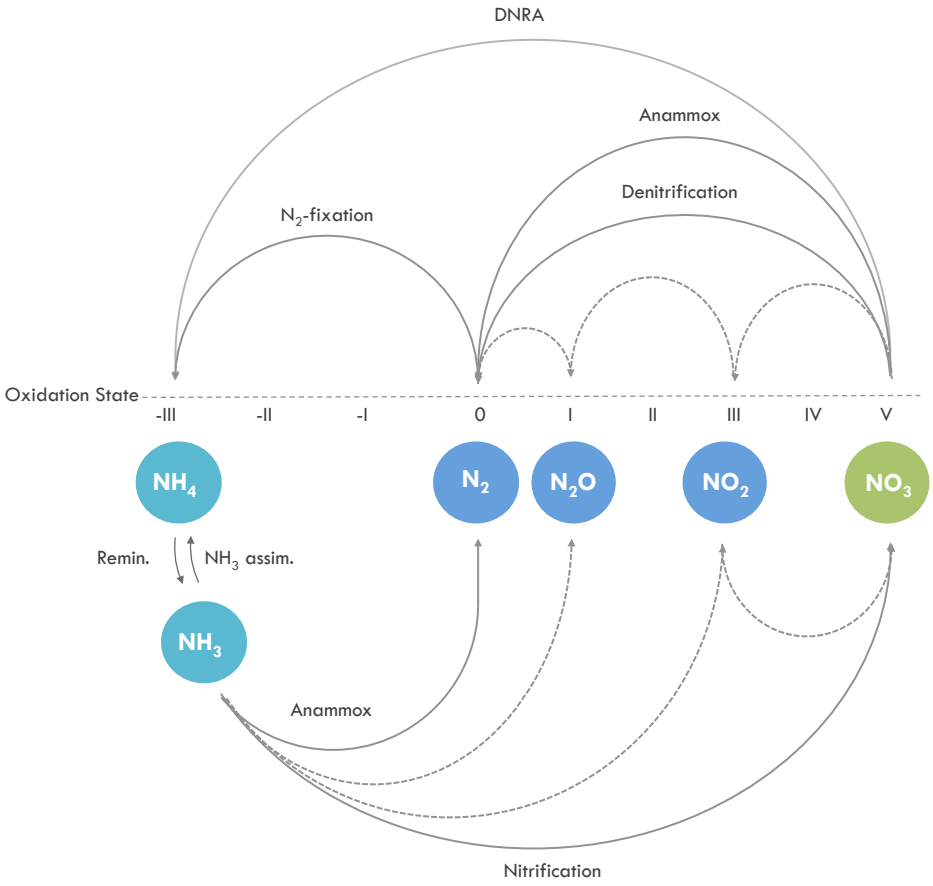

Figure 2: Nitrogen compounds and transformations within the N-cycle sorted along the oxidation state axis. Oxidation processes such as remineralisation, anaerobic ammonium oxidation (*anammox*) and nitrification are shown in the lower part of the diagram. Reduction processes such as denitrification, anammox and N_2-fixation are shown in the upper part of the diagram. Solid lines represent the different processes pointing towards the end products, while dotted lines represent the intermediate or by- products in nitrification and denitrification processes.

1.2.1. Nitrogen compounds

The nitrogen compounds are neither evenly distributed nor have the same abundance in the ocean interior. The bioavailable nitrogen compounds, i.e., NH_4^+ and NO_3^-, are relatively scarce in the ocean compared to nitrogen in its gaseous inorganic form (N_2). N_2 represents 94% of the total nitrogen budget in the ocean, whereas NO_3^- accounts only to 4% and dissolved organic nitrogen (DON) to 1%. Half of the remaining 1% is completed with particulate organic nitrogen (PON), NO_2, NH_4^+ and N_2O (Gruber, 2008).

The global depth average distribution of NO_3^- in the ocean is shown in Figure 3. NO_3^- is depleted at the sea surface due to the continuous uptake of phytoplankton, but it occupies the deep ocean in a large reservoir with an average value of 30 µmol kg^{-1}. NH_4^+ follows the same fate as that from NO_3^- in the euphotic zone but at much larger magnitude. Phytoplankton has a preference for assimilating NH_4^+ among the fixed nitrogen compounds and NH_4^+ is quickly exhausted either on its original supply from N_2-fixation or its remineralized form from the deeper layers. As a consequence, NH_4^+ concentration peaks close to the euphotic zone, where its production after remineralisation of organic matter exceeds its own consumption by phytoplankton. NH_4^+ is therefore less abundant than NO_3^- and it is completely depleted at depth. NO_2, as an intermediate compound in the nitrogen cycle, is also consumed in the euphotic zone and depleted below 100m.

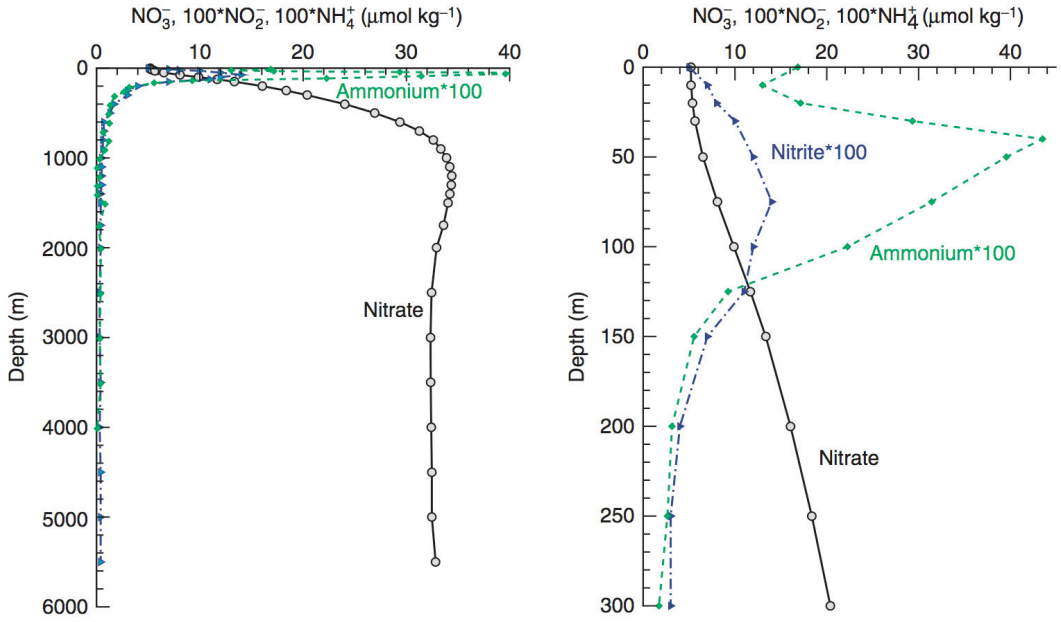

Figure 3: Global depth average of NO_3^-, NH_4^+ and NO_2 in (a) the whole water column and (b) the first 300m. Concentrations of NH_4^+ and NO_2 are augmented 100 times for intercomparison on the same unit scale. (JGOFS).

While the nitrogen pool of NO_3^- and NH_4^+ is modulated by phytoplankton demands, the distribution of N_2O is strictly linked to bacterial production processes by nitrification and denitrification (see 1.2.4 Nitrous oxide emissions). The depth distribution of N_2O and the in-situ O_2 measurements from several cruise campaigns is shown in Figure 4 (Suntharalingam and Sarmiento, 2000). Nitrification and denitrification operate together in regions where O_2 concentration falls below 5 to 20 µmol L^{-1}. In these *oxygen minimum zones* (OMZs or *oxygen deficient zones*, ODZ, in literature) N_2O production is particularly enhanced by the simultaneous production processes and N_2O concentration reaches its maximum in various oceanic locations, up to 40 to 50 nmol L^{-1}. Minima are observed in the sea surface due to gas exchange, whereas a remaining N_2O reservoir is found in the deep around 16 nmol L^{-1} (Bange et al., 2009). The O_2 consumption follows the same profile but mirrored on the concentration scale. The minimum on O_2 concentration is observed in the same depth range between 200 and 1000m deep, where the N_2O maxima are found. O_2 increases at the surface and in the deep at a global depth average of 195 µmol L^{-1} (Bianchi et al., 2012).

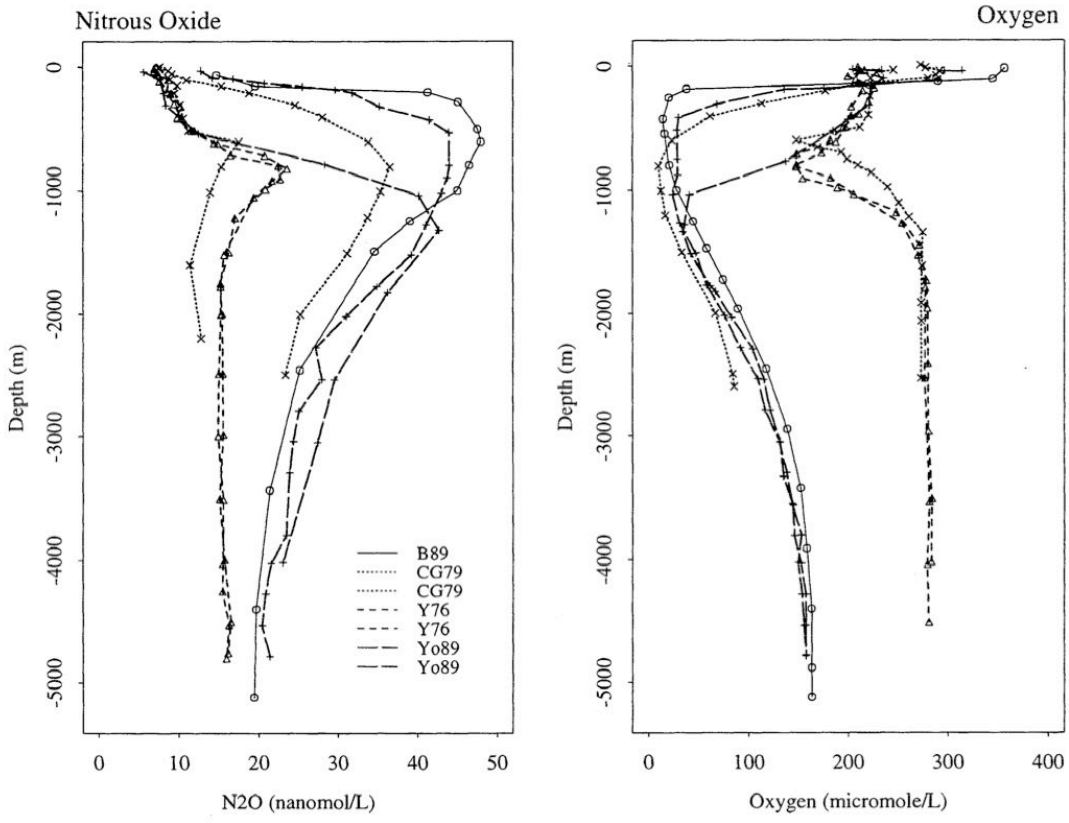

Figure 4: Global depth average profile of N_2O (in nmol L^{-1}) and the corresponding O_2 (in µmol L^{-1}) from the same measurements. The different lines correspond to the cruises from the BATS, SAGA and RITS cruise campaigns. (Suntharalingam and Sarmiento, 2000).

1.2.2. Nitrogen cycle processes

1.2.2.1. N_2-fixation

N_2-fixation is the largest source of external bioavailable nitrogen into the ocean (Gruber and Galloway, 2008). A particular group of phytoplankton known as *diazotrophs* fix dissolved N_2 in low-latitude warm waters, contributing to the fixed nitrogen pool in larger quantities than atmospheric nitrogen deposition or riverine nitrogen supply do. Despite the energetically expensive process of breaking the triple bond of N_2, resulting in a slower growth rate, diazotrophs have been succesful performing this strategy to compensate the lack of other forms of bioavailable nitrogen in their close proximity, taking advantage in the competition against the non-diazotrophs, which are nitrogen limited.

Two groups of diazotrophs are responsible for N_2-fixation in the ocean, cyanobacteria and proteobacteria (Carpenter and Capone, 2008), known as the N_2-fixers. The N_2-fixers and its unique N_2-fixation process have been studied particularly over the last two decades, when the distribution and the main environmental controls of the N_2-fixation process have been identified. N_2-fixation is fostered under high seawater temperatures above 15 to 20°C (Carpenter, 1983; Capone et al., 1997), although temperatures above 30 to 34 °C reduce their metabolims and hence the N_2-fixation capability (Fu et al., 2014). Just like any other phytoplanktonic organism, *diazotrophs* need high incoming radiation (Chen et al., 1998, Orcutt et al., 2001), and also the constant supply of PO_4 (Wu et al., 2000; Sañudo-Wilhelmy et al., 2001) but mostly Fe for activate the enzyme responsible of breaking N_2 (Falkowski, 1997; Berman-Frank et al., 2007). *Diazotrophs* are highly competitive in abscence of other forms of fixed nitrogen, i.e. NH_4^+ and NO_3^- (Capone et al., 1997; Karl et al., 2002; Holl and Montoya, 2005) and are favoured by relatively low O_2 conditions (Stuart and Pearson, 1970). Recent studies have also analyzed the diazotrophs performance under high levels of seawater CO_2 concentration (Barcelos e Ramos et al., 2007; Hutchins et al., 2007; Hutchins et al., 2013), where dissolved CO_2 plays the role of an additional nutrient, and growth rates and N_2-fixation rates increase as CO_2 concentration does. Recent studies have analyzed more in detail the interplay of the environmental conditions for N_2-fixation, going beyond single terms to combinations of them. Two examples are the studies by Dutkiewicz et al. (2012), where the N:Fe ratio regulates ultimately the N_2-fixation activity, and Deutsch et al. (2007), where the additional key term is the local N:P ratio.

Over the last years significant improvements have been made both on the observational and modelling side on N_2-fixation. The first global database of marine N_2-fixers abundance and

N_2-fixation rates was made available under the auspices of the MAREDAT project (Buitenhuis et al., 2013) by Luo et al. (2012). More than 5,000 measurements were compiled, spanning 30 years of observations, of N_2-biomass, N_2-fixation rates and metadata of temperature, Fe and O_2. The observational analysis have been completed on a global scale with modelling studies, including idealised box model analysis to estimate the global budget and their uncertainties related to changes in ocean circulation (Eugster and Gruber, 2012). N_2-fixers and N_2-fixation process have been included into the standard model output of global ocean models, gathered under the auspices of the Coupled Model Intercomparison Project 5 (CMIP5) (Taylor et al., 2012) and shown in Chapter 2.

1.2.2.2. Nitrification

Nitrifying bacteria carry out the oxidation of NH_4^+ into NO_3^-. These organisms are separated into ammonia-oxidizing bacteria plus archaea, who perform the first step from NH_4^+ to NO_2^-, and nitrite-oxidizing bacteria who finalize the process, turning NO_2^- into NO_3^-. None of these organisms is able to perform both steps simultaneously. Nitrification occurs at the lower boundary of the euphotic zone, where NH_4^+ is not longer assimilated by phytoplankton due to the abscence of light and where NH_4^+ from remineralisation of organic matter is fully available for nitrifying bacteria.

There are a few environmental controls which determine the optimum conditions for nitrification that have been identified. While N_2-fixation has a permanent supply of dissolved N_2, nitrification depends primarily on the amount of organic matter remineralised, and therefore on the export of organic matter (CEX) to depth. Nitrification is inhibited by light (Horrigan et al., 1981), although there are growing evidences that nitrification could occur in the euphotic layer. Nitrification shows its maximum around 100m deep where nitrifying bacteria is highly competitive against the phytoplankton in that depth range because of the absence of light.

As today, there are no global databases available compiling nitrification rates measurements. Only few nitrifying bacteria distributions in the open ocean have been compiled in the MAREDAT project (Buitenhuis et al., 2013). Global ocean biogeochemical models have included recently nitrification among their model output (e.g., IPSL, GFDL, CESM and CMCC, described in detail in Chapter 2).

1.2.2.3. Denitrification

Respiration of NO_3^- in low O_2 conditions leads to the reduction of NO_3^- back to the inorganic form of N_2 in a process called denitrification. The removal of bioavailable nitrogen is done by anaerobic bacteria when O_2 concentration is below 2 to 5 µmol L^{-1} (Tiedje, 1988). Dissolved O_2 concentration is therefore the main environmental control of denitrification occurrence. Denitrification is also inhibited by light, although this assumption comes automatically by the fact that OMZs are located well below 200m deep. When O_2 is completely depleted (i.e., anoxia), N_2O is consumed instead of NO_3^- (Cohen and Gordon, 1978). Sediment denitrification, based on the same biological mechanisms, is also a prominent removal process of fixed nitrogen from the ocean. The degradation of the biologically available nitrogen compounds occurs in the surface of the sediments mostly along coastal margins (Middelburg et al., 1996; Devol, 2008), but without completing the whole NO_3^- to N_2O formation process.

1.2.2.4. External nitrogen input

Atmospheric deposition of reactive nitrogen and river discharge of dissolved organic and inorganic nitrogen are the second and third most relevant external sources of nitrogen into the ocean after N_2-fixation (Gruber and Galloway, 2008). Reactive nitrogen coumpounds (NO_y, NH_x) are transported from land onto the sea surface via atmospheric deposition. These plumes of reactive nitrogen are associated with high industrialised areas close to the seaside like those from North America, India and Southeast Asia. Recent estimates of atmospheric nitrogen deposition are between 38.9 (Dentener et al. 2006) to 68 TgN yr^{-1} (Duce et al., 2008). Atmospheric nitrogen deposition alone is responsible of 3% of the global new primary production (Duce et al., 2008). Particulate and dissolved organic and inorganic nitrogen is supplied by river discharge into estuaries (Mayorga et al., 2010). Rivers contribute with 30 TgN yr^{-1} into the oceanic nitrogen budget (Gruber and Galloway, 2008). The impact on marine productivity is however larger, 5% of new primary production, than atmospheric nitrogen deposition (DaCunha et al., 2007).

1.2.3. Physical transport of nitrogen compounds

Critical as the biological supply mechanisms and nitrogen cycle transformations is the physical transport of nitrogen compounds in the ocean interior, as the ultimate mechanism responsible

of the distribution of the main nitrogen compounds. There are two basic mechanisms of transport of nitrogen compounds from the ocean interior to the euphotic layer, namely mixing and upwelling. Mixing between the subsurface and the euphotic layer supply fixed nitrogen in the remineralised forms of NH_4^+ and NO_3^- back to the surface. Upwelling in the eastern boundary currents represents one of the most important sources of nutrients into the euphotic layer. Upwelling delivers NO_3^- from its deep reservoir together with other nutrients such as PO_4 or Fe, which regulate the phytoplankton population distribution and ultimately surface NO_3^- and NH_4^+ concentrations.

1.2.4. Nitrous oxide emissions

Estimations of global oceanic N_2O emissions to the atmosphere are about 4 TgN yr^{-1} (Nevison et al., 1995; Suntharalingam et al., 2000), with a wide interval of uncertainties from 1.8 to 9.4 TgN yr^{-1} (Table 1). The oceanic N_2O emissions represents one third of all the natural sources of N_2O in the Earth System, or one fourth of all the total sources, including the anthropogenic ones (Ciais et al., 2013). Other contributions of N_2O to the atmosphere are mainly nitrification in soils and anthropogenic-related activities such as fossil fuel combustion, industrial processes and agricultural exploitation (Figure 5). The same interval of uncertainties from oceanic emissions applies to estimates of soil emissions and those from anthropogenic sources.

	N_2O (TgN yr^{-1})	Uncertainties (TgN yr^{-1})
Natural N_2O sources		
Soils under natural vegetation	6.6	3.3 - 9.0
Oceans	3.8	1.8 - 9.4
Atmospheric chemistry	0.6	0.3 - 1.2
Anthropogenic N_2O Sources	6.9	2.7 - 11.1
Total	17.9	8.1 - 30.7

Table 1: Natural and anthropogenic sources of N_2O to the atmosphere. Oceanic N_2O emissions account up to 30% of the total natural emissions and 25% of the total N_2O emissions including those from anthropogenic activities. Anthropogenic activities include fossil fuel combustion, industrial processes, agriculture, biomass and biofuel burning and human excreta. (Ciais et al., 2013).

Measurements of oceanic N_2O flux to the atmosphere and N_2O concentrations in the ocean interior are sparse in space and time domains (Nevison et al., 1995; Bange et al., 2009). The first cruises measuring N_2O concentration and N_2O sea-to-air fluxes covered long transects along the Atlantic (BLAST), western Pacific (RITS89) western Pacific and Indian ocean (SAGA2). However, the spatial coverage of oceanic N_2O concentration measurements have been mostly focused on the N_2O production hotspots at the Eastern Tropical Pacific (ETP) (Paulmier and Ruiz-Pino, 2009; Cornejo and Farias, 2012), Benguela Upwelling System (BUS) (Gutknecht et al., 2013) and Northern Indian Ocean (Naqvi et al., 2010), but very limited in the open ocean. Measurements of N_2O sea-to-air emissions from the ocean to the atmosphere show a poor spatial coverage (Nevison et al., 2004), in which any attempt of global interpolation results in very uncertain values of the actual global oceanic N_2O emissions. The lack of measurements together with the limited understanding of the N_2O production processes result in the above mentioned large interval of uncertainties when global estimates are made.

N_2O formation in the ocean is associated with two particular bacterial processes; nitrification in ocean and in soils, and water column denitrification in the ocean interior (Cohen and Gordon, 1978; Goreau et al., 1980; Elkins et al, 1978). The combination of these two processes together with N_2O consumption by the same denitrifying bacteria in complete anoxia (i.e., dissolved O_2 exhausted) yield a positive net N_2O production in the ocean interior and the subsequent sea-to-air emissions of N_2O.

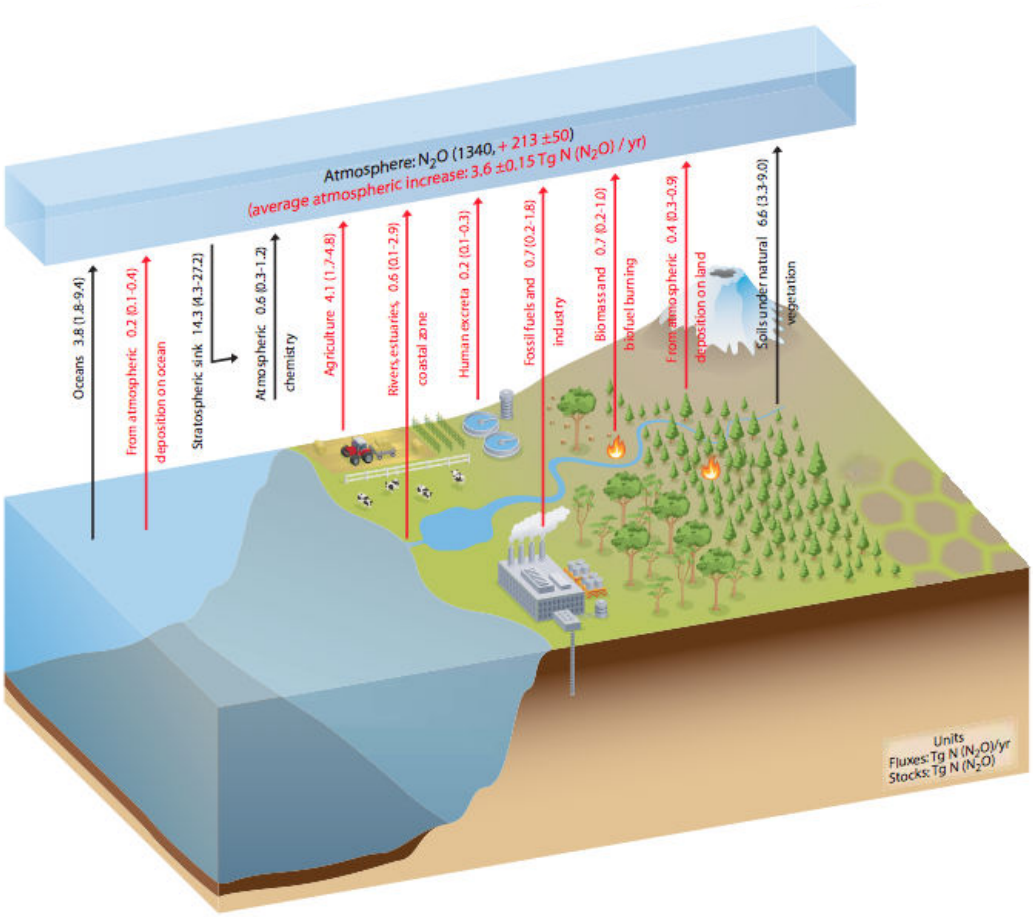

Figure 5: Contributions (in TgN yr^{-1}) to the atmospheric N_2O budget and their uncertainties from terrestrial and oceanic sources. Natural N_2O sources such as oceanic, atmospheric chemistry and soils under natural vegetation are marked in black, while the anthropogenic contributions including those from atmospheric deposition in the ocean, agriculture, coastal, human excreta, fossil fuels, industry, biomass and biofuel burning, and atmospheric deposition on land are marked in red (Ciais et al., 2013).

Natural N_2O emissions have been historically in equilibrium with the only known substantial N_2O sink, i.e., annihilation with stratospheric O_3. Ice core measurements have shown a constant N_2O atmospheric concentration of 270 ppb over the 2000 years prior to the industrial revolution, as shown in Figure 7. However, an increase in atmospheric N_2O concentration has been observed over the last two hundred years. N_2O atmospheric concentration has increased by 18% since pre-industrial times, reaching 325 ppb at present (NOAA ESRL Global Monitoring Division, Boulder, Colorado, USA, http://esrl.noaa.gov/gmd/). Changes are quite likely attributed to anthropogenic sources of N_2O that must have increased the atmospheric concentration significantly over the last two hundred years.

N_2O plays the role of a greenhouse gas (GHG) in the atmosphere. It is ranked third in radiative forcing (RF) after methane (CH_4) and carbon dioxide (CO_2) (Table 2) (Myhre et al.,

2013). Although its radiative forcing potential is lower, N_2O shows the longest lifetime of these greenhouse gases. One molecule of N_2O lasts in the atmosphere up to 131 ± 10 yr (Prather et al., 2012), exceeding by an order of magnitude the lifetime of CO_2 and CH_4. CO_2 estimated lifetime span 30 to 95 yr, while CH_4 has a shorter lifetime of 11.2 ± 1.3 yr (Prather et al., 2012). During its lifetime, N_2O is distributed from the troposphere up to the stratosphere. When N_2O reaches the stratosphere, it is annihilated in a photochemical reaction where O_3 is consumed (Crutzen, 1970; Johnston, 1971), weakening the O_3 layer. Other O_3 depletion emissions such as chlorofluorocarbons (CFCs) have been limited after the mitigation policies agreed in the *The Montreal Protocol on Substances That Deplete The Ozone Layer* in 1987. This reduction in CFCs emissions suggests that N_2O is now leading the O_3 depletion, and it might keep playing this role the next hundred years, as suggested by Ravishankara et al. (2009) (Figure 6).

Species	Concentration (ppx)	Radiative Forcing (W m^{-2})
CO_2 (ppm)	391 ± 0.2	1.82 ± 0.19
CH_4 (ppb)	1803 ± 2	0.48 ± 0.05
N_2O (ppb)	324 ± 0.1	0.17 ± 0.03

Table 2: Mole fractions and radiative forcing for the three most important greenhouse gases: carbon dioxide (CO_2), methane (CH_4) and nitrous oxide (N_2O). Concentrations are based on measurement averages (Myhre et al., 2013).

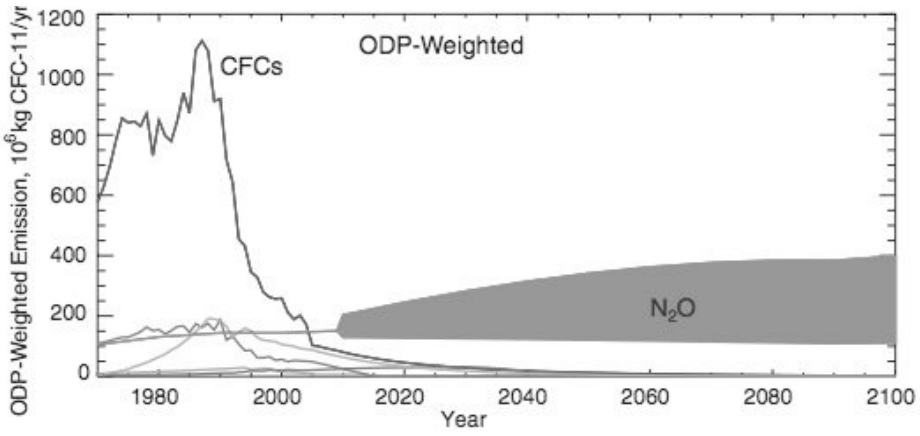

Figure 6**:** Ozone Depletion Potential (ODP) of N_2O and CFCs for present and future scenarios up to year 2100. Regulation of CFC emissions after *The Montreal Protocol on Substances That Deplete The Ozone Layer* (1987) reduced significantly the role of CFCs as the most important ozone depletion agent at the end of the 20th century. N_2O would be the main emission responsible of the O_3 depletion until 2100 (Ravishankara et al., 2009).

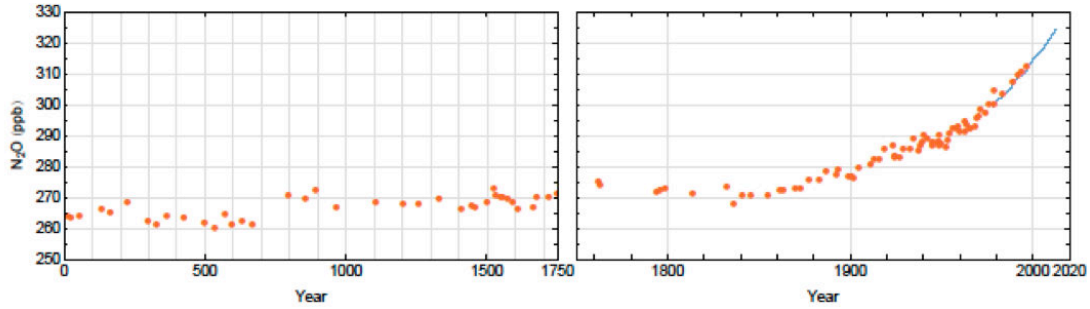

Figure 7: Atmospheric N_2O concentration (in ppb) from 0 AD to present time. Data points are from ice-core measurements (red) and direct atmospheric measurements (blue). The atmospheric N_2O concentration has experienced an 18% increase from pre-industrial to present times, reaching 325 ppb at present. (Ciais et al., 2013 and NOAA ESRL Global Monitoring Division, Boulder, Colorado, USA, http://esrl.noaa.gov/gmd/).

1.2.5. Controls of the bioavailable nitrogen pool

The contribution of inputs, losses and their intermediate processes among the different nitrogen compounds in the fixed nitrogen pools regulate primary production over vast regions of the ocean, modulating in this way the strength of the *biological pump*.

The main input of bioavailable nitrogen as NH_4^+ into the ocean is N_2-fixation. Up to 134 TgN are introduced in the fixed nitrogen pool per year via N_2-fixation according to interpolation techniques based on the compilation of measurements from Luo et al. (2012) (Table 3). This estimation is subject however to large uncertainties. Observations of N_2-fixers distribution, biomass and N_2-fixation rates show a sparse temporal and spatial coverage which cast doubts on the accuracy of its potential global extrapolation. Moreover, the measurement techniques used in this compilation of observations have been also a matter of debate. Estimates using this database could increase up to 177 TgN yr^{-1} (Grosskopf et al., 2012). On the other hand, model studies have estimated global N_2-fixation rates in the same order of magnitude, spanning 134 (Eugster and Gruber, 2012) to 137 TgN yr^{-1} (Deutsch et al., 2007), with uncertainties in the order of ± 16 to ± 34 TgN yr^{-1} respectively. Global ocean biogeochemical model estimates from the CMIP5 project (Taylor et al., 2012) increase the uncertainties up to ± 75 TgN yr^{-1}, despite the agreement on the global mean estimate of 134 TgN yr^{-1} (see Chapter 5).

The loss of fixed nitrogen in the ocean is driven by water column and sediment denitrification, in which NO_3^- is converted by denitrifying bacteria back into an inorganic form of nitrogen (N_2) in low O_2 conditions. Recent model studies estimated 30 and 85 TgN yr^{-}

[1] for water column and sediment denitrification respectively (Eugster, 2013), in the same order of magnitude than previous studies from Somes et al. (2010), Galloway et al. (2004) or Gruber (2004) (Table 3). A comparison between the estimated total input of nitrogen via N_2-fixation and the total loss of nitrogen via total denitrification suggests that at present the oceanic nitrogen budget might be at equilibrium (Gruber, 2008).

Study	N_2-fixation (TgN yr^{-1})	Total Denitrification (TgN yr^{-1})	Sediment Denitrification (TgN yr^{-1})	Water Column Denitrification (TgN yr^{-1})	Study
		115	85	30	Eugster, 2013
Luo et al., 2012	137 ± 9				
Grosskopf et al., 2012	177 ± 8				
Eugster & Gruber, 2012	134 ± 16				
		105	38	67	Somes et al., 2010
Deutsch et al., 2007	137 ± 34				
		274	193	81	Galloway et al., 2004
		245	180	65	Gruber, 2004
Carpenter et al., 1992	10				

Table 3: Estimations of N_2-fixation rates in TgN yr^{-1} combining model studies from Deutsch et al. (2007), Eugster and Gruber (2012), and observational analysis from Luo et al. (2012) and the additional corrections from Grosskopf et al. (2012) based on the former study. Estimates of water column and sediment denitrification (in TgN yr^{-1}) at present are from model estimates (Eugster, 2013; Somes et al., 2010) and geochemical estimates (Galloway et al., 2004; Gruber, 2004).

1.3. The N-cycle in the past

The scenario as today concerning natural oceanic N_2O emissions and the natural equilibrium in the fixed nitrogen pool is a consequence of historical swings over long timescales. Paleorecords indicate this natural variability and describe the cycles that the N-ctcle has been subject to in the past. The additional variability induced by anthropogenic forcings must be put in context of historical fluctuations in N_2O emissions and in the fixed nitrogen pool.

1.3.1. N_2O in the last glacial period

N_2O bubbles trapped into ice cores allow us to reconstruct past atmospheric N_2O concentrations. The atmospheric N_2O concentration has experienced significant changes over

the last 600.000 yr (Figure 8) during glacial and interglacial time periods. This variability is highly correlated with changes in temperature in the northern hemisphere, although it is not yet clear in which way causality operates (Janssen et al., 2007). Moreover, the potential contribution of the oceanic N_2O emissions to the total N_2O budget remains unknown, and so do the land emissions over the same period.

Most of the available data on past atmospheric N_2O concentration belongs to the last 100.000 yr. During this period abrupt changes and shifts in climate conditions have been observed. These changes are also known and Dansgaard-Oeschger (D-O) events. Records of atmospheric N_2O concentration are highly correlated with these abrupt D-O changes. Assuming nitrification and denitrification as the only known production pathways of N_2O in the ocean interior, changes within these processes might explain the abrupt changes observed. In fact, it has been suggested by Gruber (2004) that changes in N_2O production via denitrification or a combination of changes in denitrification and nitrification might have lead to the observed changes during D-O events. The isotopic fractionation during N_2O production allow us to differenciate the main N_2O sources. Denitrification produces *light* (N_2O and N_2) and *heavy* products (NO_3). While N_2O and N_2 escape to the atmosphere, the NO_3 isotopic signal is transferred into organic matter that is eventually stored into sediments (Suthhof et al., 2001). ^{15}N records from sediment cores support the hypothesis of a large activity of denitrification during D-O events. This behaviour has been observed in sediment cores from the Arabian Sea (Pichevin et al., 2007) and the ETP (Suthhof et al., 2001), traditional hotspots of N_2O production. However, sediment records only allow us to reconstruct denitrification activity, leaving N_2O production pathway via nitrification with significant uncertainties of how it evolved in the past, as changes in nitrification are assumed to have occurred in the last glacial period (Fluckiger et al., 2004). From the modelling perspective, model analysis of changes in oceanic N_2O have tried to explain the mechanisms behind the correlation between atmospheric N_2O concentration and the D-O events. These model experiments have focused on changes in ocean circulation as the main driver of changes in N_2O production and eventually on atmospheric N_2O concentration. One of the plausible explanations proposed in these experiments is the substantial change on the strength of the Atlantic Meridional Overturning Circulation (AMOC) during D-O events. Model studies from Schmitter and Galbraith (2008), or Goldstein et al. (2003), induced freshwater inputs in the North Atlantic, thus changing the strength of the AMOC. As a result, they obtained a highly correlated variability in atmospheric N_2O concentrations during D-O events. Whether the same mechanisms might operate in the future modulating oceanic N_2O emissions is a question which remains open.

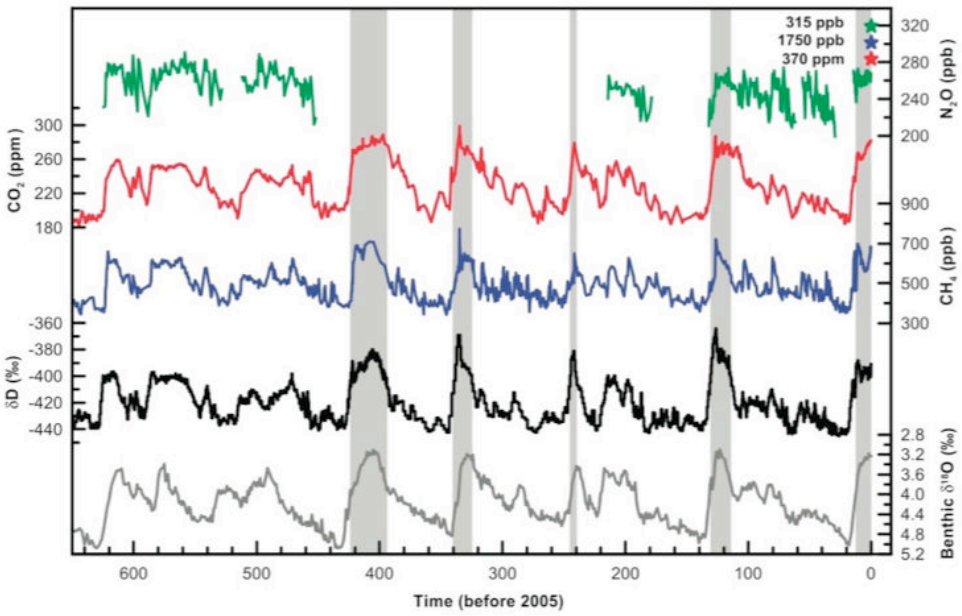

Figure 8: Atmospheric concentration of N_2O, CO_2, CH_4, ∂D and $\Delta^{18}O$ from paleorecords. Warm interglacial periods are shown in grey. (Janssen et al., 2007).

1.3.2. Swings in the nitrogen budget

Palaeorecords have shown evidence of variability of the atmospheric CO_2 concentration over glacial to interglacial periods, from 175ppm to 300ppm in the last 800 kyr (Wolff, 2011). Fluctuations in the oceanic nitrogen inventory, driven presumably by changes in the balance between N_2-fixation and denitrification, might have caused significant variations in the strength of the biological pump and therefore in atmospheric CO_2 concentration (McElroy, 1987). McElroy (1987) argued that swings in the dominance of N_2-fixation over denitrification could explain significant changes in the oceanic fixed nitrogen inventory and hence on the oceanic uptake capability of atmospheric CO_2. That would imply that N_2-fixation and denitrification can be decoupled in a way that one process can operate almost independently from the other over long time scales. Gruber (2008) suggested however that the nitrogen cycle could not be the only or major driving mechanism of the biological pump during long time periods, as compared to the hypothesis proposed by McElroy (1987). The negative feedbacks between changes in N_2-fixation and denitrification would not allow such an imbalance in the N-cycle in long time periods, as they are coupled in a way that changes in N_2-fixation are automatically translated into denitrification. In addition, changes in the nitrogen cycle are located mostly at mid- to low latitudes, whereas in carbonate chemistry changes at high latitudes via the solubility pump have larger implications on the overall CO_2 uptake capacity

of the ocean. The time scope of these hypothesis will not be tested in this thesis, that considers shorter time scales within the next hundred years.

1.4. The N-cycle in the future

Anthropogenic activities have caused perturbations in the marine N-cycle on top of its natural variability. There are direct and indirect anthropogenic induced changes to the marine environment that might change N-cycle processes and transformations. Direct anthropogenic effects include increasing levels of nitrogen supply to the oceans via river discharge due to the extensive use of fertilizers. Increasing industrialization will also increase atmospheric nitrogen deposition of reactive nitrogen compounds. All the extra amount of nitrogen into the natural N-cycle will undoubtedly lead to changes in ocean biogeochemistry. Indirect anthropogenic effects occur via higher levels of atmospheric greenhouse gas concentrations and seawater CO_2, creating three main stressors on the marine environment, namely global warming, ocean deoxygenation and ocean acidification (Gruber, 2011).

Direct and indirect anthropogenic induced changes will modify the external N supply into the ocean, N_2-fixation, nitrification and denitrification processes, with consequences on oceanic N_2O emissions, on the amount of bioavailable nitrogen and on global climate feedbacks. The oceanic regions in which global warming, ocean deoxygenation and ocean acidification operate have been summarised in Figure 9 (Gruber, 2011). Increased stratification expand at low latitudes due to higher temperatures, with subsequent changes in the nutrient supply to the euphotic layer and therefore on marine productivity (Sarmiento et al., 2004). Changes in dissolved O_2 content are also concentrated at low latitudes, particularly on the eastern boundary currents and the northern Indian Ocean. The low latitudinal effects on productivity together with the location of the OMZs in the same latitudinal band makes the N-cycle the ideal candidate to experience the manifold interactions with future oceanic stressors. Some of the most relevant N-cycle processes, namely N_2-fixation, nitrification and water column denitrification occur indeed mostly at low latitudes (see Chapter 2). These processes will experience changes in the distribution of the organisms which perform such transformations, in the metabolic efficiency of these processes, in the environmental conditions under which these processes occur and, finally, in the physical transport of the nitrogen compounds within the ocean interior.

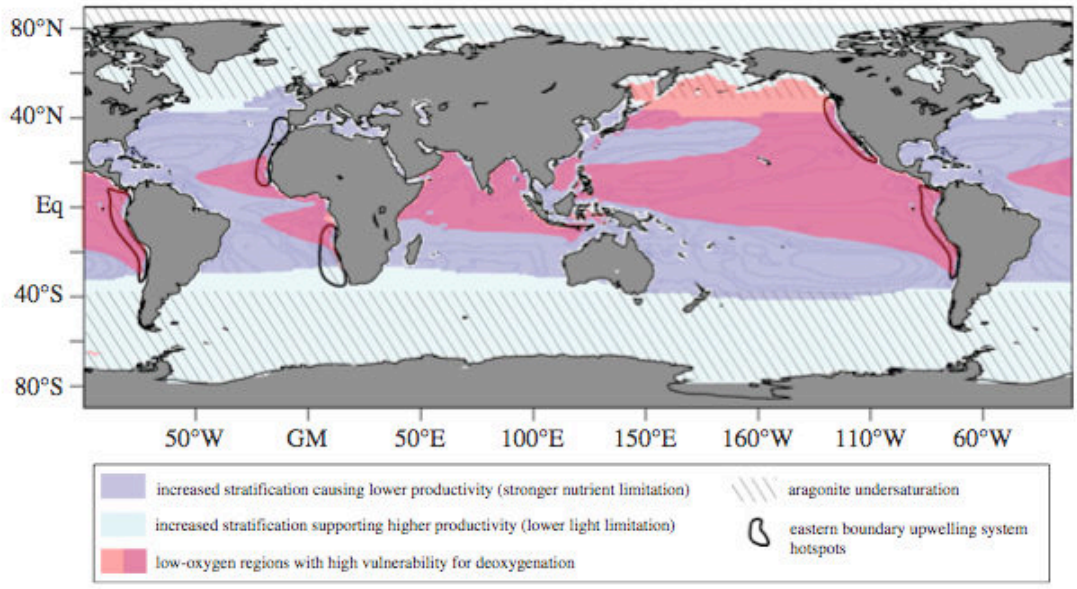

Figure 9: Oceanic regions subject to a significant impact of changes by increasing stratification leading to lower productivity (blue) and deoxygenation (pink) as a result of climate change (Gruber, 2011). The combined effects of stratification and deoxygenation are coincident in low latitudinal regions, where most of the N-cycle processes occur.

1.4.1. Impact of global warming

Global warming, as a result of higher atmospheric concentrations of CO_2 and other greenhouse gases, will increase seawater temperatures and induce higher levels of ocean stratification. This will trigger changes in mixing between the euphotic and the subsurface layers, and in the strength of nutrient upwelling at the eastern boundary currents region, causing a reduced supply of Fe, PO_4, NH_4^+ and NO_3^- in the euphotic layer.

Based on the current understading of N_2-fixation process, questions on whether N_2-fixation efficiency will change in the future due to global warming could be intuitively anticipated. First order effects will operate on the environmental controls on N_2-fixation. Changes in seawater temperature are expected, boosting N_2-fixers population growth and enhanced N_2-fixation. On the other hand, restrictions in the supply of nutrients into the euphotic layer such as Fe or PO_4, which are crucial for the diazotrophs to perform N_2-fixation, would limit substantially N_2-fixation in regions where N_2-fixers are Fe limited like in the Pacific basin. Regions where N_2-fixers are not so Fe limited, like the Arabian Sea or the North Atlantic due to dust deposition (Luo et al., 2014), might show less sensitivity to changes in Fe supply due to global warming.

Regarding nitrification, future changes in marine productivity will directly modify the total amount of NH_4^+ which is potentially oxidized. Model studies have projected a decrease in net primary production (NPP) due to a lower supply of nutrients to the euphotic layer (Steinacher et al., 2010; Bopp et al., 2013). As a consequence, less organic matter would be exported to depth, resulting in a more limited amount of NH_4^+ to be oxidized by nitrifying bacteria. It might therefore expect a decrease in ntirification rates on a global scale.

However, changes in seawater temperature will have a direct impact on ecosystem structures, including nitrifying bacteria. Whether the population of bacteria might change substantially in the future is a question which remains open.

Little is known about the effect of global warming on denitrification. There are no studies on how higher temperatures change the metabolic process of reducing NO_3^- by denitrifying bacteria. Changes in denitrifying bateria population are neither fully analyzed or understood (Freing et al., 2012).

Model studies project an increasing trend in atmospheric greenhouse gas concentration in 2100 under a variety of potential future scenarios, N_2O being the only compound which shows an increase for all the future scenarios considered (Figure 10). Dedicated analysis on specific sources of N_2O to the atmosphere have isolated the individual contribution of the terrestrial sources to the global radiative forcing (Stocker et al., 2013). Terrestrial N_2O emissions under high CO_2 business-as-usual scenario might increase by 80%, leading to a temperature increase of 0.4 to 0.5°C in 2100 in combination with CH_4 soil emissions. The magnitude of the potential contribution of future oceanic N_2O emissions to the radiative forcing remains unknown. Changes in nitrification will be translated into changes in N_2O production, particularly when it has been suggested that most of the N_2O production in the ocean interior is fuelled by the nitrification pathway (Freing et al., 2012). Therefore a decrease of N_2O production is intuitively expected if primary production decreases. Transport of N_2O from the subsurface to the air-sea interface might be affected too due to increased stratification. Finally, changes also in N_2O solubility must be considered together with the water masses which were in contact with the atmosphere at different equilibrium concentrations of N_2O.

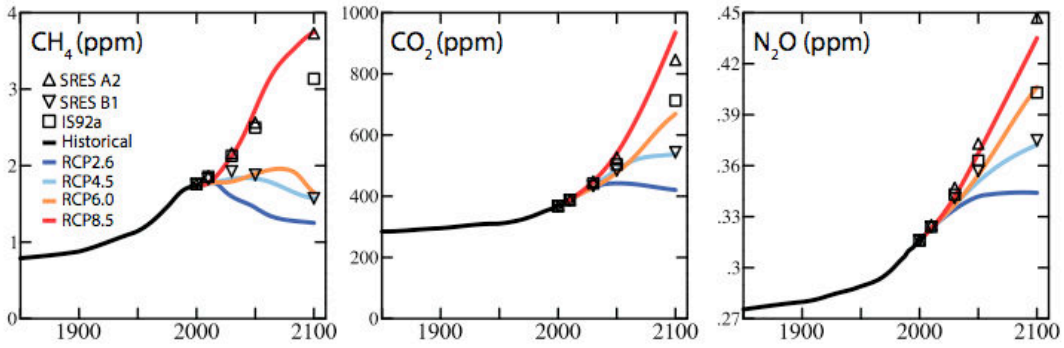

Figure 10: Historical and projected CO_2, CH_4 and N_2O concentrations in 2100 under different Representative Concentration Pathways (RCPs) scenarios. Future values beyond present time are compared to previous climate reports using the former model generations and related scenarios. N_2O atmospheric concentration is expected to increase in each of the scenarios studied, up to a 33% increase in the business-as-usual high CO_2 emissions scenario. (Meinshausen et al., 2011; Ciais et al., 2013).

1.4.2. Impact of ocean deoxygenation

Ocean deoxygenarion is a consequence of the ongoing reduced ventilation associated with increased stratification, together with lower solubility due to higher seawater temperatures (Ciais et al. 2013). This fact has been reflected in ocean general circulation and biogeochemical model future projections. Figure 11 shows the decrease of the O_2 content on a global scale by several IPCC class models, and the increase in the hypoxic (O_2 concentration < 80 $\mu molL^{-1}$) volumes from 1850 to 2100 under the high CO_2 business-as-usual scenario (Bopp et al., 2013). There are few long time records of O_2 measurements that could confirm this hypothesis (Stramma et al., 2008, Stenardo et al., 2009), but nevertheless this result is consistent with the projections made by the previous generation of global ocean biogeochemical models (Steinacher et al., 2009; Cocco et al, 2012).

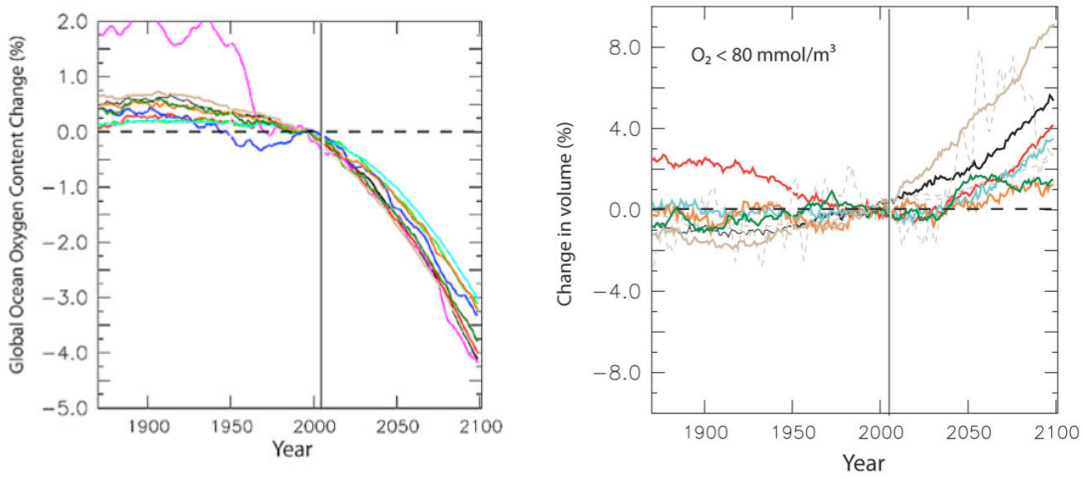

Figure 11: Model projections of changes in (a) Global oxygen content (in %) and (b) O_2 concentration below 80 mmol m^{-3} using the CMIP5 model ensemble under the business-as-usual high CO_2 emissions scenario RCP8.5 (Bopp et al., 2013).

Changes in the dissolved O_2 concentration are not expected to imprint significant changes in N_2-fixation. N_2-fixation occurs in the euphotic layer, where high levels of O_2 are observed and therefore little changes are expected on this process. Moreover, few studies report sensitivity of *diazotrophs* to O_2 levels, as they live mostly in the ocean surface. N_2-fixation does have however sensitivity to O_2, as reported by Stuart and Pearson, 1970, but future changes seem far from changing that limiting facto substantially enough.

Ocean deoxygenation might shift the boundaries of occurrence of nitrification and denitrification in the ocean interior. Nitrification is characterized by being a global process and therefore little changes are expected due to the relatively small volume of the OMZs subject to change. The expansion of the OMZs at depth will increase the occurrence of denitrification, leading to an enhanced loss of bioavailable nitrogen and an increase in N_2O production and N_2O consumption. While N_2O production in low-O_2 environments might be boosted, N_2O consumption might be boosted as well by the same denitrifying bacteria in anoxic environments (Bange et al., 2000). Culture experiments have shown a high sensitivity of N_2O production to O_2 levels (Goreau et al., 1980; Frame and Casciotti, 2010), whereas direct observations disagree with this assumption, as shown by Zamora et al., 2012, where N_2O shows a linear relationship with O_2 even at OMZs such as those in the Eastern Tropical Pacific (ETP). The evolution of the balance between N_2O production and consumption in the OMZs in the future remains unclear.

1.4.3. Impact of ocean acidification

The oceanic uptake of atmospheric CO_2 has decreased the levels of seawater pH by 0.1 units on average since pre-industrial times (Orr et al., 2004). Model projections, following the increasing atmospheric CO_2 concentration and the current absoption capacity of the ocean, suggest that pH could reach even lower levels (Steinacher et al., 2009, Bopp et al., 2013). Adaptation of phytoplankton groups and bacteria to decreased levels of seawater pH remains one of the big unknowns in biogeochemical studies. Process efficiencies and population dynamics must certainly change within changes in their environmental conditions due to ocean acidification. N_2-fixation might be favoured by increasing seawater CO_2 (Barcelos e Ramos et al., 2007, Hutchins et al., 2007, Hutchins et al., 2012), although their future evolution remains unclear. Barcelos e Ramos et al., 2007, analysed the effect of increasing levels of seawater CO_2 on particular species of N_2-fixers named *Trichodesmium*. *Trichodesmium* is supposed to be responsible of at least half of the total N_2-fixation in the global ocean. In these culture experiments CO_2 played the role of an additional nutrient, doubling N_2-fixation rates and N_2-fixers growth rates from pre-industrial to projected 2100 CO_2 levels (Figure 12a and Figure 12b).

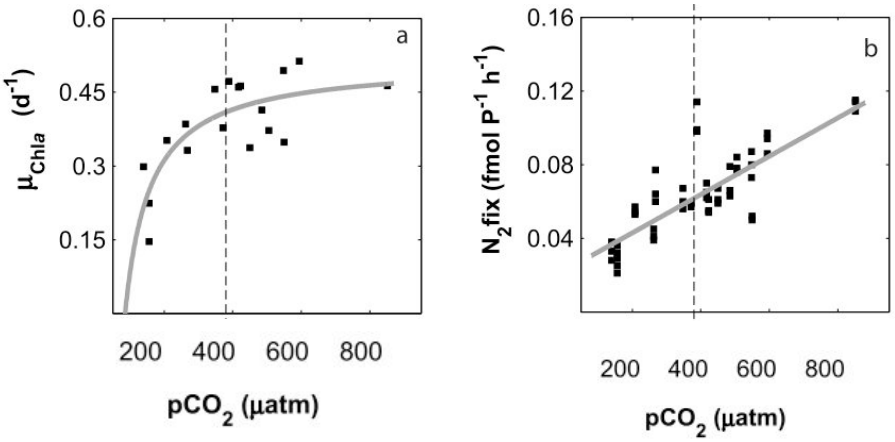

(a) *(b)*

Figure 12: Experimental results of the CO_2 fertilization effect on diazotrophs, showing (a) growth rate of *Trichodesmium* under high levels of pCO_2 fitted to a Michaelis-Menten curve and (b) N_2-fixation rates fitted to a linear function (Barcelos e Ramos et al., 2007).

Changes in N_2-fixation in other species (*Croccosphera*) in addition to *Trichodesmium* have been analysed in more detail by Hutchins et al., 2013. Results of N_2-fixation rates under high levels of seawater CO_2 on the most and less sensitive species of N_2-fixers, i.e., *Trichodesmium*

Erythraeum and *Trichodesmium Thiebautii* are shown in Figure 13. Boundaries of the response of N_2-fixers are defined by half saturation constants of 431 ppm and 65 ppm respectively. In both cases there is an increase of the N_2-fixation rates for the whole range of seawater CO_2 concentrations considered. The range of spatial changes in seawater CO_2 and the distribution of the *diazotrophs* species sensitive to these changes will ultimately determine the future evolution of N_2-fixation.

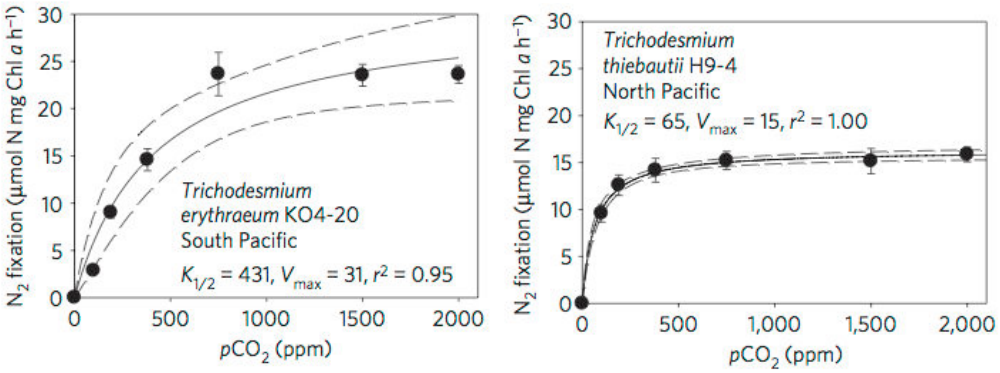

Figure 13: Experimental results of N_2-fixation rates for the most and least sensitive N_2-fixation species to seawater CO_2 fitted to a Michaelis-Menten curve in Hutchins et al., 2013, in particular (a) *Trichodesmium Erythraeum* and (b) *Trichodesmium Thiebautii*.

Nitrifying bacteria show low sensitivity to changes in seawater CO_2 levels (Badger et al., 2008, Berg et al., 2007). However, nitrification is sensitive to changes in pH, as shown by Huesemann et al. (2002). This study analysed the effect of increased levels of H^+ concentration in estuaries (Figure 14). Nitrification efficiency decreased together with pH by 50% for changes of only 1% in pH. Changes in nitrification were further explored by Beman et al. (2011), this time from an open ocean perspective. Laboratory experiments using different cultures from different oceanic basins showed the same response of nitrifying bacteria to lower pH levels. Figure 15 shows a decrease from 5% to 20% in nitrification due to a 1% change in pH. This results suggests that future ocean acidification might have a significant impact on nitrification and therefore on N_2O production.

Changes in denitrification due to lower levels of pH are unknown. Studies based on the same genetic mechanisms of denitrification in soils estimate that changes in seawater pH are not significant enough to be noticeable in denitrification (Liu et al., 2010). Therefore changes in N_2O production in the OMZs are not expected to change significantly due to changes in pH.

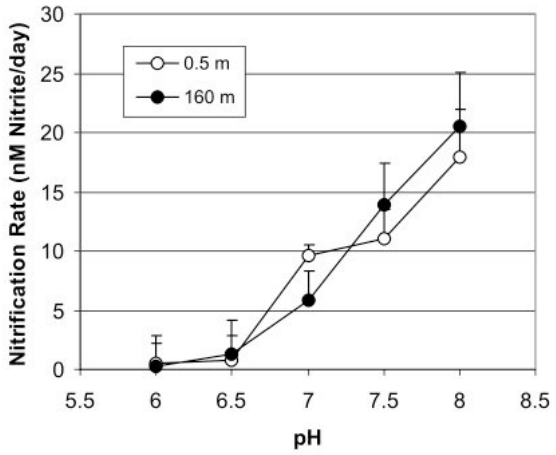

Figure 14**:** Nitrification rates for different seawater pH samples at two different depths, near surface 0.5m and deeper 160m (Huesemann et al, 2002).

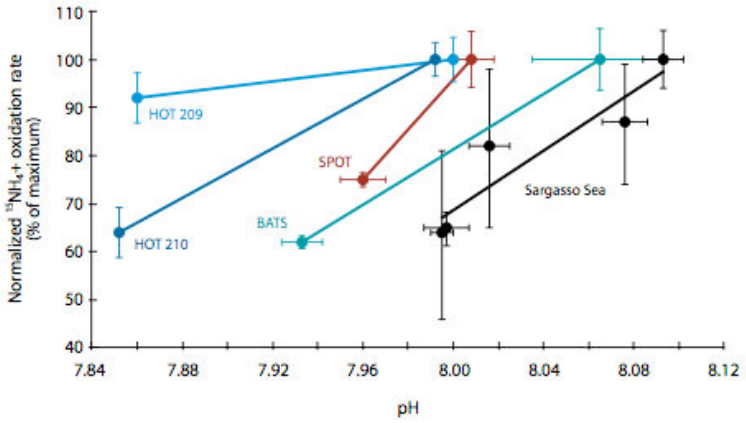

Figure 15: Nitrification rates in response to experimentally reduced levels of seawater pH from different samples at HOT, BATS, SPOT and Sargasso Sea locations (Beman et al., 2011).

1.4.4. Direct anthropogenic nitrogen inputs

In addition to changes in the marine nitrogen cycle in the ocean interior, the increasing human population will boost the use of fertilisers and the reactive nitrogen emissions, part of which will eventually end in the marine environment either via atmospheric deposition or riverine supply.

Atmospheric nitrogen deposition is expected to increase in the next century. Growing industrialized areas will produce more NO_x, NH_y and organic nitrogen compounds that will increase the supply of nitrogen on the sea surface via atmospheric deposition. Duce et al. (2008) projected an increase from 68 at present to 77 TgN yr^{-1} in year 2030, in the same order

of magnitude from the study by Dentener et al. (2004) from 38.9 to 68.9 TgN yr^{-1} over the same time period. It is estimated that in the future it could potentially equal the contribution of N_2-fixation due to larger industrialized areas in coastal regions (Duce et al., 2008, Krishnamurthy et al., 2007). Changes of N_2O production and N_2O emissions due to atmospheric nitrogen deposition from pre-industrial to present were analysed by Suntharalingam et al. (2012), which could give an estimate about future changes if atmospheric deposition increases at the same rate. Atmospheric nitrogen deposition from the previous studies estimated 20/22.1 TgN yr^{-1} in 1851, increasing by 48/16.8 TgN yr^{-1} at present (Dentener et al., 2004; Duce et al., 2008). Due to these changes over the historical period N_2O emissions were estimated to increase by 3 to 4%, following the imprint of additional nitrogen in export production with an increase of 4%.

There are many uncertainties on how river discharge might change in the future, however it is intuitively expected that the increasing population and therefore increasing food demand might also increase the use of fertilizers and other industrial processes that contribute to the N-budget in soils and hence in rivers. The extensive use of fertilizers will increase the river discharge over coastal regions and river basins. DaCunha et al. (2011) projected changes in biogeochemical markers such as primary production and export production in a variety of future scenarios up to 2050, assuming river discharge values from a world population of 12 billion inhabitants. The increase in river discharge of DIC, DOC, POC and DIN lead to an increase on export production of 6% in 2050, which might eventually be translated into an increase of N_2O emissions in the same magnitude.

1.5. Open questions

1.5.1. Future marine N_2O emissions

The evolution of oceanic N_2O emissions in the future remains largely unknown. Multiple stressors on the marine N-cycle will certainly change the N_2O production, N_2O transport and N_2O sea-to-air flux to the atmosphere, with a potential impact on the ocean contribution to the global GHG budget and the O_3 depletion process. Critical questions that have to be addressed are clustered around N_2O production, N_2O transport, other N_2O production processes and the current capabilities of models.

Many uncertainties still exist regarding the relative contribution of nitrification and denitrification to the total N_2O production budget, and how these production pathways will

evolve in the future. Although nitrification seems the dominant pathway (Freing et al., 2012), the evolution of these pathways might not be as such in the future. Changes in the volume of hypoxic and suboxic waters will definitely imply changes in the production of N_2O via denitrification. Experimentally, it has been found that N_2O shows a higher yield under suboxic regimes (Goreau et al., 1980; Frame and Casciotti, 2012), but also does the N_2O consumption, as suggested by Zamora et al. (2013). There are many uncertainties regarding the coupling between N_2O production and consumption in the boundaries and core of the OMZs respectively. Changes in the bacterial community will modify the distribution of the N_2O producers in the ocean interior. Increasing temperatures will modify the metabolism of bacteria and quite likely their abundance and distribution. The CO_2 attenuation effect on N_2O production via nitrification (Beman et al., 2011) could reinforce the projected decrease in export of organic matter to depth in 2100 (Bopp et al., 2013). The extent at which the CO_2 reduction effect is enhanced under lower levels of pH is still unknown.

The magnitude of changes in transport from the subsurface to the surface might be critical in estimating the N_2O sea-to-air flux. Oceanic stratification might enlarge the N_2O reservoir at deep, as any other biogeochemical compound produced or transported below the euphotic zone (Freing et al., 2012). Changes in N_2O solubility will modify the N_2O inventory and the gas exchange with the increasing atmospheric N_2O.

The contribution of anammox as an alternative source of N_2O remains largely unknown. It has been reported as one of the major sources of N_2O off the Namibia coast (Kuypers, 2005), but many uncertainties remain on its adequate environmental conditions, occurrence and relative contribution among the other N_2O production processes.

Uncertainties when using ocean biogeochemical models to estimate N_2O sea-to-air flux has been also a matter of debate (Zamora and Oschlies, 2014). On a single model analysis, N_2O production from surface nitrification represents 50% of the uncertainty, followed by the distribution of O_2 in the model by 24%. Other parameters that introduce uncertianties on the estimations are the N_2O consumption rate and the O_2 threshold at which N_2O production switches to N_2O consumption. Model projections of future N_2O emissions are tied to the foundational assumption of N_2O production parameterizations, i.e., the apparent oxygen utilization and its linear relationship with the excess of N_2O (Elkins et al., 1978; Butler et al., 1989). Mechanistic parameterizations based nitrification and denitrification rates as well as the N_2O formation sensitivity to changes in temperature are not available as today and this fact hamper accurate projections of N_2O production and hence N_2O sea-to-air emissions.

1.5.2. Impacts of global warming and ocean acidification on the N-cycle

Multiple effects of higher levels of dissolved CO_2 are presumed to occur in the N-cycle. Despite the experimental results on particular processes such as N_2-fixation or nitrification, the combined effects and the second order non-linearities in the fixed nitrogen pool, as well as in other biogeochemical cycles, are difficult to predict. Critical questions that have to be addressed are centered around the equilibrium between N_2-fixation and denitrification and how it might evolve in the future, and the unknown response to higher-than-ever dissolved CO_2 concentrations.

The potential compensation between the CO_2 fertilization effect on N_2-fixation (Barcelos e Ramos et al., 2007; Hutchins et al., 2007; Hutchins et al., 2013) and the CO_2 attenuation effect on nitrification (Huesemann et al., 2004; Beman et al., 2011), might play an important role on the response of the N-cycle as a whole to marine stressors. The magnitude, occurrence and local coupling or decoupling between these two processes would clarify the future response of the N-cycle in the next century. Moreover, the assumption of equilibrium between inputs and losses of fixed nitrogen at present might not be valid in the future. In addition to the arguments exposed by Gruber (2008), the role of an intermediate process between N_2-fixation and denitrification, i.e., nitrification, has not been yet discussed in detail. Changes in nitrification might change the dissolved O_2 distribution in subsurface layers, hence having direct implication in the occurrence of denitrification in the ocean interior and therefore on the negative feedback between the coupled formation-and-removal of fixed nitrogen. Spatial coupling and decoupling of changes in N_2-fixation and nitrification are also of paramount importance. The time scales over which both processes can co-exist would determine changes over longer time periods such as those observed during paleoscales.

Paleorecords have shown variations in the N-cycle associated with an specific range of changes in atmospheric CO_2 concentration, from 175ppm to 300ppm. The amplitude of periodical swings between N_2-fixation and denitrification in a context of much larger variations of atmospheric CO_2 than that from the paleoscales analyzed by McElroy must be addressed considering the range of atmospheric CO_2 estimates looming ahead, up to more than 900ppm.

1.6. Objectives and methods

The aim of this thesis is to explore and project changes in the N-cycle under global warming, ocean deoxygenation and ocean acidification on a global scale. Particular attention is paid to changes in N_2-fixation, nitrification and oceanic N_2O emissions to the atmosphere in 2100.

The main questions that are addressed in this work are which are the main sources of uncertainties in N_2O production rates and N_2O inventory estimates using state-of-the-art global ocean biogeochemical models, how will evolve the oceanic N_2O emissions to the atmosphere int he future, and what is the impact of the individual and combined effect of ocean acidification and global warming on N_2-fixation and nitrification. This thesis is organized in the five following chapters:

Chapter 2

Methods

I describe PISCES ocean biogeochemical model, particularly the way the N-cycle is represented in the model, and its coupling configuration with NEMO ocean general circulation model. I put the current PISCES and NEMO capabilities in the context of the CMIP5 models. In addition, I describe the existing databases and data-based products that are used to constrain the representation and accuracy of the main nitrogen compounds and other biogeochemical variables in models.

Chapter 3

N-cycle in CMIP5 models

I compare the model estimations and their uncertainties with N_2O inventories and N_2O production rates derived from climatologies and data-based products of temperature, salinity, O_2 and export of organic matter to depth (CEX). I identify the major sources of these deviations considering the existing parameterizations found in literature for estimating N_2O production and N_2O inventory in a steady-state fashion. The calculation method is based on offline estimations using O_2 and CEX from the CMIP5 model output archive. Data-based

products estimates are made using temperature, salinity and O_2 from the World Ocean Atlas (WOA) 1998 to WOA2009, including the oxygen-corrected World Ocean Atlas 2005 (hereinafter WOA2005*) from Bianchi et al. (2012). For CEX we use two dimensional CEX fields at 100m deep from Laws et al. (2000), Eppley et al. (1989), Schlitzer et al. (2004) and Dunne et al. (2007). The N_2O parameterizations used are those from Butler et al. (1989) and Nevison et al. (2003). N_2O inventory is compared to the measurements gathered in the MEMENTO Database (Bange et al., 2009). The PISCES ocean biogeochemical model is used additionally to analyse the temporal and spatial correlation between N_2O production and N_2O flux.

In addition, I explore the main uncertainties in the current representation of N_2-fixers biomass and N_2-fixation rates in the state-of-the-art ocean biogeochemical models, by comparing the CMIP5 model output data in the existing repositories with the database from Luo et al. (2012). Strengths and weaknesses are identified when estimating the global N_2-fixation budget and the spatial distribution of N_2-fxation occurrence. Of particular interest are the environmental controls of the N_2-fixation process, such as temperature or Fe supply, considered in each of the individual models.

Chapter 4

Oceanic N_2O emissions in the 21st century

I analyse changes in N_2O sea-to-air flux in 2100 together with the mechanisms triggered by global warming on N_2O production pathways, N_2O storage and N_2O transport in 2100 under the business as usual high CO_2 emission scenario RCP8.5. I make future projections of oceanic N_2O emissiosn using PISCES ocean biogeochemical model in the framework of the IPSL-CM5 physical forcings for the historical and future scenarios. Two different parameterisations are implemented into PISCES, inspired by Butler et al. (1989) and Jin and Gruber (2003). A dedicated box model is designed, synthesizing the main drivers of changes in N_2O sea-to-air flux in a simplified fashion. I explore the range of different magnitudes of export of organic matter in combination with mixing coefficients which modulate future N_2O oceanic emissions to expand the analysis to a wider scope of future scenarios beyond the single PISCES experiment.

Chapter 5

Impact of ocean acidification on N_2-fixation

I analyse the increase in seawater CO_2 in tandem with global warming on N_2-fixation. I estimate the effects of the individual and the combined effects on a global scale, from pre-industrial 1851 to 2100 under the business as usual high CO_2 emission scenario RCP8.5. I implement a new parameterisation in PISCES ocean biogeochemical model following the laboratory experiment results from Hutchins et al. (2013). A Michaelis-Menten function is added to the N_2-fixation parameterization assuming dissolved CO_2 playing the role of a nutrient. I analyze the separated and combined effects of ocean acidification and climate change, and estimate changes in N_2-fixation rates on a global scale, in the nutrient cycling via the relative amount of NH_4^+ in the nitrogen pool, and in primary production at the end of the century. The expansion of N_2-fixation occurrence latitudinal- and depthwise is also analyzed.

Chapter 6

Impact of ocean acidification on Nitrification

I analyze the combined effects of global warming and decreasing levels of seawater pH on nitrification. I use NEMO-PISCES ocean general circulation and biogeochemical model to analyze the individual and combined effect of the two marine stressors during the next century under the business-as-usual high CO_2 emissions scenario (RCP8.5). I developed a new parameterisation including a pH sensitive term based on Beman et al. (2011) experiments. I explored changes in nitrification efficiencies and the secondary effects of nitrification on subsurface NO_3^-, O_2 concentration, primary production and changes in N_2O production on a global scale. I take advantage of the previously N_2O parameterization included in the same fashion as in the previous experiments.

Chapter 2

Methods

2.1. Introduction

Ocean biogeochemical models are a useful tool to explore past, present and future changes in the marine N-cycle. Models allow us to study the interactions in ocean biogeochemistry between systems of several elements under different but combined physical, chemical and biological forcings.

The scope of the analysis is particularly complex when taking into account three different marine stressors, i.e., global warming, ocean deoxygenation and ocean acidification, applied to different processes: N_2-fixation, nitrification, denitrification and N_2O production. These processes involve a variety of nitrogen compounds (NO_3^-, NH_4^+ and N_2O) from the N-cycle and their coupling with C-, P-, O_2- and Fe- cycles, on top of changes in phytoplanton nutrient uptake, primary productivity, export of organic matter to depth or bacterial processes, among many others. Moreover, the ultimate purpose of ocean biogeochemical models, linking the nutrient cycling with marine CO_2 sequestration, complete the global picture analysing the

implications of changes in the N-cycle with climate feedbacks on a global scale. The complexity of these various interactions is difficult to reproduce both in laboratory experiments and also to be observed in direct measurements, which are spatially limited, temporally scarce, and difficult to analyze under the changing environment due to anthropogenic forcings.

Models were historically developed to solve questions beyond these laboratory boundaries. Since their inception in the 1940s (Riley, 1946; Riley et al., 1949), ocean biogeochemical models have evolved significantly (Figure 1). Focusing only on global models, they have experienced significant improvements over the last decades fueled primarily by the increasing computational development in the semiconductor industry over the same time period, and therefore by the increasing state variables, increasing physical model resolution and longer simulation time periods.

Starting in the 1980s, biogeochemical models were initally phosphate-based using a crude representation of geochemistry only with particulate organic matter. It was during the 1990s when the first living compartments were introduced, together with the NPZD concept, having nutrients (stands for N), phytoplankton (for P), detritus (for D) and zooplankton (for Z) as the paradigmatic and most extended biogeochemical model architecture. The sharp increase in computational capacity in the 2000s brought the ability to compute more compartments and interactions and therefore they came along with an outburst of nutrients (Fe, NH_4^+, Silicate) and more living compartments for particular phytoplankton groups and plankton functional types (PFTs). The pinnacle in model complexity has been achieved recently (Follows et al., 2007), where a myriad of phytoplankton groups compete for the existing resources, yet with a simple metabolic description of these living subgroups.

In parallel, ocean circulation models have experienced a similar development over the last decade, increasing their resolution up to 12^{th} of a degree and including mesoscale turbulent features such as eddies. As a result, coarse resolution models in the 1980s have evolved towards high resolution, eddy resolving global circulation models, coupled to the existing ocean biogeochemical models in high-end computational architectures.

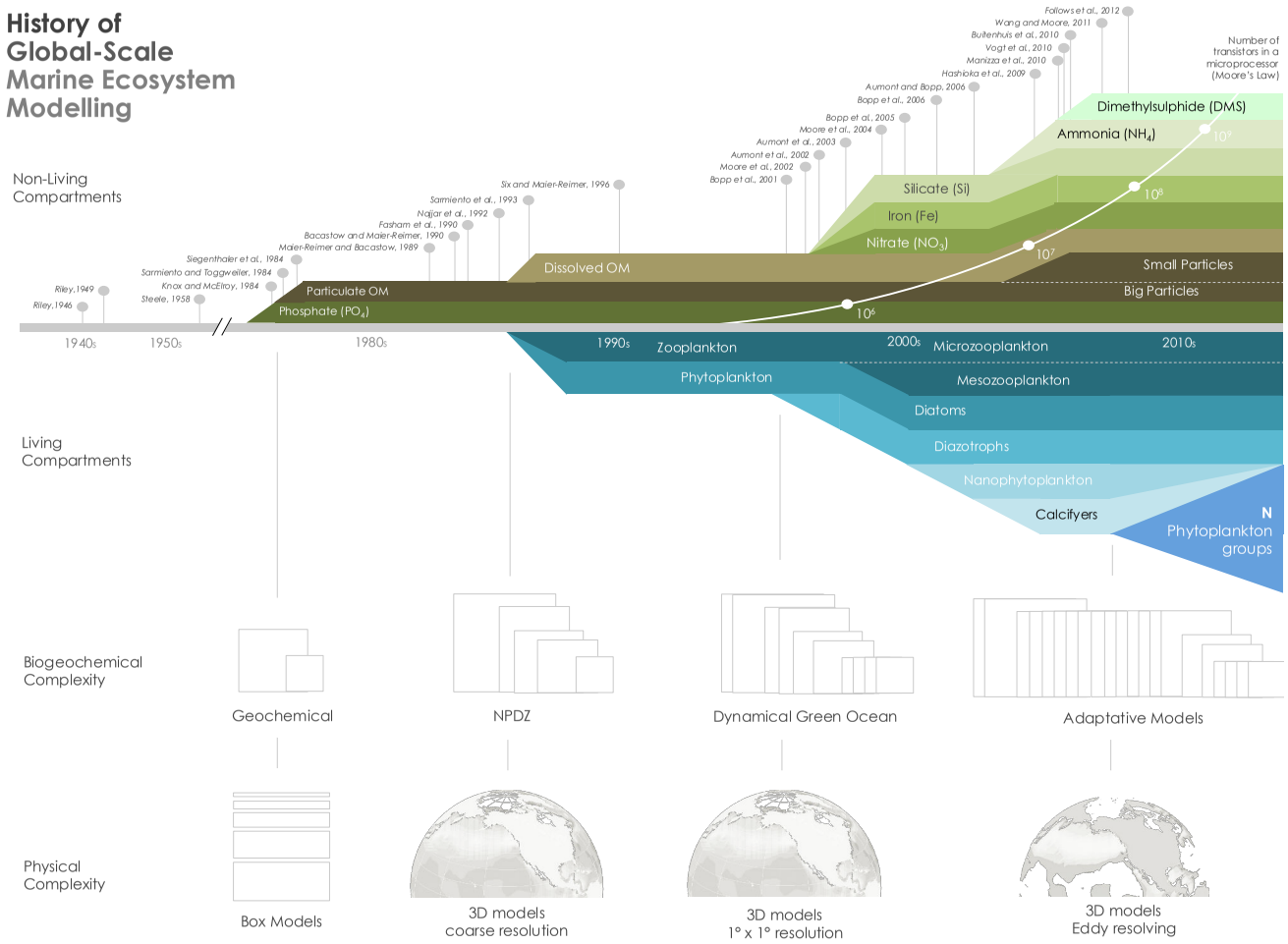

Figure 1: Timeline and major achievements in the hIstory of global scale marine ecosystem models. Non-living compartments are shown in the upper part of the diagram, while living compartments are shown in the lower part. The white curve represents the Moore's Law, showing the number of transistors in a microprocessor. Dots represent the landmarks in model development. (Vogt et al., in prep).

2.2. PISCES model

2.2.1. Structure

PISCES is an NPZD-type ocean biogeochemical model designed to address questions not only related to the carbon cycle but to other nutrients as well (Aumont and Bopp, 2006). Its representation of marine ecosystems (Figure 2) at a primary level includes five nutrients (NO_3^-, NH_4^+, PO_4, Silicate and Fe), two phytoplankton groups (nanophytoplankton and diatoms), two zooplankton sizes (micro and mesozooplankton), plus five compartments of organic matter (dissolved organic matter, big and small organic particles, dissolved Si and two types of dissolved Fe). Nutrient availability and three wavelength radiation bands (red, green and blue) limit the phytoplankton growth. Phytoplankton is either grazed by zooplankton or degraded into the organic matter pool. Zooplankton is controlled by mortality, fueling the same organic matter pool. Remineralization of the organic matter feeds the nutrients pool in addition to the external nutrient supply. PISCES uses constant Redfield ratios for C, N and P of 122:16:1 (Takahashi et al., 1985). Ratios of C:Si and C:Fe are variable and computed by the model.

Ocean biogeochemical models have been triggered mainly by the development of the carbon cycle and the analysis of marine CO_2 sequestration, being the development of other nutrients stimulated in parallel. PISCES includes among its biogeochemical processes N_2-fixation, nitrification, denitrification and production and sea-air gas exchange of N_2O due to nitrification and denitrification. In addition there is external nitrogen inputs from atmospheric nitrogen deposition and riverine nitrogen supply. These processes and the way they are embedded into PISCES are described in the following sections.

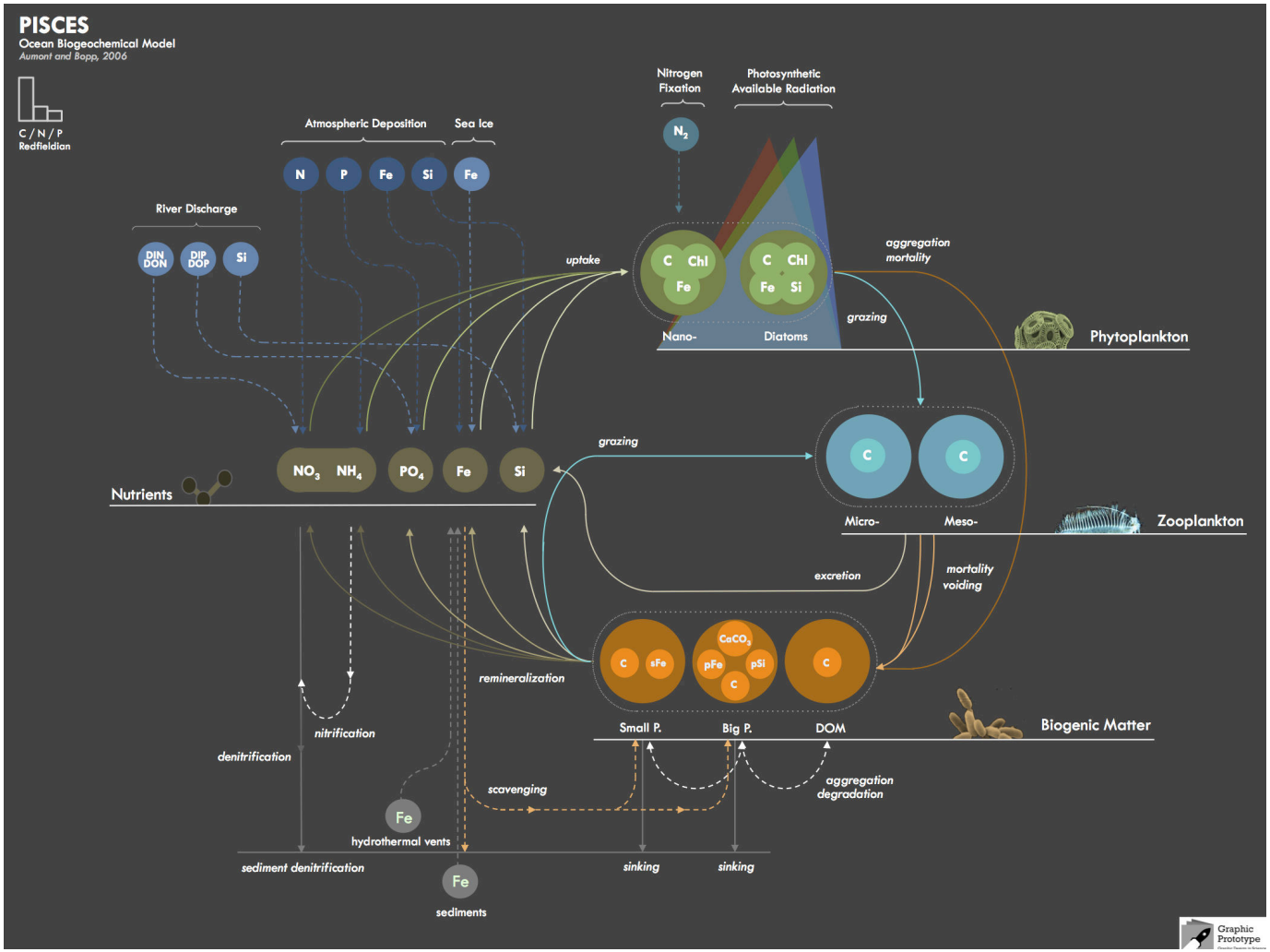

Figure 2: Diagram of the different pools in PISCES ocean biogeochemical model. The model is built upon four main compartments: nutrients (brown), phytoplankton groups (green), zooplankton types (blue) and organic matter (orange) (Aumont et al., in prep.)

2.2.2. The N-cycle in PISCES

2.2.2.1. N_2-fixation

N_2-fixation is included in PISCES as a combination of environmental limiting terms on N_2-fixation process performed by nanophytoplankton, who play the role of *diazotrophs* in the model. *Diazotrophs* are not explicitly resolved in the model and only N_2-fixation rates are diagnosed. The parameterization used in PISCES includes the following limiting terms: abundance of other nitrogen compounds other than N_2 (assumed to be in infinite supply), i.e., NO_3^- and NH_4^+, availability of Fe, incoming photosynthetic available radiation (PAR) and temperature. The combination of limiting terms modulating N_2-fixation is formulated in Eq. (1) as:

$$J_{Nfix} = \mu \cdot \frac{K_n}{K_n + [NO_3 + NH_4]} \cdot \frac{[Fe]}{K + [Fe]} \cdot (1 - e^{-I_{PAR}}) \cdot \alpha^{TEMP} \quad (1)$$

where μ is the growth rate of nanophtoyplankton, K_n is the half saturation constant of NO_3, K is the half saturation constant of Fe, PAR is the photosynthetic available radiation and TEMP is temperature. The range of variation of the different limiting terms is shown in Figure 3. N_2-fixation is inhibited above 2 to 3 μmol L^{-1} of NH_4^++ NO_3^-, below Fe concentrations of 0.05 nmol L^{-1}, below 12 to 15°C and below 20 W m^{-2} of PAR.

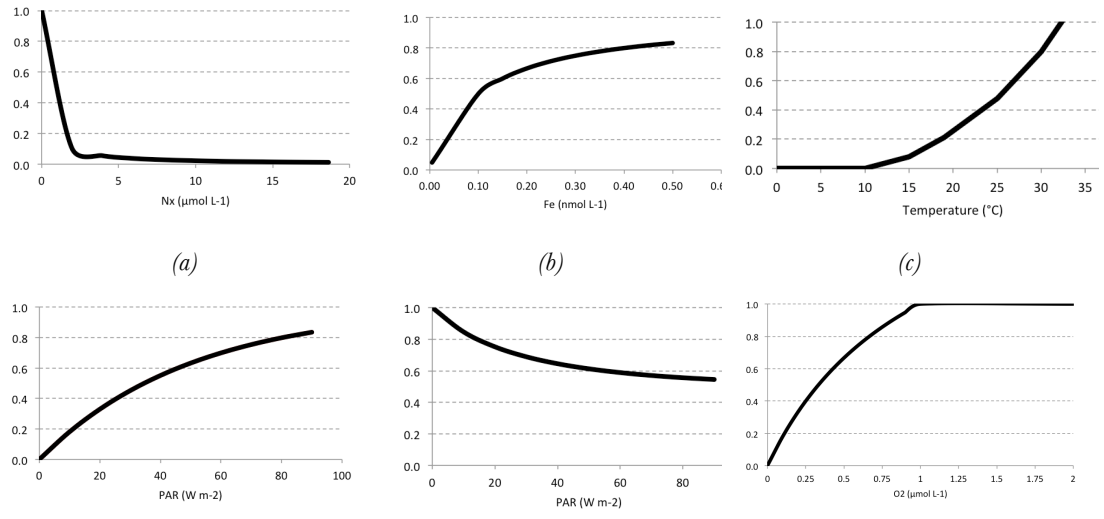

Figure 3: Offline estimates of the limiting terms in N_2-fixation in NEMO-PISCES from (a) NO_3^-+ NH_4^+ concentration (in mmol L^{-1}), (b) dissolved Fe concentration (in nmol L^{-1}), (c) Temperature (in °C), (d) Photosynthetic available radiation (PAR) (in Wm^{-2}). Offline estimates for nitrification limiting terms in NEMO-PISCES from (e) Photosynthetic available radiation (PAR) (in Wm^{-2}) and (f) O_2 concentration (in μmol L^{-1}).

The spatial distribution of vertically integrated N_2-fixation rates in PISCES at present (averaged 1985 to 2005 time period in the historical simulation) is shown in Figure 4. N_2-fixation is found mainly at low latitudes, without significant N_2-fixation activity in the subpolar and polar regions due to light and temperature restraints. Regions of high N_2-fixation rates are located in the western part of the major oceanic basin and they are inhibited by upwelling of other nitrogen compounds in the eastern boundary currents. The contribution of Fe from western river basins in the tropical Atlantic (i.e., Amazon river) supports N_2-fixation in the Atlantic. High N_2-fixation rates in the Benguela Upwelling System (BUS) show either an undersestimation of upwelling in that region or alternative transport effects in the South Atlantic in the model.

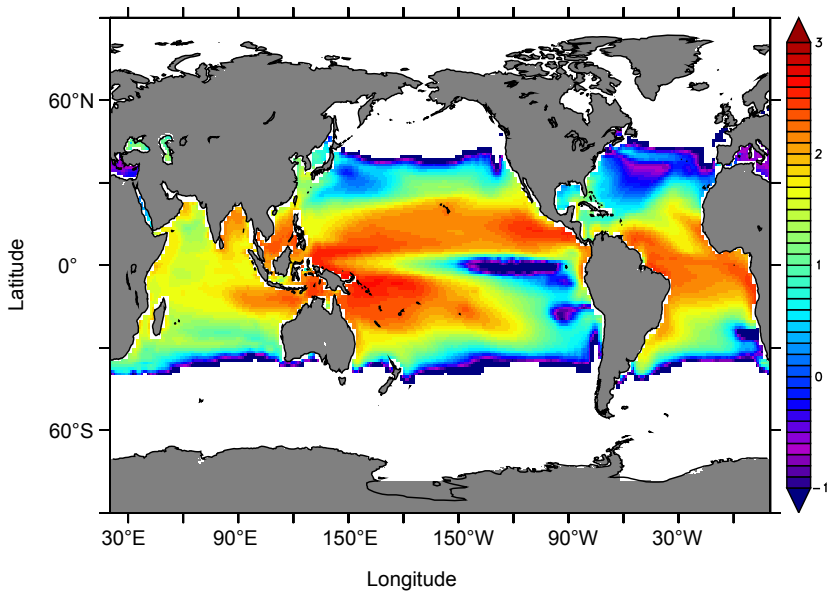

Figure 4: N_2-fixation rates (in log µmol m^{-2} d^{-1}) in PISCES model, averaged over the 1985 to 2005 time period in the historical simulation. Environmental factors regulate the occurrence of N_2-fixation performed by nanophytoplankton in the model. N_2-fixation is inhibited at high latitudes quite likely due to temperature and PAR effects.

2.2.2.2. Nitrification

Nitrification is modelled in PISCES in Eq. (2) based on the amount of carbon exported to depth which is remineralized into NH_4^+ and subject to conversion into NO_3^-. This amount is then modulated by three additional terms: the nitrification rate, light inhibition, and the attenuation of nitrification in suboxic areas:

$$Nitrif = \lambda_{NH_4} \frac{NH_4}{1 + \overline{PAR}} (1 - \Delta(O_2)) \quad (2)$$

where PAR is averaged over the mixed layer and $\Delta(O_2)$ equals to 1 at complete anoxia (i.e., dissolved O_2 concentration equal to zero). The range of values in which these limiting terms operate are shown in Figure 3. Nitrification is particularly enhanced in total abscence of light, whereas O_2 levels should be above the suboxic threshold of 1 µmol L^{-1}. Nitrification in PISCES is shown in Figure 5 using the N_2O production in high-O_2 areas for present day (averaged 1985 to 2005 time period using historical simulations) for comparison purposes with denitrification in the next section. Denitrification has not been explicitly diagnosed in our model analysis. It is assumed that the distribution of nitrifying bacteria in the model is ubiquitous in the ocean interior, so wherever there is export of organic matter to depth the model computes nitrification, consuming NH_4^+ and producing NO_3^-. There is nitrification in all of the major oceanic basins, with hotspots in the western part of the oceanic basins and the Arabian Sea. Lowest values are found in the subtropical gyres and at high latitudes both in the Arctic and the Southern Ocean.

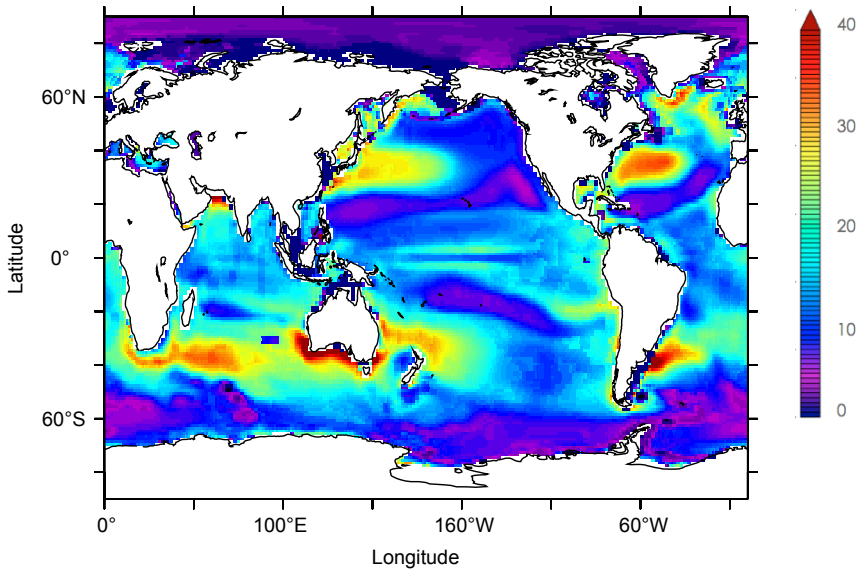

Figure 5: N_2O production via nitrification as a proxy of nitrification (in gN yr^{-1}) in PISCES averaged over the 1985 to 2005 time period using the historical simulation.

2.2.2.3. Denitrification

It is assumed in the model that denitrification operates in the water column and also in sediments. Denitrification is computed in the model where dissolved O_2 concentration falls below 6 µmol L^{-1}. Regions where water column denitrification occurs in PISCES are shown in Figure 6. Denitrification is found at ETP, Bay of Bengal and the Benguela Upwelling System. Minima are found in the subtropical gyres, Southern Ocean and Arctic regions.

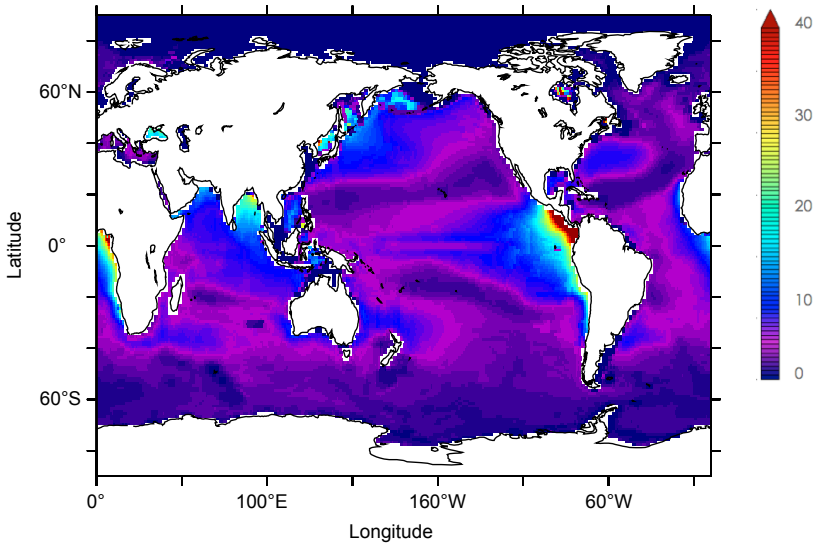

Figure 6: N_2O production via denitrification as a proxy of denitrfication occurrence (in gN yr^{-1}) in PISCES averaged over the 1985 to 2005 time period using the historical simulation.

2.2.2.4. External N input

PISCES uses the output of the INCA model (Hauglustaine et al., 2005) as an input for atmospheric nitrogen deposition fields. INCA simulates the transport and deposition of NO_x and organic nitrogen compounds, with a global atmospheric deposition of 40 TgN yr^{-1}. In PISCES, all the nitrogen from atmospheric deposition is assumed to be dissolved and it contributes directly to the nitrogen pool of nutrients. Large plumes in the vicinity of highly dense industrialised areas characterize the spatial distribution of the nitrogen deposition fields (Figure 7). North Atlantic, North Sea, western Pacific Ocean and Indian Ocean are regions where nitrogen deposition is more prominent. The distribution and magnitude of the nitrogen deposition is assumed to be constant in the model along the historical and future simulation periods.

PISCES uses the model output from the Global Erosion Model (GEM) by Ludwig et al. (1996) as an input of the riverine discharge into the ocean. This model output comprises 180 river basins with their respective supply of dissolved inorganic carbon (DIC), dissolved organic carbon (DOC), and particulate organic carbon (POC). Largest contributions correspond to the major river basins such as the Amazon river or the southeast asian continental margins (see Figure 8). Organic matter is assumed to be remineralised in estuaries and added to the nutrients pool directly with fixed stoichiometry. River discharge is assumed to be constant along historical and future simulated periods.

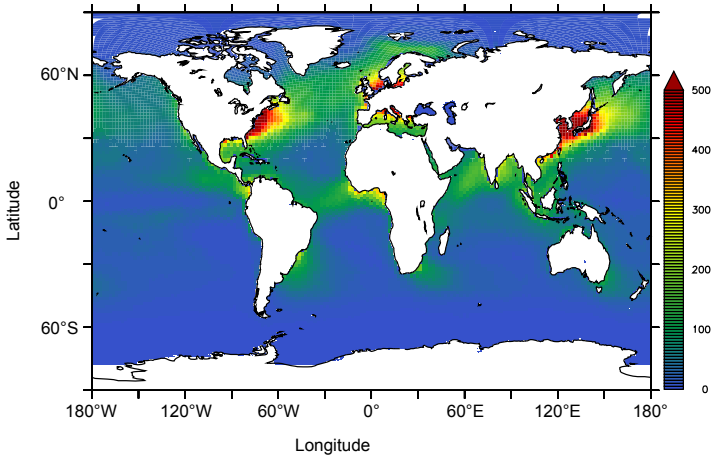

Figure 7: Atmospheric nitrogen deposition fields from INCA model (Hauglustaine et al., 2005] for the present scenario in 2000 (in mgN $m^{-2}yr^{-1}$) in World Ocean Atlas 2001 regular grid. Plumes of reactive nitrogen compounds such as NO_x and organic nitrogen extend eastward from dense industrialised areas in the western part of North Atlantic and North Pacific oceanic basins.

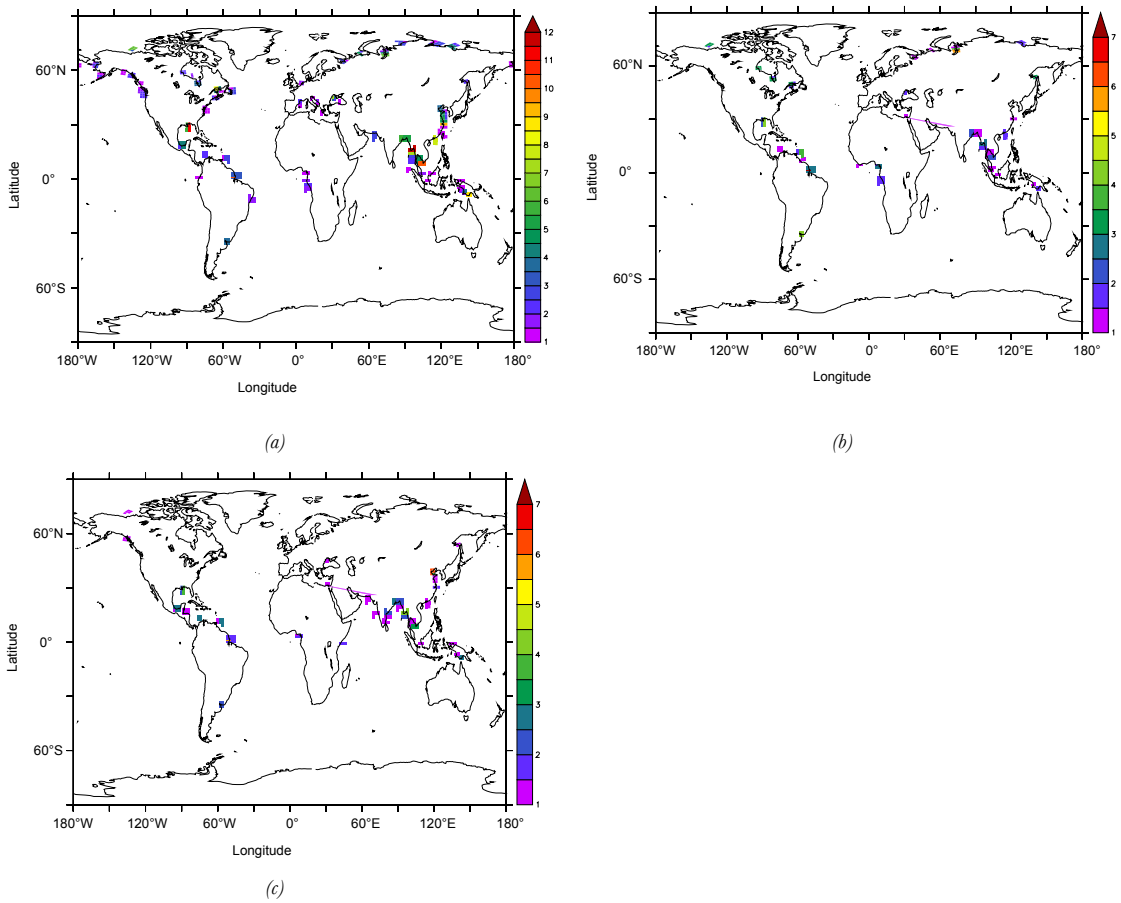

Figure 8: Location of river basins and discharge estimate from the Global Erosion Model (GEM) by Ludwig et al. (1996) in terms of (a) dissolved inorganic carbon (DIC, in TgC yr^{-1}), (b) dissolved organic carbon (DOC, in TgC yr^{-1}) and (c) particulate organic carbon (POC, in TgC yr^{-1}).

2.2.2.5. N_2O production

Nitrous oxide, from production, consumption and transport to air-sea gas exchange, is included into PISCES model. Two different parameterisations are embedded into the model. One parameterization (P.TEMP) is based on the parameterization proposed by Butler et al. (1989), where N_2O production is a linear function of O_2 consumption, plus an additional term sensitive to changes in temperature which reflect the effect of temperature on the bacteria metabolism. The parameterization in Eq. (3) is formulated as:

$$J^{P.TEMP}(N_2O) = (\gamma + \theta\, T\,)\, J(O_2)_{consumption} \tag{3}$$

where γ is a background yield (0.53 x 10^{-4} mol N_2O/mol O_2 consumed), θ is the temperature dependency of γ (4.6 x 10^{-6} mol N_2O (mol O_2)$^{-1}$ K^{-1}), T is temperature (K), and $J(O_2)_{consumption}$ is the sum of all biological O_2 consumption terms within the model.

The other parameterization (P.OMZ) is based on Jin and Gruber (2003). This parameterization shows a more mechanistic approach than the previous one, with two production pathways differentiated, one in high-O_2 conditions only due to nitrification and a low-O_2 production pathway merging the N_2O formation from nitrification and denitrification. In addition, an extra N_2O consumption term is considered, based on the growing evidences that within the 1 to 10 µmol L^{-1} concentration range of dissolved O_2, N_2O is consumed (Zamora et al., 2013). The P.OMZ parameterization is implemented as:

$$J^{P.OMZ.STEP}(N_2O) = (\alpha + \beta f(O_2))J(O_2)_{consumption} - k\, N_2O \tag{4}$$

where α is, as in Eq. (3) a background yield (0.9 · 10^{-4} mol N_2O/mol O_2 consumed), b is a yield parameter that scales the oxygen dependent function (6.2 · 10^{-4}), $f(O_2)$ is a unitless oxygen-dependent step-like modulating function, as suggested by laboratory experiments (Goreau et al., 1980). The oxygen modulating function $\beta f(O_2)$ is shown Figure 9. N_2O production is enhanced in low oxygenated regions. At complete anoxia there is no N_2O production (Bange et al., 2000). k is the 1st order rate constant of N_2O consumption close to anoxia (zero otherwise). For k we have adopted a value of 0.138 yr^{-1} following Bianchi et al. (2012) while we set the consumption regime for O_2 concentrations below 5 µmol L^{-1}. The model N_2O sea-to-air flux is shown in Figure 10. There are three major latitudinal bands of N_2O emissions, with no significant N_2O flux to the atmosphere in the subtropical gyres and high latitudes. The bands correspond to the N_2O production hotspots in the North Atlantic, Benguela Upwelling System, ETP and western basins of the Pacific and Indian oceans.

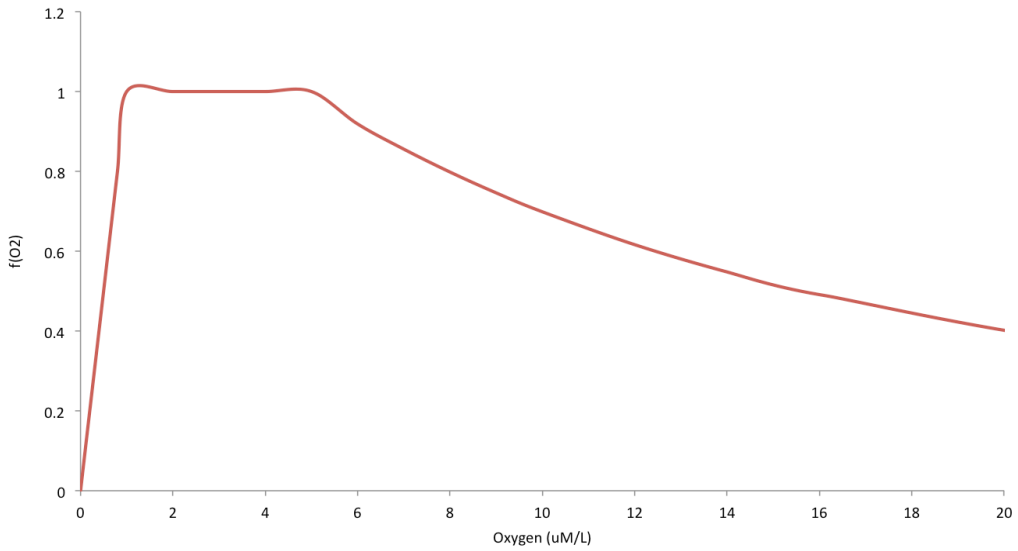

Figure 9: O_2 modulating function included into P.OMZ N_2O production parameterization, based on Goreau et al. (1980) experiments.

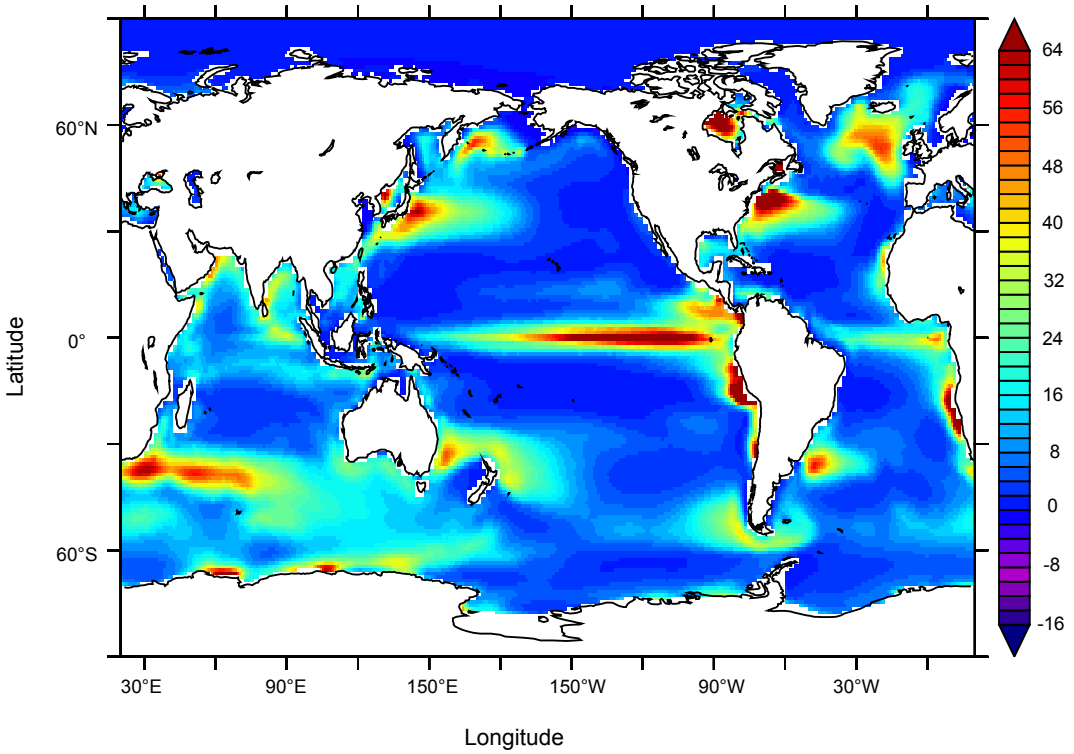

Figure 10: Sea-to-air N_2O flux (in mgN $m^{-2}yr^{-1}$) in P.OMZ parameterization averaged over the 1985 to 2005 time period in the historical simulation.

2.3. Datasets and data-based products

Historical PISCES model projections of N-cycle processes have been evaluated against the biogeochemical variables available in databases and data-based products as today. This includes O_2 from the World Ocean Atlas series, export of organic matter to depth (CEX) from Dunne et al. (2007), Eppley et al. (1989), Laws (2000) and Schlitzer et al. (2004), N_2O sea-to-air flux from Nevison et al. (2004), N_2O concentration from the MEMENTO database (Bange et al., 2009) and N_2-fixation rates from Luo et al. (2012). In all cases the existing data has been compared to the 1985 to 2005 time period from PISCES historical simulations, assuming that period as the best projected present scenario comparable to the observations.

2.3.1. World Ocean Atlas

Temperature, salinity and O_2 are used from the World Ocean Atlas data available from the 1998, 2001, 2005 and 2009 releases (Garcia et al., 2010a). Of particular interest in this study are the O_2 fields, which represent the boundaries at which nitrification and denitrification occur. Hypoxia (O_2 < 60 µmol L^{-1}) and suboxia (O_2 < 5 µmol L^{-1}) from the World Ocean Atlas 2009 (hereinafter WOA2009) are shown in Figure 11. Hypoxia is present in the three major oceanic basins. The largest hypoxic area is located in the Pacific and it expands from the ETP towards the northern hemispheric part of the basin. The hypoxic areas in the north Pacific are located around 600m deep. Hypoxia in the Indian ocean is concentrated in the Arabian Sea and the Bay of Bengal. These hypoxic areas are much shallower than those from the Pacific, around 100m deep. Two small areas of hypoxia appear in the Atlantic: the Benguela Upwelling System and the area off-coast of Senegal. Suboxia is exclusively found at the ETP and the Arabian Sea. The global volume of suboxia (0.3 x 10^6 km^3) is currently two orders of magnitude lower than that from hypoxia (77.3 x 10^6 km^3) (see Chapter 3).

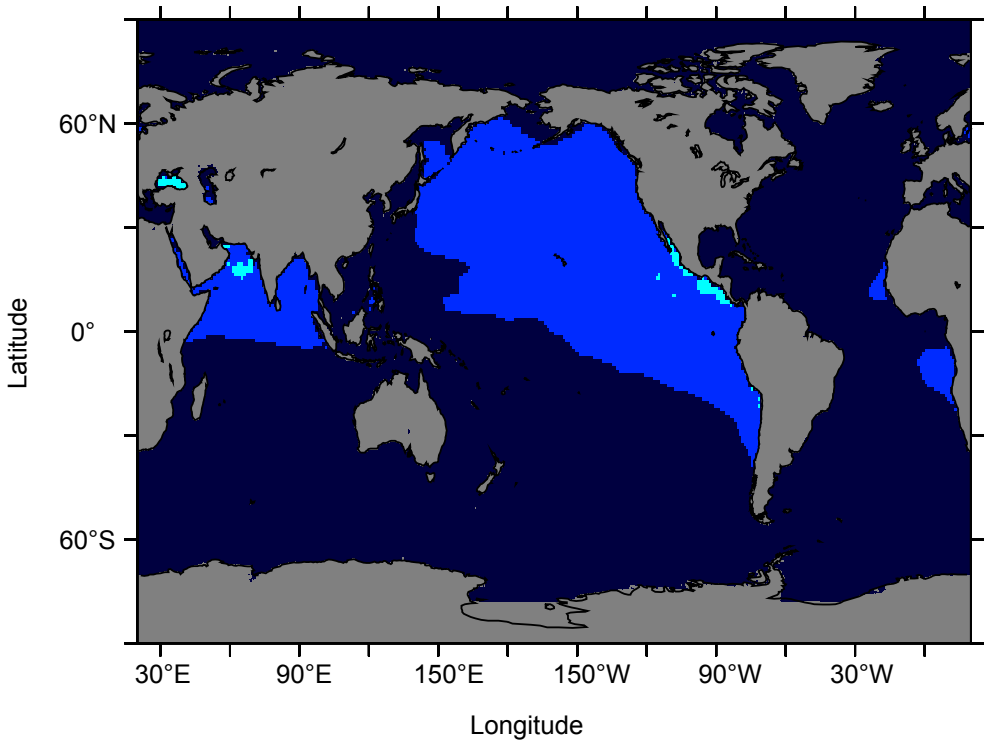

Figure 11: Occurrence in the water column of hypoxic (blue) and suboxic (light blue) regimes in WOA2009 (Garcia et al., 2010a).

2.3.2. O_2-corrected World Ocean Atlas

Considering the particular interest of this analysis in the enhanced production of N_2O in low oxygented waters, the most accurate description of the OMZs is required when looking at the N_2O production and consumption in the core of OMZs. The interpolation techniques used in the World Ocean Atlas 2005 have been revised by Bianchi et al. (2012), particularly in regions where the low O_2 regimes are found, i.e., hypoxia and suboxia. Bianchi et al. (2012) released a new data-based product (hereinafter WOA2005*) with larger hypoxic and suboxic volumes than the ones from World Ocean Atlas 2005. The extension of these O_2 regimes is shown in Figure 12a. There are no significant changes in the hypoxic extension if we compare them to the previously shown World Ocean Atlas 2009 results. However, there is a substantial change in the extension of the OMZ in the ETP. The histogram for low O_2 concentration levels below 60 µmol L^{-1} is shown in Figure 12b. The differences between WOA2005* (right, yellow) and the WOA2005 (left, dark green) are more pronounced as the dissolved O_2 concentration decreases. There is more than a two-fold increase for the suboxic regime lower than 5 µmol L^{-1}, from 0.6 x 10^6 km^3 in WOA2005 to 1.9 x 10^6 km^3 in WOA2005*.

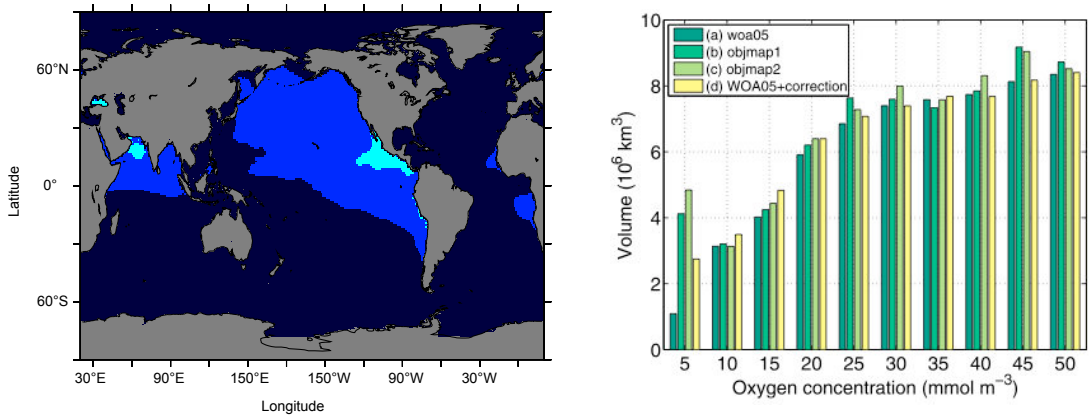

Figure 12: (a) Occurrence in the water column of hypoxic and suboxic regimes in WOA2005*. (b) Histogram of oxygen content (in 10^6 km^3) in WOA2005 (dark green) and WOA2005* (yellow) from Bianchi et al. (2012) over the low O_2 spectrum.

2.3.3. Export of Organic Matter

Four data-based products of export of organic matter are used: Eppley et al. (1989), Laws (2000), Schlitzer et al. (2004) and Dunne et al. (2007). Laws et al. (2000) derived a model based CEX product, using as model input ^{14}C observations translated into production estimates from several stations of the Joint Global Ocean Flux Study (JGOFS) programme. The observations covered the Pacific (HOT, equatorial and subarctic Pacific stations), Atlantic (BATS, Greenland polynya stations), Arabian Sea and Southern Ocean (Ross Sea station). The Laws et al. (2000) model used total production estimates, temperature and depth. Schlitzer et al. (2004) approach was based on a global inverse model, using datasets of nutrients and O_2. The model calculated the optimal CEX as the best fit between the model and the water column profiles based on the adjoint method. Dunne et al. (2007) developed a satellite-based CEX product. It used satellite data of temperature, chlorophyll and PAR from SeaWIFS and temperature from NCEP reanalysis to estimate primary production via a suite of algorithms from Behrenfeld and Falkowski (1997). Once the primary production was estimated, it was propagated through POC flux and export rates based on Dunne et al. (2005) and taking into the account the spatial variability by using the method for particle export stoichiometry proposed by Sarmiento et al. (2004).

Global estimated CEX in PgC yr^{-1} found for the references used are discussed in detail in Chapter 3. The distribution of CEX is shown in Figure 13 for each of the data-based products. In addition to coastal regions, all the data-based products spot regions of high CEX along the North Atlantic, North Pacific, Equatorial Pacific and western part of the major basins.

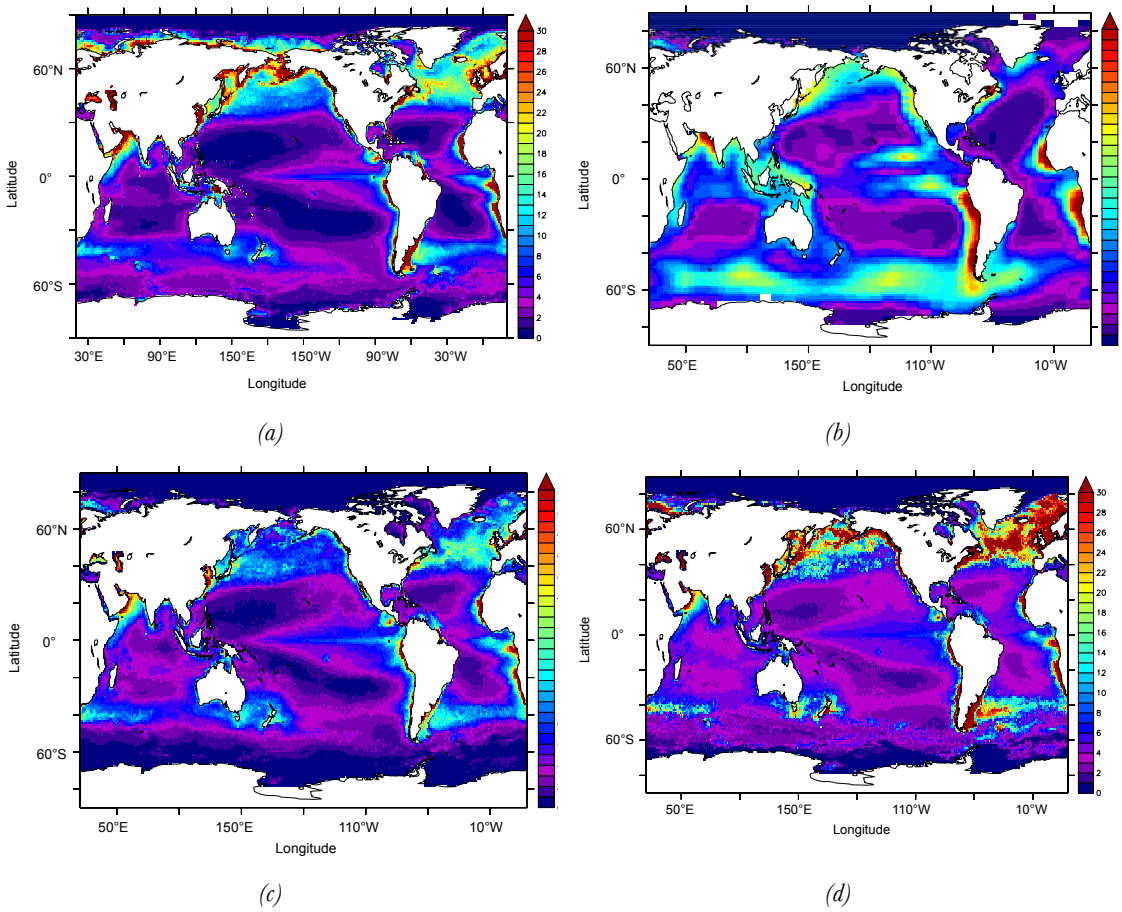

Figure 13: Export of organic matter to depth (CEX, in gC $m^{-2}d^{-1}$) at 100m in (a) Dunne et al. (2007), (b) Schlitzer et al. (2004), (c) Eppley et al. (1989) and (d) Laws (2000).

2.3.4. N_2O sea-to-air flux

Using more than 60,000 surface partial pressure N_2O measurements, Nevison et al. (2004) developed an interpolated data-based product of N_2O sea-to-air flux. The data-based product identified N_2O emission hotspots in the North Atlantic, North Pacific, Arabian Sea, ETP and the Southern Ocean, particularly in the vicinity of the Agulhas current (see Figure 14). The O_2 content in the Southern Ocean, where high levels of O_2 are present, has casted doubts on whether the Southern Ocean is such a prominent source of N_2O. Nevison et al. (2003) suggested that the bias introduced by summer-only N_2O measurements and the coincidence by chance between measurements and the model misrepresentation of N_2O production in that region could have introduced artifacts in the interpolated product.

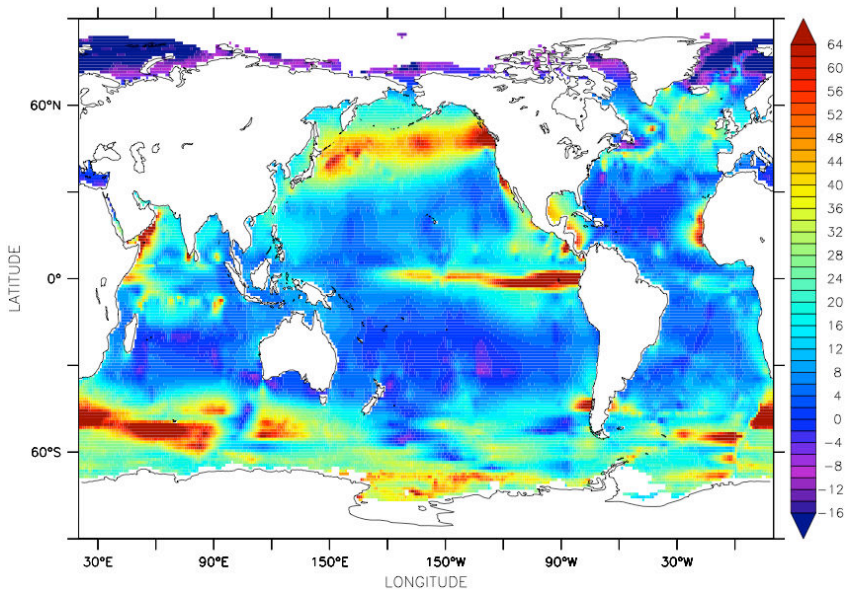

Figure 14: N_2O sea to air flux (in mgN $m^{-2}yr^{-1}$) from the interpolated data-based product of Nevison et al. (2004) using surface partial pressure N_2O measurements.

2.3.5. N_2O inventory

The largest compilation of N_2O concentration measurements from Bange et al. (2009) was used. The so-called MEMENTO database combines CH_4 and N_2O measurements. More than 120,000 surface and depth N_2O concentration samples are included along transects over the major oceanic basins (Figure 15). Despite the large number of measurements, depth profiles are only available in particular regions such as ETP, Arabian Sea and off the Senegal coast. The database also includes the in-situ dissolved O_2 concentration levels.

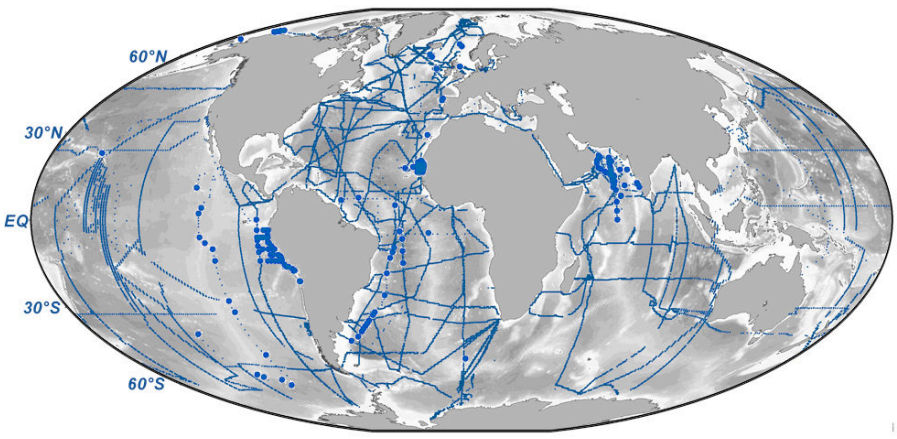

Figure 15: Available measurements of N_2O concentration comprising more than 100,000 measurements along transects (lines) and spots where depth profiles are available (blue dots) compiled in the MEMENTO database (Bange et al., 2009).

2.3.6. N_2-fixation rates

N_2-fixation rates and N_2-fixation biomass measurements have been gathered and presented by Luo et al. (2012). The compilation is part of the MAREDAT project on marine ecosystem databases, with more than 5,000 data points distributed in transects in the Atlantic, Pacific oceans and Mediterranean Sea (see Figure 16). Most of the data points are located at mid to low latitudes, where N_2-fixers are expected to be found. However, potential high latitudinal N_2-fixation has not been explored yet. The database comprises measurements of N_2-fixation biomass, N_2-fixation rates, diazotroph species responsible for N_2-fixation (*Trichodesmium*, *Unicellular Cyanobacteria -UCYN-* and *Heterocyst*) and in-situ chlorophyll, temperature, salinity, NO_3^-, PO_4 and Fe concentrations.

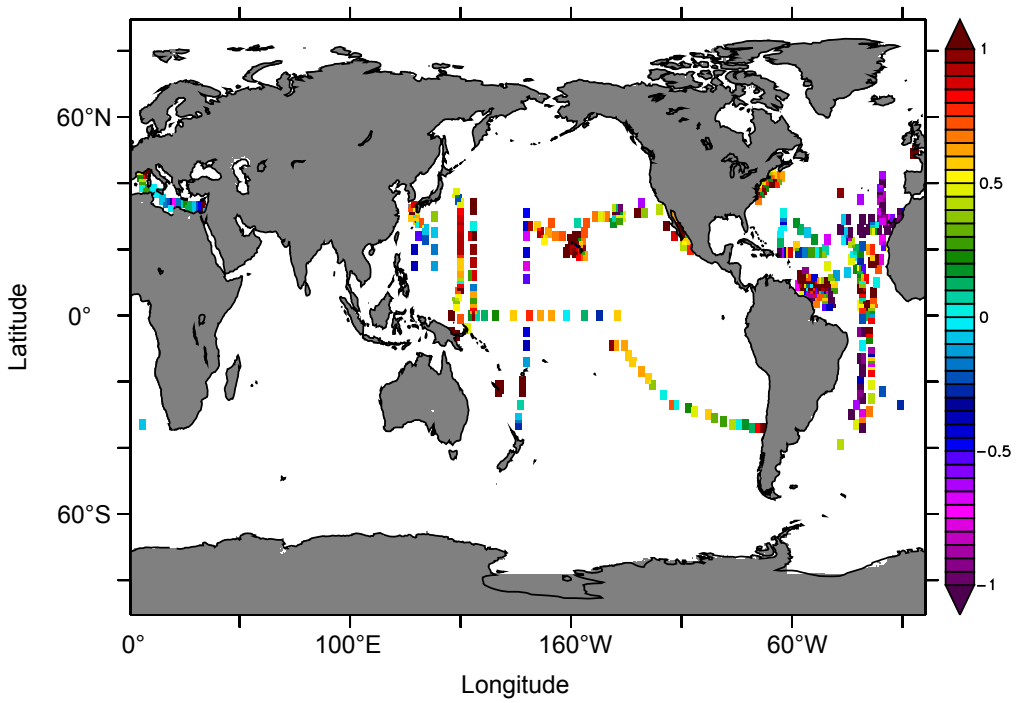

Figure 16: Mean depth-integrated N_2-fixation rates (in log(µmol N m^{-2} d^{-1})) contained in the MAREDAT database of N_2-fixation rates and N_2-fixers biomass from Luo et al. (2012).

2.4. Climate Models

2.4.1. IPSL-CM5

I use the Institut Pierre Simon Laplace (IPSL) Earth System Model (ESM) components to analyse future changes in the marine N-cycle. The IPSL-CM5 model uses PISCES (Aumont ant Bopp, 2006) as the ocean biogeochemical model in tandem with NEMO (Madec et al., 2008) as the ocean circulation model. Both models, in combination with the atmospheric module LMDZ (Hourdin et al., 2006) can be coupled to analyse present and future projections of ocean biogeochemistry and global climate feedbacks.

LMDZ model is run under different atmospheric GHG concentrations, following the Representative Concentration Pathways (RCP) IPCC standarized protocol (see Figure 17). The four scenarios (RCP2.6, RCP4.5, RCP6.0 and RCP8.5) represent four associated radiative potentials in W m^{-2} in 2100. This capability allows the IPSL-CM5 to participate in model evaluations of the same kind (ex., Coupled Model Intercomparison Project 5, CMIP5, Taylor et al., 2012) and scientific assesments (ex., Intergovernmental Panel for Climate Change, IPCC reports 2007 and 2013) on global climate projections. From the lowest to highest CO_2 emissions scenarios, NEMO responds to these forcings in terms of wind stress, radiation or temperature, and therefore with consequent changes on the ocean circulation fields. PISCES ultimately experiences these changes from the physical to the chemical perspective with a direct impact on global biogeochemical cycles.

PISCES and NEMO can be run completely decoupled from the atmospheric component. Moreover, PISCES and NEMO can be coupled in an offline fashion, where the forcing dynamic fields from NEMO online experiments (i.e., fully coupled with LMDZ) are applied as monthly or yearly averages to PISCES. All the experiments I have done in this work presented here have been offline simulations with the physical forcings derived from the coupled NEMO-LMDZ set up. A more refined temporal analysis would help us to introduce, for instance, the O_2 intra-annual variability, which is not present in this study. Nevertheless, the long-term global estimations that I try to solve within the focus of this work gives confidence on the methodology and results. Despite the disadvantages of such approach in terms of missing the variability, offline experiments are one of the great advantages in global biogeochemical model analysis, reducing enormously the computational time cost and allowing a greater number of resources to explore decadal to centennial interactions in ocean biogeochemistry.

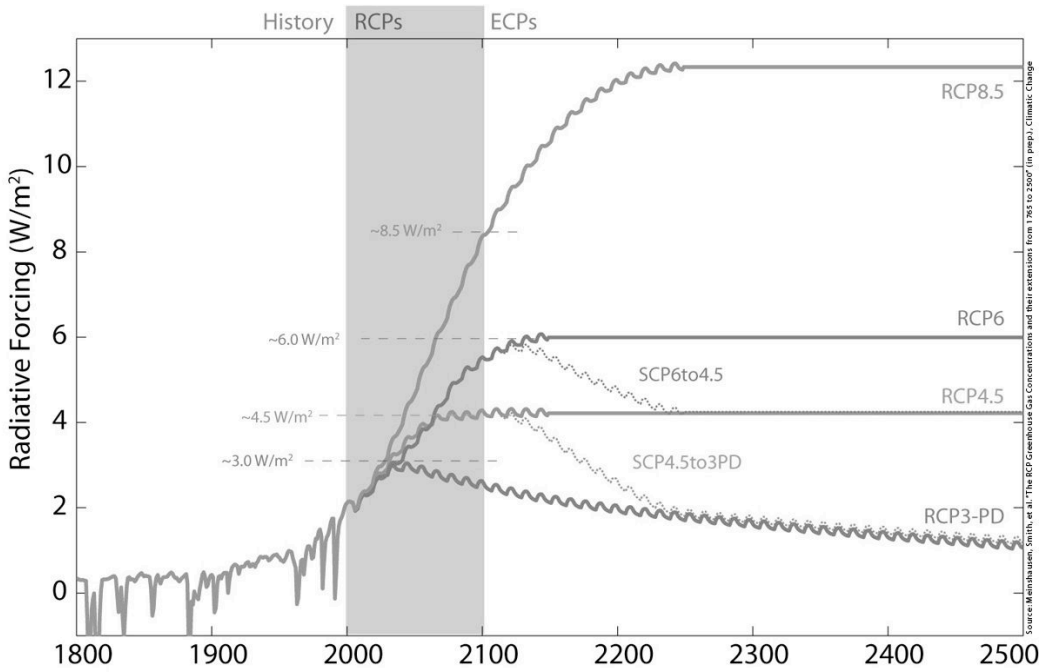

Figure 17: Representative Concentration Pathway (RCP) scenarios used as a standard protocol in the future model projections on the IPCC assessments. RCP8.5 represents the business-as-usual high CO_2 emissions scenario (IPCC, 2013).

2.4.2. CMIP5 models

Models included into the Coupled Model Intercomparison Project 5 (CMIP5, Taylor et al., 2012) are used in the model evaluation and model projections and help to frame the envelope of uncertainties when using ocean biogeochemical models to estimate oceanic N_2O and N_2-fixation (see Chapter 3). This set of models share the same scope in terms of future RCP scenarios and standarised model output variables, both for the physical and biogeochemical diagnosis, but they have different ocean circulation and ocean biogeochemical components. CMIP5 distinctive biogeochemical features have been summarized in Table 1. Models have a wide range of complexity, from basic NPDZs to more complex biogeochemical modules with dynamical stoichiometry, various PFTs or full Fe-cycle representation. IPSL-ESM is among those who have a broad representation of N-cycle processes and most of the external nitrogen input processes too. Only half of the CMIP5 models have such number of external N-input mechanisms, more than 1 phytoplankton group, nitrification or NH_4^+ among their nutrients. None of the CMIP5 models have included variable stoichiometry into the C/N ratio and other processes such as anammox are also not included. Despite the different level of degree in their complexity, intercomparison projects such as CMIP5 allow us to identify the sensitivity to additional or to the total absence of many of these components on N-cycle processes.

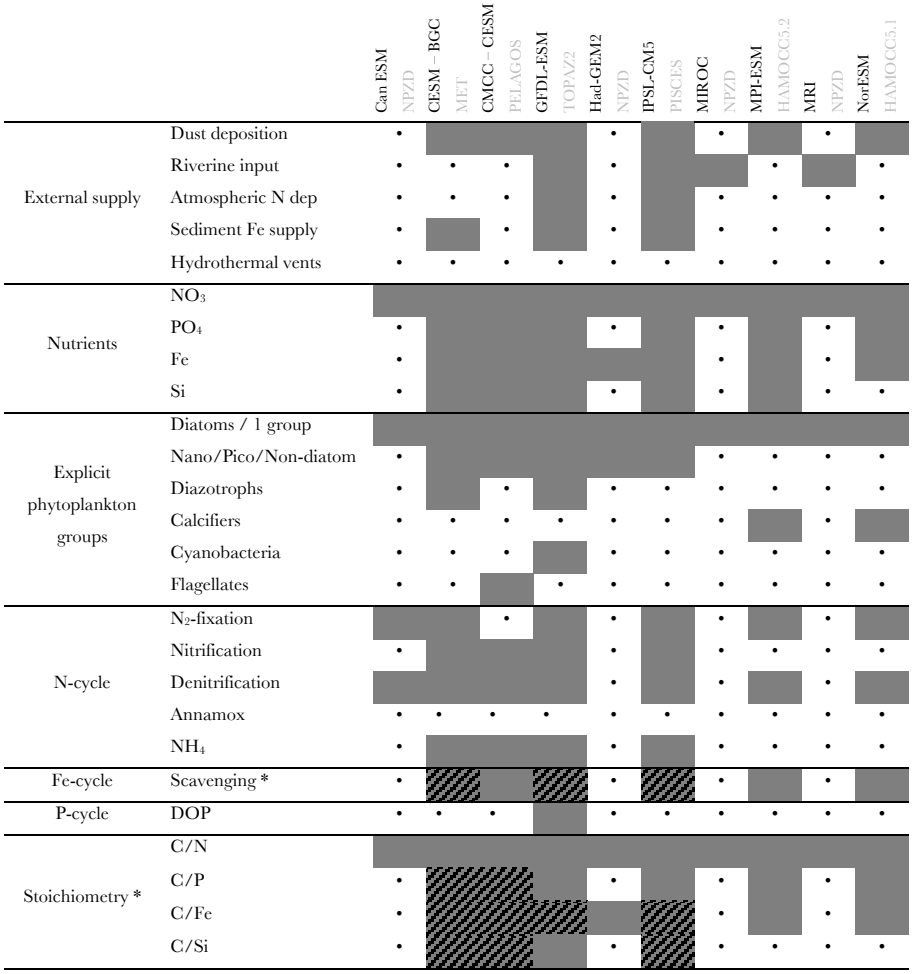

Table 1: Biogeochemical features of the CMIP5 model suite. Availability is denoted in grey, absence is marked by dots. The information has been summarised from Zahariev et al. (2008) (CanESM), Moore et al. (2004) (CESM-BGC), Vichi et al. (2007) (CMCC-CESM), Dunne et al. (2013) (GFDL-ESM), Palmer and Totterdell (2000) (Had-GEM2), Aumont and Bopp (2006) (IPSL-CM5), Watanabe et al. (2011) (MIROC), Maier-Reimer and Kriest (2005) (MPI-ESM), Yukimoto et al. (2011) (MRI) and Assman et al. (2010) (NorESM1). (Vogt et al., in prep).

2.5. Simulation Plan

2.5.1. Oceanic N_2O emissions in the 21st century

Future model projections of oceanic N_2O emissions are based on three experiments (see Table 2). The oceanic N_2O is stabilised in the ocean interior in a spin-up run (SPIN), where the total flux and the different production terms are equilibrated (see Chapter 4 for details). An historical simulation (HIST) is done for the present scenario, setting up the initial conditions and evaluating the model in terms of N_2O sea-to-air flux. The simulation RCP8.5 applies the future forcing scenario until year 2100.

Name	Description	Period	Years	Target
SPIN	Standard PISCES v3.2 with N_2O as a new tracer	Pre-industrial	50	Spin up for equilibrated N_2O sea-to-air flux.
HIST	PISCES with N_2O along the historical period	Historical 1851 to 2005	154	Achieve a realistic starting point for the future estimations of N_2O. 3.6 Tg N/yr for each parameterisation.
RCP8.5	PISCES with N_2O along the 21st century	Future 2006 to 2100	95	Estimate the future oceanic emissions of N_2O.

Table 2: Name, description, forcing period, duration and comments on the experiments for estimating the global oceanic N_2O emissions in 2100. During the spin-up, the N_2O sea-to-air flux is stabilised around the reference value of 4 TgN yr^{-1} from Nevison et al., 2003. Historical and future RCP8.5 simulations allows us to estimate present and future N_2O emissions.

2.5.2. Ocean Acidification effect on the marine N-cycle

Ocean acidification and climate change effects on N_2-fixation and nitrification are analysed in a series of simulations (see Table 3). The control (CTL) simulation sets the default scenario and identifies model drifts for further future corrections. N_2-fixation is analysed separately with high levels of atmospheric CO_2 (N2.CTL.OA) and in combination with Climate Change (N2.RCP.OA). The same approach is used for nitrification only, with NIT.CTL.OA and NIT.RCP.OA respectively. Both processes are analysed being CO_2 sensitive simultaneously in a last set of experiements only under ocean acidification (BOTH.CTL.OA) and in tandem with climate change (BOTH.RCP.OA).

Name	Description	Period	Years	Target
CTL	Control simulation without CO_2 effect on nitrification or N_2-fix	Pre-Industrial 1851 to 2100	250	Reference simulation for model drifts and analysis of ocean acidification
N2.CTL.OA	Ocean acidification on N_2-fix only.	Pre-Industrial 1851 to 2100	250	Effect of high CO_2 levels on N_2-fixation
N2.RCP.OA	Climate change + Ocean acidification on N_2-fix only	Historical + Future 1851 to 2100	250	Effec of high CO_2 levels and global warming on N_2-fix
NIT.CTL.OA	Ocean acidification on Nitrification only.	Pre-Industrial 1851 to 2100	250	Effect of high CO_2 levels on Nitrification
NIT.RCP.OA	Climate change + Ocean acidification on Nitrification	Historical + Future 1851 to 2100	250	Effec of high CO_2 levels and global warming on Nitrification
BOTH.CTL.OA	Ocean acidification on N_2-fix and Nitrification	Pre-Industrial 1851 to 2100	250	Effect of high CO_2 levels on N_2-fix and Nitrification
BOTH.RCP.OA	Climate change + Ocean acidification on N_2-fix and Nitrification	Historical + Future 1851 to 2100	250	Effec of high CO_2 levels and global warming on N_2-fix and Nitrification

Table 3: Name, description, forcing period, duration and comments on the experiments for analysing the effect of increasing levels of CO_2 on N_2-fixation in combination with nitrification. Dedicated analysis on each individual processes are done, together with the effect of climate change on top of ocean acidification.

Chapter 3

N-cycle in CMIP5 models

3.1. Introduction

Climate models for climate projections (e.g., for CMIP5 and the last IPCC assessment report) include a representation of the land and oceanic carbon cycle, as they address the questions of climate-carbon feedbacks. To do so, an explicit representation of the terrestrial and marine primary productivities is essential.

On the terrestrial side, primary productivity is mostly modelled as limited by atmospheric CO_2, temperature and water availability. Only two models (CESM and NorESM) do include nutrient limitation of plant growth by the availability in soils. On the ocean side, nutrient limitation has been used in very early ocean biogeochemical models (see Chapter 2). In CMIP5 all models include a limitation on the phytoplankton growth, as seen in Chapter 2. For instance, Figure 1 shows the surface NO_3 concentration in CMIP5 models compared to the climatology from Garcia et al. 2010b. The representation of NO_3 requires at least a minimal description of N-cycle processes. As discussed in Chapter 2, the representation of the

N-cycle in CMIP5 models is very diverse. A complete assessment of the individual representation of the N-cycle in the CMIP5 mode suite is out of the scope of this work. However, I focus in this section on two particular N-cycle processes which are relevant for the analysis, namely N_2O production and N_2-fixation. N_2O is not part of the CMIP5 model standard output. I explore how the CMIP5 models can be used to estimate N_2O production and N_2O inventories. On the contrary, N_2-fixation is included into CMIP5 models.

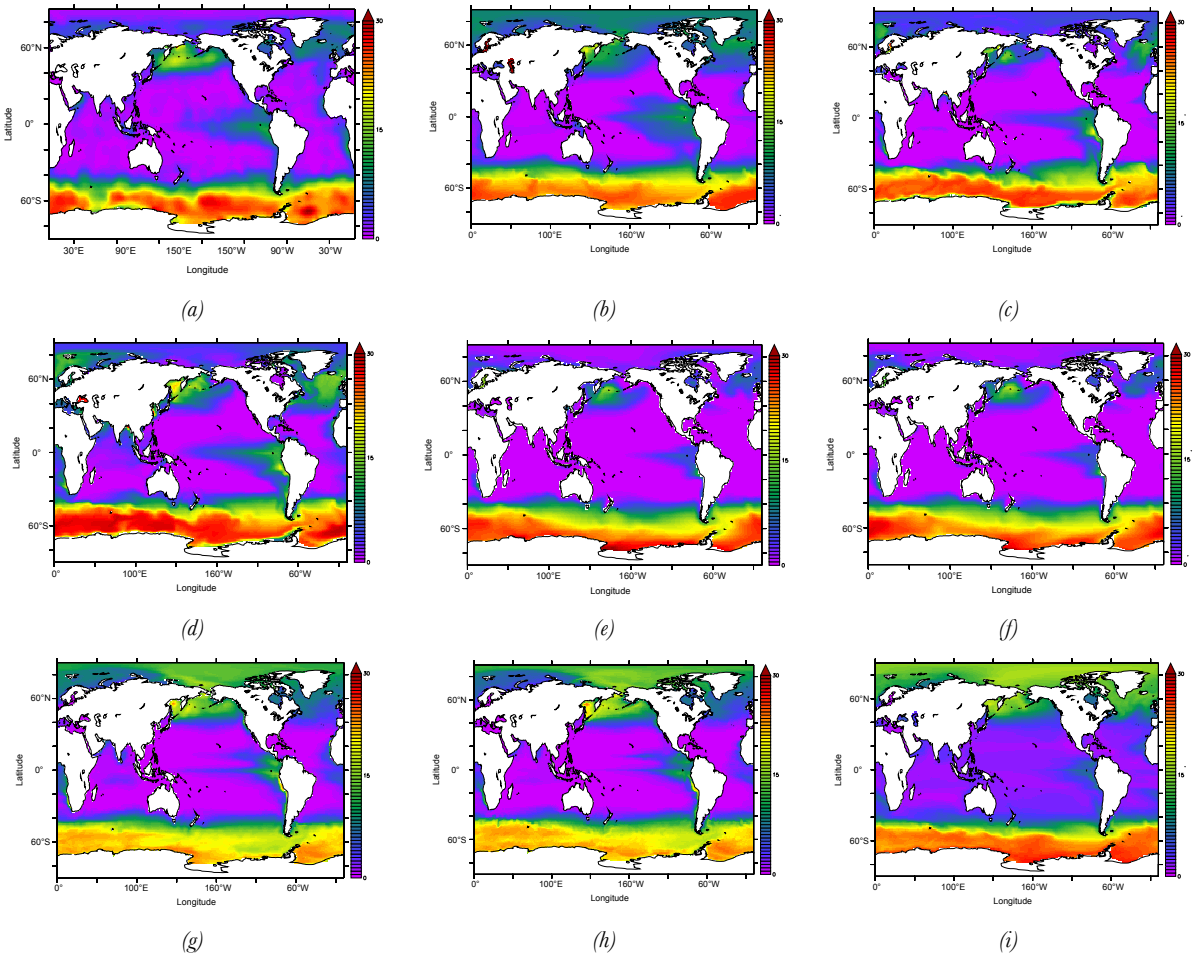

Figure 1: NO_3 distribution averaged in the upper 1000m (in mmol m^{-3}) in (a) WOA2009 (Garcia et al., 2010b), (b) CESM, (c) GFDL-2G, (d) GFDL-2M, (e) IPSL-CM5-LR, (f) IPSL-CM5-MR, (h) MPI-LR, (i) MPI-MR and (k) NorESM averaged in the 1995 to 2005 time period using the historical simulation.

The amplitude of marine N_2O production rates and N_2O inventory estimates as a result of the inherent uncertainties in ocean biogeochemcial models using the available parameterizations as today challenges the ability to calculate the oceanic contribution of N_2O to the global greenhouse gas budget. The same methodological perspective applies to model estimations of global N_2-fixation rates and N_2-fixation spatial distribution.

When studying marine N_2O, it must be considered the fact that there are many uncertainties on the processes which govern N_2O formation in the ocean interior (Zehr and Ward, 2002; Gruber and Galloway, 2008). The precise conditions under which nitrification and denitrification occur are still not fully understood. Recent studies (Yool et al., 2007; Zamora et al., 2013) have questioned assumptions such as N_2O production only in the aphotic zone (Horrigan et al., 1981), the boundaries of occurrence of denitrifcation below O_2 concentrations of 4 μmol L^{-1} (Nevison et al., 2003), exponential increase of N_2O production at low O_2 levels (Goreau et al., 1980) or N_2O consumption only close to anoxia (O_2 < 1 μmol L^{-1}) (Suntharalingam and Sarmiento, 2000; Jin and Gruber, 2003). Moreover, the relative contribution of nitrification and denitrification to the global N_2O budget is still unclear. Model studies have suggested that nitrification and denitrification contributions are about 75%/25% respectively (Suntharalingam et al., 2000; Jin and Gruber, 2003), but recent analysis of N_2O observations on a global scale increase the contribution of nitrification up to 93% of the total N_2O production (Freing et al., 2012).

Field observations of N_2O go back to the '70s and out-number laboratory experiments as information sources (Goreau et al., 1980; Frame and Casciotti, 2010). The first cruises in the 1970s (Yoshinari, 1973; Cohen et al., 1977; Elkins et al., 1978) linked the N_2O inventory to O_2 consumption in the water column in terms of the apparent O_2 utilization (AOU). First parameterisations based on N_2O measurements proposed a simple linear relationship between ΔN_2O and AOU (Elkins et al., 1978; Butler et al., 1989; Naqvi and Noronha, 1991; Law and Owens, 1990; Hahn, 1981; Oudot et al., 1990; Cohen and Gordon, 1989), where ΔN_2O is defined following Yoshinari (1973). The observed discrepancies between N_2O and the O_2 profiles, particularly the pronounced decrease in N_2O concentration at depth, lead to embodying new variables into the former N_2O parameterizations such as depth or temperature (Butler et al., 1989) to explain such differences. Complexity in N_2O parameterisations increased when N_2O was measured at the core of the OMZs at the Eastern Tropical Pacific (ETP) or Benguela Upwelling System (BUS). The split of N_2O production into nitrification and denitrification explicit terms was first suggested by Suntharalingam et al. (2000), although with a general description of the N_2O production into high-O_2 production pathway, associated only with nitrification, and low-O_2, which included both nitrification and denitrification. Jin and Gruber (2003) followed the same approach with a more detailed representation of the N_2O formation processes at the OMZs. The N_2O parameterization by Jin and Gruber (2003) included N_2O consumption below 5 μmol L^{-1} as well as a wider range of low-O_2 regimes where nitrification operates in tandem with denitrification. The step-function like dependence under low-O_2 regimes use in Jin and Gruber (2003) was based on the experimental work by Frame and Casciotti (2010). Nevison et al. (2003) adopted a broader perspective including the export of particulate organic carbon (POC) and its remineralization,

hence focusing on the drivers of the subsequent O_2 profiles and N_2O production from nitrification. A more recent study by Freing et al. (2012), the role of water mass transport was highlighted, reflecting the last time water masses were in contact with the atmosphere. Despite the increased sophistication of the N_2O parameterizations, they remain tied to its foundational assumption: the observed O_2 consumption, or altenatively to the biogeochemical driver of the O_2 profiles, i.e., the export of organic matter to depth. Microbiological experiments provided N_2O production rates per mol of ammonium (NH_4^+) oxidized, respectively mole of nitrate reduced nitrate (NO_3^-) (Mantoura et al., 1993; Bange et al., 2000; Elkins et al., 1978; Yoshida et al., 1989; Punshon and Moore, 2004; De Wilde and De Bie, 2000).

Diazotrophs distribution and the environmental controls that favour N_2-fixation occurrence suffer from the same level of uncertainties as N_2O formation in the ocean interior. The lack of measurements in a large part of the major oceanic basins together with the on-going analysis on the phytoplankton groups which are able to fix inorganic N_2 and its relative contribution to the global N_2-fixation budget leads to significant uncertainties. However, there have been many attempts on parameterizing N_2-fixation in models, particularly in regional studies. The most recent N_2-fixation parameterizations in regional models are summarized in Table 1. In general, the basic assumption is the combination of limiting terms based on previous studies on incoming radiation, temperature, PO_4 and Fe concentrations or optimum C:N cell ratios.

Study	Parameterization
Hood et al., 2001	$\mu = \mu_c^{max} \cdot \left(1 - exp\left(\frac{I}{I_Z}\right)\right)\ exp\left(-\frac{I}{I_{\beta T}}\right)$
Fennel et al., 2002	$\mu = \cdot \frac{\alpha I_{PAR}}{(\mu_c^{max} + \alpha^2 I_{PAR}^2)^{1/2}} \cdot \frac{DIP}{K + DIP} \cdot \frac{1}{3}\left[\frac{1}{6}\right]\ tanh(2(T - T_{crit}) + 1) + \frac{1}{3}\left[\frac{1}{6}\right], \quad \tau \leq \tau_{crit}$
Lenes et al., 2008	$\mu = \mu_c^{max} \cdot min\left\{\frac{I_z}{I_{SAT} - exp\left(1 - \frac{I_z}{I_{SAT}}\right)}, \frac{PO_4}{K + PO_4} + \frac{DOP}{K + DOP}, \frac{[Fe]}{K + [Fe]}\right\}$
Sonntag et al., 2011	$\mu = \mu_c^{max} \cdot \frac{\alpha I_{PAR}}{(\mu_c^{max} + \alpha^2 I_{PAR}^2)^{1/2}} \cdot\ exp\left(-\frac{(T - T_{opt})^4}{T_1 - T_2 sgn(T - T_{opt})^4}\right)$
Ye et al., 2012	$\mu = \mu_c^{max} \cdot f(T^4) \cdot min\left\{tanh\left(\frac{\alpha I_{PAR}}{\mu_c^{max}}\right), \frac{Q_{Fe} - Q_{Fe\_min}}{Q_{Fe}}, \frac{Q_P - Q_{P\_min}}{Q_P}\right\}$

Table 1: N_2-fixation parameterizations in regional models as a combination of environmental terms such as temperature, incoming radiation, PO_4 and Fe concentration or C:N cell ratios from Hood et al. (2001), Fennel et al. (2002), Lenes et al. (2008), Sonntag et al., (2011) and Ye et al. (2012).

This complexity has been transferred in part to global ocean models from the CMIP5 suite, as they seem to be in the initial stages of including N_2-fixation, at least at a comparable degree as other C-cycle processes or the regional models described above. This will be discussed in detail in section 3.2.4.

While N_2-fixation rates can be obtained from the model runs in the CMIP5 model repositories, N_2O sea-to-air emissions could only be obtained by doing transient simulations but they have not been included into the standard CMIP5 output. Thus I focus on N_2O production rates and N_2O inventories that can be computed offline based on CEX and O_2 fields from CMIP5 models. I quantify in this section the uncertainties related to the estimation of N_2O production rates and N_2O inventory using the state-of-the-art ocean biogeochemical models and the climatology data-based products available as today. I compare the estimated N_2O inventory from models and data-based products to MEMENTO, the largest available N_2O database. Moreover, we analyze the representation of N_2-fixation rates and N_2-fixation biomass in the CMIP5 mode suite. I compare the global N_2-fixation rate budget to the estimate of Luo et al. (2012) and to other global model estimates. Based on the common assumption of combining limiting terms to build the N_2-fixation parameterizations, I analyze the effect of temperature on N_2-fixation rates as the precursor of climate change effects looming ahead.

3.2. Methodology

3.2.1. CMIP5 models

The set of Earth System Models (ESM) who participated in the CMIP5 project share the same scope in terms of simulated time periods and applied forcings, with a standarized model output of relevant physical and biogeochemical variables. In this study I have analysed the output of 8 models available in the CMIP5 repositories, namely GFDL-ESM2G, GFDL-ESM2M, Hadley-GEM2, IPSL-CM5-LR, IPSL-CM5-MR, MPI-ESM-LR, MPI-ESM-MR and Nor-ESM2. Detailed model performance and model intercomparisons in terms of biogeochemical variables such as primary production, CEX and O_2 can be found in recent analysis from Bopp et al. (2013), and Steinacher et al. (2010), as well as Cocco et al. (2012) for the previous model generation.

As today, N_2O is not included in the standard output of the CMIP5 model suite (Taylor et al., 2012). To evaluate modeled N_2O production rates and inventories for present-day conditions, the ten year average over the 1995 to 2005 time period was computed for historical simulations as defined by the IPCC AR5 protocol. I use the variables on which N_2O

parameterizations are based, i.e., temperature, salinity, dissolved O_2 and export of organic carbon at 100 meters. Temperature and salinity are used for estimating oxygen saturation (O_{sat}), and AOU (Eq. (1)) in combination with O_2 in the form:

$$AOU = O_2 - O_{sat} \quad (1)$$

where O_{sat} is calculated using Weiss and Price (1980) formulas based on temperature and salinity.

On the contrary, N_2-fixation rates and N_2-fixation biomass are included into the standard output of CMIP5 models. The output of the historical simulation runs for each of the individual CMIP5 models are used, averaging the 1995 to 2005 time period as the best estimate at present.

3.2.2. Data-based products and datasets

As a reference, data-based products of temperature, salinity and O_2 were also used in this study. In order to estimate the uncertainties linked to CEX, estimates from Laws et al. (2000), Eppley et al. (1989), Schlitzer et al. (2000) and Dunne et al. (2007) were used (see Chapter 2). For all the other variables (i.e., temperature, salinity and O_2), I use the World Ocean Atlas 1998, 2005 and 2009 (Levitus et al., 2010), as well as the O_2-corrected World Ocean Atlas 2005 (hereinafter WOA2005*) from Bianchi et al. (2012). For consistency, all the data-based products as well as the model output were regridded into a regular 1° x 1° grid with 33 vertical levels, i.e., that from the World Ocean Atlas 2001 (Garcia and Gordon, 2001). The same formulas from Weiss and Price (1980), were used to estimate O_{sat} and subsequently AOU from the data-based products.

The N_2O inventories obtained from the CMIP5 models and data-based products are compared to the MEMENTO database (Bange et al., 2009), comprising observations of in-situ O_2 and N_2O concentration from more than a hundred cruises. The observations span 30 years, from 1970 to 2010. I have calculated the mean of this period and compared it to the 1995 to 2005 time period in CMIP5 models and data-based products.

N_2-fixation rates and N_2-fixation biomass from Luo et al. (2012) are used as a reference, as well as the global estimate of N_2-fixation rates per oceanic basin and the total rate from the same study.

3.2.3. N_2O Parameterizations

I estimate the N_2O production rates and N_2O inventory at steady-state (e.g., Nevison et al., 2003; Bianchi et al., 2012) from the semi-empirical formulas proposed by Nevison et al. (2003) and Butler et al. (1989).

3.2.3.1. N_2O Production rates

N_2O production rates in Nevison et al. (2003) are derived from Eq. (2) using the remineralisation rate of particulate organic carbon (POC) in the water column, modulated by the O_2 concentration as:

$$J(N_2O) = R_{N:C} \cdot \left[\frac{a_1}{O_2} + a_2\right] \cdot \frac{\partial \phi^{POC}}{\partial z} \quad (2)$$

where $R_{N:C}$ = 16:106, a_1 = 0.26 mol N_2O/mol N x mmol O_2 m^{-3} and a_2 = $-6 \cdot 10^{-4}$ mol N_2O/mol N. N_2O production is only considered for dissolved O_2 concentrations above 4 µmol L^{-1} below which N_2O consumption occurs (Nevison et al., 2003). The relative contribution of N_2O production to the total N_2O budget in higher oxygenated waters was suggested to amount to around 93% leaving only a minor contribution to low O_2 environments (Freing et al., 2012). Moreover, N_2O consumption estimates in the interior of the OMZs could be underestimated and might counterbalance the N_2O production in such regions (Zamora et al., 2012). N_2O production is assumed to be inhibited by light (Horrigan et al., 1981) and is assumed zero over the top first 100 m. The with-depth evolution of export fluxes of POC in the water column is required to estimate the N_2O production from Eq. (2) POC fluxes were reconstructed following Bianchi et al. (2012). This approach assumes that the decline with depth of POC fluxes follows a power law below 100 m (Martin et al., 1987), but imposes exponents of 0.80 and 0.36 for high, respectively and low-O_2 environments. I used 0.85 and 0.35 respectively. Following this approach allowed to compare N_2O production rate estimates across the water column for a variety of model output and CEX compilations. In order to test the robustness of this reconstruction methodology, I calculated the correlation coefficient between the original, three-dimensional CEX field and the reconstructed one for POC fluxes after Dunne et al. (2007). For this purpose I used two and three-dimensional CEX combined with O_2 from WOA2005*. I obtained a correlation coefficient of r^2 = 0.96, with an overestimation of 13% in total N_2O production (Figure 2a) I further evaluated this approach be comparing two and three-dimensional CEX fields from PISCES ocean biogeochemical model, i.e., the biogeochemical module of the CMIP5 IPSL-CM5 model. The correlation between the reconstructed export from the two-dimensional output and the original three-

dimensional model output is $r^2 = 0.91$ with an underestimation of 22% in the N_2O production rate on a global scale compared to the original three dimensional CEX (Figure 2b).

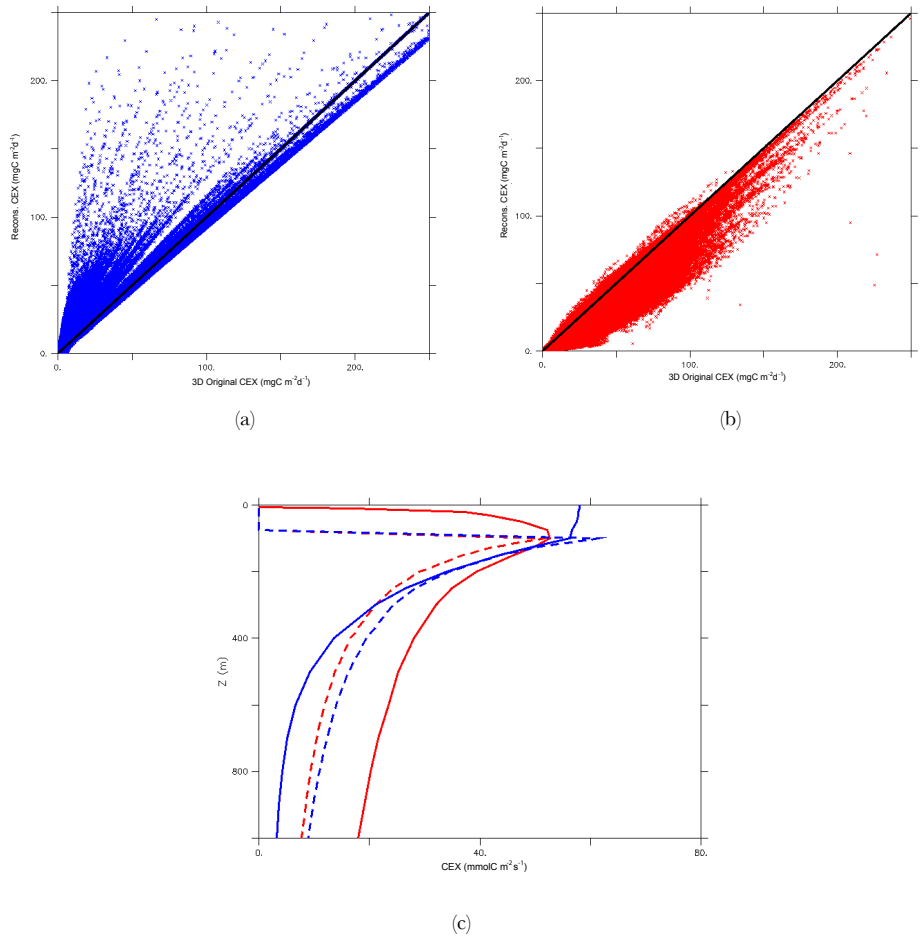

Figure 2: Scatter plots for (a) original 3D CEX vs Reconstructed CEX from 2D CEX at 100m from Dunne et al. (2007) and (b) original 3D CEX vs Reconstructed CEX from 2D at 100m from PISCES. The black line is the 1:1 line. (c) Global average depth profiles of PISCES (red) original 3D export, reconstructed 3D export (dashed red) and Dunne et al. (2007) original 3D export (blue) and reconstructed 3D export (dashed blue) with oxygen from WOA2005*.

3.2.3.2. N_2O Inventory

The N_2O inventory is estimated after parameterizations by Nevison et al. (2003) and Butler et al. (1989). I calculate in both parameterizations the excess of N_2O (ΔN_2O in equation (3)), defined by Yoshinari et al. (1976), as the difference between the actual N_2O concentration and the N_2O in equilibrium with the atmospheric N_2O concentration (N_2O_{sat}) in the form:

$$\Delta N_2O = [N_2O]_{obs} - [N_2O]_{sat} \quad (3)$$

where N_2O_{sat} was calculated according to Weiss and Price (1980) using temperature and salinity. A value of 300 ppbv for the atmospheric N_2O concentration is selected in the

calculation of N_2O_{sat} (Nevison et al., 2003). N_2O inventory results are shown in actual N_2O concentration, or N_2O_{obs} in Eq. (3). Following Butler et al. (1989) (hereinafter Butler), ΔN_2O is given by :

$$\Delta N_2O = \alpha \cdot AOU + \beta \cdot T \cdot AOU \tag{4}$$

where α is 0.125 x 10^{-4} mol N_2O / mol O_2 and β is 0.0093 x 10^{-3} mol N_2O / mol O_2 K. Estimates of ΔN_2O after Nevison et al. (2003) (hereinafter Nevison) were obtained following Eq. (5) :

$$\Delta N_2O = R_{N:O_2} \left[\frac{\mu}{O_2} + \kappa\right] \cdot e^{-\frac{z}{z_e}} \tag{5}$$

where μ = 0.31, k = -4 · 10^{-4}, z_e = 3000m and $R_{N:O2}$ = 16:170. ΔN_2O is restricted after Nevison et al. (2003) to dissolved O_2 concentrations above 4 µmol L^{-1}. Figure 3 shows the N_2O yield per mol of O_2 consumed for Butler and Nevison as an offline estimate for temperatures ranging 5 to 25°C. Butler shows a higher temperature sensitivity, particularly below 150 µmol L^{-1} of dissolved O_2, doubling the yield in this temperature range. Nevison shows less sensitivity to changes in temperature, having the same exponential-like yield in the hypoxic regions, where O_2 falls below 60 µmol L^{-1}.

The analysis of global budgets of N_2O production and N_2O inventory is restricted to depths between 100m and 1000m, where most of the N_2O is potentially produced and transported to the atmosphere for sea-to-air gas exchange (Suntharalingam and Sarmiento, 2000).

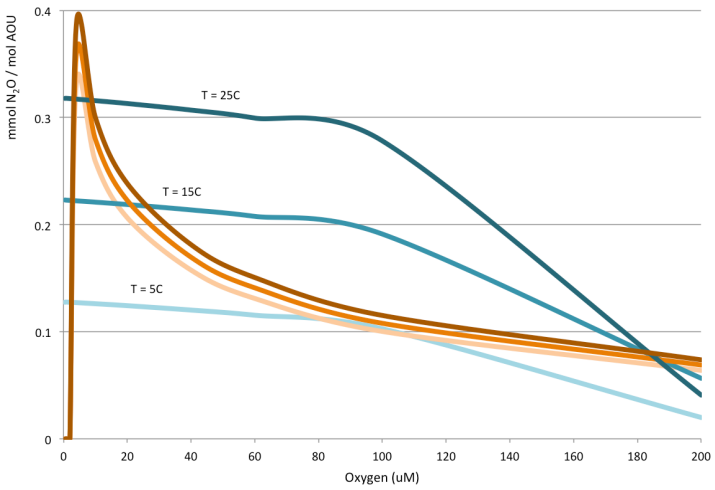

Figure 3: N_2O yield (in mmol) per O_2 consumed (in mol) compared to O_2 concentration (in µmol L^{-1}) in Butler et al. (1989) (blue) and Nevison et al. (2003) (orange) parameterisations for temperatures ranging 5°C (light) to 25°C (dark).

3.2.4. N_2-fixation parameterization in CMIP5 models

CMIP5 models have explicit representation of N_2-fixation. However, there is a wide variety of interpretations of the environmental conditions leading to N_2-fixation as well as in the variables used. Table 2 summarizes the different approaches used by the CMIP5 model suite. Models can be clustered into those with explicit representation of *diazotrophs*, i.e., CanESM, GFDL and CESM, and those who use the phytoplankton growth to compute the N_2-fixation rates, i.e., IPSL and MPI. However, there is another alternative organization by the way the N_2-fixation is implemented. One family of models (CanESM, IPSL and GFDL) are based on a combination of environmental terms such as other forms of bioavailable nitrogen (NH_4^+ + NO_3^-), Fe, PAR, O_2 or temperature. The other family of models (CESM and MPI) rely on ratios. While CESM defines an optimum N:C ratio within the cell and N_2-fixation is performed depending on the deficit in that ratio, MPI assumes N_2-fixation based on the PO_4 to NO_3^- ratio. In this way, there is a wide variety of parameterizations which depend on a second order on the representation of the biogeochemical variables included in the parameterizations within the models themselves.

Model	Limiting terms	Parameterisation
CanESM	Diazotrophs N_x comp. PAR	$J_{Nfix} = [N^{Diaz}] \cdot \frac{K_n}{K_n + [NO_3 + NH_4]} \cdot I_{PAR}(0)e^{-kz}$
IPSL-CM5	N_x comp. PAR Temperature Fe	$J_{Nfix} = \mu \cdot \frac{K_n}{K_n + [NO_3 + NH_4]} \cdot \frac{[Fe]}{K + [Fe]} \cdot (1 - e^{-I_{PAR}}) \cdot \alpha^{TEMP}$
GFDL-ESM	Diazotrophs N_x comp. O_2	$J_{Nfix} = [N^{Diaz}] \cdot \frac{K_n}{K_n + [NO_3 + NH_4]} \cdot \frac{K}{K + [O_2]}$
CESM	Diazotrophs N:C ratio	$J_{Nfix} = [N^{Diaz}] \cdot N/C$
MPI-ESM	N_x comp. $PO_4 : NO_3^-$ ratio	$J_{Nfix} = \mu \cdot (PO_4 \cdot R_{N:P} - NO_3)$

Table 2: N_2-fixation parameterizations as a combination of limiting terms such as NO_3, PO_4, NH_4, Fe, photosynthetic available radiation (PAR) or temperature (TEMP) in CanESM, IPSL-CM5, GFDL-ESM, CESM and MPI-ESM models from the CMIP5 model suite. Three of the models (CanESM, GFDL-ESM and CESM) include an explicit representation of diazotrophs while the remaining models assume a fraction of phytoplankton fixing N_2 (Taylor et al., 2012).

3.3. N_2O from CMIP5 models

3.3.1. N_2O production rates

Data-based CEX and O_2 products estimate a global N_2O production rate of 11.29 ± 4.94 TgN yr^{-1} (Table 3). Discrepancies in data-based CEX and O_2 products, which span 9.51 TgN yr^{-1} in Dunne et al. (2007) to 14.87 TgN yr^{-1} for Schlitzer et al. (2000) are reflected in the uncertainty in N_2O production estimations. Of particular interest is the high CEX scenario suggested by Schlitzer et al. (2000), with around 50% increase in N_2O production compared to the mean of the data-based products. Compared to the data-based products, CMIP5 models underestimate the global production rates of N_2O with a total of 5.33 ± 2.21 TgN yr^{-1}, where the uncertainties are about a half of that from data-based products. Based on the calculation method applied, CEX and O_2 are the main drivers of changes in estimating N_2O production rates and will be discussed in the next section.

CMIP5 models show a good agreement with data-based products on the major CEX hotspots in the ocean, found at ETP, Indian Ocean, North Pacific, North Atlantic and Subantarctic regions (Figure 4a and Figure 4b). Discrepancies are found in the misrepresented Benguela Upwelling system, the overestimation of CEX in the Southern Ocean and in underestimating in coastal margins. Overall, dense export areas above 30 mmolC m^{-2} d^{-1} are not well represented in the CMIP5 model suite.

Despite their diversity in the calculation methods and particle sinking processes, CMIP5 models show a low spread in CEX values at 100m depth (Bopp et al., 2013). This result is surprising when looking at the dispersion in CEX estimates from data-based products, where little amount of observations at depth are taken into account and hence they rely mostly on interpretation of satellite data, leading to a bigger spread in uncertainties. This fact suggests that CMIP5 models are quite likely targeting a common global CEX value. In case models were more independent, that would leave room for even wider intervals of uncertainties when estimating oceanic N_2O.

The uncertainties in N_2O estimates derived from data-based CEX products and CMIP5 models seem indeed driven by the dispersion of the CEX values in both cases, despite having very different O_2 fields (Bopp et al., 2013) contributing to the O_2 term using Eq. (2). Only in well oxygenated models such as Had-GEM2 and IPSL-CM5-LR with 2.4 and 1.2 x 10^6 km^3 on hypoxic volume (O_2 < 20 µmol L^{-1}) compared to 15.9 x 10^6 km^3 from the WOA2005*, estimates are below 5 TgN yr^{-1}.

	Dunne et al., 2007	Schlitzer et al., 2000	Eppley et al., 1989	Laws et al., 2000	OBS Mean	GFDL 2G	GFDL 2M	HAD GEM2	IPSL CM5 LR	IPSL CM5 MR	MPI ESM MR	MPI ESM LR	NOR ESM	CMIP5 Mean
CEX (Pg C/yr)	9.84	11.39	8.03	11.1	10.1 ±3.1	4.90	7.30	5.38	6.53	6.93	7.27	7.97	7.76	6.75 ±2.20
N_2Op (Tg N/yr)	9.51	14.87	9.80	10.96	11.29 ±4,94	4.79	6.69	3.76	4.06	5.49	6.48	6.28	5.13	5.33 ±2.21

Table 3: Export of organic matter (CEX) at 100m (in PgC yr^{-1}) and estimations of the global N_2O production rates (in TgN yr^{-1}) from CEX data-based products using O_2 from the WOA2005* and averaged 1995 to 2005 time period in CMIP5 historical simulations.

The spatial distribution of the main N_2O production regions is similar from CMIP5 models and from data-based CEX and O_2 products, but a significant drop by an order of magnitude (Figure 4c and Figure 4d) is observed where the maxima are, i.e., North Atlantic, North Pacific, Arabian Sea, Bay of Bengal and coastal margins of the ETP. Minima in the subtropical gyres are overestimated by CMIP5 models.

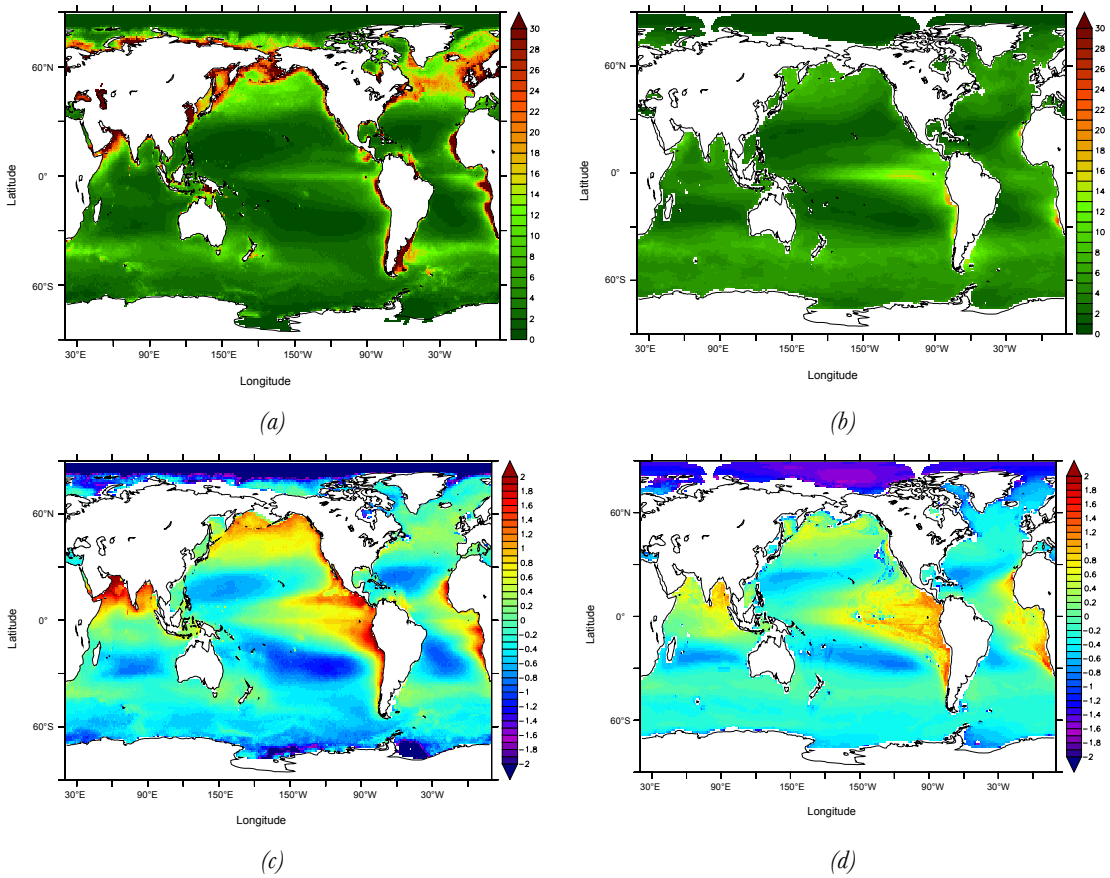

Figure 4: Export of organic matter (CEX) (in mmol C m^{-2} d^{-1}) at 100m from (a) Dunne et al. (2007) and (b) CMIP5 model mean in the 1995 to 2005 averaged time period. N_2O production rates, in log(nmol N m^{-2} s^{-1}) estimated from of (c) Dunne et al. (2007) using O_2 from WOA2005*, and (d) CMIP5 Mean.

Reasons behind the underestimation point towards the high CEX in data-based products in coastal margins associated with low O_2 areas in the Arabian Sea or upwelling regions such as ETP or BUS. N_2O production is enhanced in these regions following the calculation method applied, i.e., boosted by steeper CEX profiles in the reconstruction process, therefore more remineralization of organic matter and hence more nitrification. CMIP5 models are generally low resolution models. They have a similar yet deficient representation of coastal margin processes, hence attributing a lower amount of CEX than some data-based products (e.g., Dunne et al., 2007). This fact might explain the underestimation of N_2O production rates within the CMIP5 models compared to those from data-based products.

3.3.1.1. Drivers of uncertainties in estimating N_2O production

In order to quantify the individual contribution of CEX and O_2 to the uncertainties in N_2O production, I calculate independently N_2O production using the spectrum of CEX from the CMIP5 models in combination with a CMIP5 averaged O_2 field. Conversely, I estimate N_2O production with a single CEX profile but applying the individual O_2 distribution from each of the CMIP5 models.

Table 4 shows the uncertainties derived from such calculations. The uncertainty in global N_2O production derived from different CEX ($\pm$ 2.53 TgN yr^{-1}) is larger than from O_2 ($\pm$ 1.73 TgN yr^{-1}), supporting the hypothesis of the smaller influence of O_2 than CEX when estimating N_2O production rates. This estimation is however strongly biased by the calculation method I have applied, where, if O_2 is the same in all cases and therefore all Martin et al. (1987) curves are equal, the only variable that matters ultimately is the value of export at 100m. In other words, only the absolute value of CEX at 100m drives the uncertainties in N_2O production in this sensitivity analysis. This is shown in Figure 5a, where deviations from the average have all the same depth profile and they all depend on the starting value of CEX at 100m for the subsequent CEX reconstruction. The uncertainty due to the different O_2 fields is lower when estimating global N_2O production, but it shows a more pronounced spatial variability. Changes in O_2 across CMIP5 models trigger changes in the boundaries between the two regimes of the Martin et al. (1987) curves. This depth variability is shown in Figure 5b, where discrepancies from the CMIP5 mean reflect the variety in O_2 fields from the CMIP5 models throughout the water column. Changes in CEX, due to the calculation method applied, introduce more uncertainties in the global N_2O production budget, while O_2 dominates on the spatial variability of N_2O production locally. The impact of O_2 dispersion in making N_2O estimations is more prominent in the N_2O inventory calculation, as discussed in detail in the next section.

	GFDL 2G	GFDL 2M	HAD GEM2	IPSL CM5 LR	IPSL CM5 MR	MPI ESM MR	MPI ESM LR	NOR ESM	CMIP5 Mean
N_2Op (TgN yr^{-1}) Variable CEX	4.56	6.10	4.98	5.73	6.07	7.29	8.15	7.54	6.30 ± 2.53
N_2Op (TgN yr^{-1}) Variable O_2	5.98	6.33	4.25	4.04	5.13	5.31	4.81	4.07	4.99 ± 1.73

Table 4: Estimations of the global N_2O production rates (in TgN yr^{-1}) from averaged 1995 to 2005 time period in CMIP5 historical simulations. The first row explores the variability in CEX using constant CMIP5 averaged O2. The second row considers the O2 spectrum from CMIP5 models with constant CMIP5 averaged CEX.

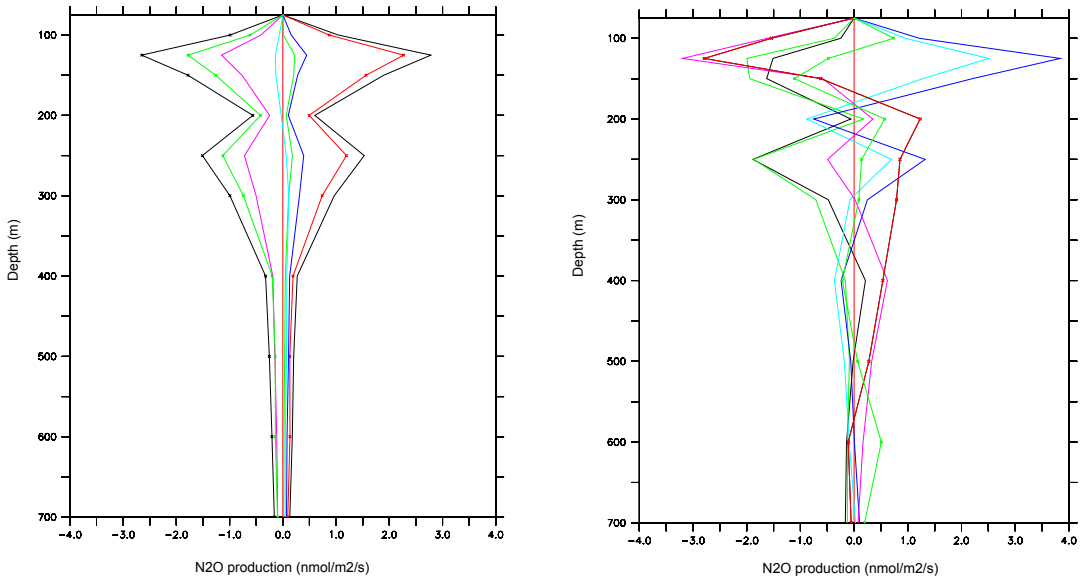

(a) *(b)*

Figure 5: Depth averaged changes in N_2O production compared to the average for (a) CMIP5 models using the averaged CMIP5 O_2 with individual CEX and (b) CMIP5 models using the averaged CMIP5 CEX with individual O_2 fields, being GFDL-2G (black), GFDL-2M (red), IPSL-LR(blue), IPSL-MR (green), MPI-MR (cyan), MPI-LR (purple), HadESM (dot-black) and NorESM (dot-red).

3.3.2. N_2O inventory

The N_2O reservoir estimated from the averaged World Ocean Atlas is 211 ± 22 TgN. Uncertainties are around 10% of the total N_2O inventory in the upper 1000m when using Butler parameterization, and less than 5%, i.e., 197 ± 8 TgN when using Nevison (Table 5). If I take into account the oxygen corrected WOA2005*, with larger volumes for both hypoxic and suboxic regimes of 80.9 and 15.9 x 10^6 km^3 compared to 77.3 and 0.3 x 10^6 km^3 on

WOA2009, N_2O inventory estimate falls within the range of uncertainty from the World Ocean Atlas. The slight decrease in the amount of N_2O from Butler to Nevison might be caused by the fact that Nevison parameterization only computes areas where O_2 is greater than 4 µmol L^{-1}, hence excluding the cores of the OMZs in the Arabian Sea and the ETP, where Butler parameterization, on the contrary, does apply. Large reservoirs of N_2O are found in the main N_2O production areas, namely Arabian Sea, Bay of Bengal, ETP and North Pacific, whereas Southern Ocean, Pacific subtropical gyre and North Atlantic show the absence of N_2O content (Figure 6a and Figure 6c). Changes between Butler and Nevison parameterization can be observed in few spots in the core of the OMZ in the ETP and Arabian Sea, where Nevison threshold applies and no N_2O inventory is calculated as a consequence of the steady-state analysis. In a transient simulation, N_2O would be advected from other regions into the core of the ETP using the same parameterization.

Uncertainties using data-based products such as World Ocean Atlas must be interpreted with caution. The World Ocean Atlas versions are built upon its predecessors, except for the WOA2005*, so little variations are expected among the different versions when I estimate the global N_2O inventory. World Ocean Atlas versions are therefore very homogeneous, with roughly the same amount of hypoxic and suboxic volumes with an average of 74.9 and 0.4 x 10^6 km^3 respectively.

The CMIP5 averaged model ensemble estimation of the content of N_2O in the ocean in the first 1000m is in the same order of magnitude compared to the reference estimate using WOA2005*. Butler estimate of 193 ± 51 TgN falls within the data-based products estimates of 212 ± 22 TgN, while Nevison estimate is lower, with 169 ±27 TgN compared to the observed 197 ± 8 TgN (Table 5), quite likely due to the bigger OMZs in some of the CMIP5 models and therefore the exclusion of the N_2O inventory calculation below the 4 µmol L^{-1} threshold. The heterogeneous O_2 profiles of the different CMIP5 models lead to a significant increase in the uncertainties. Significant discrepancies are found among the CMIP5 models when it comes to represent dissolved O_2 concentration, particularly on hypoxic and suboxic regimes. On average, CMIP5 models have large areas of suboxia or even anoxia, with an order of magnitude difference from the reference values of WOA2005* and the World Ocean Atlas mean. On an individual level, models are clustered around higher or lower values compared to the reference value for O_2 regimes below 60, 20 and 5 µmol L^{-1} (Figure 7). This result challenges the idealised selection of an adequate individual model to estimate global oceanic N_2O. None of the CMIP5 models match the observed hypoxic or suboxic volumes.

The spatial distribution of the N_2O inventory in the CMIP5 models reflects the underestimation in all the high N_2O productive regions using the Butler parameterisation, yet with an overall agreement on the location of the largest reservoirs (Figure 6b and Figure 6d). Discrepancies with WOA2005* derived estimates are more prominent when using Nevison

parameterization. Large variations in the OMZ extension in certain models such as GFDL-ESM where hypoxia below 20 µmol L^{-1} reaches 62.6 x 10^6 km^3 and suboxia below 5 µmol L^{-1} is 38.2 x 10^6 km^3 compared to WOA2005* of 15.9 and 1.9 x 10^6 km^3 respectively cause a significant distortion in the spatial distribution due to the Nevison excluding regime in steady state analysis, showing the non-zero N_2O inventory only in the ocean interior.

	WOA 1998	WOA 2005	WOA 2005*	WOA 2009	WOA Mean	GFDL -2G	GFDL -2M	HAD GEM2	IPSL CM5 LR	IPSL CM5 MR	MPI MR	MPI LR	Nor ESM	CMIP5 Mean
Hypoxic vol. (10^6 km^3)	70.55	76.94	80.90	77.26	74.92 ± 7.57	120.20	123.50	24.71	71.07	267.2	140.9	126.0	92.2	122.0 ±140.0
Suboxic vol. (10^6 km^3)	0.24	0.60	1.94	0.28	0.37 ± 0.39	38.16	33.59	0.38	0.38	1.78	45.61	51.00	47.67	29.10 ±48.00
Butler N_2O (Tg N)	213	221	202	199	211 ± 22	209	210	177	165	152	217	219	192	193 ± 51
Nevison N_2O (Tg N)	194	202	198	196	197 ± 8	192	183	167	161	149	163	177	161	169 ± 27

Table 5: O_2 volume (in 10^6 km^3) in WOA98, WOA05, WOA2005*, WOA09 and averaged historical 1995 to 2005 time period CMIP5 model simulations for hypoxia (O_2 < 60 µmol L^{-1}) and suboxia (O_2 < 5 µmol L^{-1}). N_2O inventory (in TgN) usgin Butler and Nevison parameterization in the upper 1000m for WOA98, WOA05, WOA2005*, WOA09 and averaged historical 1995 to 2005 time period CMIP5 model simulations.

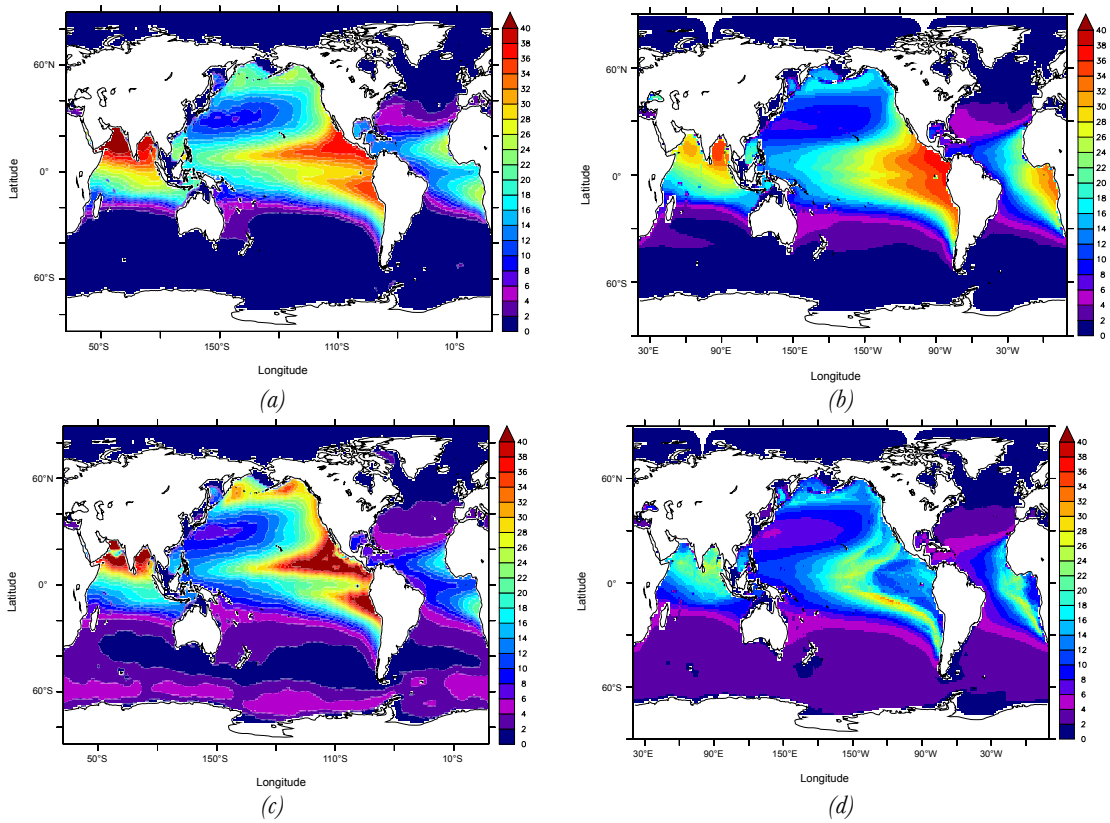

Figure 6: Vertically integrated N_2O inventory estimations for (a) WOA05* using Butler, (b) CMIP5 model mean using Butler, (c) WOA05* using Nevison and (d) CMIP5 model mean using Nevison parameterization.

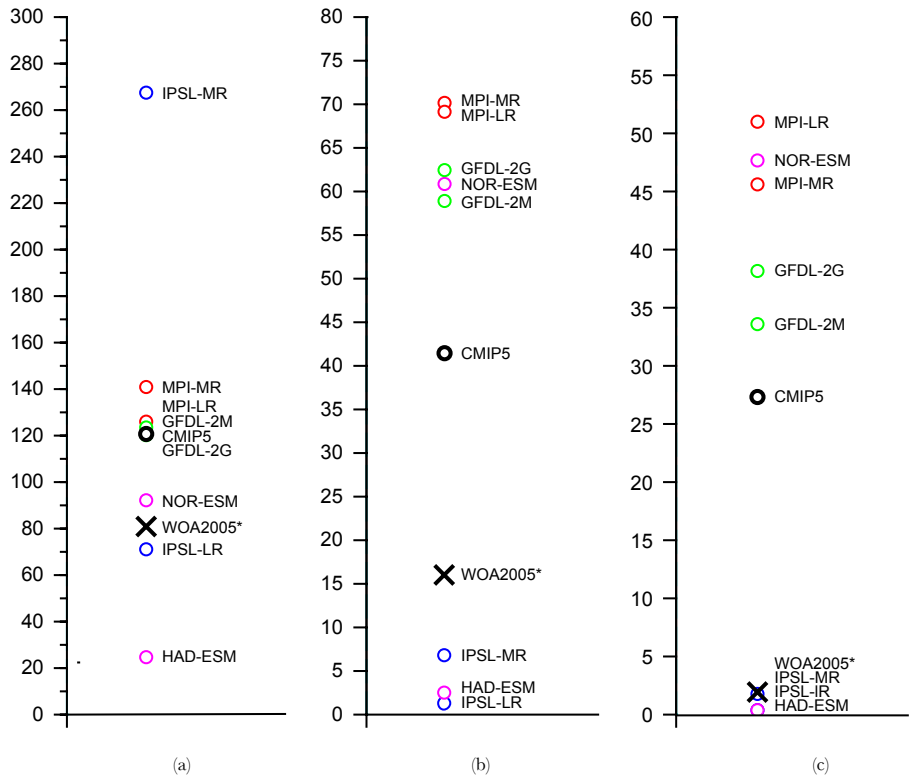

Figure 7: O_2 volume (in 10^6 km^3) in WOA2005* and CMIP5 models for (a) hypoxia (O_2 < 60 µmol L^{-1}), (b) hypoxia (O_2 < 20 µmol L^{-1}), and (c) suboxia (O_2 < 5 µmol L^{-1}).

3.3.2.1. N_2O inventory estimates and observations

The N_2O inventory derived from this steady-state calculation is compared to the distribution of N_2O available in the MEMENTO database (Bange et al., 2009). Table 6 summarizes the standard deviation and correlation coefficients between WOA2005* with respect to MEMENTO database. Standard deviation in the WOA2005* estimates are larger than that from MEMENTO, from 20/21 nmol in Butler/Nevison parameterization to 16 nmol in the observations depending on the parameterization. Correlation coefficients between MEMENTO data points sampled over the WOA2005* estimates shows 0.43 to 0.39 when using Butler and Nevison respectively. Figure 8a and Figure 8b show the global depth average of the different WOA data-based products and the MEMENTO database. WOA derived N_2O is underestimated in the first 1000m, quite likely due to the abscence of an explicit representation of enhanced N_2O production in the low O_2 regions in Butler and Nevison parameterizations and also to the MEMENTO measurements biased towards OMZ regions with higher than usual N_2O concentrations. However, the residual N_2O concentration in the

deep is well represented in the estimates, at around 16 nmol.

The relationship between WOA2005* O_2 concentration and N_2O inventory is shown in Figure 8c and Figure 8d. The linear relationship from Butler is in good agreement along most of the O_2 spectrum but fails at capturing the low O_2 levels, where observed N_2O concentration peaks around 80 nmol L^{-1} and then drops close to anoxic conditions. On the contrary, Nevison does a better job at the OMZs reproducing the maximum, but with a smaller spread in its values throughout the rest of the O_2 regimes.

When I compare the CMIP5 model performance against the MEMENTO database, the standard deviation of the CMIP5 model mean matches the observed value of 16 nmol L^{-1} when using Butler. In addition, the correlation between CMIP5 mean and MEMENTO is slightly higher than in the WOA case, reaching $r^2 = 0.51$ using Butler parameterization (Table 6).

The CMIP5 global depth average of N_2O shows a similar profile to the observations in the upper 1000m, but still lacking the enhancement of the N_2O production at the core of the OMZs (Figure 9a and Figure 9b). Surprisingly this is observed more prominently using Butler parameterization than using Nevison. The exclusion of high N_2O values in Nevison might explain this counterintuitive result. Similar to WOA, Butler fails at reproducing high N_2O measurements at low O_2 levels but it reproduces most of the linear section of higher O_2 regimes (Figure 9c and Figure 9d). Without N_2O values at very low O_2 in Nevison, the comparison lacks the characteristic higher exponential profile at low O_2 despite the good agreement along the rest of the O_2 spectrum.

	WOA2005* Butler	WOA2005* Nevison	CMIP5 Butler	CMIP5 Nevison	MEMENTO
Standard deviation (in nmol N_2O)	20	21	15	10	16
Correlation coefficient with observations	0.43	0.39	0.51	0.47	-

Table 6: Standard deviation and correlation coefficient between N_2O estimates using Butler and Nevison parameterization in WOA2005* and 1995 to 2005 averaged time period CMIP5 historical simulation compared to MEMENTO database (Bange et al., 2009). Global depth (in m) average N_2O inventory profile (in nmol L^{-1}) for the CMIP5 models and MEMENTO database using (a) Butler parameterization and (b) Nevison parameterization.

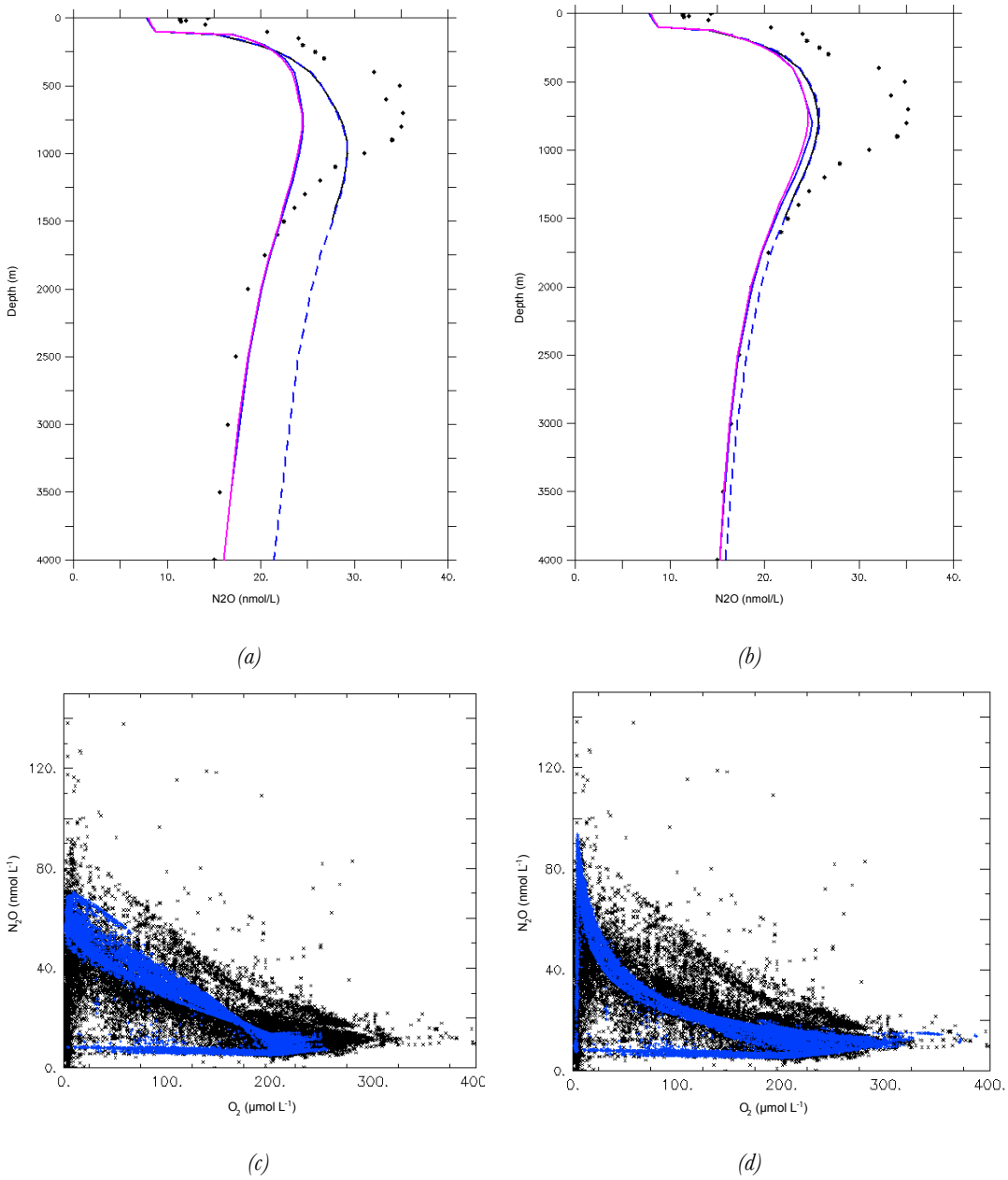

Figure 8: Global depth average (in m) of N_2O inventory (in nmol L^{-1}) in MEMENTO database (dots) and WOA1998 (blue), WOA2005* (dashed blue) and WOA2009 (purple) N_2O inventory estimations using (a) Butler and (b) Nevison parameterization. Scatter plot of O_2 (in µmol L_{-1}) vs N_2O (in nmol L^{-1}) in MEMENTO dabase (black) under (c) WOA2005* using Butler parameterization and (d) WOA2005* using Nevison parameterization.

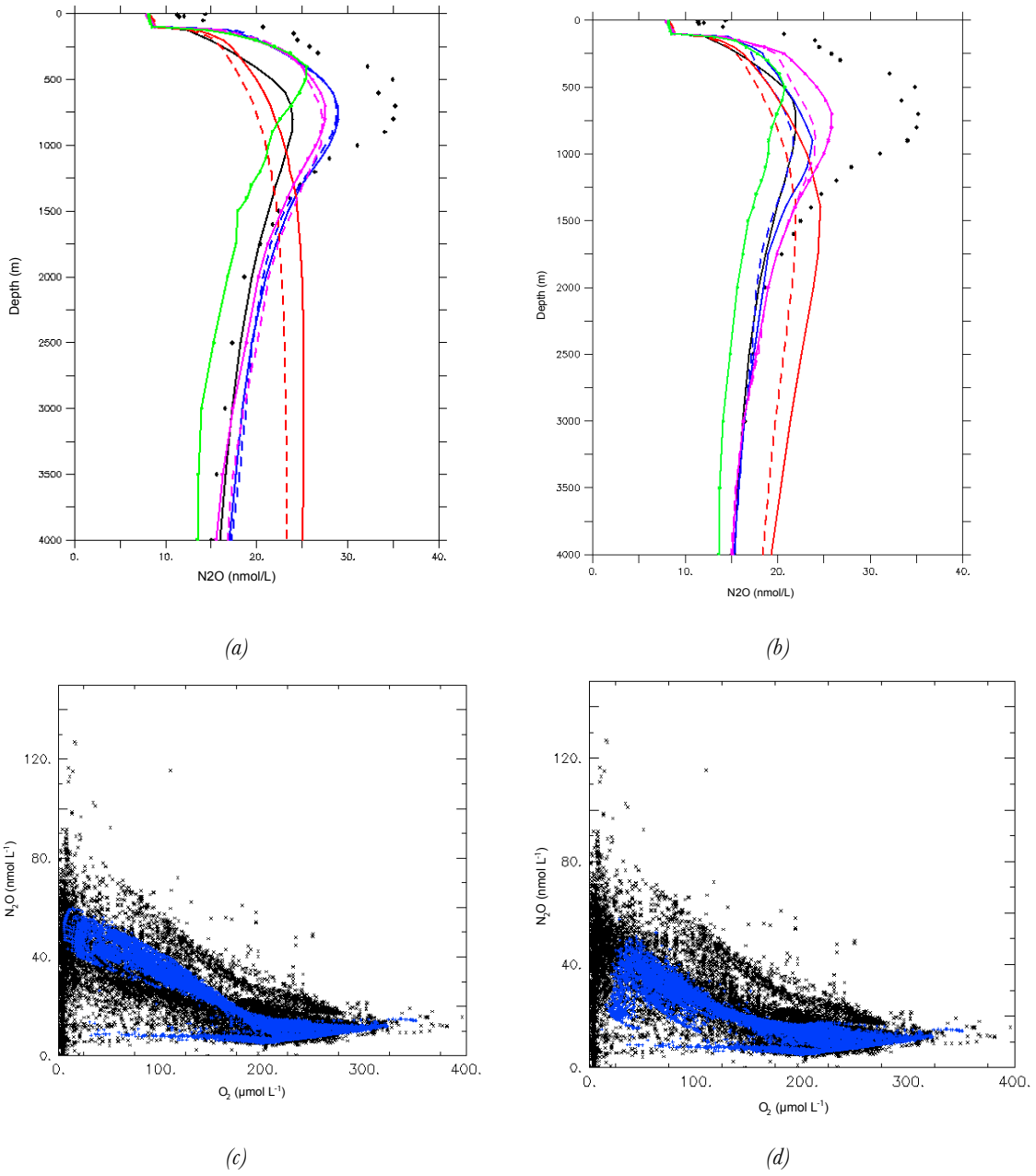

Figure 9: Global depth average (in m) of N_2O inventory (in nmol L^{-1}) in MEMENTO database (dots) and CMIP5 models using (a) Butler and (b) Nevison parameterizations. Scatter plot of O_2 (in µmol L_{-1}) vs N_2O (in nmol L^{-1}) in MEMENTO dabase (black) under (c) CMIP5 using Butler parameterization and (d) CMIP5 using Nevison parameterization.

3.4. N_2-fixation in CMIP5 models

3.4.1. N_2-fixation rates

CMIP5 estimates of the global nitrogen fixation agree with estimations based on observations and model analysis. CMIP5 models estimate 134 TgN yr^{-1} on average at present, although with an uncertainty of ± 75 TgN yr^{-1} (Table 7). The absolute value is close to the estimate of Luo et al. (2012) of 137 ± 9 TgN yr^{-1} and also to the model based estimates of Deutsch et al. (2007) of 137 ± 34 TgN yr^{-1} and Eugster and Gruber (2012) of 134 ± 16 TgN yr^{-1}. However, the CMIP5 estimate is below the revised estimation by Grosskopf et al. (2012) of 177 ± 8 TgN yr^{-1}. The spread in the CMIP5 estimates is a consequence of the distribution of model estimates, from the lowest of 75 TgN yr^{-1} in IPSL-LR to 184 TgN yr^{-1} of MPI-LR. The relative contribution of the different ocean basins to the total N_2-fixation rates is consistent with the observations from Luo et al. (2012). The North Atlantic and Pacific dominate over their southern counterparts, whereas on a global scale the Pacific ocean remains as the biggest contributor.

Model	North Atlantic	South Atlantic	North Pacific	South Pacific	Indian	Total (Tg N/y)
CanESM	19	11	46	33	29	140
CESM	25	19	41	31	44	165
GFDL-2M	21	15	40	31	26	139
IPSL-LR	7	8	27	21	9	75
IPSL-MR	9	9	33	23	18	96
MPI-LR	13	14	57	55	21	184
MPI-MR	4	7	55	45	14	142
CMIP5 mean	14	12	43	34	23	134 ± 75
OBS	32	2	56	46	-	137 ± 9
Deutsch et al., 2007						137 ± 34
Grosskopf et al., 2012						177 ± 8
Eugster & Gruber, 2012						134 ± 16

Table 7: Global N_2-fixation rates estimations (in TgN yr^{-1}) in CMIP5 models, observations from Luo et al. (212) and Grosskopf et al. (2012) and model studies from Deutsch et al. (2007) and Eugster and Gruber (2012). Grosskopf commented on the measurements techniques in Luo et al., 2012, suggesting an underestimation based on the technical method measuring N_2-fixation rates. The observations value from Luo et al. (2012) is based on interpolated 3° by 3° bins..

Spatial distribution of N_2-fixation in CMIP5 models are shown in Figure 10. On average, CMIP5 models locate the N_2-fixation occurrence at low to mid latitudes in the Indian Ocean, western and eastern parts of the Pacific ocean and equatorial Atlantic. Lower N_2-fixation rates are found at high latitudes, particularly in the Arctic and Southern Ocean. Despite the homogeneous values found on average, significant discrepancies are found among the CMIP5 models. CanESM, CESM and IPSL-CM5 models estimate N_2-fixation in the western part of the major oceanic basins. The inhibition of N_2-fixation due to other forms of nitrogen compounds shift the N_2-fixation occurrence far from the eastern boundary currents, where upwelling of nutrients contribute to the limiting terms included in these parameterizations. Moreover, the Fe supply in the western part of the Pacific as well as in the Atlantic together with the river supply of large rivers such as the Amazon contribute to boost N_2-fixation in this family of models on that regions. This set of CMIP5 models also have in common a strong temperature limitation, as shown by the lack of N_2-fixation occurrence beyond 40° N/S. On the other hand, GFDL and MPI project high N_2-fixation rates particluarly in upwelling regions. The need of PO_4 in MPI parameterization demands the presence of potential N_2-fixers close to the eastern boundary currents, whereas diazotrophs in GFDL are present also in such regions (see section 3.4.2).

Despite the discrepancies, CMIP5 models accurately describe the minima at high latitudes, the maxima of the tropical and sub-tropical N_2-fixation (Figure 11) and the envelope of maxima at 20°N and 20°S. Only two models, MPI-LR/MR and GFDL-2M show N_2-fixers at higher latitudes. It must be mentioned that N_2-fixation rates in Luo et al. (2012) dabatase are biased towards the expected niches of N_2-fixation occurrence at low latitudes, without any measurements at high latitudes. Whether the projection of MPI and GFDL models is plausible is a question which remains open.

On average, CMIP5 models simulate N_2-fixation particularly for temperatures above 20°C (Figure 12), where N_2-fixation rates are enhanced compared to cooler regimes. There is however a non-zero N_2-fixation rates in all of the temperature spectrum which seems unrealistic. Observations show how significant N_2-fixation activity kicks in for temperatures above 15°C, with higher N_2-fixation rates around 25°C and an upper limit on temperatures of 30°C.

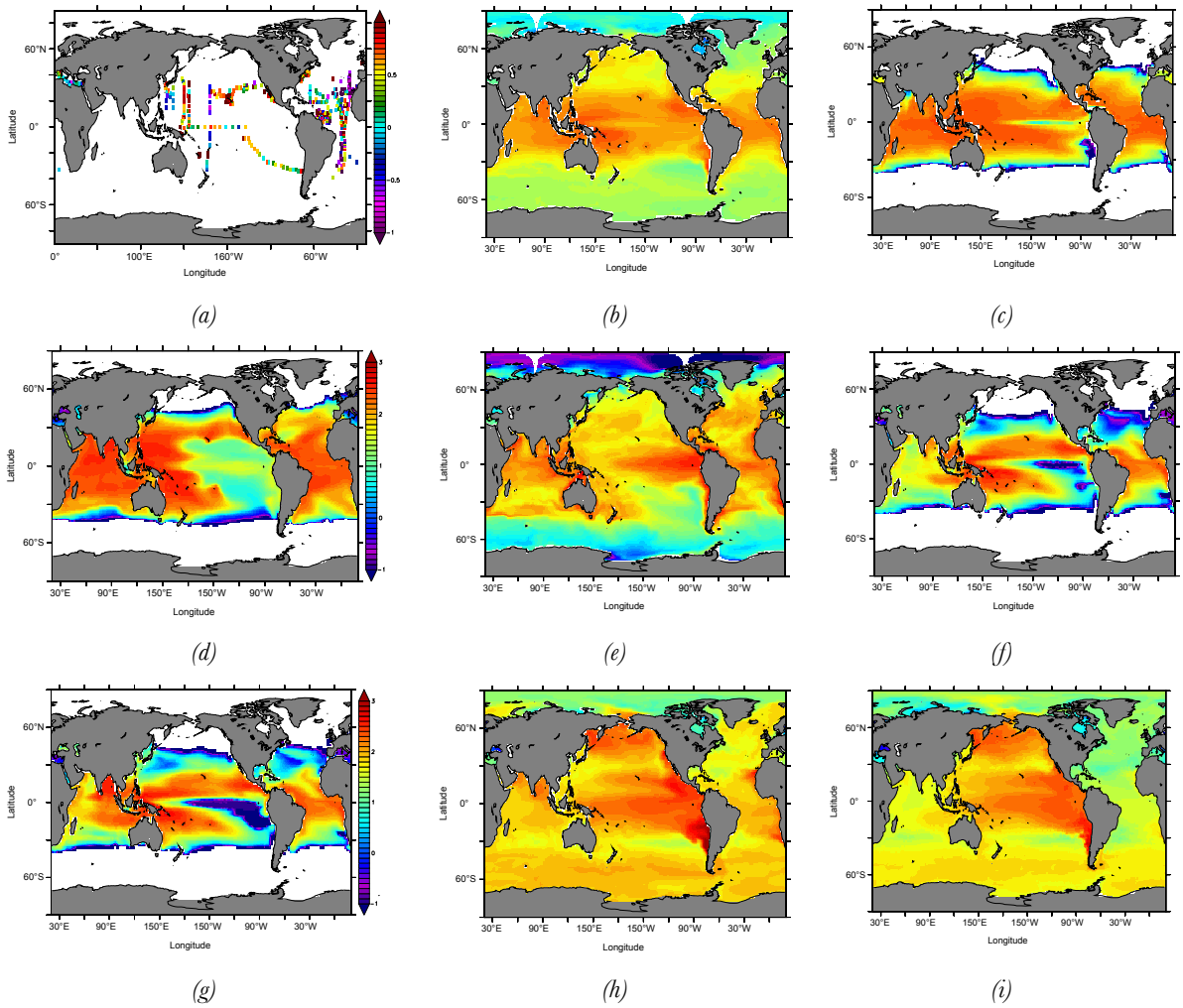

Figure 10: Depth integrated N_2-fixation rates (in log (μmolN m^{-2} d^{-1})) in CMIP5 models. (a) Luo et al. (2012), (b) CMIP5 mean, (c), CanESM, (d) CESM, (e) GFDL-2M, (f) IPSL-LR (g) IPSL-MR, (h) MPI-LR and (i) MPI-MR.

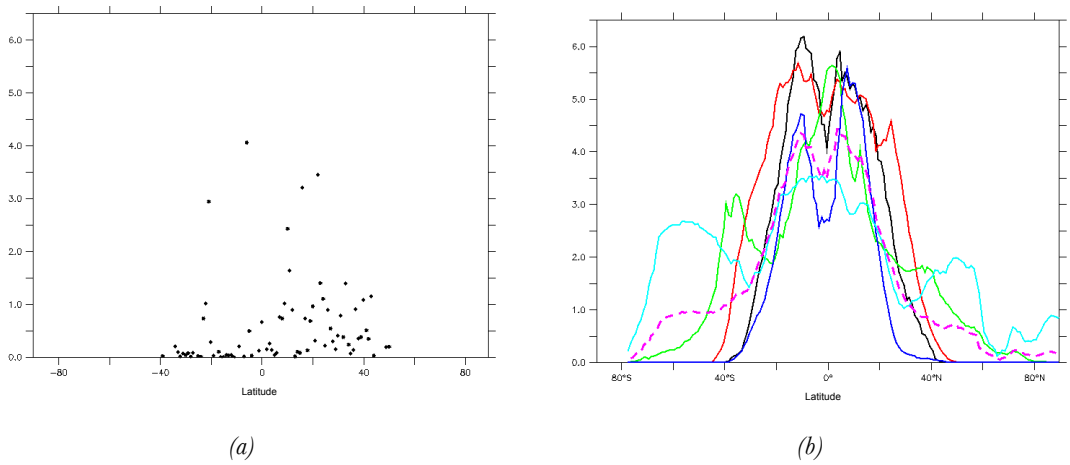

Figure 11: Latitudinal depth integrated N_2-fixation rate (in log(uMm^{-2}d^{-1})) in (a) Luo et al. (2012) database and (b) CMIP5 mean (dashed pink) and the CMIP model suite: CanESM (black), CESM (red), GFDL-2M (green), IPSL-LR(blue) and MPI-MR (cyan) (Taylor et al., 2012).

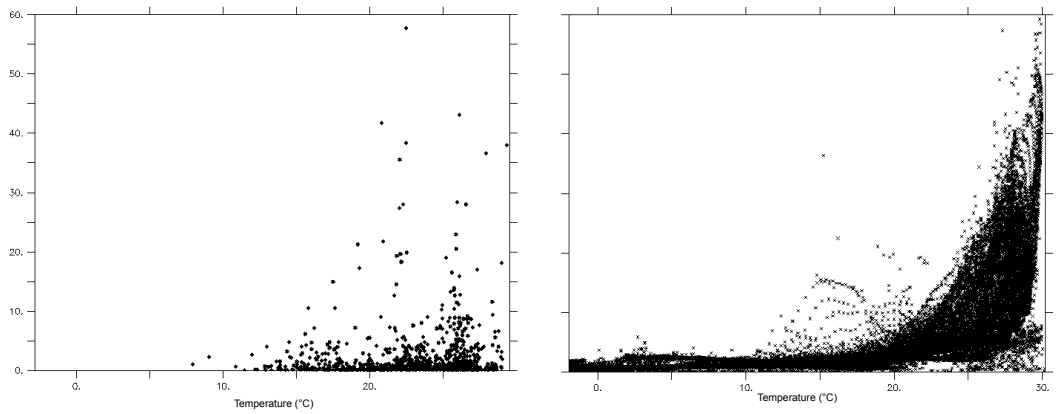

(a) *(b)*

Figure 12: Depth integrated N_2-Fixation rates (in µmolN m^{-2} d^{-1}) over the temperature range (in °C) in (a) Luo et al. (2012) database and (b) CMIP5 model mean over the 1995 to 2005 time period.

3.4.2. N_2-fixers biomass

Two of the CMIP5 models include *diazotrophs* as an explicit phytoplankton group in their state variables. While the distribution of diazotrophs in CESM is mostly in the western part of the oceanic basins, the distribution in the case of GFDL model is almost the opposite, occupying the eastern boundary currents and even in a small magnitude in the Southern Ocean (Figure 13). This fact casts doubts on the current ability of CMIP5 models representing diazotrophs explicitly.

Overall, there are significant gaps in the N_2-fixation rates data coverage at present which hampers an adequate validation of the models on a global scale, but provide valuable information on a local scale. Observations are gathered mostly around the Atlantic and western Pacific oceans, without any measurements in the Indian Ocean and high latitudes such as the Southern Ocean. Global interpolations derived from this database must be interpreted with caution due to the large oceanic areas where no datapoints are found. In addition, the heterogeneous and rather simplistic representation of N_2-fixation rates in CMIP5 models is not encouraging as today. Opposite patterns among the CMIP5 model suite increases the level of uncertainty when estimating present and potential future scenarios.

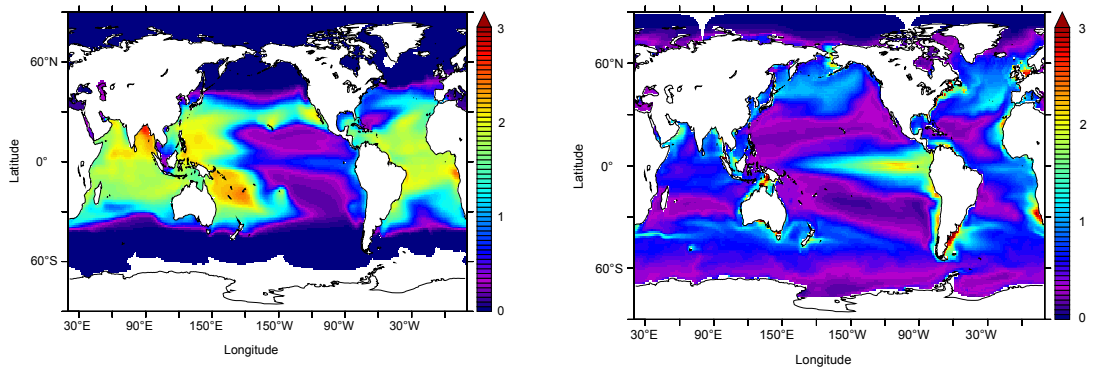

(a) (b)

Figure 13: Concentration (in mgC m^{-3}) of diazotrophs averaged over the 1995-2005 period in the upper 100m in (a) CESM model and (b) GFDL model.

3.5. Conclusions

CMIP5 models underestimate the N_2O production rates compared to steady-state data-based product calculations. Underestimation of CEX is reflected on N_2O production rates estimates based on the reconstruction methodology proposed in this analysis and the parameterisations used. The uncertainties in CMIP5 models are significant, around 50% of the total value of 5.33 TgN yr^{-1}, but nevertheless lower than those from CEX data-based products. Coarse resolution in coastal margins as well as remineralisation, sinking trajectories and CEX attenuation processes in CMIP5 models contribute to the uncertainties associated with N_2O estimations. O_2 variability among CMIP5 models has a limited effect in N_2O production rates estimates.

Recent model intercomparison studies have assessed global CEX fields for present-day and future conditions (Steinacher et al., 2010; Bopp et al., 2013). Uncertainties and deviations from existing data-based products have been identified in the same studies. Fixed and variable coefficients of the regenerated production set the first order uncertainties on CEX. Remineralization (Martin et al., 1987; Klaas and Archer, 2002) and sinking particle trajectories to the ocean interior (Martin et al., 1987) contribute to second order deviations. O_2, however, remains as one of the biggest challenges in current biogeochemical modeling. Ocean circulation has been identified as the main source of uncertainties in modelled O_2, including changes in deep circulation and upwelling dynamics, together with the associated biogeochemical response in terms of nutrient supply, CEX and subsequent remineralization (Cocco et al., 2012; Bopp et al., 2013). Dissolved O_2 concentration in OGCBMs also shows high sensitivity to the nature and resolution of the coupled atmospheric forcings (e.g., Marti et al., 2010). Models are challenged too by the poor representation of the intrinsic natural

variability of O_2 (Froelicher et al., 2009). Present and future estimations are also under debate regarding the modelled amplitude of the O2 fluctuations, similar to that of the natural O_2 variability (Cocco et al., 2012). As a consequence, the representation of O_2 in ocean biogeochemical models is subject to a significant uncertainty in its distribution, let alone the O_2 regimes such as hypoxia (O_2 < 60 µmol L^{-1}) or suboxia (O_2 < 5 µmol L^{-1}). With respect to estimating N_2O production rates and inventories particular attention is paid to the OMZs because of the high yield of N_2O production at low-O_2 regimes. Models exhibit a significant variability capturing this feature in regions such as the Arabian Sea, Bay of Bengal, northern Pacific and the eastern upwelling systems in ETP or BUS (e.g., Resplandy et al., 2012, on the Arabian Sea).

The major N_2O inventory reservoirs are also underestimated in CMIP5 models compared to those based on the WOA according to the calculation method used. The broad spectrum of O_2 content in the CMIP5 models hamper an accurate estimation of the N_2O inventory, with large uncertainties on the global budget. It is not the aim of this study to discuss the O_2 fields in CMIP5 models in detail, but this fact remains substantial as long as the modelling community rely on parameterizations based on dissolved O_2 for calculating the N_2O inventory in the ocean interior. An alternative approach using mechanistic parameterizations in models based on nitrification and denitrification rates might contribute to reduce the uncertainty in estimating the ocean N_2O contribution to the climate system. However, the O_2 threshold at which nitrification and denitrification occur still relates the O_2 fields and the capability of OGCBMs making accurate N_2O estimations.

CMIP5 model estimations and future projections must be therefore used with caution within the framework described in this study. The ultimate climate feedback question on N_2O remains on the sea-to-air flux rather than on the N_2O production itself. Mechanisms leading to changes in the N_2O flux due to changes in CEX, O_2, ocean circulation, N_2O transport and N_2O gas exchange must be explored in transient simulations, but being aware of the significant uncertainties on the N_2O produced and N_2O stored in the ocean interior.

What ultimately matters for evaluating the contribution of oceanic N_2O to the total greenhouse gas budgets is the actual N_2O sea-to-air flux. Translate the uncertainties of N_2O production into N_2O flux in a steady-state analysis is not a straight forward exercise. It has been traditionally assumed that all the N_2O produced in the ocean interior is eventually outgassed to the atmosphere, but there are some non-linearities that must be taken into account in this steady-state methodology. Making use of transient PISCES simulations, I analyse the correlation between N_2O production and N_2O flux. Figure 14 shows the correlation between N_2O production and N_2O flux on global annual averages from 1851 to 2100. There is a positive correlation between N_2O production and N_2O flux to the atmosphere. Intuitively there is an increasing flux with increasing production, which suggest

that most of the N_2O produced in the upper 1000m is eventually outgassed on short timescales, with a significant role of ocean circulation and N_2O transport in the subsurface.

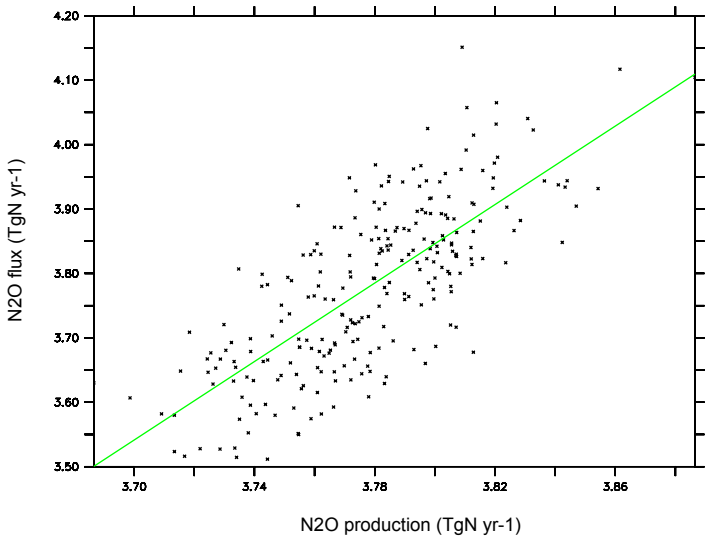

Figure 14: Scatter plots between N_2O flux and N_2O production from annual averaged 1851 to 2100 period in PISCES model historical runs plus RCP8.5 future simulations using a Butler-like parameterization of N_2O production.

Another source of uncertainties which is not captured in this steady-state analysis is the interannual variability of N_2O emissions, that must be considered when estimating N_2O sea-to-air flux in models. A high correlation of tropospheric N_2O with the ENSO index has been observed (Thompson et al., 2013). Changes in ocean circulation and N_2O transport from the subsurface to the atmosphere interface might explain such correlation. For instance, the accumulation of N_2O in the subsurface at the ETP might be diminished during La Niña episodes, where enhanced upwelling would transport more N_2O than usual to the surface, facilitating in this way gas exchange with the atmosphere and therefore a potential significant signature on tropospheric N_2O.

The CMIP5 model community accurately describes the total budget of N_2-fixation compared to the most up-to-date N_2-fixation database. The relative contribution of the different ocean basins to the total N_2-fixation budget is also well represented in the total budget estimations. Latitudinal maxima and minima are identified at around 20°N, 20°S and the Equator, following the pattern observed in the database. Limiting terms such as temperature are in good agreement with the observations, with higher N_2-fixation rates at temperatures in the range of 15°C to 20°C. Inconsistencies among the CMIP5 models are observed in regions sensitive to the availability to other forms of nitrogen, such as upwelling zones in the Eastern Subtropical Pacific. These differences could lead to different responses to climate change,

where is quite likely that oligotrophic regions will tend to increase. More complex, up-to-date approaches on N:P:Fe ratios and data validation are needed.

Chapter 4

Oceanic N_2O emissions in the 21st century

Introduction

For the first time, a future projection of marine N2O emissions in 2100 is presented in the climate science community. Based on PISCES model and the IPSL-CM5 business-as-usual high CO_2 emissions scenario, we implemented two different parameterizations in the model and run historial and future simulations, from 1851 to 2100. These two parameterizations allow us to analyze changes in high- and low- O_2 production pathways. We evaluate changes in 2100 in N_2O production pathways, N_2O storage in the ocean interior and N_2O sea-to-air fluxes. In addition, we use a box model to focus on the main drivers of future changes, namely export of organic matter to depth (CEX) and mixing between the surface and subsurface layers. The results are framed in the context of natural sources of N_2O and the contribution to the radiative forcing feedback compared to N_2O soil emissions on a global scale.

This study has been submitted to *Biogeosciences* as:

"Oceanic N_2O emissions in the 21st century"
J. Martinez-Rey, L. Bopp, M. Gehlen, A. Tagliabue and N. Gruber

Biogeosciences Discuss., 11, 1–40, 2014
www.biogeosciences-discuss.net/11/1/2014/
doi:10.5194/bgd-11-1-2014

Biogeosciences
Discussions
Open Access

Oceanic N_2O emissions in the 21st century

J. Martinez-Rey[1], L. Bopp[1], M. Gehlen[1], A. Tagliabue[2], and N. Gruber[3]

[1]Laboratoire des Sciences du Climat et de l'Environnement, IPSL, CEA/CNRS/UVSQ, Bat. 712, Orme des Merisiers, 91191 CE Saclay, Gif-sur-Yvette, France
[2]School of Environmental Sciences, University of Liverpool, 4 Brownlow Street, Liverpool L69 3GP, UK
[3]Environmental Physics, Institute of Biogeochemistry and Pollutant Dynamics, ETH, CHN E31.2, Universitaetstrasse 16, 8092 Zürich, Switzerland

Received: 16 September 2014 – Accepted: 15 October 2014 – Published:

Correspondence to: J. Martinez-Rey (jorge.martinez-rey@lsce.ipsl.fr)

Published by Copernicus Publications on behalf of the European Geosciences Union.

Abstract

The ocean is a substantial source of nitrous oxide (N_2O) to the atmosphere, but little is known on how this flux might change in the future. Here, we investigate the potential evolution of marine N_2O emissions in the 21st century in response to anthropogenic climate change using the global ocean biogeochemical model NEMO-PISCES. We implemented two different parameterizations of N_2O production, which differ primarily at low oxygen (O_2) conditions. When forced with output from a climate model simulation run under the business-as-usual high CO_2 concentration scenario (RCP8.5), our simulations suggest a decrease of 4 to 12 % in N_2O emissions from 2005 to 2100, i.e., a reduction from 4.03/3.71 to 3.54/3.56 Tg N yr^{-1} depending on the parameterization. The emissions decrease strongly in the western basins of the Pacific and Atlantic oceans, while they tend to increase above the Oxygen Minimum Zones (OMZs), i.e., in the Eastern Tropical Pacific and in the northern Indian Ocean. The reduction in N_2O emissions is caused on the one hand by weakened nitrification as a consequence of reduced primary and export production, and on the other hand by stronger vertical stratification, which reduces the transport of N_2O from the ocean interior to the ocean surface. The higher emissions over the OMZ are linked to an expansion of these zones under global warming, which leads to increased N_2O production associated primarily with denitrification. From the perspective of a global climate system, the averaged feedback strength associated with the projected decrease in oceanic N_2O emissions amounts to around -0.009 W m^{-2} K^{-1}, which is comparable to the potential increase from terrestrial N_2O sources. However, the assesment for a compensation between the terrestrial and marine feedbacks calls for an improved representation of N_2O production terms in fully coupled next generation of Earth System Models.

1 Introduction

Nitrous oxide (N_2O) is a gaseous compound responsible for two key feedback mechanisms within the Earth's climate. First, it acts as a long-lived and powerful greenhouse gas (Prather et al., 2012) ranking third in anthropogenic radiative forcing after carbon dioxide (CO_2) and methane (CH_4) (Myrhe et al., 2013). Secondly, the ozone (O_3) layer depletion in the future might be driven mostly by N_2O after the drastic reductions in CFCs emissions start to show their effect on stratospheric chlorine levels (Ravishankara et al., 2009). The atmospheric concentration of N_2O is determined by the natural balance between sources from land and ocean and the destruction of N_2O in the atmosphere largely by reaction with OH radicals (Crutzen, 1970; Johnston, 1971). The natural sources from land and ocean amount to ~ 6.6 and $3.8\,\mathrm{Tg\,N\,yr^{-1}}$, respectively (Ciais et al., 2013). Anthropogenic activities currently add an additional $6.7\,\mathrm{Tg\,N\,yr^{-1}}$ to the atmosphere that caused atmospheric N_2O to increase by 18 % since pre-industrial times (Ciais et al., 2013), reaching 325 ppb in the year 2012 (NOAA ESRL Global Monitoring Division, Boulder, Colorado, USA, http://esrl.noaa.gov/gmd/).

Using a compilation of 60 000 surface ocean observations of the partial pressure of N_2O (pN_2O), Nevison et al. (1995) computed a global ocean source of $4\,\mathrm{Tg\,N\,yr^{-1}}$, with a large range of uncertainty from 1.2 to $6.8\,\mathrm{Tg\,N\,yr^{-1}}$. Model derived estimates also differ widely, i.e., between 1.7 and $8\,\mathrm{Tg\,N\,yr^{-1}}$ (Nevison et al., 2003; Suntharalingam et al., 2000). These large uncertainties are a consequence of too few observations and of poorly known N_2O formation mechanisms, reflecting a general lack of understanding of key elements of the oceanic nitrogen cycle (Gruber and Galloway, 2008; Zehr and Ward, 2002), and of N_2O in particular (e.g., Zamora et al., 2012; Bange et al., 2009; Freing et al., 2012, among others). A limited number of interior ocean N_2O observations were made available only recently (Bange et al., 2009), but they contain large temporal and spatial gaps. Information on the rates of many important processes remains insufficient, particularly in natural settings. There are only few studies from a limited number of specific regions such as the Arabian Sea, Central and North Pacific, the Bedford Basin and the Scheldt estuary, which can be used to derive and test model parameterizations (Mantoura et al., 1993; Bange et al., 2000; Elkins et al., 1978; Yoshida et al., 1989; Punshon and Moore, 2004; De Wilde and De Bie, 2000).

N_2O is formed in the ocean interior through two major pathways and consumed only in oxygen minimum zones through denitrification (Zamora et al., 2012). The first production pathway is associated with nitrification (conversion of ammonia, NH_4^+, into nitrate, NO_3^-), and occurs when dissolved O_2 concentrations are above $20\,\mu\mathrm{mol\,L^{-1}}$. We subsequently refer to this pathway as the high-O_2 pathway. The second production pathway is associated with a series of processes when O_2 concentrations fall below $\sim 5\,\mu\mathrm{mol\,L^{-1}}$ and involve a combination of nitrification and denitrification (hereinafter referred to as low-O_2 pathway) (Cohen and Gordon, 1978; Goreau et al., 1980; Elkins et al., 1978). As nitrification is one of the processes involved in the aerobic remineralization of organic matter, it occurs nearly everywhere in the global ocean with a global rate at least one order of magnitude larger than the global rate of water column denitrification (Gruber, 2008). A main reason is that denitrification in the water column is limited to the OMZs, which occupy only a few percent of the total ocean volume (Bianchi et al., 2012). This is also the only place in the water column where N_2O is being consumed.

The two production pathways have very different N_2O yields, i.e., fractions of nitrogen-bearing products that are transformed to N_2O. For the high-O_2 pathway, the yield is typically rather low, i.e., only about 1 in several hundred molecules of ammonium escapes as N_2O (Cohen and Gordon, 1979). In contrast, in the low-O_2 pathway, and particularly during denitrification, this fraction may go up to as high as 1 : 1, i.e., that all nitrate is turned into N_2O (Tiedje, 1988). The relative contribution of the two pathways to global N_2O production is not well established. Sarmiento and Gruber (2006) suggested that the two may be of equal importance, but more recent estimates suggest that the high-O_2 production pathway dominates global oceanic N_2O production (Freing et al., 2012).

Two strategies have been pursued in the development of parameterizations for N_2O production in global biogeochemical models. The first approach builds on the impor-

tance of the nitrification pathway and its close association with the aerobic remineralization of organic matter. As a result the production of N_2O and the consumption of O_2 are closely tied to each other, leading to a strong correlation between the concentration of N_2O and the apparent oxygen utilization (AOU). This has led to the development of two sets of parameterizations, one based on concentrations, i.e., directly as a function of AOU (Butler et al., 1989) and the other based on the rate of oxygen utilization, i.e. OUR (Freing et al., 2009). Additional variables have been introduced to allow for differences in the yield, i.e., the ratio of N_2O produced over oxygen consumed, such as temperature (Butler et al., 1989) or depth (Freing et al., 2009). In the second approach, the formation of N_2O is modeled more mechanistically, and tied to both nitrification and denitrification by an O_2 dependent yield (Suntharalingam and Sarmiento, 2000; Nevison et al., 2003; Jin and Gruber, 2003). Since most models do not include nitrification explicitly, the formation rate is actually coupled directly to the remineralization of organic matter. Regardless of the employed strategy, all parameterizations depend to first order on the amount of organic matter that is being remineralized in the ocean interior, which is governed by the export of organic carbon to depth. The dependence of N_2O production on oxygen levels and on other parameters such as temperature only acts at second order. This has important implications not only for the modeling of the present-day distribution of N_2O in the ocean, but also for the sensitivity of marine N_2O to future climate change.

Over this century, climate change will perturb marine N_2O formation in multiple ways. Changes in productivity will drive changes in the export of organic matter to the ocean interior (Steinacher et al., 2010; Bopp et al., 2013) and hence affect the level of marine nitrification. Ocean warming might increase the rate of N_2O production during nitrification. Changes in carbonate chemistry (Bindoff et al., 2007) might cause changes in the C : N ratio of the exported organic matter (Riebesell et al., 2007), altering not only the rates of nitrification, but also the ocean interior oxygen levels (Gehlen et al., 2011). Finally, the expected general loss of oxygen (Keeling et al., 2010; Cocco et al., 2012; Bopp et al., 2013) could substantially affect denitrification and the N_2O production.

Models used for IPCC's 4th assessment report estimated a decrease between 2 and 13 % in primary production (PP) under the business-as-usual high CO_2 concentration scenario A2 (Steinacher et al., 2010). A more recent multi-model analysis based on the models used in IPCC's 5th assessment report also suggest a large reduction of PP down to 18 % by 2100 for the RCP8.5 scenario (Bopp et al., 2013). In these simulations, the export of organic matter is projected to decrease between 6 and 18 % in 2100 (Bopp et al., 2013), with a spatially distinct pattern: in general, productivity and export are projected to decrease at mid- to low-latitudes in all basins, while productivity and export are projected to increase in the high-latitudes and in the South Pacific subtropical gyre (Bopp et al., 2013). A wider spectrum of responses was reported regarding changes in the ocean oxygen content. While all models simulate decreased oxygen concentrations in response to anthropogenic climate change (by about 2 to 4 % in 2100), and particularly in the mid-latitude thermocline regions, no agreement exists with regard to the hypoxic regions, i.e., those having oxygen levels below 60 $\mu mol\,L^{-1}$ (Cocco et al., 2012; Bopp et al., 2013). Some models project these regions to expand, while others project a contraction. Even more divergence in the results exists for the suboxic regions, i.e., those having O_2 concentrations below 5 $\mu mol\,L^{-1}$ (Keeling et al., 2010; Deutsch et al., 2011; Cocco et al., 2012; Bopp et al., 2013), although the trend for most models is pointing towards an expansion. At the same time, practically none of the models is able to correctly simulate the current distribution of oxygen in the OMZ (Bopp et al., 2013). In summary, while it is clear that major changes in ocean biogeochemistry are looming ahead (Gruber, 2011), with substantial impacts on the production and emission of N_2O, our ability to project these changes with confidence is limited.

In this study, we explore the implications of these future changes in ocean physics and biogeochemistry on the marine N_2O cycle, and make projections of the oceanic N_2O emissions from year 2005 to 2100 under the high CO_2 concentration scenario RCP8.5. We analyze how changes in biogeochemical and physical processes such as net primary production (NPP), export production and vertical stratification in this cen-

tury translate into changes in oceanic N_2O emissions to the atmosphere. To this end, we use the NEMO-PISCES ocean biogeochemical model, which we have augmented with two different N_2O parameterizations, permitting us to evaluate changes in the marine N_2O cycle at the process level, especially with regard to production pathways in high and low oxygen regimes. We demonstrate that while future changes in the marine N_2O cycle will be substantial, the net emissions of N_2O appear to change relatively little, i.e., they are projected to decrease by about 10 % in 2100.

2 Methodology

2.1 NEMO-PISCES model

Future projections of the changes in the oceanic N_2O cycle were performed using the PISCES ocean biogeochemical model (Aumont and Bopp, 2006) in offline mode with physical forcings derived from the IPSL-CM5A-LR coupled model (Dufresne et al., 2013). The horizontal resolution of NEMO ocean general circulation model is $2° \times 2° \cos Ø$ (Ø being the latitude) with enhanced latitudinal resolution at the equator of 0.5°. PISCES is a biogeochemical model with five nutrients (NO_3, NH_4, PO_4, Si and Fe), two phytoplankton groups (diatoms and nanophytoplankton), two zooplankton groups (micro and mesozooplankton), and two non-living compartments (particulate and dissolved organic matter). Phytoplankton growth is limited by nutrient availability and light. Constant Redfield C : N : P ratios of 122 : 16 : 1 are assumed (Takahashi et al., 1985), while all other ratios, i.e., those associated with chlorophyll, iron, and silicon (Chl : C, Fe : C and Si : C) vary dynamically.

2.2 N_2O parameterizations in PISCES

We implemented two different parameterizations of N_2O production in NEMO-PISCES. The first one, adapted from Butler et al. (1989) follows the oxygen consumption approach, with a temperature dependent modification of the N_2O yield (P.TEMP). The second one is based on Jin and Gruber (2003) (P.OMZ), following the more mechanistic approach, i.e., it considers the different processes occurring at differing oxygen concentrations in a more explicit manner.

The P.TEMP parameterization assumes that the N_2O production is tied to nitrification only with a yield that is at first order constant. This is implemented in the model by tying the N_2O formation in a linear manner to O_2 consumption. A small temperature dependence is added to the yield to reflect the potential impact of temperature on metabolic rates. The production term of N_2O, i.e., $J^{\mathrm{P.TEMP}}(N_2O)$, is then mathematically formulated as:

$$J^{\mathrm{P.TEMP}}(N_2O) = (\gamma + \theta T) J(O_2)_{\mathrm{consumption}} \quad (1)$$

where γ is a background yield (0.53×10^{-4} mol N_2O (mol O_2 consumed)$^{-1}$), θ is the temperature dependency of γ (4.6×10^{-6} mol N_2O (mol O_2)$^{-1}$ K^{-1}), T is temperature (K), and $J(O_2)_{\mathrm{consumption}}$ is the sum of all biological O_2 consumption terms within the model. Although this parameterization is very simple, a recent analysis of N_2O observations supports such an essentially constant yield, even in the OMZ of the Eastern Tropical Pacific (Zamora et al., 2012).

The P.OMZ parameterization, formulated after Jin and Gruber (2003), assumes that the overall yield consists of a constant background yield and an oxygen dependent yield. The former is presumed to represent the N_2O production by nitrification, while the latter is presumed to reflect the enhanced production of N_2O at low oxygen concentrations, in part driven by denitrification, but possibly including nitrification as well. This parameterization includes the consumption of N_2O in suboxic conditions. This gives:

$$J^{\mathrm{P.OMZ}}(N_2O) = (\alpha + \beta f(O_2)) J(O_2)_{\mathrm{consumption}} - k N_2O \quad (2)$$

where α is, as in Eq. (1), a background yield (0.9×10^{-4} mol N_2O (mol O_2 consumed)$^{-1}$), β is a yield parameter that scales the oxygen dependent function (6.2×10^{-4}), $f(O_2)$

is a unitless oxygen-dependent step-like modulating function, as suggested by laboratory experiments (Goreau et al., 1980) (Fig. S1, Supplement), and k is the 1st order rate constant of N_2O consumption close to anoxia (zero otherwise). For k, we have adopted a value of 0.138 yr^{-1} following Bianchi et al. (2012) while we set the consumption regime for O_2 concentrations below 5 $\mu mol\,L^{-1}$.

The P.OMZ parameterization permits us to separately identify the N_2O formation pathways associated with nitrification and those associated with low-oxygen concentrations (nitrification/denitrification). Specifically, we consider the source term $\alpha J(O_2)_{consumption}$ as that associated with the nitrification pathway, while we associated the source term $\beta f(O_2) J(O_2)_{consumption}$ with the low-oxygen processes (Fig. S2, Supplement).

We employ a standard bulk approach for simulating the loss of N_2O to the atmosphere via gas exchange. We use the formulation of Wanninkhof et al. (1992) for estimating the gas transfer velocity, adjusting the Schmidt number for N_2O and using the solubility constants of N_2O given by Weiss and Price (1980). We assume a constant atmospheric N_2O concentration of 284 ppb in all simulations.

2.3 Experimental design

NEMO-PISCES was first spun up during 3000 years using constant pre-industrial dynamical forcings fields from IPSL-CM5A-LR (Dufresne et al., 2013) without activating the N_2O parameterizations. This spin-up phase was followed by a 150 yr long simulation, forced by the same dynamical fields now with N_2O production and N_2O sea-to-air flux embedded. The N_2O concentration at all grid points was prescribed initially to 20 $nmol\,L^{-1}$, which is consistent with the MEMENTO database average value of 18 $nmol\,L^{-1}$ below 1500 m (Bange et al., 2009). During the 150 yr spin-up, we diagnosed the total N_2O production and N_2O sea-to-air flux and adjusted the α, β, γ and θ parameters in order to achieve a total N_2O sea-to-air flux in the two parameterizations at equilibrium close to 3.85 $Tg\,N\,yr^{-1}$ (Ciais et al., 2013). In addition, the relative contribution of the high-O_2 pathway in the P.OMZ parameterization was set to 75 % of the total N_2O production. This assumption is based on growing evidence that nitrification is the dominant pathway of N_2O production on a global scale, based on estimations considering N_2O production along with water mass transport (Freing et al., 2012).

Projections in NEMO-PISCES of historical (from 1851 to 2005) and future (from 2005 to 2100) simulated periods were done using dynamical forcing fields from IPSL-CM5A-LR. These dynamical forcings were applied in an offline mode, i.e. monthly means of temperature, velocity, wind speed or radiative flux were used to force NEMO-PISCES. Future simulations used the business-as-usual high CO_2 concentration scenario (RCP8.5) until year 2100. Century scale model drifts for all the biogeochemical variables presented, including N_2O sea-to-air flux, production and inventory, were removed using an additional control simulation with IPSL-CM5A-LR pre-industrial dynamical forcing fields from year 1851 to 2100. Despite the fact that primary production and the export of organic matter to depth were stable in the control simulation, the air–sea N_2O emissions drifted (an increase of 5 to 12 % in 200 yr depending on the parameterization) due to the short spin-up phase (150 yr) and to the choice of the initial conditions for N_2O concentrations.

3 Present-day oceanic N_2O

3.1 Contemporary N_2O fluxes

The model simulated air–sea N_2O emissions show large spatial contrasts, with flux densities varying by one order of magnitude, but with relatively small differences between the two parameterizations (Fig. 1a and b). This is largely caused by our assumption that the dominant contribution (75 %) to the total N_2O production in the P.OMZ parameterization is the nitrification pathway, which is then not so different from the P.TEMP parameterization, where it is 100 %. As a result, the major part of N_2O is produced close to the subsurface via nitrification, contributing directly to imprint changes

into the sea-to-air N_2O flux without a significant meridional transport (Suntharalingam and Sarmiento, 2000).

Elevated N_2O emission regions ($> 50\,mg\,N\,m^{-2}\,yr^{-1}$) are found in the Eastern Tropical Pacific, in the northern Indian ocean, in the northwestern Pacific, in the North Atlantic and in the Agulhas Current. In contrast, low fluxes ($< 10\,mg\,N\,m^{-2}\,yr^{-1}$) are simulated in the Atlantic and Pacific subtropical gyres and southern Indian Ocean.

The regions of high N_2O emissions are in both parameterizations generally consistent with the data product of Nevison et al. (1995) (Fig. 1c), especially in the equatorial latitudes. The largest discrepancies occur in the North Pacific and Southern Ocean. The high N_2O emissions observed in the North Pacific are not well represented by our model, with a significant shift towards the western part of the Pacific basin, similar to other modeling studies (e.g., Goldstein et al., 2003; Jin and Gruber, 2003). The OMZ, located at approximately 600 m deep in the North Pacific, might be underestimated in our model, which in turn might suppress one potential N_2O source. Minor discrepancies between model and observations also occur in the Southern Ocean, a region whose role in global N_2O fluxes remains debated due to the lack of observations and the occurrence of potential artifacts due to interpolation techniques (e.g., Suntharalingam and Sarmiento, 2000; Nevison et al., 2003). In particular, the modeled N_2O flux maxima peak at around 40° S, i.e., around 10° N to that estimated by Nevison et al. (1995) (Fig. 1d).

3.2 Contemporary N_2O concentrations and the relationship to O_2

The model results at present day were evaluated against the MEMENTO database (Bange et al., 2009), which contains about 25 000 measurements of co-located N_2O and dissolved O_2 concentrations. Table 1 summarizes the SD and correlation coefficients for P.TEMP and P.OMZ compared to MEMENTO. The SD of the model output is very similar to MEMENTO, i.e., around $16\,nmol\,L^{-1}$ of N_2O. However, the correlation coefficients between the sampled data points from MEMENTO and P.TEMP/P.OMZ are 0.49 and 0.42, respectively.

Figure 2 compares the global average vertical profile of the observed N_2O against the results from the two parameterisations. The in-situ observations show three characteristic layers: the upper 100 m layer with low ($\sim 10\,nmol\,L^{-1}$) N_2O concentration due to gas exchange keeping N_2O close to its saturation concentration, the mesopelagic layer, between 100 and 1500 m, where N_2O is enriched via nitrification and denitrification in the OMZs, and the deep ocean beyond 1500 m, with a relatively constant concentration of $18\,nmol\,L^{-1}$ on average. Both parameterizations underestimate the N_2O concentration in the upper 100 m, where most of the N_2O is potentially outgassed to the atmosphere. In the second layer, P.OMZ shows a good correlation with the observations, whereas P.TEMP is too low by $\sim 10\,nmol\,L^{-1}$. Below 1500 m, both parameterizations simulate too high N_2O compared to the observations. This may be caused by the lack or underestimation of a sink process in the deep ocean, or by the too high concentrations used to intialize the model, which persist due to the rather short spin-up time of only 150 yr.

The analysis of the model simulated N_2O concentrations as a function of model simulated O_2 shows the differences between the two parameterizations more clearly (Fig. 3a and b). Such a plot allows us to assess the model performance with regard to N_2O (Jin and Gruber, 2003), without being subject to the strong potential biases introduced by the model's deficiencies in simulating the distribution of O_2. This is particularly critical in the OMZs, where all models exhibit strong biases (Cocco et al., 2012; Bopp et al., 2013) (see also Fig. 3c). P.TEMP (Fig. 3a) slightly overestimates N_2O for dissolved O_2 concentrations above $100\,\mu mol\,L^{-1}$, and does not fully reproduce neither the high N_2O values in the OMZs nor the N_2O depletion when O_2 is almost completely consumed. P.OMZ (Fig. 3b) overestimates the N_2O concentration over the whole range of O_2, with particularly high values of N_2O above $100\,nmol\,L^{-1}$ due to the exponential function used in the OMZs. There, the observations suggest concentrations below $80\,nmol\,L^{-1}$ for the same low O_2 values, consistent with the linear trend observed for higher O_2, which seems to govern over most of the O_2 spectrum, as suggested by Zamora et al. (2012). The discrepancy at low O_2 concentration may also stem from

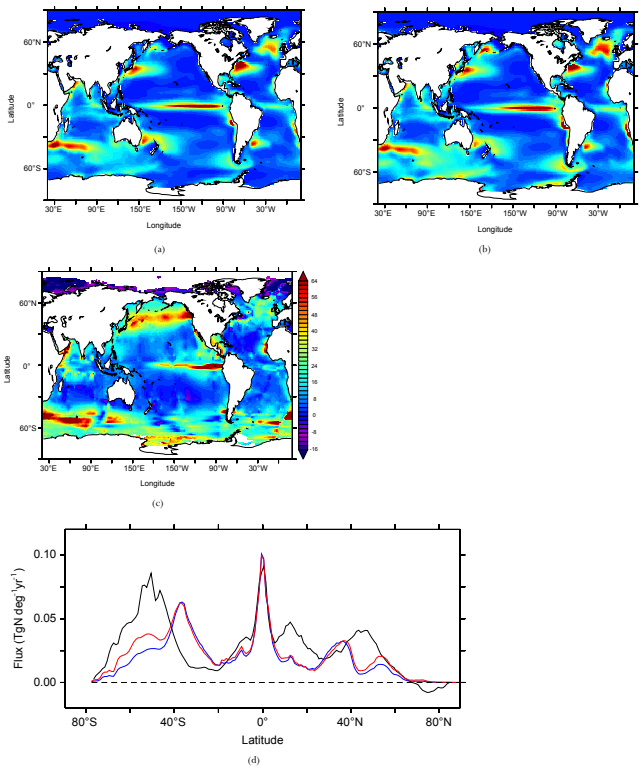

Figure 1. N_2O sea-to-air flux (in mg N m^{-2} yr^{-1}) from **(a)** P.TEMP parameterzation averaged for the 1985 to 2005 time period in the historical simulation, **(b)** P.OMZ parameterization over the same time period, **(c)** data product of Nevison et al. (1995) and **(d)** latitudinal N_2O sea-to-air flux (in Tg N deg^{-1} yr^{-1}) from Nevison et al. (1995) (black), P.TEMP (blue) and P.OMZ (red).

Table 1. SD and correlation coefficients between P.TEMP and P.OMZ parameterizations with respect to MEMENTO database observations (Bange et al., 2009).

	P.TEMP	P.OMZ	OBS
SD (in nmol N_2O L^{-1})	12	18	16
Correlation coefficient with obs.	0.49	0.42	–

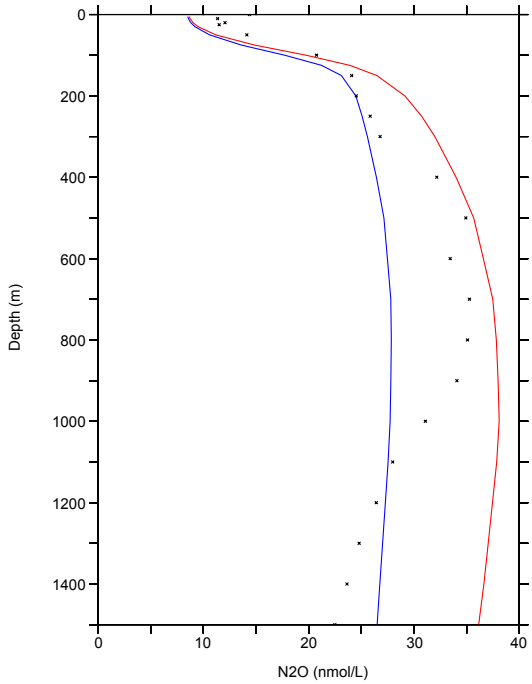

Figure 2. Global average depth profile of N_2O concentration (in nmol L^{-1}) from the MEMENTO database (dots) (Bange et al., 2009), P.TEMP (blue) and P.OMZ (red). Model parameterizations are averaged over the 1985 to 2005 time period from the historical simulation.

our choice of a too low N_2O consumption rate under essentially anoxic conditions. The O_2 distribution in the model (Fig. 3c) shows a deficient representation of the OMZs, with higher concentrations than those from observations in the oxygen-corrected World Ocean Atlas (Bianchi et al., 2012). The rest of the O_2 spectrum is well represented in our model. Finally, it should be considered that most of the MEMENTO data points are from OMZs and therefore N_2O measurements could be biased towards higher values than the actual open ocean average, where our model performs better.

4 Future oceanic N_2O

4.1 N_2O sea-to-air flux

The global oceanic N_2O emissions decrease relatively little over the next century (Fig. 4a) between 4 and 12 %. Namely, in P.TEMP, the emissions decrease by 0.15 from 3.71 Tg N yr^{-1} in 1985–2005 to 3.56 Tg N yr^{-1} in 2080–2100 and in P.OMZ, the decrease is slightly larger at 12 % i.e., amounting to 0.49 Tg N yr^{-1} from 4.03 to 3.54 Tg N yr^{-1}. Notable is also the presence of a negative trend in N_2O emissions over the 20th century, most pronounced in the P.OMZ parameterization. Considering the change over the 20th and 21st centuries together, the decreases increase to 7 and 15 %.

These relatively small global decreases mask more substantial changes at the regional scale, with a mosaic of regions experiencing a substantial increase and regions experiencing a substantial decrease (Fig. 4b and c). In both parameterizations, the oceanic N_2O emissions decrease in the northern and south western oceanic basins (e.g., the North Atlantic and Arabian Sea), by up to 25 mg N m^{-2} yr^{-1}. In contrast, the fluxes are simulated to increase in the Eastern Tropical Pacific and in the Bay of Bengal. For the Benguela Upwelling System (BUS) and the North Atlantic a bi-modal pattern emerges in 2100. As was the case for the present-day distribution of the N_2O fluxes,

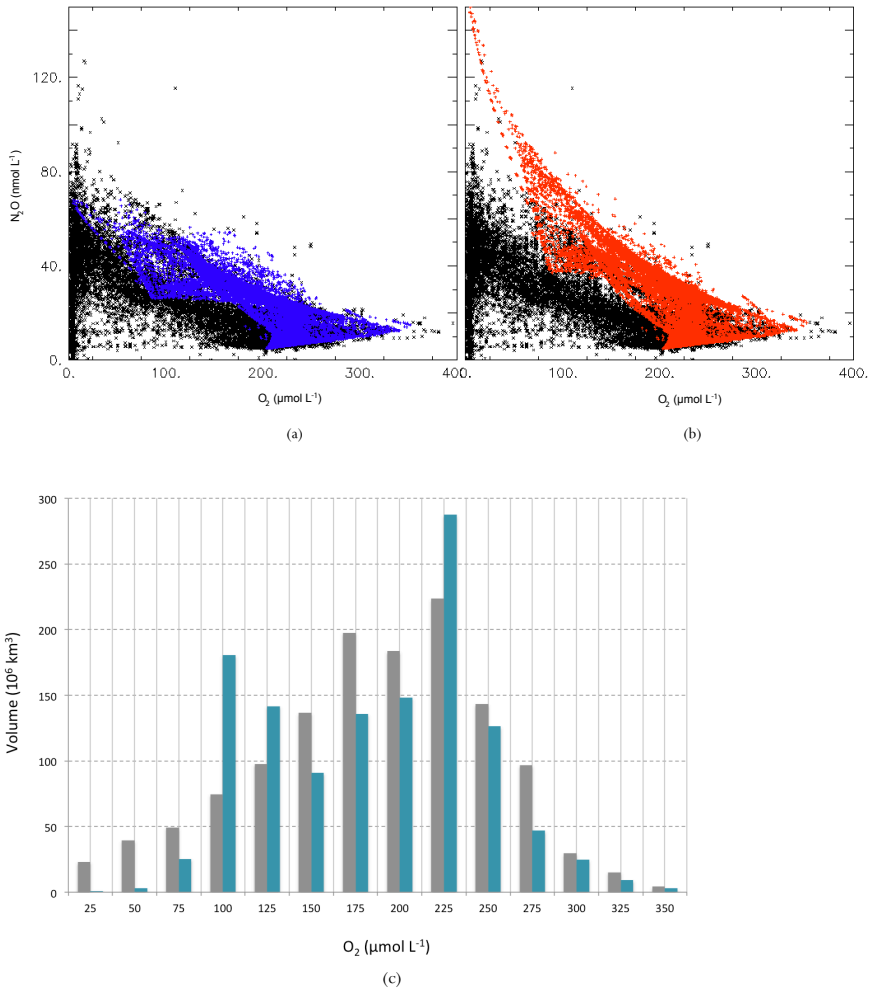

Figure 3. Relationship between O_2 concentration (in $\mu mol\,L^{-1}$) and N_2O concentration (in $nmol\,L^{-1}$) in the MEMENTO database (black) (Bange et al., 2009), compared to model **(a)** P.TEMP (blue) and **(b)** P.OMZ (red) parameterizations averaged over the 1985 to 2005 time period from the historical simulation. **(c)** Distribution of O_2 concentration in NEMO-PISCES 1985 to 2005 averaged time period (blue) compared to the oxygen corrected World Ocean Atlas (grey) from Bianchi et al. (2012).

the overall similarity between the two parameterizations is a consequence of the dominance of the nitrification (high-O_2) pathway in both parameterizations.

Nevertheless there are two regions where more substantial differences between the two parameterizations emerge: the region overlying the oceanic OMZ at the BUS and the Southern Ocean. In particular, the P.TEMP parameterization projects a larger enhancement of the flux than P.OMZ at the BUS, whereas the emissions in the Southern Ocean are enhanced in the P.OMZ parameterization.

4.2 Drivers of changes in N_2O emissions

The changes in N_2O emissions may stem from a change in net N_2O production, a change in the transport of N_2O from its location of production to the surface, or any combination of the two, which includes also changes in N_2O storage. Next we determine the contribution of these mechanisms to the overall decrease in N_2O emissions that our model simulated for the 21st century.

4.2.1 Changes in N_2O production

In both parameterizations, global N_2O production is simulated to decrease over the 21st century. The total N_2O production in P.OMZ decreases by 0.41 $Tg\,N\,yr^{-1}$ in 2080–2100 compared to the mean value over 1985–2005 (Fig. 5a). The parameterization P.OMZ allows to isolate the contributions of high- and low-O_2 and will be analysed in greater detail in the following sections. N_2O production via the high-O_2 pathway in P.OMZ decreases in the same order than total production, by 0.35 $Tg\,N\,yr^{-1}$ in 2080–2100 compared to present. The N_2O production in the low-O_2 regions remains almost constant across the experiment. In P.TEMP parameterization, the reduction in N_2O production is much weaker than in P.OMZ due to the effect of the increasing temperature. N_2O production decreases by 0.07 $Tg\,N\,yr^{-1}$ in 2080–2100 compared to present (Fig. 5b).

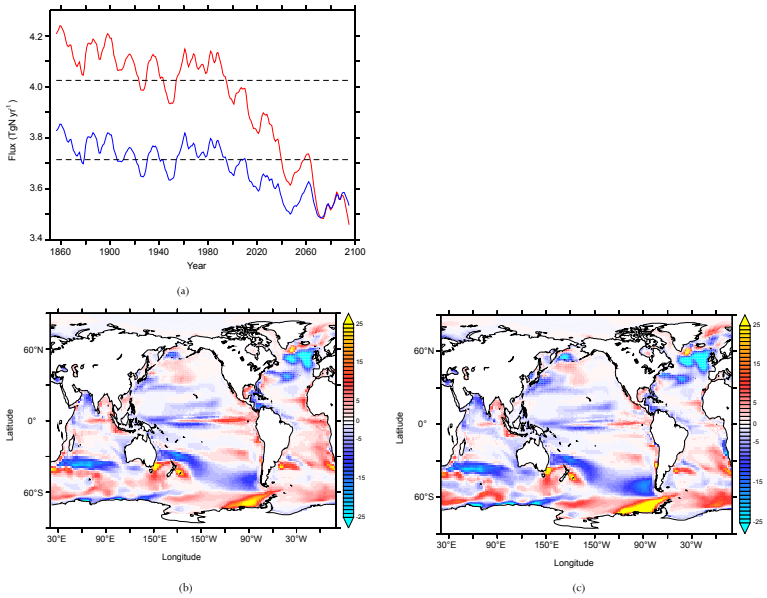

Figure 4. (a) N_2O sea-to-air flux (in $Tg\,N\,yr^{-1}$) from 1851 to 2100 in P.TEMP (blue) and P.OMZ (red) using the historical and future RCP8.5 simulations. Dashed lines indicate the mean value over the 1985 to 2005 time period. Change in N_2O sea-to-air flux ($mg\,N\,m^{-2}\,yr^{-1}$) from the averaged 2080–2100 to 1985–2005 time periods in future RCP8.5 and historical simulations in **(b)** P.TEMP and **(c)** P.OMZ parameterizations.

The vast majority of the changes in the N_2O production in the P.OMZ parameterization is caused by the high-O_2 pathway with virtually no contribution from the low-O_2 pathway (Fig. 5a). As the N_2O production in this pathway is solely driven by changes in the O_2 consumption (Eq. 2), which in our model is directly linked to export production, the dominance of this pathway implies that primary driver for the future changes in N_2O production in our model is the decrease in export of organic matter (CEX). It was simulated to decrease by $0.97\,Pg\,C\,yr^{-1}$ in 2100, and the high degree of correspondence in the temporal evolution of export and N_2O production in Fig. 5a confirms this conclusion.

The close connection between N_2O production associated with the high-O_2 pathway and changes in export production is also seen spatially (Fig. 5c), where the spatial pattern of changes in export and changes in N_2O production are extremely highly correlated (shown by stippling). Most of the small deviations are caused by lateral advection of organic carbon, causing a spatial separation between changes in O_2 consumption and changes in organic matter export.

As there is an almost ubiquitous decrease of export in all of the major oceanic basins except at high latitudes, N_2O production decreases overall as well. Hotspots of reductions exceeding $-10\,mg\,N\,m^{-2}\,yr^{-1}$ are found in the North Atlantic, the western Pacific and Indian basins (Fig. 5c). The fewer places where export increases, are also the locations of enhanced N_2O production. For example, a moderate increase of $3\,mg\,N\,m^{-2}\,yr^{-1}$ is projected in the Southern Ocean, South Atlantic and Eastern Tropical Pacific. The general pattern of export changes, i.e., decreases in lower latitudes, increase in higher latitudes, is consistent generally with other model projection patterns (Bopp et al., 2013), although there exist very strong model-to-model differences at the more regional scale.

Although the global contribution of the changes in the low-O_2 N_2O production is small, this is the result of regionally compensating trends. In the model's OMZs, i.e., in the Eastern Tropical Pacific and in the Bay of Bengal, a significant increase in N_2O production is simulated in these locations (Fig. 5d), with an increase of more than $15\,mg\,N\,m^{-2}\,yr^{-1}$. This increase is primarily driven by the expansion of the OMZs in our model (shown by stippling), while changes in export contribute less. In effect, NEMO-PISCES projects a 20 % increase in the hypoxic volume globally, from 10.2 to $12.3 \times 10^6\,km^3$, and an increase in the suboxic volume from 1.1 to $1.6 \times 10^6\,km^3$ in 2100 (Fig. 5e). Elsewhere, the changes in the N_2O production through the low-O_2 pathway are dominated by the changes in export, thus following the pattern of the changes seen in the high-O_2 pathway. Overall these changes are negative, and happen to nearly completely compensate the increase in production in the OMZs, resulting in the near constant global N_2O production by the low-O_2 production pathway up to year 2100.

4.2.2 Changes in storage of N_2O

A steady increase in the N_2O inventory is observed from present to 2100. The pool of oceanic N_2O down to 1500 m, i.e., potentially outgassed to the atmosphere, increases by 8.9 Tg N from 1985–2005 to year 2100 in P.OMZ, whereas P.TEMP is less sensitive to changes with an increase of 4.0 Tg N on the time period considered (Fig. 6a).

This increase in storage of N_2O in the ocean interior shows an homogeneous pattern for P.TEMP, with particular hotspots in the North Pacific, North Atlantic and the eastern boundary currents in the Pacific (Fig. 6b). The spatial variability is more pronounced in P.OMZ (Fig. 6c), related in part to the enhanced production associated with OMZs. Most of the projected changes in storage are associated with shoaling of the mixed layer depth (shown by stippling), suggesting that increase in N_2O inventories is caused by increased ocean stratification. Enhanced ocean stratification, in turn, occurs in response to increasing sea surface temperatures associated with global warming (Sarmiento et al., 2004).

4.2.3 Effects of the combined mechanisms on N_2O emissions

The drivers of the future evolution of oceanic N_2O emissions emerge from the preceding analysis. Firstly, a decrease in the high-O_2 production pathway driven by a reduced

organic matter remineralization reduces N_2O concentrations below the euphotic zone. Secondly, the increased N_2O inventory at depth is caused by increased stratification and therefore to a less efficient transport to the sea-to-air interface, leading to a less N_2O flux.

The global changes in N_2O flux, N_2O production and N_2O storage for P.OMZ are presented in Fig. 7. Changes in N_2O flux and N_2O production are mostly of the same sign in almost all of the oceanic regions in line with the assumption of nitrification being the dominant contribution to N_2O production. Changes in N_2O production close to the subsurface are translated into corresponding changes in N_2O flux. There is only one oceanic region (Sub-Polar Pacific) where this correlation does not occur. N_2O inventory increases in all of the oceanic regions. The increase in inventory is particularly pronounced at low latitudes along the eastern boundary currents in the Equatorial and Tropical Pacific. Figure 7 shows how almost all the relevant changes in N_2O production and storage are related to low-latitude processes, with little or no contribution from changes in polar regions.

The synergy among the driving mechanisms can be explored with a box model pursuing two objectives. First, to reproduce future projections assuming that the only mechanisms ruling the N_2O dynamics in the future were those that we have proposed in our hypothesis, i.e., increased stratification and reduction of N_2O production in high-O_2 regions. Secondly, to explore a wider range of values for both mixing (i.e., degree of stratification) and efficiency of N_2O production in high-O_2 conditions.

To this end, a box model was designed to explore the response of oceanic N_2O emissions to changes in export of organic matter (hence N_2O production only in high-O_2 conditions) and changes in the mixing ratio between deep (> 100 m) and surface (< 100 m) layers. We divided the water column into two compartments: a surface layer in the upper 100 m where 80 % of surface N_2O concentration is outgassed to the atmosphere (Eq. 3), and a deeper layer beyond 100 m, where N_2O is produced from remineralization as a fraction of the organic matter exported in the ocean interior (Eq. 4). The N_2O reservoirs in the surface and in the deep layer are allowed to exchange. The exchange is regulated by a mixing coefficient v:

$$\text{surface } N_2O; \quad \frac{dN_2O^s}{dt} = -v \cdot \left(N_2O^s - N_2O^d\right) - \kappa \cdot N_2O^s \tag{3}$$

$$\text{deep } N_2O; \quad \frac{dN_2O^d}{dt} = v \cdot \left(N_2O^s - N_2O^d\right) + \varepsilon \cdot \Phi^{POC} \tag{4}$$

where N_2O^s is N_2O in the surface, N_2O^d is N_2O in the deep reservoir, Φ^{POC} is the flux of POC into the lower compartment, v is the mixing coefficient between both compartments, k is the fraction of N_2O^s outgassed to the atmosphere and ε the fraction of POC leading to N_2O^d formation (Fig. S3 and Table S1, Supplement). Equations (3) and (4) are solved for a combination of POC fluxes and mixing coefficients, reflecting the increasing stratification and the decrease in export production projected by year 2100 (Sarmiento et al., 2004; Bopp et al., 2013).

A decrease in the N_2O flux is observed for a wide range of boundary conditions simulating reduced mixing and export of POC (Fig. 8a). The equivalent of the transient NEMO-PISCES simulation, i.e., a −10 % decrease in N_2O flux, is achieved for a −8 % decrease in export in the box model. The most extreme scenario explored with the box model suggests a −20 % decrease in N_2O flux, although these associated values of mixing and export are clearly unrealistic, from a nearly total stagnation of ocean circulation between the deep and surface layers to an attenuation of export of −20 % in the global ocean.

The projected increase in N_2O storage in the deep reservoir is reproduced by the box model (Fig. 8b) at a wide range of changes particularly in mixing. Changes in mixing dominate over changes in export as drivers of the increase in the N_2O reservoir at depth. A 25 % decrease in mixing leads to an increase in storage similar to the one projected with NEMO-PISCES (+10 %), independently of changes in export of organic matter.

In general, the interplay between mixing and export of organic matter operates differently when N_2O flux or N_2O inventory are considered. The box model experiment

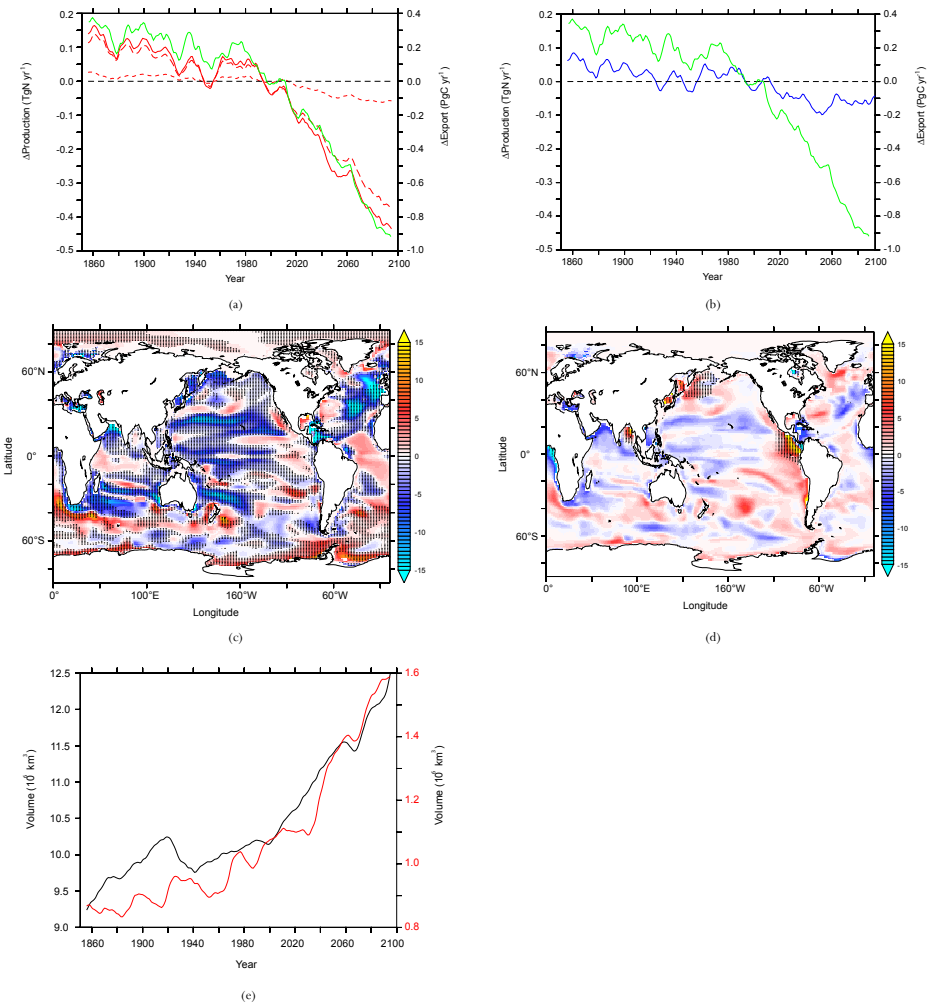

Figure 5. (a) Anomalies in export of organic matter at 100 m (green), low-O_2 production pathway (short dashed red), high-O_2 production pathway (long dashed red) and total P.OMZ production (red) from 1851 to 2100 using the historical and future RCP8.5 simulations. **(b)** Anomalies in export of organic matter at 100 m (green) and P.TEMP production (blue) over the same time period. **(c)** Change in high-O_2 production pathway of N_2O (in $mg\,N\,m^{-2}\,yr^{-1}$) in the upper 1500 m between 2080–2100 to 1985–2005 averaged time periods. Hatched areas indicate regions where change in export of organic matter at 100 m deep have the same sign as in changes in high-O_2 production pathway. **(d)** Change in low-O_2 production pathway of N_2O (in $mg\,N\,m^{-2}\,yr^{-1}$) in the upper 1500 m between 2080–2100 to 1985–2005 averaged time periods. Hatched areas indicate regions where oxygen minimum zones ($O_2 < 5\,\mu mol\,L^{-1}$) expand. **(e)** Volume (in $10^6\,km^3$) of hypoxic (black, $O_2 < 60\,\mu mol\,L^{-1}$) and suboxic (red, $O_2 < 5\,\mu mol\,L^{-1}$) areas in the 1851 to 2100 period in NEMO-PISCES historical and future RCP8.5 simulations.

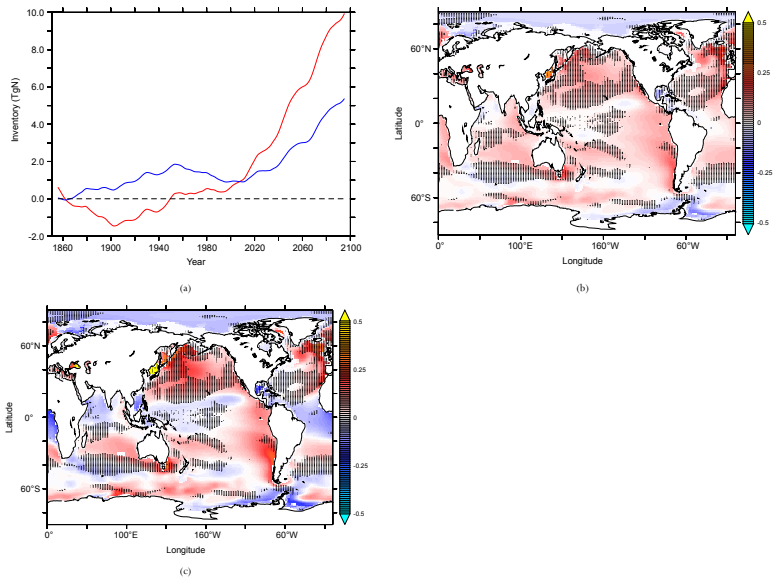

Figure 6. (a) Anomalies in N_2O inventory (in Tg N) from 1851 to 2100 in P.TEMP (blue) and P.OMZ (red) using the historical and future RCP8.5 simulations in the upper 1500 m. Change in vertically integrated N_2O concentration (in mg N m^{-2}) in the upper 1500 m using NEMO-PISCES model mean from the averaged 2080–2100 to 1985–2005 time periods in future RCP8.5 and historical scenarios respectively in **(b)** P.TEMP and **(c)** P.OMZ. Hatched areas indicate regions where mixed layer depth is reduced by more than 5 m in 2080–2100 compared to 1985–2005.

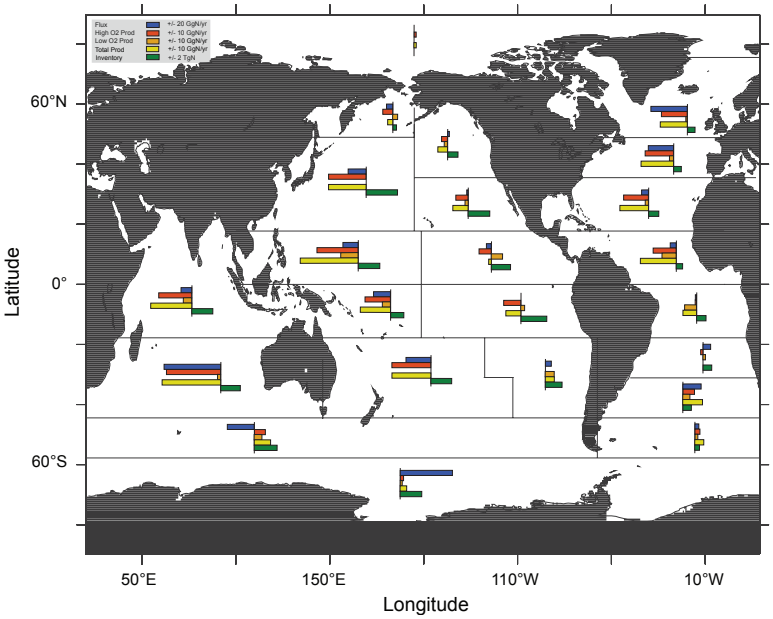

Figure 7. Change in the whole water column in N_2O sea-to-air flux (blue), high-O_2 production pathway (red), low-O_2 production pathway (orange), total N_2O production (yellow) and N_2O inventory (green) for P.OMZ from the averaged 2080–2100 to present 1985–2005 averaged time period in the NEMO-PISCES historical and future RCP8.5 simulations (based on Mikaloff-Fletcher et al. (2006) oceanic regions).

suggests that the evolution of the N_2O reservoir is driven almost entirely by changes in mixing, while changes of mixing and export of organic matter have similar relevance when modulating N_2O emissions.

5 Caveats in estimating N_2O using ocean biogeochemical models

The use of O_2 consumption as a proxy for the actual N_2O production expand the uncertainties in N_2O model estimations. Future model development should aim at the implementation of mechanistic parameterizations of N_2O production based on nitrification and denitrification rates. Further, in order to determine accurate O_2 boundaries for both N_2O production and N_2O consumption at the core of OMZs additional measurements and microbial experiments are needed. The contribution of the high-O_2 pathway that was considered in this model analysis might be a conservative estimate. Freing et al. (2012) suggested that the high-O_2 pathway could be responsible of 93 % of the total N_2O production. Assuming that changes in the N_2O flux are mostly driven by N_2O production via nitrification, that would suggest a larger reduction in the marine N_2O emissions in the future. Moreover, Zamora et al. (2012) observed a higher than expected N_2O consumption at the core of the OMZ in the Eastern Tropical Pacific, occurring at an upper threshold of 10 µmol L^{-1}. The contribution of OMZs to total N_2O production remains an open question. N_2O formation associated with OMZs might be counterbalanced by its own local consumption, leading to the attenuation of the only increasing source of N_2O attributable to the projected future expansion of OMZs (Steinacher et al., 2010; Bopp et al., 2013). Finally, the accurate representation of subsurface O_2 concentration remains as a major challenge for ocean biogeochemical models, as shown by Bopp et al. (2013).

The combined effect of climate change and ocean acidification has not been analyzed in this study. N_2O production processes might be altered by the response of nitrification to increasing levels of seawater pCO_2 (Huesemann et al., 2002; Beman et al., 2011). Beman et al. (2011) reported a reduction in nitrification in response to decreasing pH. This result suggests that N_2O production might decrease beyond what we have estimated only due to climate change. Conversely, negative changes in the ballast effect could potentially reinforce nitrification at shallow depth in response to less efficient POC export to depth and shallow remineralization (Gehlen et al., 2011). Regarding N_2O formation via denitrification, changes in seawater pH as a consequence of higher levels of CO_2 might not be substantial enough to change the N_2O production efficiency, assuming a similar response of marine denitrifiers as reported for denitrifying bacteria have in terrestrial systems (Liu et al., 2010). Finally, the C : N ratio in export production (Riebesell et al., 2007) might increase in response to ocean acidification, potentially leading to a greater expansion of OMZs than simulated here (Oschlies et al., 2008; Tagliabue et al., 2011), and therefore to enhanced N_2O production associated with the low-O_2 pathway.

Changes in atmospheric nitrogen deposition have not been considered in this study. It has been suggested that due to anthropogenic activities the additional amount of reactive nitrogen in the ocean could fuel primary productivity and N_2O production. Estimates are however low, around 3–4 % of the total oceanic emissions (Suntharalingam et al., 2012).

Longer simulation periods could reveal additional effects on N_2O transport beyond changes in upwelling or meridional transport of N_2O close to the subsurface (Suntharalingam and Sarmiento, 2000). Eventual ventilation of the N_2O reservoir at high latitudes could shed light into the role of upwelling regions as an important source of N_2O. Additional studies using other ocean biogeochemical models might also yield alternative values using the same parameterizations. N_2O production is particularly sensitive to the distribution and magnitude of export of organic matter and O_2 fields defined in models.

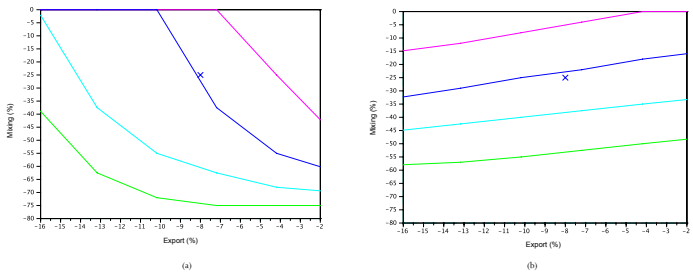

Figure 8. Constant regimes of **(a)** N_2O sea-to-air flux (in percentage of the historical flux: 95 % pink, 90 % blue, 85 % cyan and 80 % green) and **(b)** N_2O concentration in the deep (in percentage of the historical concentration: 90 % pink, 110 % blue, 125 % cyan and 150 % green) in 2100 as a result of a reduction in the export coefficient ε (in %) and in the mixing coefficient μ (in %) in the box model.

6 Contribution of future N_2O to climate feedbacks

Changes in the oceanic emissions of N_2O to the atmosphere will have an impact on atmospheric radiative forcing, with potential feedbacks on the climate system. Based on the estimated 4 to 12 % decrease in N_2O sea-to-air flux over the 21st century under RCP8.5, we estimated the feedback factor for these changes as defined by Xu-Ri et al. (2012). Considering the reference value of the pre-industrial atmospheric N_2O concentration of 280 ppb in equilibrium, and its associated global N_2O emissions of $11.8\,\mathrm{Tg\,N\,yr^{-1}}$, we quantify the resulting changes in N_2O concentration per degree for the two projected emissions in 2100 using P.TEMP and P.OMZ. The model projects changes in N_2O emissions of -0.16 and $-0.48\,\mathrm{Tg\,N\,yr^{-1}}$ respectively, whereas surface temperature is assumed to increase globally by 3 °C on average according to the physical forcing used in our simulations. These results yield -0.05 and $-0.16\,\mathrm{Tg\,N\,yr^{-1}\,K^{-1}}$, or alternatively -1.25 and $-3.8\,\mathrm{ppb\,K^{-1}}$ for P.TEMP and P.OMZ respectively. Using Joos et al. (2001) we calculate the feedback factor in equilibrium for projected changes in emissions to be -0.005 and $-0.014\,\mathrm{W\,m^{-2}\,K^{-1}}$ in P.TEMP and P.OMZ.

Stocker et al. (2013) projected changes in terrestrial N_2O emissions in 2100 using transient model simulations leading to feedback strengths between +0.001 and $+0.015\,\mathrm{W\,m^{-2}\,K^{-1}}$. Feedback strengths associated with the projected decrease of oceanic N_2O emissions are of the same order of magnitude as those attributable to changes in the terrestrial sources of N_2O, yet opposite in sign, suggesting a compensation of changes in radiative forcing due to future increasing terrestrial N_2O emissions. At this stage, potential compensation between land and ocean emissions is to be taken with caution, as it relies of a single model run with constant atmospheric N_2O.

7 Conclusions

Our simulations suggest that anthropogenic climate change could lead to a global decrease in oceanic N_2O emissions during the 21st century. This maximum projected de-

crease of 12 % in marine N_2O emissions for the business-as-usual high CO_2 emissions scenario would compensate for the estimated increase in N_2O fluxes from the terrestrial biosphere in response to anthropogenic climate change (Stocker et al., 2013), so that the climate–N_2O feedback may be more or less neutral over the coming decades.

The main mechanisms contributing to the reduction of marine N_2O emissions are a decrease in N_2O production in high oxygenated waters as well as an increase in ocean vertical stratification that acts to decrease the transport of N_2O from the subsurface to the surface ocean. Despite the decrease in both N_2O production and N_2O emissions, simulations suggest that the global marine N_2O inventory may increase from 2005 to 2100. This increase is explained by the reduced transport of N_2O from the production zones to the air–sea interface.

Differences between the two parameterizations used here are modest, and the role of warming in P.TEMP or higher N_2O yields at low-O_2 concentrations in P.OMZ does not translate into significant differences in our model projections. The dominant high-O_2 N_2O production pathway drives not only the general decrease in N_2O emissions but also the homogeneousness between the two parameterizations considered.

The N_2O production pathways demand however a better understanding in order to enable an improved representation of processes in models. At a first order, the efficiencies of the production processes in response to higher temperatures or increased seawater pCO_2 are required. Second order effects such as changes in the O_2 boundaries at which nitrification and denitrification occur must be also taken into account. In the absence of process-based parameterizations, N_2O production parameterizations will still rely on export of organic carbon and oxygen levels. Both need to be improved in global biogeochemical models.

The same combination of mechanisms (i.e., change in export production and ocean stratification) have been identified as drivers of changes in oceanic N_2O emissions during the Younger Dryas by Goldstein et al. (2003). The N_2O flux decreased, while the N_2O reservoir was fueled by longer residence times of N_2O caused by increased stratification. Whether these mechanisms are plausible drivers of changes beyond year 2100 remains an open question that needs to be addressed with longer simulations.

The Supplement related to this article is available online at doi:10.5194/bgd-11-1-2014-supplement.

Acknowledgements. We thank Cynthia Nevison for providing us the N_2O sea-to-air flux dataset. We thank Annette Kock and Herman Bange for the availability of the MEMENTO database (https://memento.geomar.de). Comments by Parvadha Suntharalingam improved significantly this manuscript. Nicolas Gruber acknowledges the support of ETH Zürich. This work has been supported by the European Union via the Greencycles II FP7-PEOPLE-ITN-2008, number 238366. We thank Christian Ethé for help analyzing PISCES model drift.

References

Aumont, O. and Bopp, L.: Globalizing results from ocean in situ iron fertilization studies, Global Biogeochem. Cy., 20, GB2017, doi:10.1029/2005gb002591, 2006.

Bange, H. W., Rixen, T., Johansen, A. M., Siefert, R. L., Ramesh, R., Ittekkot, V., Hoffmann, M. R., and Andreae, M. O.: A revised nitrogen budget for the Arabian Sea, Global Biogeochem. Cy., 14, 1283–1297, doi:10.1029/1999gb001228, 2000.

Bange, H. W., Bell, T. G., Cornejo, M., Freing, A., Uher, G., Upstill-Goddard, R. C., and Zhang, G.: MEMENTO: a proposal to develop a database of marine nitrous oxide and methane measurements, Environ. Chem., 6, 195–197, doi:10.1071/en09033, 2009.

Beman, J. M., Chow, C.-E., King, A. L., Feng, Y., Fuhrman, J. A., Andersson, A., Bates, N. R., Popp, B. N., and Hutchins, D. A.: Global declines in oceanic nitrification rates as a consequence of ocean acidification, P. Natl. Acad. Sci. USA, 108, 208–213, doi:10.1073/pnas.1011053108, 2011.

Bianchi, D., Dunne, J. P., Sarmiento, J. L., and Galbraith, E. D.: Data-based estimates of suboxia, denitrification, and N_2O production in the ocean and their sensitivities to dissolved O_2, Global Biogeochem. Cy., 26, GB2009, doi:10.1029/2011gb004209, 2012.

Bindoff, N., Willebrand, J., Artale, V., Cazenave, A., Gregory, J., Gulev, S., Hanawa, K., Le Quere, C., Levitus, S., Norjiri, Y., Shum, C., Talley, L., and Unnikrishnan, A.: Observations: oceanic climate change and sea level, in: Climate Change 2007: The Physical Science Basis. Contribution of Working Group I to the Fourth Assessment Report of the Intergovernmental Panel on Climate Change, 2007.

Bopp, L., Resplandy, L., Orr, J. C., Doney, S. C., Dunne, J. P., Gehlen, M., Halloran, P., Heinze, C., Ilyina, T., Séférian, R., Tjiputra, J., and Vichi, M.: Multiple stressors of ocean ecosystems in the 21st century: projections with CMIP5 models, Biogeosciences, 10, 6225–6245, doi:10.5194/bg-10-6225-2013, 2013.

Butler, J. H., Elkins, J. W., Thompson, T. M., and Egan, K. B.: Tropospheric and dissolved N_2O of the west pacific and east-indian oceans during the El-Niño Southern Oscillation event of 1987, J. Geophys. Res.-Atmos., 94, 14865–14877, doi:10.1029/JD094iD12p14865, 1989.

Ciais, P., Sabine, C., Bala, G., Bopp, L., Brovkin, V., Canadell, J., Chhabra, A., DeFries, R., Galloway, J., Heimann, M., Jones, C., Le Quéré, C., Myneni, R. B., Piao, S., and Thornton, P.: Carbon and other biogeochemical cycles, in: Climate Change 2013: The Physical Science Basis. Contribution of Working Group I to the Fifth Assessment Report of the Intergovernmental Panel on Climate Change, 2013.

Cocco, V., Joos, F., Steinacher, M., Frölicher, T. L., Bopp, L., Dunne, J., Gehlen, M., Heinze, C., Orr, J., Oschlies, A., Schneider, B., Segschneider, J., and Tjiputra, J.: Oxygen and indicators of stress for marine life in multi-model global warming projections, Biogeosciences, 10, 1849–1868, doi:10.5194/bg-10-1849-2013, 2013.

Cohen, Y. and Gordon, L. I.: Nitrous-oxide in oxygen minimum of eastern tropical north pacific – evidence for its consumption during denitrification and possible mechanisms for its production, Deep-Sea Res., 25, 509–524, doi:10.1016/0146-6291(78)90640-9, 1978.

Cohen, Y. and Gordon, L. I.: Nitrous-oxide production in the ocean, J. Geophys. Res.-Oceans, 84, 347–353, doi:10.1029/JC084iC01p00347, 1979.

Crutzen, P. J.: Influence of nitrogen oxides on atmospheric ozone content, Q. J. Roy. Meteor. Soc., 96, 320–326, doi:10.1002/qj.49709640815, 1970.

de Wilde, H. P. J. and de Bie, M. J. M.: Nitrous oxide in the Schelde estuary: production by nitrification and emission to the atmosphere, Mar. Chem., 69, 203–216, doi:10.1016/s0304-4203(99)00106-1, 2000.

Deutsch, C., Brix, H., Ito, T., Frenzel, H., and Thompson, L.: Climate-forced variability of ocean hypoxia, Science, 333, 336–339, doi:10.1126/science.1202422, 2011.

Dufresne, J. L., Foujols, M. A., Denvil, S., Caubel, A., Marti, O., Aumont, O., Balkanski, Y., Bekki, S., Bellenger, H., Benshila, R., Bony, S., Bopp, L., Braconnot, P., Brockmann, P., Cadule, P., Cheruy, F., Codron, F., Cozic, A., Cugnet, D., de Noblet, N., Duvel, J. P., Ethe, C., Fairhead, L., Fichefet, T., Flavoni, S., Friedlingstein, P., Grandpeix, J. Y., Guez, L., Guilyardi, E., Hauglustaine, D., Hourdin, F., Idelkadi, A., Ghattas, J., Joussaume, S., Kageyama, M., Krinner, G., Labetoulle, S., Lahellec, A., Lefebvre, M. P., Lefevre, F., Levy, C., Li, Z. X., Lloyd, J., Lott, F., Madec, G., Mancip, M., Marchand, M., Masson, S., Meurdesoif, Y., Mignot, J., Musat, I., Parouty, S., Polcher, J., Rio, C., Schulz, M., Swingedouw, D., Szopa, S., Talandier, C., Terray, P., Viovy, N., and Vuichard, N.: Climate change projections using the IPSL-CM5 Earth System Model: from CMIP3 to CMIP5, Clim. Dynam., 40, 2123–2165, doi:10.1007/s00382-012-1636-1, 2013.

Elkins, J. W., Wofsy, S. C., McElroy, M. B., Kolb, C. E., and Kaplan, W. A.: Aquatic sources and sinks for nitrous-oxide, Nature, 275, 602–606, doi:10.1038/275602a0, 1978.

Freing, A., Wallace, D. W. R., Tanhua, T., Walter, S., and Bange, H. W.: North Atlantic production of nitrous oxide in the context of changing atmospheric levels, Global Biogeochem. Cy., 23, GB4015, doi:10.1029/2009gb003472, 2009.

Freing, A., Wallace, D. W. R., and Bange, H. W.: Global oceanic production of nitrous oxide, Philos. T. R. Soc. B, 367, 1245–1255, doi:10.1098/rstb.2011.0360, 2012.

Gehlen, M., Gruber, N., Gangstø, R., Bopp, L., and Oschlies, A.: Biogeochemical consequences of ocean acidification and feedbacks to the earth system, in: Ocean Acidification, 230–248, 2011.

Goldstein, B., Joos, F., and Stocker, T. F.: A modeling study of oceanic nitrous oxide during the Younger Dryas cold period, Geophys. Res. Lett., 30, 1092, doi:10.1029/2002gl016418, 2003.

Goreau, T. J., Kaplan, W. A., Wofsy, S. C., McElroy, M. B., Valois, F. W., and Watson, S. W.: Production of NO_2^- and N_2O by nitrifying bacteria at reduced concentrations of oxygen, Appl. Environ. Microb., 40, 526–532, 1980.

Gruber, N.: The marine nitrogen cycle: overview of distributions and processes, in: Nitrogen in the Marine Environment, 2nd edn., 1–50, 2008.

Gruber, N.: Warming up, turning sour, losing breath: ocean biogeochemistry under global change, Philos. T. R. Soc. A, 369, 1980–1996, doi:10.1098/rsta.2011.0003, 2011.

Gruber, N. and Galloway, J. N.: An Earth-system perspective of the global nitrogen cycle, Nature, 451, 293–296, doi:10.1038/nature06592, 2008.

Huesemann, M. H., Skillman, A. D., and Crecelius, E. A.: The inhibition of marine nitrification by ocean disposal of carbon dioxide, Mar. Pollut. Bull., 44, 142–148, doi:10.1016/s0025-326x(01)00194-1, 2002.

Jin, X. and Gruber, N.: Offsetting the radiative benefit of ocean iron fertilization by enhancing N_2O emissions, Geophys. Res. Lett., 30, 2249, doi:10.1029/2003gl018458, 2003.

Johnston, H.: Reduction of stratospheric ozone by nitrogen oxide catalysts from supersonic transport exhaust, Science, 173, 517–522, doi:10.1126/science.173.3996.517, 1971.

Joos, F., Prentice, I. C., Sitch, S., Meyer, R., Hooss, G., Plattner, G. K., Gerber, S., and Hasselmann, K.: Global warming feedbacks on terrestrial carbon uptake under the Intergovernmental Panel on Climate Change (IPCC) emission scenarios, Global Biogeochem. Cy., 15, 891–907, doi:10.1029/2000gb001375, 2001.

Keeling, R. F., Koertzinger, A., and Gruber, N.: Ocean deoxygenation in a warming world, Ann. Rev. Mar. Sci., 2, 199–229, doi:10.1146/annurev.marine.010908.163855, 2010.

Liu, B., Morkved, P. T., Frostegard, A., and Bakken, L. R.: Denitrification gene pools, transcription and kinetics of NO, N_2O and N_2 production as affected by soil pH, FEMS Microbiol. Ecol., 72, 407–417, doi:10.1111/j.1574-6941.2010.00856.x, 2010.

Mantoura, R. F. C., Law, C. S., Owens, N. J. P., Burkill, P. H., Woodward, E. M. S., Howland, R. J. M., and Llewellyn, C. A.: Nitrogen biogeochemical cycling in the northwestern indian-ocean, Deep-Sea Res. Pt. II, 40, 651–671, 1993.

Myhre, G., Shindell, D., Bréon, F.-M., Collins, W., Fuglestvedt, J., Huang, J., Koch, D., Lamarque, J.-F., Lee, D., Mendoza, B., Nakajima, T., Robock, A., Stephens, G., Takemura, T., and Zhang, H.: Anthropogenic and natural radiative forcing, in: Climate Change 2013: The Physical Science Basis. Contribution of Working Group I to the Fifth Assessment Report of the Intergovernmental Panel on Climate Change, 2013.

Nevison, C., Butler, J. H., and Elkins, J. W.: Global distribution of N_2O and the Delta N_2O-AOU yield in the subsurface ocean, Global Biogeochem. Cy., 17, 1119, doi:10.1029/2003gb002068, 2003.

Nevison, C. D., Weiss, R. F., and Erickson, D. J.: Global oceanic emissions of nitrous-oxide, J. Geophys. Res.-Oceans, 100, 15809–15820, doi:10.1029/95jc00684, 1995.

Oschlies, A., Schulz, K. G., Riebesell, U., and Schmittner, A.: Simulated 21st century's increase in oceanic suboxia by CO_2-enhanced biotic carbon export, Global Biogeochem. Cy., 22, GB4008, doi:10.1029/2007gb003147, 2008.

Prather, M. J., Holmes, C. D., and Hsu, J.: Reactive greenhouse gas scenarios: systematic exploration of uncertainties and the role of atmospheric chemistry, Geophys. Res. Lett., 39, L09803, doi:10.1029/2012gl051440, 2012.

Punshon, S. and Moore, R. M.: Nitrous oxide production and consumption in a eutrophic coastal embayment, Mar. Chem., 91, 37–51, doi:10.1016/j.marchem.2004.04.003, 2004.

Ravishankara, A. R., Daniel, J. S., and Portmann, R. W.: Nitrous oxide (N_2O): the dominant ozone-depleting substance emitted in the 21st century, Science, 326, 123–125, doi:10.1126/science.1176985, 2009.

Resplandy, L., Lévy, M., Bopp, L., Echevin, V., Pous, S., Sarma, V. V. S. S., and Kumar, D.: Controlling factors of the oxygen balance in the Arabian Sea's OMZ, Biogeosciences, 9, 5095–5109, doi:10.5194/bg-9-5095-2012, 2012.

Riebesell, U., Schulz, K. G., Bellerby, R. G. J., Botros, M., Fritsche, P., Meyerhoefer, M., Neill, C., Nondal, G., Oschlies, A., Wohlers, J., and Zoellner, E.: Enhanced biological carbon consumption in a high CO_2 ocean, Nature, 450, 545–548, doi:10.1038/nature06267, 2007.

Sarmiento, J. L., Slater, R., Barber, R., Bopp, L., Doney, S. C., Hirst, A. C., Kleypas, J., Matear, R., Mikolajewicz, U., Monfray, P., Soldatov, V., Spall, S. A., and Stouffer, R.: Response of ocean ecosystems to climate warming, Global Biogeochem. Cy., 18, GB3003, doi:10.1029/2003gb002134, 2004.

Steinacher, M., Joos, F., Frölicher, T. L., Bopp, L., Cadule, P., Cocco, V., Doney, S. C., Gehlen, M., Lindsay, K., Moore, J. K., Schneider, B., and Segschneider, J.: Projected 21st century decrease in marine productivity: a multi-model analysis, Biogeosciences, 7, 979–1005, doi:10.5194/bg-7-979-2010, 2010.

Stocker, B. D., Roth, R., Joos, F., Spahni, R., Steinacher, M., Zaehle, S., Bouwman, L., Xu, R., and Prentice, I. C.: Multiple greenhouse-gas feedbacks from the land biosphere under future climate change scenarios, Nat. Clim. Change, 3, 666–672, doi:10.1038/nclimate1864, 2013.

Suntharalingam, P. and Sarmiento, J. L.: Factors governing the oceanic nitrous oxide distribution: simulations with an ocean general circulation model, Global Biogeochem. Cy., 14, 429–454, doi:10.1029/1999gb900032, 2000.

Suntharalingam, P., Sarmiento, J. L., and Toggweiler, J. R.: Global significance of nitrous-oxide production and transport from oceanic low-oxygen zones: a modeling study, Global Biogeochem. Cy., 14, 1353–1370, doi:10.1029/1999gb900100, 2000.

Suntharalingam, P., Buitenhuis, E., Le Quere, C., Dentener, F., Nevison, C., Butler, J. H., Bange, H. W., and Forster, G.: Quantifying the impact of anthropogenic nitrogen deposi-

tion on oceanic nitrous oxide, Geophys. Res. Lett., 39, L07605, doi:10.1029/2011gl050778, 2012.

Tagliabue, A., Bopp, L., and Gehlen, M.: The response of marine carbon and nutrient cycles to ocean acidification: large uncertainties related to phytoplankton physiological assumptions, Global Biogeochem. Cy., 25, GB3017, doi:10.1029/2010gb003929, 2011.

Takahashi, T., Broecker, W. S., and Langer, S.: Redfield ratio based on chemical-data from isopycnal surfaces, J. Geophys. Res.-Oceans, 90, 6907–6924, doi:10.1029/JC090iC04p06907, 1985.

Tiedje, J. M.: Ecology of denitrification and dissimilatory nitrate reduction to ammonium, in: Biology of Anaerobic Microorganisms, 179–244, 1988.

Wanninkhof, R.: Relationship between wind-speed and gas-exchange over the ocean, J. Geophys. Res.-Oceans, 97, 7373–7382, doi:10.1029/92jc00188, 1992.

Weiss, R. F. and Price, B. A.: Nitrous-oxide solubility in water and seawater, Mar. Chem., 8, 347–359, doi:10.1016/0304-4203(80)90024-9, 1980.

Yoshida, N., Morimoto, H., Hirano, M., Koike, I., Matsuo, S., Wada, E., Saino, T., and Hattori, A.: Nitrification rates and N-15 abundances of N_2O and NO_3^- in the western north pacific, Nature, 342, 895–897, doi:10.1038/342895a0, 1989.

Zamora, L. M., Oschlies, A., Bange, H. W., Huebert, K. B., Craig, J. D., Kock, A., and Löscher, C. R.: Nitrous oxide dynamics in low oxygen regions of the Pacific: insights from the MEMENTO database, Biogeosciences, 9, 5007–5022, doi:10.5194/bg-9-5007-2012, 2012.

Zehr, J. P. and Ward, B. B.: Nitrogen cycling in the ocean: new perspectives on processes and paradigms, Appl. Environ. Microb., 68, 1015–1024, doi:10.1128/aem.68.3.1015-1024.2002, 2002.

Chapter 5

Impact of ocean acidification on N_2-fixation

Abstract

Biological N_2-fixation by marine organisms is the main contributor of external reactive nitrogen into the ocean, adding ~140 Tg of new reactive nitrogen in the ocean every year. The planktonic organisms responsible for fixing this nitrogen from the atmosphere will experience large modifications in their future environment due to anthropogenic climate change and ocean acidification. While the potential effects of global warming on N_2-fixers have been explored, there is new evidence that increasing levels of seawater CO_2 could boost N_2-fixation rates. Laboratory experiments have shown that *Trichodesmium* doubles its N_2-

fixation rates at higher CO_2 environments of nearly 800 ppm compared to present 400 ppm (Hutchins et al., 2013). This study addresses changes in N_2 fixation over this century in response to both global warming and ocean acidification. To this end, a novel and experimentally-derived parameterization of N_2-fixation is added to the ocean general circulation and biogeochemical model NEMO-PISCES. Evolution of N_2-fixation rates in the 21st century under the business-as-usual high CO_2 representative concentration pathway (RCP8.5) are presented. Changes in the spatial and temporal evolution of N_2-fixation rates due to ocean acidification are consistent with the predicted CO_2 fertilization effect. In response to ocean acidification, the N_2-fixation rates increase by 22% on a global scale in 2100 compared to 61.5 TgN at present. Global warming decreases this acidification-induced trend due to the role of other limiting terms that regulate the ability of diazotrophs to complete the N_2-fixation process. But in summary, the CO_2 fertilization effect counterbalances the decrease in nutrient (Fe, PO_4) supply due to increased stratification in the climate change scenario (where present 68.3 TgN yr^{-1} drop to 41.5 TgN yr^{-1} in 2100), and keeps the change in N_2-fixation rates positive at the end of the century, reaching an absolute value of 68.6 TgN yr^{-1}. These results are of exploratory nature, since the lack of observations limits the evaluation of N_2-fixation in models for present day conditions and leaves large uncertainties on projections of N_2-fixation in the future.

5.1. Introduction

Nitrogen (N_2) fixation is the most important source of external reactive nitrogen into the ocean (Gruber and Galloway, 2008). Luo et al. (2012), based on a compilation of 5,000 measurements spanning 30 years of observations of marine N_2-fixers abundance and N_2-fixation rates, estimated that 134 Tg of fixed nitrogen are introduced per year in the ocean. Grosskopf et al. (2013) revised the measurement techniques which were used during these campaigns, rising the estimate to 177 TgN yr^{-1}. These observational estimates have been completed with modelling studies over the last decade: idealized box models have been used to calculate the global budget and its uncertainties related to changes in ocean circulation (Eugster and Gruber 2012). Recent model estimates are 134 ± 16 (Eugster and Gruber, 2012) and 137 ± 34 TgN yr^{-1} (Deutsch et al., 2007). In all cases global N_2-fixation rate estimates exceed by a factor of two to five those of the other two major external sources of reactive nitrogen: atmospheric nitrogen deposition, ranging from 39 to 68 TgN yr^{-1} (Dentener et al. 2006; Duce et al., 2008), and riverine nitrogen supply, with 30 TgN yr^{-1} (Gruber and Galloway, 2008).

N_2-fixation is performed by diazotrophs, a particular group of phytoplankton. They use N_2-fixation as a nutrient supply mechanism. In the absence of other forms of nitrogen (i.e., nitrate, NO_3^-, and ammonium, NH_4^+), diazotrophs are able to break the triple bond of gaseous N_2 producing fixed nitrogen as NH_4^+ (Falkowski et al., 1997). The energetically expensive process of breaking the triple bond of N_2 allows diazotrophs to compensate the lack of other forms of bioavailable nitrogen in their environment. The cost of N_2-fixation results in a slower growth rate compared to non-diazotrophs. These so-called N_2-fixers simultaneously perform photosynthesis and N_2-fixation during daylight (Chen et al., 1998; Orcutt et al., 2001). Diazotrophs are favoured by a variety of environmental conditions such as incoming radiation, high temperature (Carpenter, 1983; Capone et al., 1997), high oxygen (O_2) concentrations (Stuart and Pearson, 1970), iron (Fe) (Falkowski, 1997; Berman-Frank et al., 2007) and phosphate (PO_4) supply (Sañudo-Wilhelmy et al., 2001) on top of the required abscence of NH_4^+ and NO_3^- (Capone et al., 1997; Karl et al., 2002; Holl and Montoya, 2005).

These environmental conditions under which N_2-fixation occurs are subject to changes in response to anthropogenic climate change. Increasing atmospheric CO_2 concentrations due to fossil fuel combustion, land-use change and cement production (Myhre et al., 2012) drive major changes in the marine environment: global warming, ocean deoxygenation and ocean acidification (Gruber, 2011). The recent and future evolution of these 3 stressors could be at the origin of large perturbations of marine ecosystems particularly at low latitudes, where most of the N-cycle processes occur (Gruber and Galloway, 2008).

Global warming will increase seawater temperature, stratification and reduce nutrient supply into the euphotic layer (Sarmiento et al., 2004). Studies of the response of two important N_2-fixers, *Trichodesmium* and *Croccosphera*, to changes in temperature suggest higher growth rates, with an upper metabolic boundary at 32°C. They also indicate potential changes in their stoichiometry (Fu et al., 2014). Global warming will also introduce changes in water density resulting in increased stratification. A more stratified ocean will limit the supply of nutrients to the euphotic layer (Sarmiento et al., 2004). A shortage in the supply of Fe, PO_4, NH_4^+ and NO_3^- into the surface layers is expected, which can potentially modify the optimal environmental conditions for diazotrophs.

The oceanic uptake of CO_2 from the atmosphere has changed the seawater carbonate chemistry, increasing the concentration of dissolved CO_2. The response of diazotrophs to increasing levels of CO_2 has been studied over the last decade (Riebesell, 2004, Barcelos e Ramos et al., 2007; Hutchins et al., 2007; Hutchins et al., 2013, Shi et al., 2012). While some studies do not report any CO_2 sensitive response in N_2-fixation growth and N_2-fixation rates (Shi et al., 2012), Barcelos e Ramos et al. (2007) analysed the effect of increasing levels of seawater CO_2 in *Trichodesmium* laboratory cultures and its positive effect on N_2-fixation. CO_2

played the role of an additional nutrient, doubling N_2-fixation and growth rates from pre-industrial to projected CO_2 levels in year 2100 of 750 µatm. This CO_2 fertilization effect was analysed more in detail by Hutchins et al. (2013) on the two genera of diazotrophs responsible of at least half of the total N_2-fixation in the ocean: *Trichodesmium* and *Croccosphera*. Different species of *Trichodesmium* and *Croccosphera* were studied under high CO_2 environmental conditions. The increasing seawater CO_2 concentration boosted the N_2-fixation rates, although with different sensitivities depending on the species. Half saturation constants for the CO_2 fertilization effect span from 61ppm for *Trichodesmium Thiebautii* to 435ppm for *Trichodesmium Erythraeum*.

In this study we analyse the combined effects of global warming and ocean acidification on N_2-fixation. We use the NEMO-PISCES ocean general circulation and biogeochemical model to analyse the combined effect of these two stressors on diazotrophy over this century under the RCP8.5 high CO_2 emissions scenario. We introduced a CO_2 sensitive term to an existing parameterization for N_2-fixation. We quantify the strength of the CO_2 fertilization effect, along with that of climate change alone, as well as the interplay of different terms and their role in modulating the N_2-fixation over the 21th century.

5.2. Methodology

5.2.1. PISCES Model

Future projections of changes in the N-cycle were done using the PISCES ocean biogeochemical model (Aumont and Bopp, 2006) with physical forcings derived from the IPSL-CM5A-LR coupled model (Dufresne et al., 2013). PISCES is a biogeochemical model with five nutrients (NO_3^-, NH_4^+, PO_4, Si and Fe), two phytoplankton groups (diatoms and pico/nanophytoplankton), two zooplankton groups (micro and mesozooplankton), and two non-living organic carbon compartments (particulate and dissolved organic matter pools). Phytoplankton growth is limited by nutrient availability and light. Constant Redfield C:N:P ratios of 122:16:1 are assumed (Takahashi et al., 1985), while all other ratios Chl:C, Fe:C and Si:C are explicitly computed by the model and can vary dynamically. The horizontal resolution used in this study is 2° x 2° cos Ø (Ø being the latitude), with enhanced latitudinal resolution at the equator of 0.5°.

5.2.2. CO_2 sensitive term on N_2-fixation

Whereas PISCES does not include an explicit diazotroph group, N_2-fixation is explicitly represented in the model. It is assumed that N_2-fixation is performed by a fraction of the nanophytoplankton functionnal group. N_2-fixation (Eq (1)) is parameterized as a combination of terms modulating a maximal N_2-fixation rate:

$$J_{Nfix} = \mu \cdot \frac{K_n}{K_n + [NO_3 + NH_4]} \cdot \frac{[Fe]}{K + [Fe]} \cdot (1 - e^{-I_{PAR}}) \cdot \alpha^{TEMP} \cdot \frac{pCO_2}{K_{1/2} + pCO_2} \quad (1)$$

where μ is the growth rate of nanophytoplankton, K_n is the half saturation constant for NO_3 (0.26×10^{-6} μmol N L^{-1}), K is the half saturation constant for Fe (0.1 nmolFe L^{-1}), I_{PAR} is the incoming radiation (in W m^{-2}) and *TEMP* is temperature (in °C). The range of values for each of the different terms is shown in the Supplementary Material. In addition to the existing terms a seawater pCO_2 limiting function is introduced. The term corresponds to a Michaelis-Menten function based on the experimental results by Hutchins et al. (2013). Oceanic pCO_2 is assumed to be constant over the euphotic layer. $K_{1/2}$ is the half saturation constant. We use a $K_{1/2}$ of 431 ppm, which corresponds to the most sensitive species to changes in CO_2, *Trichodesmium erythraeum* (Hutchins et al., 2013). The minimum $K_{1/2}$ of 65ppm shows an almost constant response of N_2-fixation rates to variable pCO_2 in PISCES (see Supplementary Material).

5.2.3. Experiment Design

Changes in future N_2-fixation rates were studied using pre-industrial, historical and future dynamical forcing fields from IPSL-CM5A-LR (Dufresne et al., 2012). These dynamical forcings were applied in a decoupled (or *offline*) model configuration as monthly means of wind stress, radiation and other physical parameters. The reason behind this simplification is the saving in computational capacity compared to the fully coupled high temporal resolution configuration. Offline experiments allow us to run several experiments without losing significant performance on a centennial scope. Climate change and ocean acidification impacts are assessed for scenario RCP8.5.

Table 1 summarizes the simulations used to analyse the effect of ocean acidification alone and the combined effect of ocean acidification and climate change on marine N_2-fixation. Firstly, a control simulation was run with pre-industrial physical forcings and constant atmospheric CO_2 of 278 ppm (hereinafter CTL). Then we isolated the effect of ocean acidification on N_2-

fixation using the same pre-industrial circulation fields, but variable and increasing atmospheric CO_2 (hereinafter OA). Finally, ocean acidification and climate change effects were included in the same historical and RCP8.5 model run (hereinafter CCOA), with a reference model run only with climate change, but constant atmospheric CO_2 (hereinafter CC). Century scale model drifts for all the biogeochemical variables presented were removed using the control simulation.

Name	NEMO Physical Forcing	Atmospheric CO_2	N_2-fixation
CTL	Pre-Industrial	278 ppm	OFF
OA	Pre-Industrial	variable	ON
CC	Historical + RCP8.5	278 ppm	OFF
CCOA	Historical + RCP8.5	variable	ON

Table 1: Simulations using NEMO-PISCES model to analyse the individual and combined effects of ocean acidification and climate change on marine N_2-fixation. 'ON' means CO_2 sensitive while 'OFF' means independent of CO_2.

5.3. Model Evaluation

5.3.1. N_2-fixation

N_2-fixation in our model is evaluated against the compilation of N_2-fixation rate measurements by Luo et al. (2012). Our model underestimates the total N_2-fixation rate (Table 2). NEMO-PISCES estimates ~69 TgN yr-1 of fixed nitrogen on a global scale, which is below the estimate of 134 ± 9 TgN yr^{-1} from observations. However, the relative contribution of the different oceanic basins in the model is consistent with the observations. On a global scale the Pacific ocean remains the largest contributor of fixed nitrogen into the surface ocean in the model and in the observations.

	North Atlantic	North Pacific	Indian	Total (TgN yr^{-1})
PISCES	16.1	40.9	11.3	68.3
Luo et al. (2012)	34	102	-	137 ± 9

Table 2: Total N_2-fixation rates in PISCES for the averaged 1985 to 2005 simulated time period compared to the estimated global N_2-fixation budget from Luo et al. (2012).

The modelled N_2-fixation is located at low latitudes (Figure 1a), with little to no variation between eastern and western part of the oceanic basins except in the Pacific. Minima are found in the North Atlantic and the upwelling regions in the eastern south Pacific. Compared to observations (Figure 1b), the model has smoother transitions between minima and maxima. Maxima in observations reach 5790 µmolN $m^{-2}d^{-1}$, whereas in the model the maximum rates peak at 445 µmolN $m^{-2}d^{-1}$. The model accurately describes the tropical and sub-tropical N_2-fixation distribution (Figure 1c), with close to zero N_2-fixation rates outside the latitude band from 40°N to 40°S. However, some observations fall outside the model envelope, particularly towards the north. Regarding temperature, as one of the most important controls on N_2-fixation (Figure 1d), the modeled N_2-fixation rates are centered around 20°C, while the measurements show the highest values of N_2-fxation rates around 25°C. Higher N_2-fixation activity is observed in general for warmer temperatures, being 30°C the upper limit in both cases.

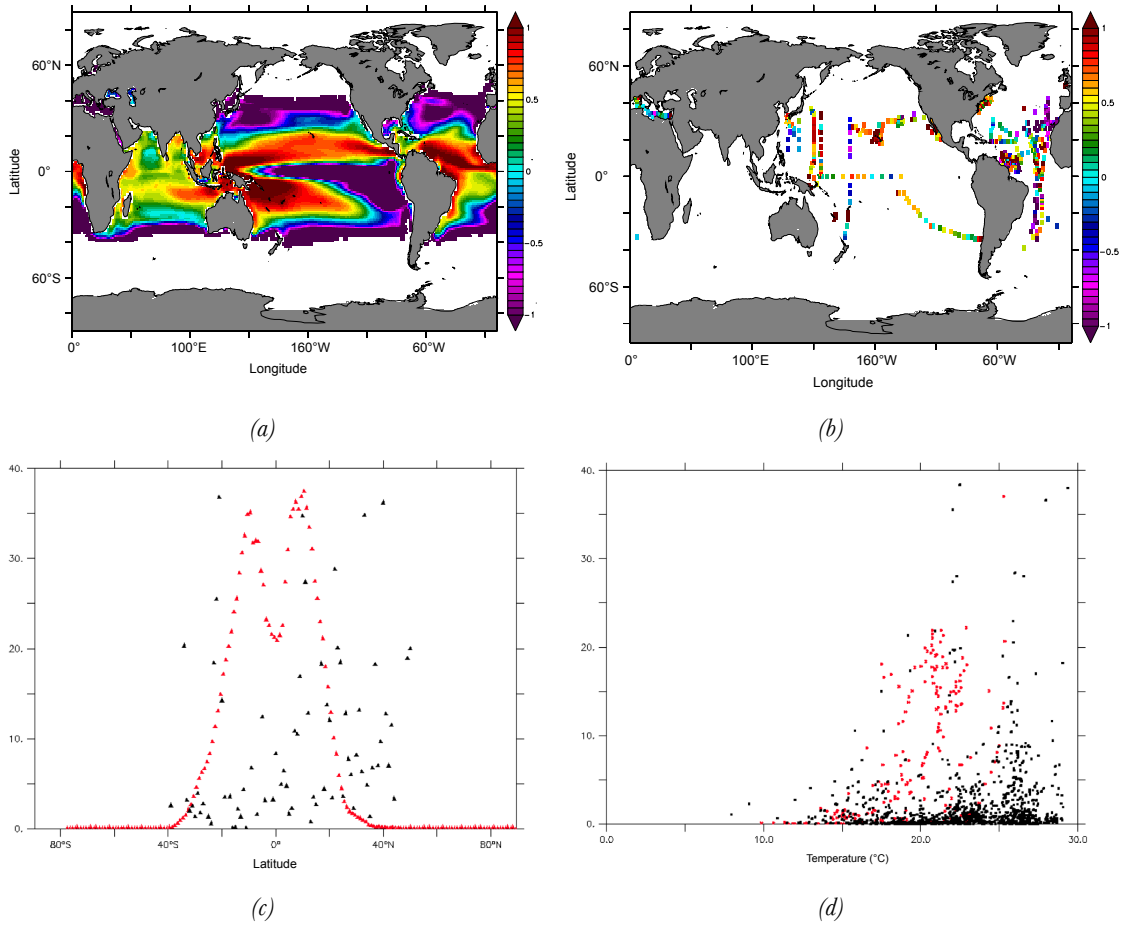

Figure 1: (a) Vertically integrated N_2-fixation rates (in log µmolN $m^{-2}d^{-1}$) in PISCES averaged over the 1985 to 2005 simulated time period. (b) Vertically integrated N_2-fixation rates from Luo et al. (2012) data compilation. (c) Latitudinal integrated N_2-fixation rates from PISCES (red) averaged over the 1985 to 2005 simulated time period and Luo et al. (2012) database (black). (d) Scatter plot of vertically integrated N_2-fixation rates and temperature (in °C) in PISCES (red) averaged over the 1985 to 2005 simulated time period and Luo et al. (2012) database (black).

5.4. Projections of N_2-fixation over the 21st century

5.4.1. Ocean acidification

Global N_2-fixation rates are presented as twenty year averages for pre-industrial (1851-1871), present-day (1985-2005) and future (2080-2100) conditions. Global N_2-fixation rates increase slightly between pre-industrial and present-day from 61.5 to 64.2 TgN yr^{-1} to reach 74.9 TgN yr-1 at the end of this century (Figure 2a). This change represents a 22% increase at the end of the century compared to the pre-industrial average. N_2-fixation rates are particularly enhanced in the western part of the Pacific and Atlantic basins (Figure 2b). There are few localized areas around 10°N in the Caribbean Sea and western Pacific for which a slight decrease is projected. For the Indian ocean, to the contrary, no significant change in N_2-fixation is projected in response to ocean acidification. The increase in N_2-fixation rates is driven entirely by the CO_2 effect. Figure 3 shows the corresponding evolution of atmospheric pCO_2 from 278ppm in 1851 to 850 ppm in year 2100. Changes in the CO_2 term span 0.46 to 0.76 over the same time period.

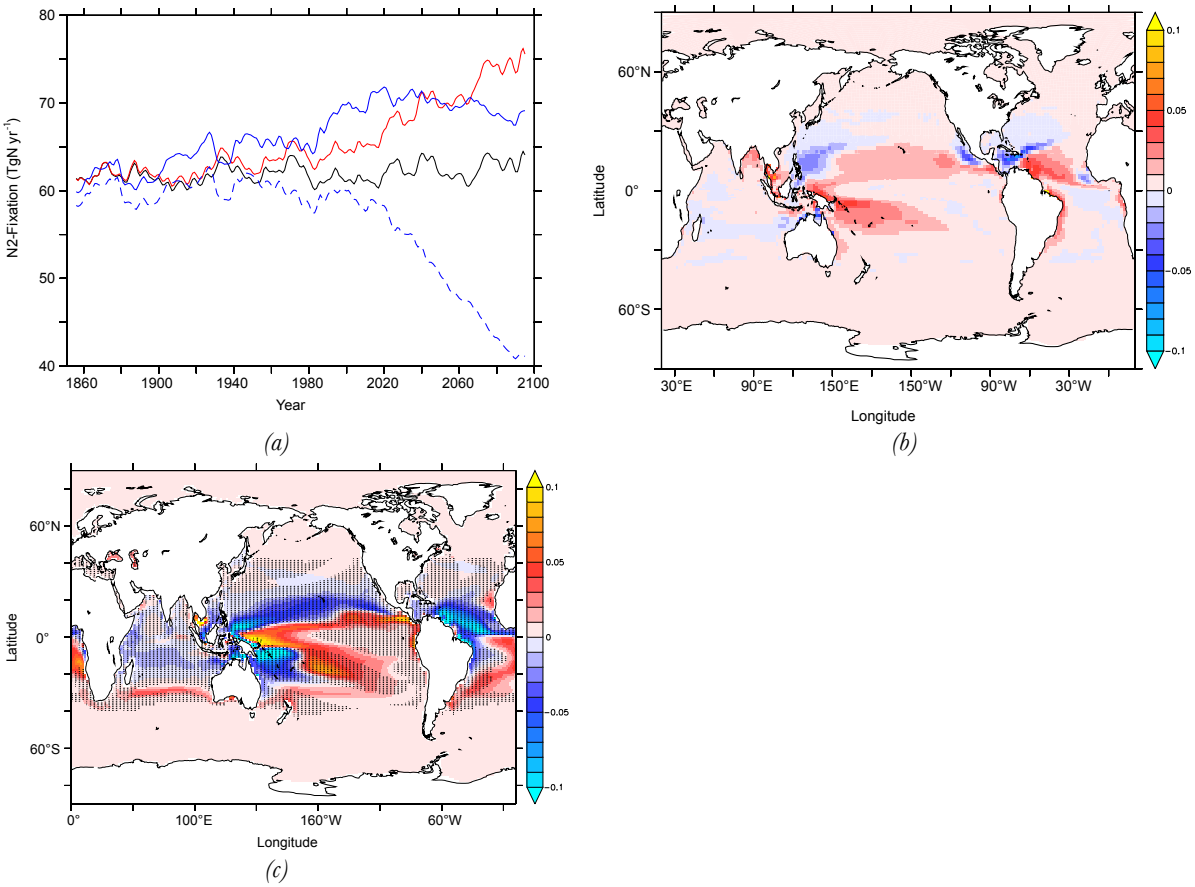

Figure 2: (a) N_2-fixation rates (in TgN yr^{-1}) in CTL (black), CC (dashed blue), OA (red) and CCOA (blue) simulations. (b) ΔN_2-fixation (in µmolN $m^{-2}d^{-1}$) in the upper 100m from 2100 to 2005 in the OA run. (c) ΔN_2-fixation (in µmolN $m^{-2}d^{-1}$) in the upper 100m from 2100 to 2030 in the CCOA run. Stippled regions show changes in the limiting term due to other forms of nitrogen which have the same sign as changes in N_2-fixation.

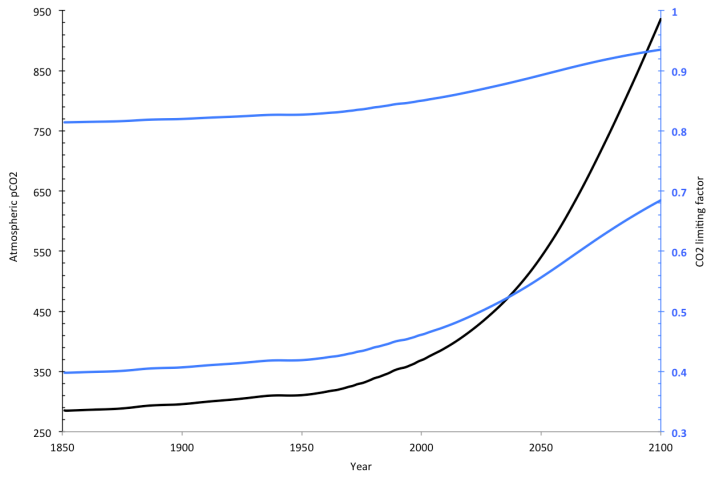

Figure 3: Surface pCO_2 (left axis, in ppm) and the CO_{2lim} term (right axis) associated with *Trichodesmium thiebautii* (upper curve, $K_{1/2}$ = 65 ppm) and *Trichodesmium erythraeum* (lower curve, $K_{1/2}$ = 431 ppm) from Hutchins et al. (2013) included into the N_2-fixation PISCES parameterisation along the simulated 1851 to 2100 time period.

5.4.2. Climate Change and Ocean Acidification

The evolution of N_2 fixation under future conditions of climate change and ocean acidification (CCAO) is shown in Figure 2a. There is a steady increase in N_2-fixation rates from 61.3 TgN yr^{-1} in 1851-1871 to 70.5 TgN yr^{-1} in 2010-2030, and a slight decrease down to 68.6 TgN yr^{-1} thereafter until the end of the century. These fluctuations are attributed to climate change (CCOA model run), as they were not observed in the variable pCO2 scenario alone (OA model run). The change in N_2-fixation in the future remains however positive, compared to the default climate change only (CC model run) scenario, where N_2-fixation drops to 41.5 TgN yr^{-1} in 2080-2100 compared to the projected 68.6 TgN yr^{-1} in CCOA. Our results suggest that the CO_2 effect counterbalances the stratification effect and the shortage in the supply of nutrients on N_2-fixation due to climate change. Spatial changes in N_2-fixation rates between these two regimes are shown in Figure 2c. There is a contrasted bimodal pattern, with a decrease in the western Pacific and north Atlantic and an increase in the equatorial Pacific and the subtropical gyre both in the Pacific and Atlantic oceans.

5.5. Discussion

5.5.1. Ocean acidification

Higher N_2-fixation rates drive changes in the nutrient cycling, wich in turn modulate the regional response to ocean acidification alone. More NH_4^+ is added into the euphotic layer, as shown in Figure 4, where the percentage of NH_4^+ contributing to the DIN pool in the upper 100m is plotted. The relative amount of NH_4^+ increases by 5% compared to pre-industrial times over the 21st century. Fueling the pool of DIN translates into higher net primary production (NPP) (Figure 5a). There is a steady 5% increase, from 37.7 PgC yr^{-1} in pre-industrial times to 39.6 PgC yr^{-1} at the end of the 21st century. The increase in NPP is spatially highly correlated with changes in N_2-fixation (Figure 5b).

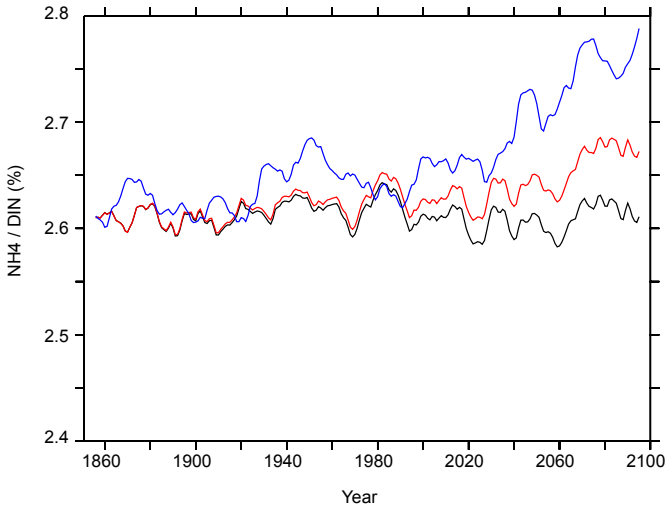

Figure 4: NH_4^+ / DIN concentration (in %) in the upper 100m in CTL (black), OA (red) and CCOA (blue).

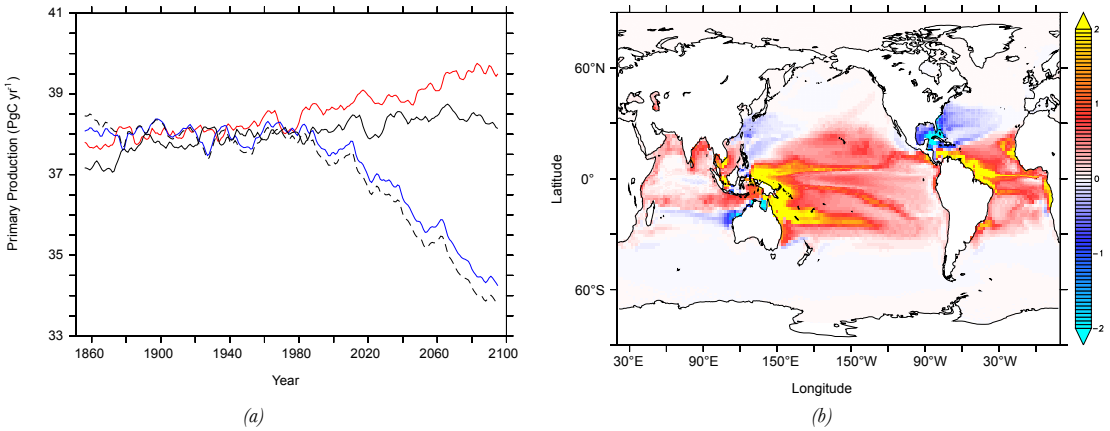

Figure 5: (a) Primary production (in PgC yr^{-1}) in CTL (black), CC (dashed black), OA (red) and CCOA (blue). (b) Change in primary production from 2100 to 2005 in OA.

5.5.2. Climate change and ocean acidification

Analyzing the terms modulating N_2-fixation, we observe different behaviours depending on the location (Figure 6). For the North Pacific and Atlantic stations, N_2-fixation rates decrease because of increased inhibition by the Nx term, i.e., more nitrogen is available in these regions. In contrast, the Southern stations, in the Pacific and Atlantic, show that the Fe and CO_{2lim} terms are modulating N_2-fixation. In the South Pacific, the increase in N_2-fixation is triggered by the CO_{2lim} term, as the other ones remain constant. In the south Atlantic the contribution mostly arises from the Fe term, but also from CO_{2lim} and Nx. On a global scale, the effect of the Nx term is more pronounced towards the end of the century, smoothing the sharp increase in global N_2-fixation rates observed from the 2005 to 2030 time period due to the contribution of the Fe and CO_2 terms.

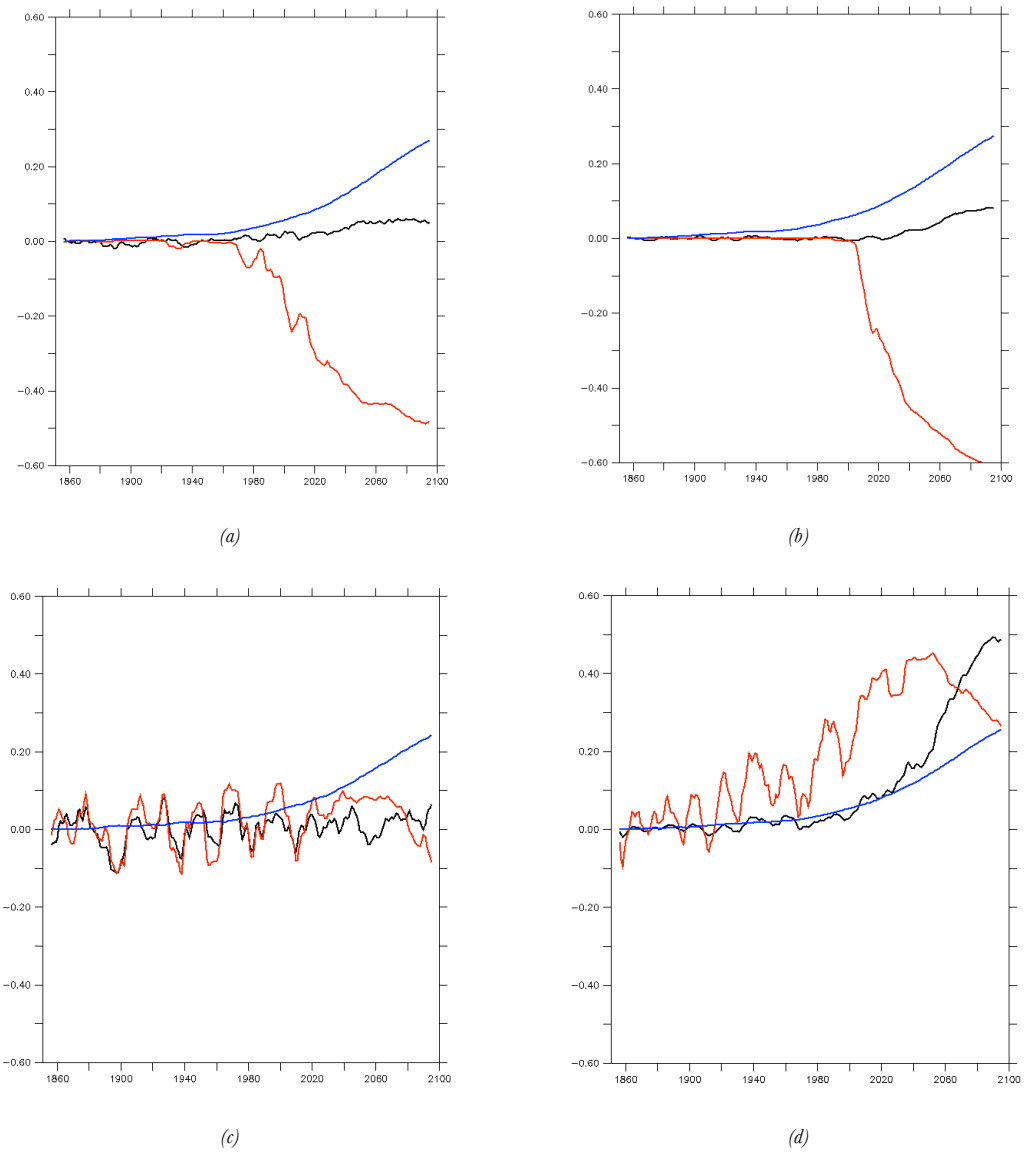

(a) *(b)*

(c) *(d)*

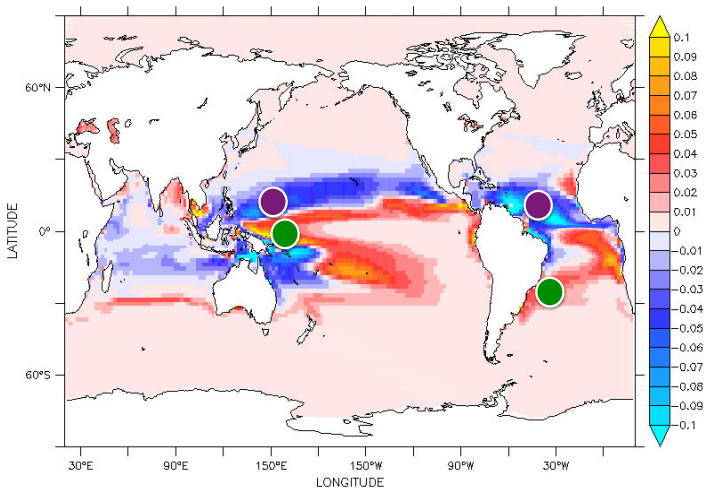

(e)

Figure 6: N_2-fixation terms in CCOA: CO_{2lim} (blue), Fe (black) and other forms of nitrogen N_x (red) in the stations at (a) North Pacific, (b) North Atlantic, (c) South Pacific and (d) South Atlantic described in (e).

Repercussions of adding climate change expand to the following issues. The relative amount of NH_4^+ in the DIN pool in the upper 100m increases globally beyond the OA scenario values (Figure 4), showing the decrease in the supply of NO_3^- from the subsurface due to increased stratification and increasing the relative amount of NH_4^+ in the euphotic layer. Changes in nutrient supply are reflected by an increase in global PP (Figure 5a) compared to the default CC model run in 2100. In the CCOA scenario, the model estimates 0.48 PgC yr^{-1} more than in the climate change only scenario. This 2% increase does not counterbalance the global decrease due to increased stratification and the limiting nutrient supply to the euphotic layer. An additional effect is observed when climate change operates in tandem with ocean acidification. N_2-fixation occurrence is expanded latitudinally and depthwise. Figure 7a shows the expansion of N_2-fixation from the averaged 1985-2005 to 2080-2100 time periods. At the surface level, N_2-fixation expands towards higher latitudes, mostly in the northern hemisphere reaching 60°N in coastal areas in the Pacific and in the North Atlantic. Depthwise, N_2-fixation expands in the Pacific subtropical gyres, Indian Ocean and western Atlantic basins. A further analysis on changes in the water column shows how increasing temperatures trigger positive changes below 40m deep, while negative changes in N_2-fixation are located above this depth boundary (Figure 7b).

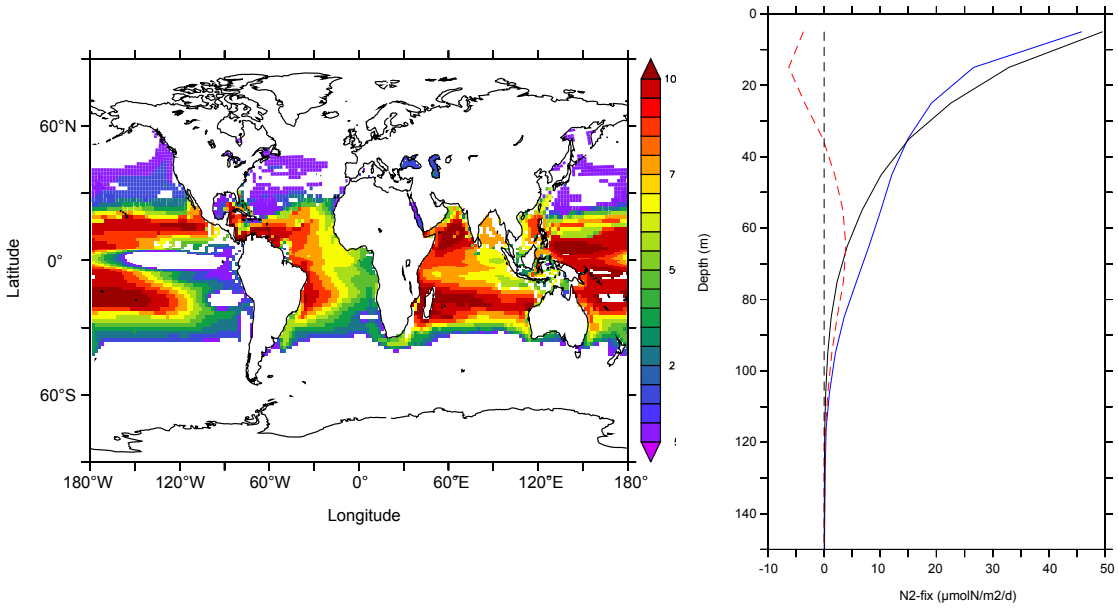

(a) *(b)*

Figure 7: (a) Maximum depth (in m) of new occurrence of N_2-fixation from 2005 to 2100 due to climate change in combination with ocean acidification. (b) Global depth average of N_2-fixation rates in 2100 (blue), 2005 (black), and the difference between the two (in red).

The most sensitive N_2-fixation scenario has been studied in this work. In an idealised ocean where *Trichodesmium Erythreaeum* (i.e., the higher half saturation constant observed in laboratory experiments from Hutchins et al. (2013)) performs all the oceanic N_2-fixation, the extra amount of NH_4^+ pumped into the nutrient pool does not counterbalance the effect of climate change on marine productivity, but increases nevertheless the marine primary production by 2% in the CCOA scenario. Considering a more realistic and heterogeneous combination of diazotroph species and assuming a less sensitive scenario on average (the minimum half saturation constant is 65 ppm compared to a maximum of 431 ppm used in our model), it is plausible that the actual increase in PP in reality will be less than the one estimated in the model. In addition, we must take into account the other nitrogen fixers whose response to higher levels of *pCO2* remains unknown. While the CO_2 fertilization effect is manifest, we must however consider this model analysis as the most sensitive response for N_2-fixers in the future.

The expansion of the N_2-fixers in the oligotrophic gyres as well as in High Nutrient Low Chlorophyll regions (HNLC) (Morel et al., 1991) gives a substantial niche-specific expansion against the non-diazotrophs. This expansion of the N_2-fixers niches towards higher latitudes might set a new arena for species competition against the non-diazotrophs, where studies such as those from Dutkiewicz et al. (2012) might determine which species are dominant. Subtle

interplays between the N_2-fixation limiting terms must be considered also in certain regions where an expansion of the N_2-fixers is observed. For instance, Luo et al. (2013) showed how N_2-fixation activity is anticorrelated with dust deposition in the North Atlantic, therefore an scenario where Fe is already saturated leads to other nutrient supply mechanisms from the subsurface as the ultimate control on the diazotrophs population and hence on the groups competition. Despite their slower growth rate, the CO_2 fertilization effect and the expansion of their niches due to increasing temperature show how diazotrophs might be ultimately favoured by the marine stressors looming ahead.

The effects of ocean acidification have been bracketed in the experiments from 278 to almost 950 ppm of atmospheric pCO_2. Palaeorecords have shown evidences of variability on the atmospheric CO_2 concentration over glacial/interglacial periods from 175 ppm to 300 ppm in the last 800 kyr (Wolff, 2011). Our experiments have explored a larger pCO_2 range that did not cause a dramatic effect on PP on a global scale, even in the most sensitive scenario of ubiquitous *Trichodesmium Erythraeum*. This fact suggest that N_2-fixation, if ruled only by the CO_2 fertilization effect, could not experience variations enough to alter the marine primary production on a global scale, as proposed by McElroy (1983). Whether N_2-fixation, as the main source of external nitrogen, has been dominant over denitrification, the most important removal process of fixed nitrogen, must be addressed in terms of inhibition or decoupling of each of the processes, rather than a particular enhancement or fertilization effect on N_2-fxation alone.

Changes in N_2-fixation in the future must be studied in parallel with increasing atmospheric deposition of reactive nitrogen compounds. It has been suggested that atmospheric deposition could potentially equal the contribution of N_2-fixation in the future because of growing industrialised areas (Duce et al., 2008, Krishnamurthy et al., 2007). It is intuitively expected that the increasing population and therefore increasing food demand might also increase the use of fertilizers. The impact on marine productivity from river discharge is larger (5%) than the atmospheric nitrogen deposition, focused mostly in coastal margins (DaCunha et al., 2007).

5.6. Model caveats

PISCES does not explicitly resolve diazotrophs. Notwithstanding more observations are required to validate and improve the model representation of this phytoplankton group. Measurements of N_2-fixers biomass and N_2-fixation rates show a sparse temporal and spatial coverage, which casts doubts on the accuracy of its potential global interpolation for global N_2-fixation rates estimates and diazotrophs distribution. In addition, diazotrophs is a buoyant phytoplankton group. The highest concentration can be found in the surface layers of the ocean. The depthwise projected expansion of N_2-fixation in the model is ultimately a numerical issue based on the assumptions made on occurrence and controls on N_2-fixation rather than a more realistic approximation. Therefore results on the expansion depthwise are more related to a prescribed threshold of a minimum N_2-fixation rate in the model that must be interpreted with caution, particularly regarding N_2-fixation below 100m.

N_2-fixation parameterization in the model is a rather simple yet sufficient representation of the process. Recent studies have included the interplay among the adequate environmental conditions for N_2-fixation, going beyond single terms such as nutrient availability, light or temperature to combinations of them. Dutkiewicz et al. (2012) suggested that the local Fe:N ratio might regulate N_2-fixation activity in the Pacific and the dominant phytoplankton group among diazotrophs and non-diazotrophs, whereas in Deutsch et al. (2007) the N:P ratio seems the crucial term for N_2-fixation occurrence. More sophisticated parameterizations should be considered in present and future studies on N_2-fixation. In order to keep the nitrogen conservation in the ocean, the maximum rate of N_2-fixation in the model is diagnosed from the total loss of nitrogen via water column denitrification over the averaged pre-industrial period., and then evolves free during the simulated period. This assumption suggests that global N_2-fixation rates could be actually larger than that shown in the model evaluation.

5.7. Summary and conclusions

The CO_2 fertilization effect reported by Hutchins et al. (2013) has been quantified on a global scale using NEMO-PISCES ocean biogeochemical model. Assuming an single ubiquitous dominant diazotroph species (*Trichodesmium Erythraeum*), highly sensitive to seawater CO_2, the model estimates a 22% increase in N_2-fixation rates at the end of the century compared to its preindustrial value. This CO_2 fertilization effect propagates along the nutrient cycling, pumping more NH_4^+ into the euphotic layer and supplying more nutrients to low-latitudinal

phytoplankton. A minor increase in primary productivity is observed, which is highly correlated to the analyzed changes in N_2-fixation in space and time domains.

When the effect of climate change is superimposed, the ocean acidification effect on N_2-fixers counterbalances the stratification effect on decreased N_2-fixation. The limited supply of other nutrients from the deeper layers is compensated by the CO_2 fertilization effect, leading to a positive change in N_2-fixation rates in 2100. Primary production is still driven by the limited supply of nutrients from the deep, but nevertheless it experiences a slight increase which might be negligible if an heterogeneous, less CO_2 sensitive, combination of diazotrophs were considered in the model. N_2-fixation is projected to expand poleward into the HNLC regions and also depthwise, defining new realms of conflict in resouce competition with all the other non-diazotrophs.

Characterization of N_2-fixers in contemporary ocean biogeochemical models is however in its awakenings. Richer databases of abundance and N_2-fixation rates are needed for model validation, as well as complex N_2-fixation parameterizations to project accurate responses of present and future oceanic N-cycle to different marine stressors.

5.8. Acknowledgements

We thank Yawei Luo and the MAREDAT project for providing the N_2-fixers biomass and N_2-fixation rates database. Nicolas Gruber acknowledges the support of ETH Zürich. This work has been supported by the European Union via the Greencycles II FP7-PEOPLE-ITN-2008, number 238366.

5.9. References

Aumont, O., and Bopp, L.: Globalizing results from ocean in situ iron fertilization studies, Global Biogeochemical Cycles, 20, 10.1029/2005gb002591, 2006.

Barcelos e Ramos, J., Biswas, H., Schulz, K. G., LaRoche, J., and Riebesell, U.: Effect of rising atmospheric carbon dioxide on the marine nitrogen fixer Trichodesmium, Global Biogeochemical Cycles, 21, 10.1029/2006gb002898, 2007.

Berman-Frank, I., Cullen, J. T., Shaked, Y., Sherrell, R. M., and Falkowski, P. G.: Iron availability, cellular iron quotas, and nitrogen fixation in Trichodesmium, Limnology and Oceanography, 46,

1249-1260, 2001.

Capone, D. G., Zehr, J. P., Paerl, H. W., Bergman, B., and Carpenter, E. J.: Trichodesmium, a globally significant marine cyanobacterium, Science, 276, 1221-1229, 10.1126/science.276.5316.1221, 1997.

Carpenter E. J.: Nitrogen fixation by marine *Oscillatoria* (Trichodesmium) in the World's oceans, Nitrogen in the marine environment, 65–103, 1983.

Chen, Y. B., Zehr, J. P., and Mellon, M.: Growth and nitrogen fixation of the diazotrophic filamentous nonheterocystous cyanobacterium Trichodesmium sp IMS 101 in defined media: Evidence for a circadian rhythm, Journal of Phycology, 32, 916-923, 10.1111/j.0022-3646.1996.00916.x, 1996.

da Cunha, L. C., Buitenhuis, E. T., Le Quere, C., Giraud, X., and Ludwig, W.: Potential impact of changes in river nutrient supply on global ocean biogeochemistry, Global Biogeochemical Cycles, 21, 10.1029/2006gb002718, 2007.

Dentener, F., Drevet, J., Lamarque, J. F., Bey, I., Eickhout, B., Fiore, A. M., Hauglustaine, D., Horowitz, L. W., Krol, M., Kulshrestha, U. C., Lawrence, M., Galy-Lacaux, C., Rast, S., Shindell, D., Stevenson, D., Van Noije, T., Atherton, C., Bell, N., Bergman, D., Butler, T., Cofala, J., Collins, B., Doherty, R., Ellingsen, K., Galloway, J., Gauss, M., Montanaro, V., Mueller, J. F., Pitari, G., Rodriguez, J., Sanderson, M., Solmon, F., Strahan, S., Schultz, M., Sudo, K., Szopa, S., and Wild, O.: Nitrogen and sulfur deposition on regional and global scales: A multimodel evaluation, Global Biogeochemical Cycles, 20, 10.1029/2005gb002672, 2006.

Deutsch, C., Sarmiento, J. L., Sigman, D. M., Gruber, N., and Dunne, J. P.: Spatial coupling of nitrogen inputs and losses in the ocean, Nature, 445, 163-167, 10.1038/nature05392, 2007.

Duce, R. A., LaRoche, J., Altieri, K., Arrigo, K. R., Baker, A. R., Capone, D. G., Cornell, S., Dentener, F., Galloway, J., Ganeshram, R. S., Geider, R. J., Jickells, T., Kuypers, M. M., Langlois, R., Liss, P. S., Liu, S. M., Middelburg, J. J., Moore, C. M., Nickovic, S., Oschlies, A., Pedersen, T., Prospero, J., Schlitzer, R., Seitzinger, S., Sorensen, L. L., Uematsu, M., Ulloa, O., Voss, M., Ward, B., and Zamora, L.: Impacts of atmospheric anthropogenic nitrogen on the open ocean, Science, 320, 893-897, 10.1126/science.1150369, 2008.

Dufresne, J. L., Foujols, M. A., Denvil, S., Caubel, A., Marti, O., Aumont, O., Balkanski, Y., Bekki, S., Bellenger, H., Benshila, R., Bony, S., Bopp, L., Braconnot, P., Brockmann, P., Cadule, P., Cheruy, F., Codron, F., Cozic, A., Cugnet, D., de Noblet, N., Duvel, J. P., Ethe, C., Fairhead, L., Fichefet, T., Flavoni, S., Friedlingstein, P., Grandpeix, J. Y., Guez, L., Guilyardi, E., Hauglustaine, D., Hourdin, F., Idelkadi, A., Ghattas, J., Joussaume, S., Kageyama, M., Krinner, G., Labetoulle, S., Lahellec, A., Lefebvre, M. P., Lefevre, F., Levy, C., Li, Z. X., Lloyd, J., Lott, F., Madec, G., Mancip, M.,

Marchand, M., Masson, S., Meurdesoif, Y., Mignot, J., Musat, I., Parouty, S., Polcher, J., Rio, C., Schulz, M., Swingedouw, D., Szopa, S., Talandier, C., Terray, P., Viovy, N., and Vuichard, N.: Climate change projections using the IPSL-CM5 Earth System Model: from CMIP3 to CMIP5, Climate Dynamics, 40, 2123-2165, 10.1007/s00382-012-1636-1, 2013.

Dutkiewicz, S., Ward, B. A., Monteiro, F., and Follows, M. J.: Interconnection of nitrogen fixers and iron in the Pacific Ocean: Theory and numerical simulations, Global Biogeochemical Cycles, 26, 10.1029/2011gb004039, 2012.

Eugster, O., and Gruber, N.: A probabilistic estimate of global marine N-fixation and denitrification, Global Biogeochemical Cycles, 26, 10.1029/2012gb004300, 2012.

Falkowski, P. G.: Evolution of the nitrogen cycle and its influence on the biological sequestration of CO2 in the ocean, Nature, 387, 272-275, 10.1038/387272a0, 1997.

Fu, F.-X., Yu, E., Garcia, N. S., Gale, J., Luo, Y., Webb, E. A., and Hutchins, D. A.: Differing responses of marine N-2 fixers to warming and consequences for future diazotroph community structure, Aquatic Microbial Ecology, 72, 33-46, 10.3354/ame01683, 2014.

Grosskopf, T., Mohr, W., Baustian, T., Schunck, H., Gill, D., Kuypers, M. M. M., Lavik, G., Schmitz, R. A., Wallace, D. W. R., and LaRoche, J.: Doubling of marine dinitrogen-fixation rates based on direct measurements, Nature, 488, 361-364, 10.1038/nature11338, 2012.

Gruber, N., and Galloway, J. N.: An Earth-system perspective of the global nitrogen cycle, Nature, 451, 293-296, 10.1038/nature06592, 2008.

Gruber, N.: Warming up, turning sour, losing breath: ocean biogeochemistry under global change, Philosophical Transactions of the Royal Society a-Mathematical Physical and Engineering Sciences, 369, 1980-1996, 10.1098/rsta.2011.0003, 2011.

Holl, C. M., and Montoya, J. P.: Interactions between nitrate uptake and nitrogen fixation in continuous cultures of the marine diazotroph Trichodesmium (Cyanobacteria), Journal of Phycology, 41, 1178-1183, 10.1111/j.1529-8817.2005.00146.x, 2005.

Hutchins, D. A., Fu, F. X., Zhang, Y., Warner, M. E., Feng, Y., Portune, K., Bernhardt, P. W., and Mulholland, M. R.: CO2 control of Trichodesmium N-2 fixation, photosynthesis, growth rates, and elemental ratios: Implications for past, present, and future ocean biogeochemistry, Limnology and Oceanography, 52, 1293-1304, 10.4319/lo.2007.52.4.1293, 2007.

Hutchins, D. A., Fu, F.-X., Webb, E. A., Walworth, N., and Tagliabue, A.: Taxon-specific response of marine nitrogen fixers to elevated carbon dioxide concentrations, Nature Geoscience, 6, 790-795, 10.1038/ngeo1858, 2013.

Karl, D., Michaels, A., Bergman, B., Capone, D., Carpenter, E., Letelier, R., Lipschultz, F., Paerl, H.,

Sigman, D., and Stal, L.: Dinitrogen fixation in the world's oceans, Biogeochemistry, 57, 47-+, 10.1023/a:1015798105851, 2002.

Krishnamurthy, A., Moore, J. K., Zender, C. S., and Luo, C.: Effects of atmospheric inorganic nitrogen deposition on ocean biogeochemistry, Journal of Geophysical Research-Biogeosciences, 112, 10.1029/2006jg000334, 2007.

Luo, Y. W., Doney, S. C., Anderson, L. A., Benavides, M., Bode, A., Bonnet, S., ... & Zehr, J. P.: Database of diazotrophs in global ocean: abundances, biomass and nitrogen fixation rates, Earth System Science Data Discussions, 5(1), 47-106, 2012.

McElroy, M. B.: Marine biological-controls on atmospheric CO_2 and climate, Nature, 302, 328-329, 10.1038/302328a0, 1983.

Morel, F. M. M., Rueter, J. G., and Price, N. M.: Iron nutrition of phytoplankton and its possible importance in the ecology of ocean regions with high nutrient and low biomass. Oceanography, 4(2), 56-61, 1991.

Myhre, G., Shindell, D., Bréon, F.-M., Collins, W., Fuglestvedt, J., Huang, J., Koch, D., Lamarque, J.-F., Lee, D., Mendoza, B., Nakajima, T., Robock, A., Stephens, G., Takemura, T. and Zhang, H.: Anthropogenic and Natural Radiative Forcing. In: Climate Change 2013: The Physical Science Basis. Contribution of Working Group I to the Fifth Assessment Report of the Intergovernmental Panel on Climate Change, 2013.

Orcutt, K. M., Lipschultz, F., Gundersen, K., Arimoto, R., Michaels, A. F., Knap, A. H., and Gallon, J. R.: A seasonal study of the significance of N-2 fixation by Trichodesmium spp. at the Bermuda Atlantic Time-series Study (BATS) site, Deep-Sea Research Part Ii-Topical Studies in Oceanography, 48, 1583-1608, 10.1016/s0967-0645(00)00157-0, 2001.

Riebesell, U.: Effects of CO(2) enrichment on marine phytoplankton, Journal of Oceanography, 60, 719-729, 10.1007/s10872-004-5764-z, 2004.

Sañudo-Wilhelmy, S. A., Kustka, A. B., Gobler, C. J., Hutchins, D. A., Yang, M., Lwiza, K., Burns, J., Capone, D. G., Raven, J. A., and Carpenter, E. J.: Phosphorus limitation of nitrogen fixation by Trichodesmium in the central Atlantic Ocean, Nature, 411, 66-69, 10.1038/35075041, 2001.

Sarmiento, J. L., Slater, R., Barber, R., Bopp, L., Doney, S. C., Hirst, A. C., Kleypas, J., Matear, R., Mikolajewicz, U., Monfray, P., Soldatov, V., Spall, S. A., and Stouffer, R.: Response of ocean ecosystems to climate warming, Global Biogeochemical Cycles, 18, 10.1029/2003gb002134, 2004.

Stewart, W. D. P., and Pearson, H. W.: Effects of aerobic and anaerobic conditions on growth and metabolism of blue-green algae, Proceedings of the Royal Society Series B-Biological Sciences, 175, 293-+, 10.1098/rspb.1970.0024, 1970.

Takahashi, T., Broecker, W. S., and Langer, S.: Redfield ratio based on chemical-data from isopycnal surfaces, Journal of Geophysical Research-Oceans, 90, 6907-6924, 10.1029/JC090iC04p06907, 1985.

Taylor, K. E., Stouffer, R. J., and Meehl, G. A.: An overview of CMIP5 and the experiment design, Bulletin of the American Meteorological Society, 93, 485-498, 10.1175/bams-d-11-00094.1, 2012.

Wolff, E. W.: Greenhouse gases in the Earth system: a palaeoclimate perspective, Philosophical Transactions of the Royal Society a-Mathematical Physical and Engineering Sciences, 369, 2133-2147, 10.1098/rsta.2010.0225, 2011.

5.10. Supplementary Material

5.10.1. N_2-fixation parameterization terms

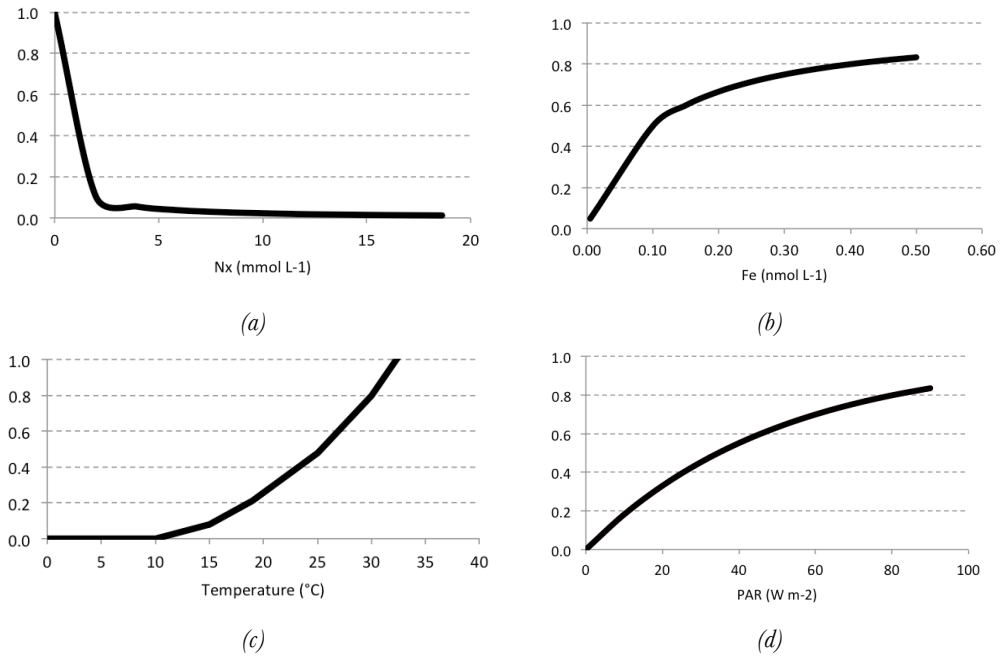

Figure 8: Offline estimates of the terms in N_2-fixation in NEMO-PISCES from (a) NO_3^-+ NH_4^+ concentration (in mmol L^{-1}), (b) dissolved Fe concentration (in nmol L^{-1}), (c) Temperature (in °C), (d) Photosynthetic available radiation (PAR) (in Wm^{-2}).

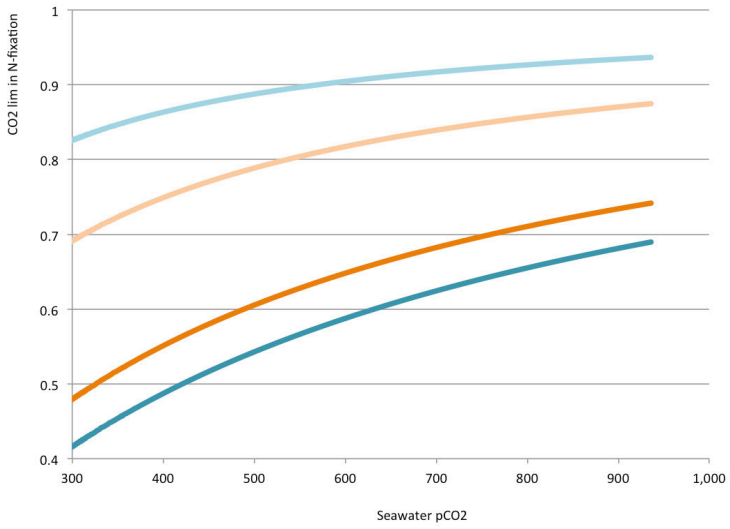

Figure 9: Offline estimates of the CO_2 term in N_2-fixation for the minimum (light) and maximum (dark) half saturation constants for *Trichodesmium* (blue) and *Croccosphera* (orange) species.

5.10.2. Carbonate chemistry

The model ΔpCO_2 shows a good spatial correlation with Takahashi et al. (2009) data product (Figure 10a and Figure 10b), simulating positive ΔpCO_2 (outgassing) at low latitudes and in the Southern Ocean, whereas negative values are located in the subtropical gyres and in the Arctic. The main discrepancies are found at the North Atlantic gyre and a particular hotspot of negative ΔpCO_2 in the vicinity of the Antarctic peninsula. The meridional mean of modeled and observed ΔpCO_2 are similar except at high northern latitudes (Figure 10c). Overall, discrepancies are found outside the low-latitude band where N_2-fixation occurs.

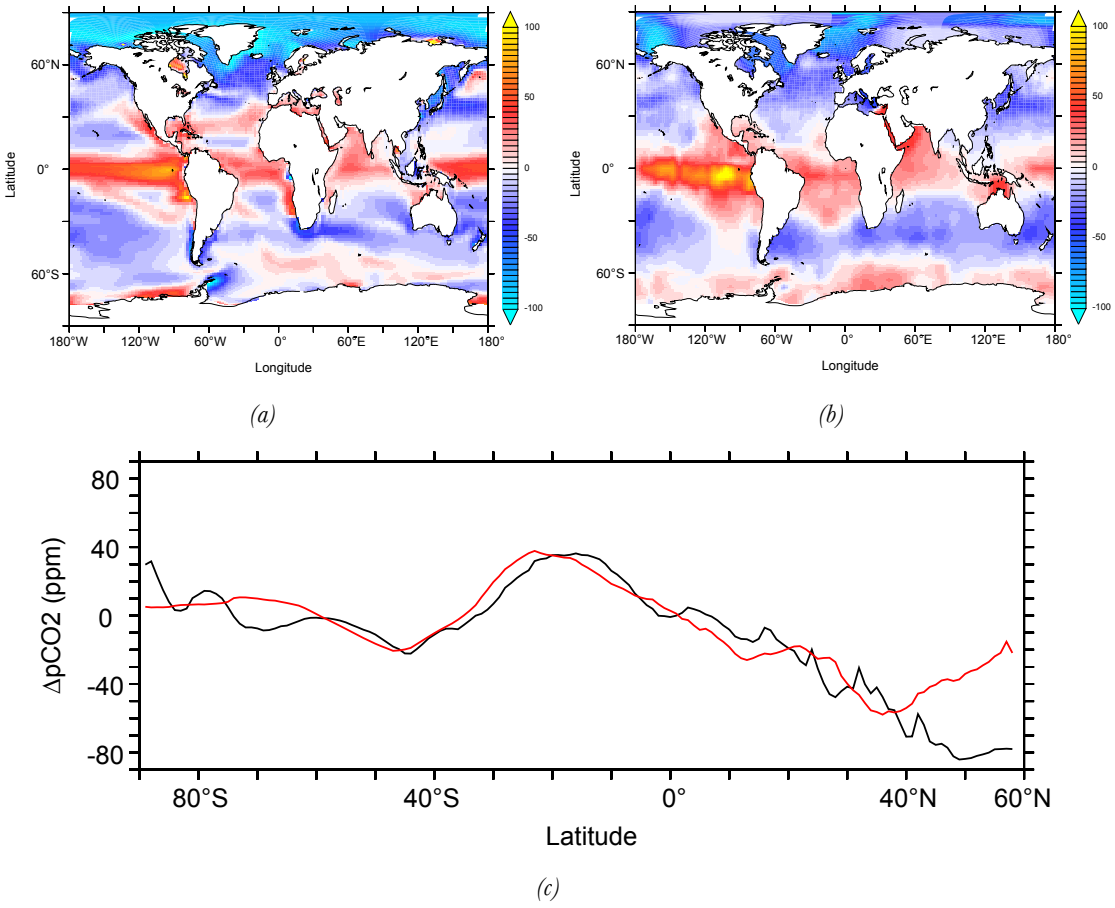

Figure 10: ΔpCO_2 (in ppm) in (a) PISCES averaged over the 1985 to 2005 simulated time period and (b) Takahashi et al. (2009). (c) Latitudinal average (in ppm) of NEMO-PISCES averaged over the 1985 to 2005 simulated time period (black) and Takahashi et al. (2009) (red).

Chapter 6

Impact of ocean acidification on nitrification

Abstract

The response of the marine nitrogen cycle (N-cycle) to global warming and ocean acidification remains highly uncertain. Changes in N_2-fixation, nitrification and denitrification due to these future marine stressors will drive changes in the bioavailable nitrogen pool (i.e., ammonium (NH_4^+) and nitrate (NO_3^-)). While NH_4^+ is produced by N_2-fixers, NO_3^- production is based on nitrification of remineralised organic matter. The NO_3^- produced from nitrification and other recycled products of organic matter fuel the so-called *regenerated* primary productivity, in contrast to the *new* primary production fuelled exclusively by external sources of bioavailable nitrogen into the euphotic zone. Nitrification is also responsible of the N_2O formation in the ocean, which contributes significantly to global greenhouse gas emissions. Decreasing levels of seawater pH could modify nitrification rates, as laboratory experiments have shown how nitrification rates decrease when pH is experimentally decreased. Changes in

the spatial and temporal evolution of nitrification due to ocean acidification might have implications on nutrient cycling, oxygen (O_2) concentration and N_2O production on a global scale. In our study the nitrification parameterization is modified in the ocean biogeochemical model PISCES, introducing a pH sensitive term. Changes in year 2100 under the business-as-usual high CO_2 emissions scenario (RCP8.5) are presented. Nitrification experiences a significant drop of 16% in year 2100 due to ocean acidification alone. This decrease is exacerbated in combination with climate change, with an additional 5% triggered by less productivity and hence less export of organic matter to depth. The decrease in nitrification translates into more O_2 in the subsurface (> 3 µmol L^{-1}) and a potential decrease of N_2O production by -0.15 TgN yr^{-1} due to ocean acidification alone. N_2O production and global nutrient cycling are projected to be significantly altered on a global scale, expanding the impact of ocean acidification onto new interactions among the oceanic biogeochemical realms.

6.1. Introduction

Nitrogen is frequently a limiting nutrient for phytoplankton activity and abundance (Moore et al., 2013). Bioavailable (or fixed) nitrogen compounds in the form of ammonia (NH_4^+) and nitrate (NO_3^-) fuel marine primary production along with phosphate (PO_4), iron (Fe) and other micronutrients. Marine productivity therefore relies on the physical and biological mechanisms which affect the quantities and chemical forms of fixed nitrogen supplied into the euphotic layer. The biological mechanisms are N_2-fixation, as the main source of external N fueling new production, nitrification, responsible for the conversion of NH_4^+ into NO_3^- supporting in part *regenerated* primary production, and denitrification, removing NO_3^- back into the inorganic form of N, i.e., N_2.

Nitrifying bacteria are responsible for the two-step oxidation of NH_4^+ into NO_3^-. These organisms are separated into a group of ammonia-oxidizing bacteria and archaea, that perform the first step from NH_4^+ to NO_2^-, and a second group of nitrite-oxidizing bacteria that finalise the process, turning NO_2^- into NO_3^-. None of these groups of organisms is able to perform both steps. Nitrification occurs most rapidly at the lower boundary of the euphotic zone, where NH_4^+ from remineralization of organic matter is no longer assimilated by phytoplankton due to the absence of light and NH_4^+ is fully available for nitrifying archaea and bacteria (Smith et al., 2014). At the same time, nitrification strongly depends on the amount of organic matter remineralized, and therefore on the export of organic matter to depth (CEX). Phytoplankton and nitrifier demand for N are therefore intertwined, and a variety of different feedbacks may shift this balance, in turn altering downstream

biogeochemical cycling.

Anthropogenic activities are causing perturbations on the marine N-cycle in general and on nitrification in particular. Increasing atmospheric CO_2 concentrations due to fossil fuel combustion induce three main stressors on the marine environment: global warming, ocean deoxygenation and ocean acidification (Gruber, 2011). The ubiquitous presence of nitrifying bacteria in the ocean suggests that nitrification will be certainly influenced in the future by the three marine stressors.

The response of nitrifying bacteria to changes in temperature remains unclear (Freing et al., 2012). Increasing temperatures might modify metabolic rates and bacterial nitrification efficiency. Global warming will also introduce changes in water density resulting in increased stratification. A more stratified ocean will trigger changes in mixing and upwelling regions, reducing the supply of nutrients to the euphotic layer (Sarmiento et al., 2004). This shortage of Fe, PO_4, NH_4^+ and NO_3^- could reduce primary production (PP) up to 18% following recent model projections (Bopp et al., 2013). As a consequence, less organic matter will be exported below the euphotic zone, resulting in less NH_4^+ that can be oxidized by nitrifying bacteria.

O_2 consumption during remineralisation could also be influenced by changes in CEX, leading to changes in the volume of the oxygen minimum zones (OMZs), where O_2 concentrations are below 5 to 20 µmol L^{-1} and denitrification-induced loss of fixed nitrogen occurs. Ocean deoxygenation may also shift the boundaries of occurrence of nitrification and denitrification in the ocean interior. If OMZs expand, the occurrence of nitrification might be significantly reduced, tied however to a substantial spatial variability that models project in the future (Bopp et al., 2013). An underappreciated aspect of nitrification is that it is also a significant sink for dissolved oxygen: in the consumption of Redfieldian organic matter, ca. 20% of oxygen consumption is due to nitrification (Ward, 2008).

Concurrent with these changes oceanic uptake of atmospheric CO_2 leads to ocean acidification, which has increased H^+ ion concentrations and decreased pH on seawater by 0.1 units on average since pre-industrial times (Orr et al., 2004). Model projections suggest that pH could drop to even lower levels in year 2100 (Bopp et al., 2013), decreasing by 0.35 pH units under the business-as-usual high CO_2 emission scenario. Acclimation and adaptation of phytoplankton and bacteria to decreased levels of seawater pH remain open questions when analysing the effects of ocean acidification (Joint et al., 2010). Concerning nitrification in particular, the nitrifying bacteria themselves have shown a low sensitivity to changes in seawater CO_2 (Badger et al., 2008; Berg et al., 2007). However, nitrification appears highly sensitive to changes in pH (Rudd et al., 1988, Huesemann et al., 2003, Beman et al., 2011), and even pure cultures of nitrifiers grown in idealized settings are sensitive to changing pH. Beman et al. (2011) analyzed the effect of experimentally increased levels of H^+ concentration in different regions of the Atlantic and the Pacific Oceans, finding that

nitrification rates decreased with pH. These result suggests that ocean acidification might have a significant impact on nitrification on a global scale. Changes in nitrification will lead ultimately to changes in oceanic N_2O production. N_2O is a powerful greenhouse gas (Ciais et al., 2013) that is likely to be the leading ozone depleting agent in the next century (Ravishankara et al., 2009). Formed as a by-product of the nitrification process (Freing et al., 2012, Zamora et al., 2012), oceanic N_2O emissions under the effect of ocean acidification have been suggested to decrease by up to 20% due to ocean acidification (Beman et al., 2011). pH driven changes in nitrification may have large climate impacts because changes in nitrification will lead ultimately to changes in oceanic N_2O production.

In this study we analyze the combined effect of global warming and ocean acidification on nitrification using the NEMO-PISCES ocean general circulation and biogeochemical model. This allows us to isolate the individual and combined effects of warming and acidification over the next century under the business-as-usual high CO_2 emissions scenario (RCP8.5). We developed a new parameterization including a pH sensitive term in nitrification to explore changes in nitrification efficiencies and the secondary effects of nitrification on subsurface NO_3^-, O_2 concentrations, primary productivity and N_2O production on a global scale.

6.2. Methods

6.2.1. Ocean circulation and biogeochemical model

Future projections of changes in the N-cycle were performed using the NEMO-PISCES ocean biogeochemical model (Aumont and Bopp, 2006) with physical forcings derived from the IPSL-CM5A-LR coupled model (Dufresne et al., 2013). The physical model horizontal resolution is 2° x 2° cos Ø, with enhanced latitudinal (Ø) resolution at the equator of 0.5°. PISCES is a biogeochemical model with five nutrients (NO_3^-, NH_4^+, PO_4, Si and Fe), two phytoplankton groups (diatoms and nanophytoplankton), two zooplankton groups (micro and mesozooplankton), and two non-living compartments (particulate and dissolved organic matter pools). Phytoplankton growth is limited by nutrient availability and light. Constant Redfield C:N:P ratios of 122:16:1 are assumed (Takahashi et al., 1985), while all other ratios Chl:C, Fe:C and Si:C are explicitly computed by the model and can vary dynamically.

6.2.2. Nitrification parameterization in PISCES

Nitrification in PISCES model is parameterized (Eq. (1)) based on the NH_4^+ concentration modulated by the incoming radiation, reduced in suboxic (O_2 < 5 µmol L^{-1}) waters, and attenuated by pH, in the form:

$$Nitrif = \lambda_{NH_4} \frac{NH_4}{1 + PAR} \left(1 - \Delta(O_2)\right)(\alpha \cdot log[H^+] + \beta) \quad (1)$$

where PAR is the Photosynthetic Available Radiation averaged over the mixed layer, $\Delta(O_2)$ defines the suboxic (equal to 1) or oxic (equal to 0) regimes, $[H^+]$ is the hydrogen ion concentration, α is - 2.475 and ß equals -18.8. The linear pH modulating function that is the last term in Eq. (1) is based on the Beman et al. (2011) results of global experimental data which found that, changes in nitrification rates were related to proportional changes in pH. Nitrification PISCES is shown in Figure 1. The assumption in the model of ubiquitous nitrifying bacteria links directly the CEX occurrence to nitrification. Nitrification is therefore present in the western part of the major oceanic basins at mid- to low-latitudes and reduced in the subtropical gyres.

We included in PISCES an N_2O production term based on the parameterization by Jin and Gruber (2003) and included into the N_2O emissions analysis in Chapter 4. This parameterization allows us to diagnose separately in the model output the N_2O production in high oxygenated areas due to nitrification alone and the low O_2 pathway due to the combined production of N_2O from nitrification and denitrification in suboxic regions.

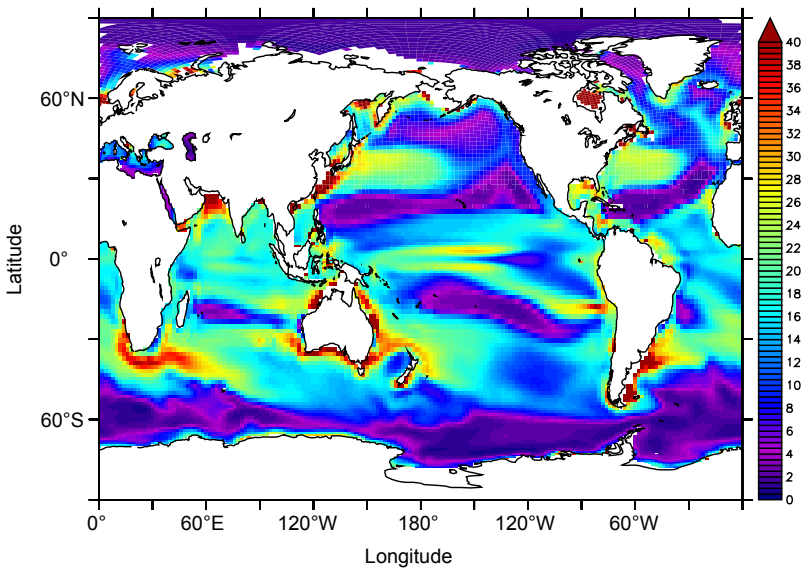

Figure 1: Depth integrated nitrification rates (in gN $m^{-2}yr^{-1}$) in NEMO-PISCES averaged over the 1985 to 2005 time period using the historical simulation run.

6.2.3. Experiment Design

Changes in nitrification rates due to ocean acidification are studied using pre-industrial, present and future dynamical forcing fields from IPSL-CM5A-LR (Dufresne et al., 2012). The model used variable CO_2 atmospheric concentration from 278 ppm in 1851 to 850 ppm in 2100. These dynamical forcings were applied in an offline fashion as monthly means. Future projections in NEMO-PISCES model of historical (from 1851 to 2005) and future (from 2005 to 2100) simulated periods were done using dynamical forcing fields from IPSL-CM5A-LR. Century scale model drifts for all the biogeochemical variables presented were removed using a control simulation with the default IPSL-CM5A-LR pre-industrial dynamical forcing fields from year 1851 to 2100.

Table 1 summarizes the simulations planned to analyze the effect of ocean acidification and the combined effect of ocean acidification and climate change on nitrification. The control simulation assumes constant atmopsheric CO_2 and pre-industrial circulation fields (CTL). We study the effect of ocean acidification alone on nitrification by changing the constant CO_2 to the variable 1851 to 2100 CO_2 values (OA). We superimpose the effect of climate change on the previous run by using the historical and future RCP8.5 IPCC scenario forcing fields with variable CO_2 (CCOA). Finally, we run a model simulation with future forcing fields but constant atmospheric CO_2 (CC) as a reference run.

Name	NEMO Physical Forcing	Atmospheric CO_2	CO_2 sensitive nitrification
CTL	Pre-Industrial	278 ppm	OFF
OA	Pre-Industrial	variable	ON
CC	Historical + RCP8.5	278 ppm	OFF
CCOA	Historical + RCP8.5	variable	ON

Table 1: Simulations using NEMO-PISCES model to analyse the individual and combined effects of ocean acidification and climate change on nitrification. 'ON' means CO_2 sensitive while 'OFF' means independent of CO_2.

6.3. Nitrification under future marine stressors

6.3.1. Impact of ocean acidification on nitrification

Changes in nitrification rates due to decreasing levels of seawater pH concentration are substantial. Figure 2a shows a 16% decrease from 12.4 TgN yr^{-1} in 1985-2005 to 10.4 TgN yr^{-1} in 2080-2100. Nitrification remains almost constant from pre-industrial to present, where pH declines by around 1% from its pre-industrial value of 8.06. The decrease in nitrification from 1985-2005 to 2080-2100 is almost ubiquitous (Figure 2b) except in the subtropical gyres in the Atlantic and Pacific basins and the Southern Ocean, where simulated nitrification was already very low.

The modelled changes in nitrification are caused by the overall decrease in pH. Figure 3a shows that the averaged pH in the 100m to 200m deep band from 1851 to 2100 decreases from 8.06 to 7.66. The pH_{lim} term decreases in our model from 1.2 to 0.3 over the same time period. pH decreases by around 0.4 units over the major oceanic basins, which represents a 5% decrease from 1985-2005 and this directly reduces nitrification (as parameterized in Eq (1)). An exception is the Southern Ocean, where the upwelling of older water masses minimizes the decrease in pH (Figure 3b).

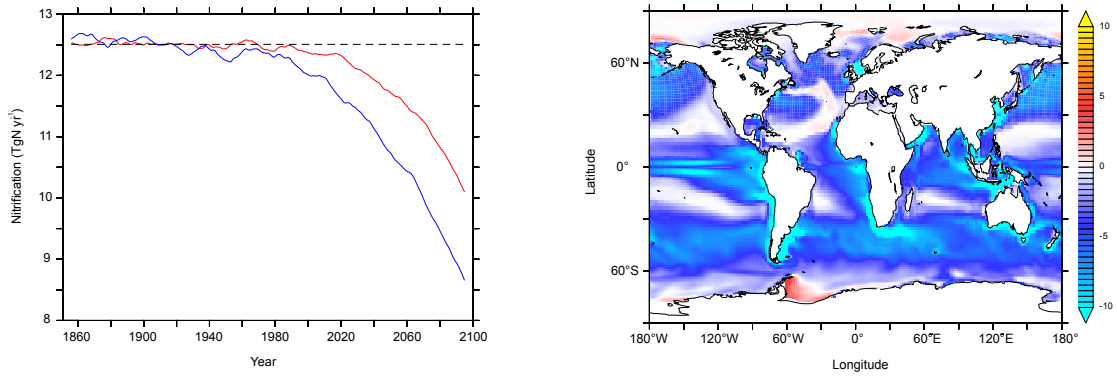

(a) *(b)*

Figure 2: (a) Nitrification in OA (red) and CCOA (blue) from 1851 to 2100. (b) Changes in nitrification in OA, from 2080-2100 to 1985-2005 averaged time periods in the historical plus future RCP8.5 simulations.

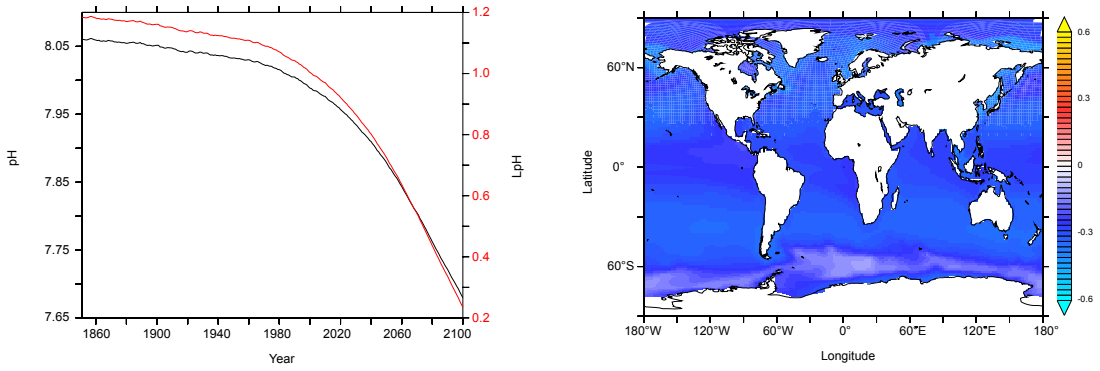

(a) *(b)*

Figure 3: (a) Averaged seawater pH between 100m and 200m deep (left axis) and pH sensitive term (right axis) included into the nitrification NEMO-PISCES parameterization from the simulated 1851 to 2100 time period. (b) Change in pH in OA from 2080-2100 to 1985-2005 averaged time periods in the historical plus future RCP8.5 simulations.

The consequences of less nitrification are not significant in the relative amount of NO_3^- and in the subsurface O_2. The amount of relative contribution of NO_3^- to the total pool of fixed N in the first 500m decreases from 99.6% (1851-1871) to 98.9% by 2080-2100 (Figure 4a) and occurs mostly in eastern boundary currents and the Indian Ocean (Figure 4b). The shift towards the eastern part of the oceanic basins suggests that the reduction in the NO_3^- signal is transported eastward from changes in nitrification which occur mostly in the western part of the oceanic basins, and therefore where less NO_3^- is produced. Minor changes in the O_2 concentration due to reduced nitrification also occur. The O_2 concentration at 100m deep on average increases mostly at the eastern boundary currents at low- to mid-latitudes (Figure 5a), following the pattern found for changes in the NO_3^- signal and driven by less O_2 consumption during nitrification. O_2 concentration increase by around 3 µmol L^{-1}. Figure 5b shows changes in the volume of hypoxia (O_2 concentration < 60 µmol L^{-1}) and suboxia (O_2 concentration < 5 µmol L^{-1}) from 1851 to year 2100. The hypoxic volume decreases from 9.8 to 9.7 x 10^6 km^3, i.e. only by 1% due to less O_2 consumption associated with reduced nitrification rates, while the suboxic volume remains constant. It must be noted that, on average, suboxic areas such as the OMZs are found between 400 and 800m deep, and therefore they are not sensitive to changes in O_2 concentration the subsurface layers.

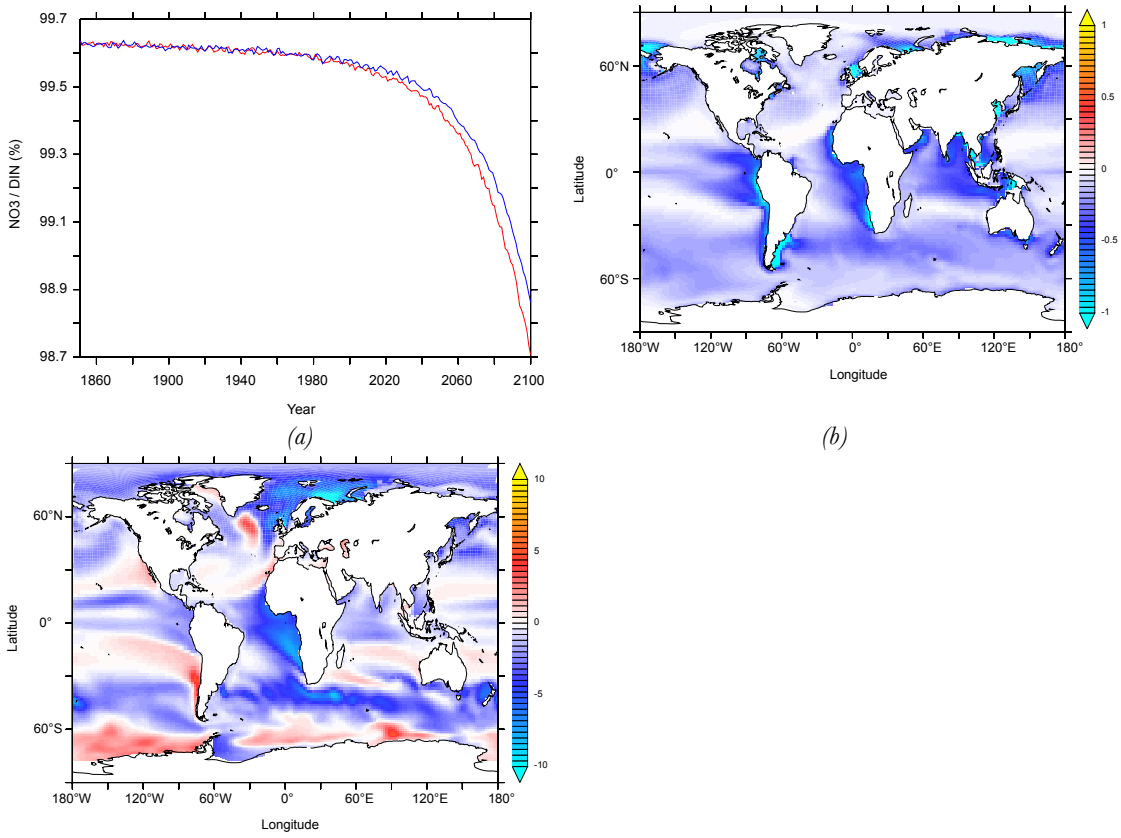

Figure 4: (a) NO_3^- / DIN (in %) in the upper 500m deep band in OA (red) and CCOA (blue). (b) Change of NO_3^- (in gN m^{-2}) ratio averaged on the upper 500m deep band in the OA run from 2080-2100 to 1851-1871 averaged time periods. (c) Change of NO_3^- (in gN m^{-2}) averaged in the upper 500m deep band in the 2080-2100 time period between OA and CCOA model runs.

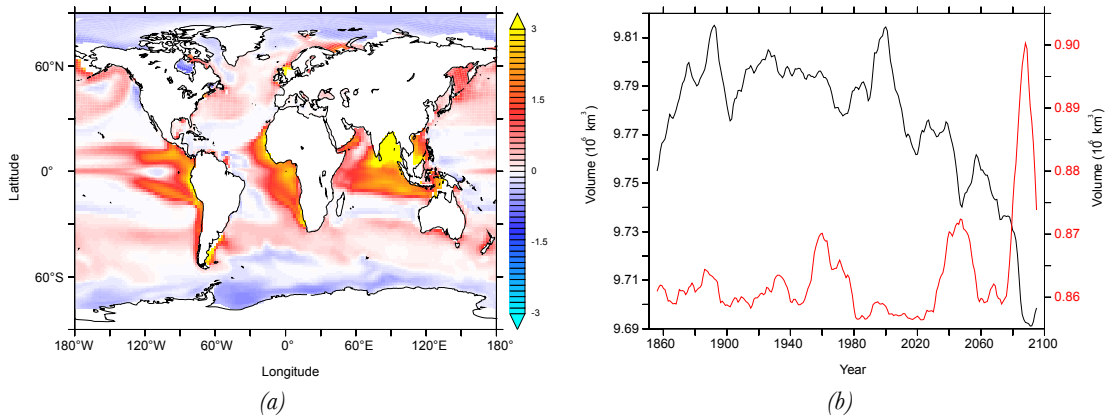

Figure 5: (a) Change of O_2 concentration at 100m (in µmol L^{-1}) between 2080-2100 and 1851-1871 time periods. (b) Hypoxic (<60 µmol L^{-1}, black, left axis) and suboxic (<5 µmol L^{-1}, red, right axis) volumes (in 10^6 km^3) from 1851 to 2100 in OA simulation run.

6.3.2. Impact of climate change and ocean acidification on nitrification

Climate change exacerbates the effect of ocean acidification on nitrification. An additional drop of 8% over the OA scenario is found by the year 2100 (Figure 2a). While changes in pH are similar in OA and CCOA scenarios, the shortage of nutrient supply to the euphotic layer drives the additional drop in nitrification. A less productive ocean leads to less export of organic matter to depth and hence to a more pronounced decrease in nitrification rates.

The effect of climate change on the relative abundance of NO_3^- in the nitrogen pool is similar to the effect of ocean acidification alone. Changes in the spatial distribution of NO_3^- in the first 500m from the CCOA to the OA scenario are shown in Figure 4c. Climate change induces reductions in the NO_3^- distribution in the subpolar regions, eastern boundary currents in the south Atlantic and in the Arctic basins, whereas an increase is observed in the Southern Ocean.

6.3.3. Nitrification impact on primary production and N_2O production

The significant changes in nitrification we observed do not translate into prominent changes in primary production. There is a 0.3% increase, from 38.4 PgC yr^{-1} in 1985-2005 time period to 38.5 PgC yr^{-1} in 2080-2100 (Figure 6) quite likely due to model drift. The minor changes in primary production that were obtained in the OA scenario due to the pH effect are also present in the CCOA scenario. The drop in primary production due to climate change alone (CC) is very similar to the CCOA results.

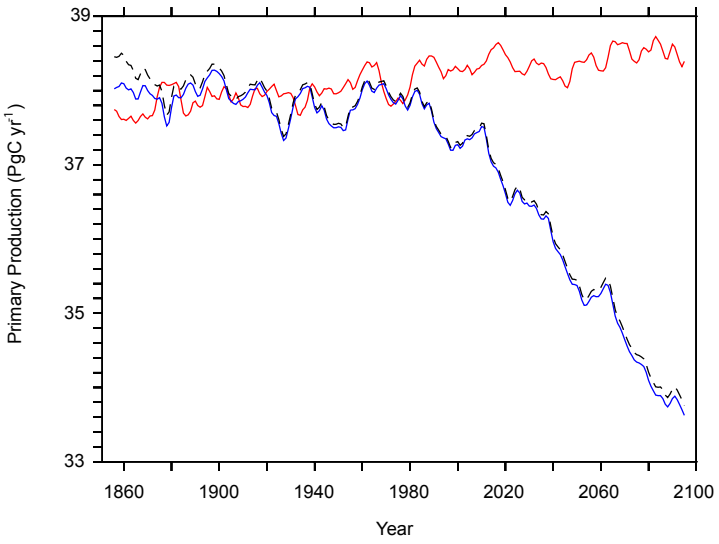

Figure 6: Primary production (in PgC yr^{-1}) in OA (red), CCOA (blue) and CC (dashed black) from 1851 to 2100 in NEMO-PISCES historical plus future RCP8.5 model run.

The most relevant impact in terms of global climate feedbacks is the effect on N_2O production. From 2080-2100 to 1851-1871 averaged time periods, the model projects a decrease of 0.15 TgN yr^{-1} in N_2O production due to the effect of pH alone on nitrification (Figure 7a). This decrease occurs in the major oceanic basins (Figure 7b), in regions coincident with those where a pronounced decrease in nitrification rates were predicted. The effect of climate change on N_2O production via nitrification reinforces the mechanisms induced by ocean acidification. Increased stratification with the associated lesser export of OM and more reduced nitrification leads to a significant 12% drop in N_2O production in the climate change only scenario (CC) (see Chapter 4). When the effect of ocean acidification is considered in tandem with climate change, there is the additional 0.15 TgN yr^{-1} decrease in N_2O production. This means that overall, when both stressors are combined, the N_2O production via nitrification is reduced by 0.65 TgN yr^{-1} by 2080-2100. Changes in N_2O production via nitrification occur mostly close to the subsurface and therefore might have a significant imprint into the N_2O sea-to-air fluxes.

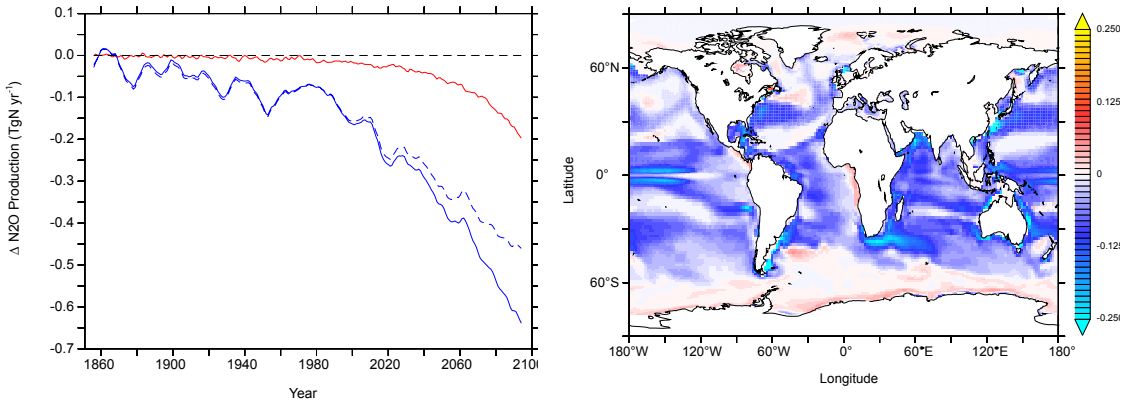

(a) *(b)*

Figure 7: (a) Anomalies in N_2O production from nitrification (in TgN yr^{-1}) in OA (red), CC (dashed blue) and CCOA (blue) from 1851 to 2100. (b) Change in N_2O production (in gN $m^{-2}yr^{-1}$) in OA from 2080-2100 to 1851-1871 averaged time periods.

6.4. Discussion

Despite the simulated decrease in nitrification, the pool of nutrients does not experience a significant change, particularly on the amount of NO_3^- in the subsurface. Changes in NO_3 due to decreased nitrification were minor compared with the effects of ocean warming. These effects are particularly notable in upwelling regions, where stratification reduces the upward

flux of NO_3^-. Moreover, changes in NO_3^- do not translate into changes in PP on a global scale, as expected from the 16% decrease in nitrification we obtained in the model projections. Yool et al. (2007) suggested that nitrification is responsible for ~30% of PP on a global scale. That would imply that our results trigger a 5 to 6% change in PP in 2100 if the same relative contribution of NO_3^- from nitrification applies. Therefore changes in nitrification appear to be second order effects against physical transport of nutrients on changes in PP.

Assuming nitrification as the dominant N_2O production pathway, there is a first order effect of decreasing pH on the efficiency of nitrification, which leads to significant changes in N_2O production at the end of the century. However, there is a secondary impact on the efficiency of N_2O production itself under lower pH that has not been considered in this analysis. Studies have shown how decreased pH on N_2O production yield on terrestrial bacteria are not relevant (Liu et al., 2012). Changes in seawater pH only represent a small fraction of these minimal changes observed by Liu et al. (2012). Experiments where marine N_2O production is analyzed under low pH are still missing. However, the ultimate question on N_2O production are the estimated changes in N_2O sea-to-air flux. Using Beman et al. (2011) estimates, the 16% drop in nitrification we have projected might trigger a decrease of 0.4 TgN yr^{-1} in sea-to-air N_2O emissions, which is comparable to the effect of climate change alone (Martinez-Rey et al., submitted), and could compensate other sources such as N_2O from fossil fuel combustion, atmospheric chemistry (0.6 TgN yr^{-1}), biomass and biofuel burning (0.4 TgN yr^{-1}) or contributions from estuaries and coastal environments (0.6 TgN yr^{-1}).

Palaeorecords have shown evidences for variability on the atmospheric CO_2 concentration over glacial/interglacial periods from 175ppm to 300ppm in the last 800 kyr (Wolff, 2011). Our experiments have explored a much more pronounced CO_2 range that did not cause a dramatic effect on NO_3^- fueling primary production or subsurface O_2 concentration. However, we did see modifications to N_2O production and eventually N_2O sea-to-air fluxes. Therefore nitrification, as the potential dominant N_2O production pathway, might have controlled the N_2O fluctuations seen over interglacial periods. McElroy (1983) suggested that the oceanic N-budget might have modulated the strength of the biological pump over these paleotimescales, with direct implications for the atmospheric CO_2 concentration and climate. Changes in the dominance of N_2-fixation over denitrification may explain dramatical changes in the oceanic N inventory and hence on the ocean uptake of atmospheric CO_2 (McElroy, 1983). One of the basic assumptions of this hypothesis is the self controlling mechanism of the N-cycle over long time periods, based on the fact that increasing N_2-fixation leads to more primary production, which in turn export more organic matter to depth, consuming more O_2 and finally expanding the OMZs where denitrifying bacteria operate removing bioavailable nitrogen. From our model study we have observed how changes in nitrification due to elevated concentrations of CO_2 may drive this sequence of events in the opposite direction,

increasing the amount of subsurface O_2 in the ocean interior and suppresing the removal of nitrogen from the nutrients pool via denitrification. Whether changes in nitrification could break the N_2 fixation – denitrification feedback mechanism is a question which remains open.

6.5. Model caveats

NEMO-PISCES is a particularly high-O_2 model compared to other ocean biogeochemical models used in the Coupled Model Intercomparison Project 5. Oxygen concentrations reflect the balance between physical supply and biological consumption. Physical supply is projected to change with ocean warming, leading to an expansion of low oxygen regions such as OMZs, supplemented by a general decrese in oxygen solubility due to warming. NEMO-PISCES underestimates by an order of magnitude the total volume of hypoxic and suboxic waters and underestimated ocean deoxygenation might overestimate the niches of nitrifying bacteria. This highlights the complexity of biological responses to ocean deoxygenation, where those processes that consume oxygen are, by definition, sensitive to oxygen concentrations. Nitrification is one of these processes and is also sensitive to pH. This creates a link between ocean acidification and deoxygenation, where the decline in nitrification due to acidification leads to less oxygen consumption, a negative feedback on ocean deoxygenation. This effect is clearly evident in the ocean's low oxygen regions such as the eastern Pacific Ocean, Benguela upwelling and Arabian Sea / Bay of Bengal. This leads to a surprinsingly sharp increase in oxygen concentrations between 100-200m due to the joint effects of ocean acidification and stratification on oxygen consumption via nitrification.

In addition to O_2, CMIP5 models tend to understimate the global export of organic matter to depth (Steinacher et al., 2009; Bopp et al., 2013). The drop in nitrification might be larger than the one estimated in this analysis on a global scale. Changes in the NO_3^- pool, but mostly N_2O production, which seems the most sensitive variable in our study, and the one which shows the highest correlation with changes in ntirification, might decrease even more.

Introducing an explicit representation of bacteria in the model, as well as additional data on specific metabolic sensitivities to temperature or dissolved CO_2 might help the model to refine the analysis of changes in the biogeochemical regulators below the euphotic layer.

6.6. Summary and conclusions

Ocean acidification decreases significantly nitrification rates globally. The decrease is ubiquitous, particularly where CEX hotspots occur in the western part of the major oceanic basins and is triggered by a global decrease in pH. However, these changes do not alter particularly the pool of NO_3^- in the subsurface layers, hence transport and advection from other locations still play the dominant role in modulating the distribution and abundance of NO_3^- in the future. We find an increase in O_2 below the euphotic layer although changes are not significant enough to be reflected into the hypoxic and suboxic volumes, where denitrification occurs. Ocean acidification has a notable impact on N_2O production. N_2O production via nitrification is assumed to dominate over the denitrification N_2O production pathway. An additional drop at the end of the century by changes in seawater pH reinforces the negative feedback of future marine stressors on marine N_2O production.

When climate change operates in tandem with ocean acidification, it dominates over the largest part of the biogeochemical changes we have evaluated in our study, except to nitrification itself. In this fashion, a less productive ocean triggers the major part of changes in the subsurface NO_3^- pool. The N_2O production shows the largest contribution of the effect of ocean acidification, with an additional drop from the climate change only scenario. This decrease due to ocean acidification is distributed uniformly in the major ocean basins and therefore expected to have an imprint into the N_2O sea to air fluxes.

This work shows the implication of ocean acidification on global climate feedbacks. On short timescales, the CO_2 attenuation effect has implications on N_2O production and eventually oceanic N_2O emissions to the atmosphere. On longer timescales, it casts doubts on the coupling between N_2-fixation and denitrification, as the effect of nitrification on subsurface O_2 might buffer the signal from N_2-fixation to denitrification. Further work on these issues should explore the combined effect of ocean acidification and climate change on N_2-fixation, nitrification and denitrification simultaneously, for a comprehensive understanding of the effect of the multiple interactions among future stressors on the marine N-cycle.

6.7. Acknowledgements

We thank John Dunne for providing the export of organic matter fields. This work has been supported by the European Union via the Greencycles II FP7-PEOPLE-ITN-2008, number 238366.

6.8. References

Aumont, O., and Bopp, L.: Globalizing results from ocean in situ iron fertilization studies, Global Biogeochemical Cycles, 20, 10.1029/2005gb002591, 2006.

Badger, M. R., and Bek, E. J.: Multiple Rubisco forms in proteobacteria: their functional significance in relation to CO(2) acquisition by the CBB cycle, Journal of Experimental Botany, 59, 1525-1541, 10.1093/jxb/erm297, 2008.

Beman, J. M., Chow, C.-E., King, A. L., Feng, Y., Fuhrman, J. A., Andersson, A., Bates, N. R., Popp, B. N., and Hutchins, D. A.: Global declines in oceanic nitrification rates as a consequence of ocean acidification, Proceedings of the National Academy of Sciences of the United States of America, 108, 208-213, 10.1073/pnas.1011053108, 2011.

Berg, I. A., Kockelkorn, D., Buckel, W., and Fuchs, G.: A 3-hydroxypropionate/4-hydroxybutyrate autotrophic carbon dioxide assimilation pathway in archaea, Science, 318, 1782-1786, 10.1126/science.1149976, 2007.

Bopp, L., Resplandy, L., Orr, J. C., Doney, S. C., Dunne, J. P., Gehlen, M., Halloran, P., Heinze, C., Ilyina, T., Seferian, R., Tjiputra, J., and Vichi, M.: Multiple stressors of ocean ecosystems in the 21st century: projections with CMIP5 models, Biogeosciences, 10, 6225-6245, 10.5194/bg-10-6225-2013, 2013.

Ciais, P., Sabine, C., Bala, G., Bopp, L., Brovkin, V., Canadell, J., Chhabra, A., DeFries, R., Galloway, J., Heimann, M., Jones, C., Le Quéré, C., Myneni, RB., Piao, S. and Thornton, P.: Carbon and Other Biogeochemical Cycles. In: Climate Change 2013: The Physical Science Basis. Contribution of Working Group I to the Fifth Assessment Report of the Intergovernmental Panel on Climate Change, 2013.

Cohen, Y., and Gordon, L. I.: Nitrous-oxide in oxygen minimum of eastern tropical north pacific - evidence for its consumption during denitrification and possible mechanisms for its production, Deep-Sea Research, 25, 509-524, 10.1016/0146-6291(78)90640-9, 1978.

Dufresne, J. L., Foujols, M. A., Denvil, S., Caubel, A., Marti, O., Aumont, O., Balkanski, Y., Bekki, S., Bellenger, H., Benshila, R., Bony, S., Bopp, L., Braconnot, P., Brockmann, P., Cadule, P., Cheruy, F., Codron, F., Cozic, A., Cugnet, D., de Noblet, N., Duvel, J. P., Ethe, C., Fairhead, L., Fichefet, T., Flavoni, S., Friedlingstein, P., Grandpeix, J. Y., Guez, L., Guilyardi, E., Hauglustaine, D., Hourdin, F., Idelkadi, A., Ghattas, J., Joussaume, S., Kageyama, M., Krinner, G., Labetoulle, S., Lahellec, A., Lefebvre, M. P., Lefevre, F., Levy, C., Li, Z. X., Lloyd, J., Lott, F., Madec, G., Mancip, M., Marchand, M., Masson, S., Meurdesoif, Y., Mignot, J., Musat, I., Parouty, S., Polcher, J., Rio, C., Schulz, M., Swingedouw, D., Szopa, S., Talandier, C., Terray, P., Viovy, N., and Vuichard, N.:

Climate change projections using the IPSL-CM5 Earth System Model: from CMIP3 to CMIP5, Climate Dynamics, 40, 2123-2165, 10.1007/s00382-012-1636-1, 2013.

Dunne, J. P., Sarmiento, J. L., and Gnanadesikan, A.: A synthesis of global particle export from the surface ocean and cycling through the ocean interior and on the seafloor, Global Biogeochemical Cycles, 21, 10.1029/2006gb002907, 2007.

Elkins, J. W., Wofsy, S. C., McElroy, M. B., Kolb, C. E., and Kaplan, W. A.: Aquatic sources and sinks for nitrous-oxide, Nature, 275, 602-606, 10.1038/275602a0, 1978.

Freing, A., Wallace, D. W. R., and Bange, H. W.: Global oceanic production of nitrous oxide, Philosophical Transactions of the Royal Society B-Biological Sciences, 367, 1245-1255, 10.1098/rstb.2011.0360, 2012.

Goreau, T. J., Kaplan, W. A., Wofsy, S. C., McElroy, M. B., Valois, F. W., and Watson, S. W.: Production of NO_2^- and N_2O by nitrifying bacteria at reduced concentrations of oxygen, Applied and Environmental Microbiology, 40, 526-532, 1980.

Gruber, N.: The marine nitrogen cycle: Overview of distributions and processes. In: Nitrogen in the marine environment, 2nd edition, 1-50, 2008.

Gruber, N.: Warming up, turning sour, losing breath: ocean biogeochemistry under global change, Philosophical Transactions of the Royal Society a-Mathematical Physical and Engineering Sciences, 369, 1980-1996, 10.1098/rsta.2011.0003, 2011.

Horrigan, S. G., Carlucci, A. F., and Williams, P. M.: Light inhibition of nitrification in sea-surface films, Journal of Marine Research, 39, 557-565, 1981.

Huesemann, M. H., Skillman, A. D., and Crecelius, E. A.: The inhibition of marine nitrification by ocean disposal of carbon dioxide, Marine Pollution Bulletin, 44, 142-148, 10.1016/s0025-326x(01)00194-1, 2002.

Jin, X., and Gruber, N.: Offsetting the radiative benefit of ocean iron fertilization by enhancing N2O emissions, Geophysical Research Letters, 30, 10.1029/2003gl018458, 2003.

Liu, B., Morkved, P. T., Frostegard, A., and Bakken, L. R.: Denitrification gene pools, transcription and kinetics of NO, N2O and N-2 production as affected by soil pH, Fems Microbiology Ecology, 72, 407-417, 10.1111/j.1574-6941.2010.00856.x, 2010.

McElroy, M. B.: Marine biological-controls on atmospheric CO_2 and climate, Nature, 302, 328-329, 10.1038/302328a0, 1983.

Orr, J. C., Fabry, V. J., Aumont, O., Bopp, L., Doney, S. C., Feely, R. A., Gnanadesikan, A., Gruber, N., Ishida, A., Joos, F., Key, R. M., Lindsay, K., Maier-Reimer, E., Matear, R., Monfray, P., Mouchet, A., Najjar, R. G., Plattner, G. K., Rodgers, K. B., Sabine, C. L., Sarmiento, J. L., Schlitzer,

R., Slater, R. D., Totterdell, I. J., Weirig, M. F., Yamanaka, Y., and Yool, A.: Anthropogenic ocean acidification over the twenty-first century and its impact on calcifying organisms, Nature, 437, 681-686, 10.1038/nature04095, 2005.

Ravishankara, A. R., Daniel, J. S., and Portmann, R. W.: Nitrous Oxide (N_2O): The Dominant Ozone-Depleting Substance Emitted in the 21st Century, Science, 326, 123-125, 10.1126/science.1176985, 2009.

Rudd, J. W. M., Kelly, C. A., Schindler, D. W., and Turner, M. A.: Disruption of the nitrogen cycle in acidified lakes. Science, 240(4858), 1515-1517, 1988.

Sarmiento, J. L., Slater, R., Barber, R., Bopp, L., Doney, S. C., Hirst, A. C., Kleypas, J., Matear, R., Mikolajewicz, U., Monfray, P., Soldatov, V., Spall, S. A., and Stouffer, R.: Response of ocean ecosystems to climate warming, Global Biogeochemical Cycles, 18, 10.1029/2003gb002134, 2004.

Steinacher, M., Joos, F., Frolicher, T. L., Bopp, L., Cadule, P., Cocco, V., Doney, S. C., Gehlen, M., Lindsay, K., Moore, J. K., Schneider, B., and Segschneider, J.: Projected 21st century decrease in marine productivity: a multi-model analysis, Biogeosciences, 7, 979-1005, 2010.

Takahashi, T., Broecker, W. S., and Langer, S.: Redfield ratio based on chemical-data from isopycnal surfaces, Journal of Geophysical Research-Oceans, 90, 6907-6924, 10.1029/JC090iC04p06907, 1985.

Wolff, E. W.: Greenhouse gases in the Earth system: a palaeoclimate perspective, Philosophical Transactions of the Royal Society a-Mathematical Physical and Engineering Sciences, 369, 2133-2147, 10.1098/rsta.2010.0225, 2011.

Yoshioka, T., and Saijo, Y.: Photoinhibition and recovery of nh-4+-oxidizing bacteria and no-2-oxidizing bacteria, Journal of General and Applied Microbiology, 30, 151-166, 10.2323/jgam.30.151, 1984.

Zamora, L. M., Oschlies, A., Bange, H. W., Huebert, K. B., Craig, J. D., Kock, A., and Loescher, C. R.: Nitrous oxide dynamics in low oxygen regions of the Pacific: insights from the MEMENTO database, Biogeosciences, 9, 5007-5022, 10.5194/bg-9-5007-2012, 2012.

6.9. Supplementary Material

As today, there are neither databases of nitrification rates available nor a global nitrification estimate. The estimate of the total amount of NH_4 in the ocean interior is around 340 ± 68 TgN (Gruber, 2008). The model estimate of 196 TgN is below the JGOFS interpolated value, but still close to the observations. Therefore, we evaluate in this section the environmental factors impacting nitrification: pH and export of organic matter to depth.

6.9.1. Carbonate chemistry

The model pH shows a good spatial correlation with the GLODAP-derived pH in the first 100m to 200m deep band, where most of the nitrification occurs (Figure 8). NEMO-PISCES identifies the regions of relatively lower pH in the upwelling regions in the Atlantic and Pacific basins, North Pacific and Bay of Bengal. Discrepancies are found in the higher pH values in the subtropical gyres in GLODAP compared to NEMO-PISCES.

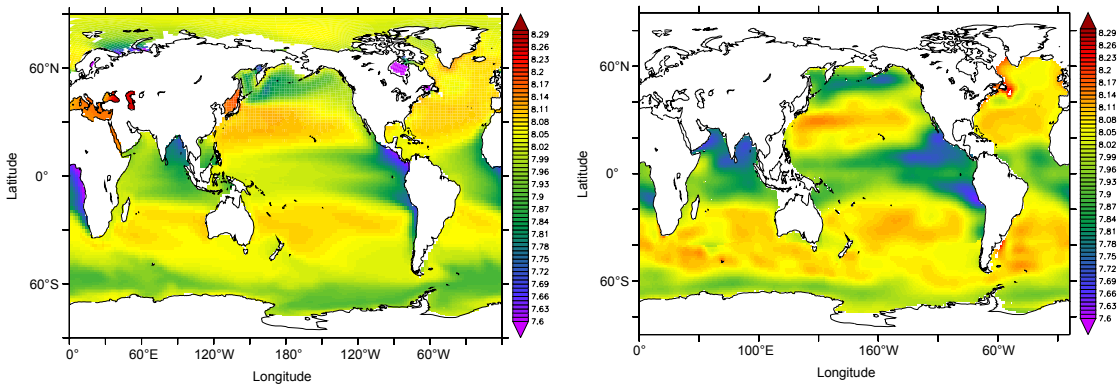

Figure 8: Averaged pH (in pH units) in the 100m to 200m deep band on (a) NEMO-PISCES averaged over the simulated 1995 to 2005 time period and (b) GLODAP pH estimate averaged over the same deep band.

6.9.2. Export of organic matter

As a proxy of nitrification occurrence below the euphotic zone, where ubiquitous nitrifying bacteria is assumed to exist, we analyse the model output in terms of CEX. CEX eventually leads to remineralisation of organic matter and hence to nitrification in the ocean interior. The model estimate of 6.53 PgC yr^{-1} is below the recent estimate from Dunne et al. (2007) estimate of 9.84 PgC yr^{-1}. Coarse resolution models have a similar yet deficient representation

of coastal margin processes, hence attributing all CEX to the ocean interior (Figure 9) rather than along the continental margins. Nevertheless, a good agreement with the major CEX cores is found at the Eastern Tropical Pacific (ETP), Indian Ocean, North Pacific, North Atlantic and Subantarctic regions. Discrepancies are found in the misrepresented Benguela Upwelling system and the overestimation of CEX in the Southern Ocean, in addition to the above mentioned coastal margins. From an overall perspective, high CEX regions above 30 mmolC $m^{-2}d^{-1}$ are not well represented in our model.

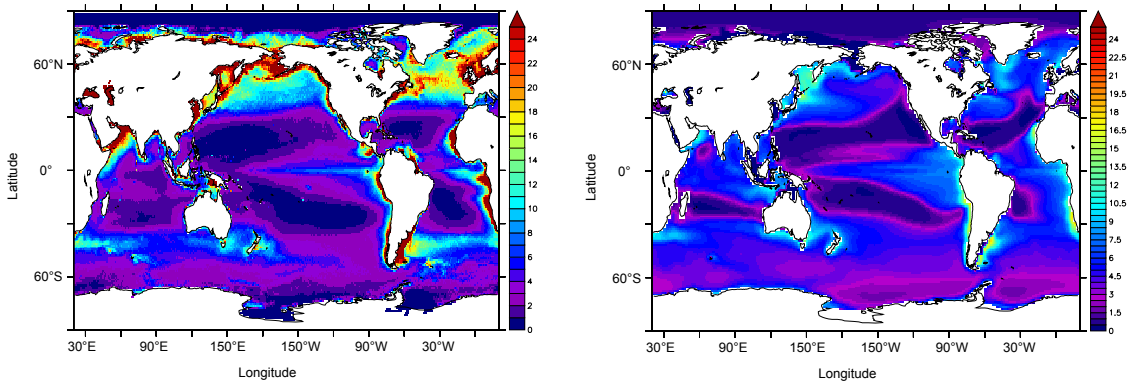

Figure 9: Export of organic matter (in mmolC $m^{-2}d^{-1}$) at 100m from (a) CEX data-based product from Dunne et al. (2007) and (b) NEMO-PISCES averaged over the 1995 to 2005 time period in the historical simulation.

Chapter 7

Conclusions and Perspectives

7.1. Conclusions

In this thesis I have explored the changes in the marine N-cycle due to the effect of climate change, ocean deoxygenation and ocean acidification. Making use of earth system models, future changes in N_2-fixation, nitrification and N_2O production were assessed. From a global perspective, the N-cycle processes that modulate the bioavailable nitrogen appear as a self regulating mechanism in response to future marine stressors. While N_2-fixation is enhanced due to higher levels of CO_2, nitrification is attenuated by the same simultaneous effect. The marine N_2O production experiences the combined effect of ocean biogeochemical and circulation changes. The ocean produces less N_2O in the future, which in turn is captured by a reduced ventilation increasing its storage in the ocean interior. Overall the marine N-cycle does not respond as a positive feedback in the climate system to the external anthropogenic forcings looming ahead. Details on the various N-cycle responses I found to marine stressors are listed in the following sections.

7.1.1. N-cycle in CMIP5 models

The offline analysis of the CMIP5 models have shed light into the current strengths and weaknesses this suite of models have as today. Considering the development of the N-cycle in

global biogeochemical models secondary to that of the carbon cycle, the state of models is encouraging to pursue further developments and gives confidence in future simulations as well as in identifying the interactions among the main drivers of changes in the N-cycle. Models identify the major N_2O production and N_2O inventory hotspots and the way CEX and O_2 shape the present and future evolution of marine N_2O based on the available parameterizations. N_2O model projections using CMIP5 individual models must be framed in this set of strengths and weaknesses. Removing the O_2 dependency on N_2O production parameterizations and an accurate estimation of CEX, particularly in coastal margins, would reduce significantly the uncertainties on N_2O estimates. Moreover, models match the global N_2-fixation rates and identify temperature as one of the main environmental controls of N_2-fixation occurrence. In particular, the main findings are:

- Compared to data-based products and model derived estimates, CMIP5 models underestimate N_2O production on a global scale. Despite the good match in the location of the major N_2O production areas, the magnitude of this production carries the understimation in CEX, which eventually turns into N_2O production based on current parameterizations available. CMIP5 model estimates introduce a 50% uncertainty over the total estimated value. Reasons behind these uncertainties are the different CEX attenuation processes, sinking profiles, remineralization and coarse resolution in CMIP5 models, which hamper an accurate representation of export of organic matter to depth. O_2 fields are secondary in the uncertainties when estimating N_2O production. However, CMIP5 models seem clustered around a targeted CEX value rather than using independent approaches. Even the model estimates found in literature show a larger spectrum of values than those from CMIP5 models. These model estimates are based on a variety of calculation methods and tied to the uncertainties of different data sources such as ^{14}C or satellite derived data. Similar independent approaches on the ocean biogeochemical model community could expand the uncertainties in CEX and hence in N_2O production found in this study.

- The magnitude of the actual N_2O inventory at depth estimated by CMIP5 models strongly depends on the O_2 fields. CMIP5 models show a wide spectrum of volumes regarding the low O_2 regimes, where N_2O production is enhanced. In general, CMIP5 models are highly oxygenated, as shown by the fact that N_2O inventory is underestimated compared to the WOA2005* estimates. However, the N_2O reservoirs in CMIP5 models are found where data-based products estimate the N_2O storage. This result gives us confidence on the location and hence on the physical mechanisms

of transport of deep N_2O to the sea-to-air interface in order to estimate the total N_2O sea-to-air flux accurately.

- Global N_2-fixation rates are accurately estimated by the CMIP5 model suite compared to the most recent N_2-fixation rates database from Luo et al. (2012). The relative contribution of each of the individual oceanic basins are reflected in all of the model estimates, being the Pacific the largest contributor of NH_4 via N_2-fixation. Spatialwise there are strong features in CMIP5 models such as the low latitudinal occurrence and the temperature threshold of 15 to 20°C at which N_2-fixation kicks in. On the contrary, there are inconsistencies among the CMIP5 models representing N_2-fixation in upwelling regions such as the ETP, and hence on the sensitivity of N_2-fixation process to other forms of bioavailable nitrogen. The addition of explicit PFTs show also large discrepancies as today.

7.1.2. Oceanic N_2O emissions in the 21st century

Future marine N_2O emissions are projected to decrease in 2100 under the business as usual high CO_2 emissions scenario. Assuming a dominant N_2O production via nitrification, changes in primary production and hence on export of organic matter to depth are translated into N_2O formation in the ocean interior. Simultaneously, stratification enlarges the N_2O reservoir at depth, leading to an overall decrease of 4 to 12% in N_2O sea-to-air emissions. The most remarkable findings regarding climate system feedbacks and regulating mechanisms are the following:

- Changes in oceanic N_2O emissions in 2100 are of the same magnitude in terms of radiative forcing as the increase from terrestrial N_2O sources over the same time period. The model estimate of 4 to 10% decrease in N_2O sea-to-air flux yields a change in radiative forcing of -0.005 and -0.014 W $m^{-2}K^{-1}$ in the two parameterizations considered, which is in the envelope of +0.001 and +0.015 W m^{-2} K^{-1} estimated by Stocker et al. (2013). This potential compensation in 2100 is estimated by a single model analysis and it must be however interpreted with caution.

- Two mechanisms operate in tandem in the reduction of oceanic N_2O emissions in 2100. N_2O production via nitrification is reduced when primary productivity decreases due to increased stratification and less supply of nutrients into the euphotic layer. In addition, the same changes in ocean circulation retard the N_2O transport from the

subsurface to the sea-to-air interface for gas exchange. As a result, the N_2O reservoir in the deep increases while N_2O sea-to-air flux decreases.

- There is a maximum of a 20% decrease in N_2O sea-to-air flux when these mechanisms are considered as the only means of change in 2100. Simple box model analysis show the boundary of change in N_2O emissions, which correspond to a 20% decrease in export of organic matter to depth and the almost interruption of mixing between the subsurface and the surface layers.

- The model analysis is almost independent of the parameterization used. If nitrification is the main N_2O production pathway in the ocean interior, other variables included into N_2O parameterizations such as temperature, higher N_2O yield in low O_2 regimes or N_2O consumption in the core of the OMZs are not significant when estimating changes in N_2O on a global scale over centennial timescales. However, there are room for changes if the same model projections are done with a different O_2 fields, where N_2O production via denitrification in tandem with nitrification in OMZs could contribute differently to global N_2O production.

7.1.3. Impact of ocean acidification on N_2-fixation

The CO_2 fertilization effect reported originally by Barcelos e Ramos et al. (2007) and particularly analyzed by Hutchins et al. (2013) has been quantified on a global scale using an ocean biogeochemical model. The study has shown that diaztrophs might be one of the winning groups in future climage change and ocean acidification scenarios. Despite their slower growth rate, the CO_2 fertilization effect compensates the lack of nutrients from global warming. Moreover, the model projects an expansion of their niches due to increasing temperature. The most sensitive N_2-fixation species to changes in dissolved CO_2 has been studied in this work. Assuming an single ubiquitous dominant diazotroph species (*Trichodesmium Erythraeum*), highly sensitive to seawater CO_2, the model estimates a 22% increase in N_2-fixation rates at the end of the century compared to its preindustrial value. Other major results are listed below:

- The most sensitive scenario, where *Trichodesmium Erythreaeum* responds to high levels of dissolved CO_2, increases the amount of NH_4 in the surface layers and contributes to a 2% increase in primary production at the end of the century. An heterogeneous combination of other species of diazotrophs responding to high CO_2 might not have

an imprint into primary production. Changes in primary production due to this CO_2 fertilization effect are highly spatial correlated with changes in N_2-fixation.

- When the response of N_2-fixation to CO_2 is so sensitive, the global N_2-fixation rate in 2100 under climate change is able to increase compared to present estimated values. The additional contribution of CO_2 as a nutrient compensates the effect of climate change, which plummets N_2-fixation rate on a global scale due to a limited supply of nutrients to diazotrophs.

- Diazotrophs are favoured both by ocean acidification and global warming. While increasing CO_2 enhances their metabolism with less nutrient limitation, increasing temperatures allow diazotrophs to expand latitudinally and depthwise. N_2-fixers in 2100 could migrate beyond 40°N/S and also reach easily the boundaries of the euphotic layer if temperature increases. Diazotrophs would therefore compete in new regions for the existing nutrients against all the non-diazotroph groups.

- The model analysis expands from 278 to 950ppm of atmospheric CO_2, where changes in primary production are not significant compared to the variations observed in CO_2 in the past. This fact contributes to the interpretation of paleorecords and the role that N_2-fixation and its coupling with denitrification has played in the past. Theories like those from McElroy (1983) or Gruber (2008) on the strength of the biological pump due to N_2-fixation / denitrification must be revised.

7.1.4. Impact of ocean acidification on nitrification

This work shows some of the consequences of ocean acidification on global climate feedbacks. On short timescales, the CO_2 attenuation effect has implications on N_2O production and eventually on oceanic N_2O emissions to the atmosphere. On longer timescales, it casts doubts on the coupling between N_2-fixation and denitrification, as the effect of nitrification on subsurface O_2 might buffer the signal from N_2-fixation to denitrification. Assuming nitrification as the dominant N_2O production pathway, there is a first order effect of decreasing pH on the efficiency of nitrification, which leads to significant changes in N_2O production at the end of the century. Despite the simulated decrease in nitrification, the pool of nutrients does not experience a significant change, particularly on the amount of NO_3 in the subsurface. Changes in NO_3 do not translate into changes in PP on a global scale, as

expected from the 16% decrease in nitrification obtained in the model projections. Particular conclusions that must be highlighted are:

- The model projects a significant 16% decrease in nitrification rates at the end of the century. The ubiquitous decrease in pH is translated into less nitrification in all of the major oceanic basins, based on the model assumption that nitrifying bacteria is present wherever there is export of organic matter to depth.

- The bioabailable nitrogen pool does not experience significant changes in the subsurface. The factors modulating the distribution and abundance of the fixed nitrogen pool still rely mostly on physical transport effects rather than on the biological mechanisms under lower levels of CO_2.

- Nitrous oxide production is the most sensitive process to changes when nitrification depends on pH. The model assumes that nitrification is the dominant N_2O production pathway, and therefore the decrease in nitrification in inherited by N_2O production on a global scale. When climate change operates in tandem with ocean acidification, the N_2O production drops at the same rate as that from climate change alone. Due to the high correlation between subsurface N_2O production and N_2O sea-to-air flux, the drop in N_2O production because of climate change and ocean acidification suggests that changes in oceanic N_2O emissions could offset the terrestrial increase projected by Stocker et al. (2012).

- The changes observed in nitrification casts doubts on whether changes in N_2-fixation via primary production have a direct effect on the occurrence and magnitude of denitrification once O_2 is consumed during remineralization in the subsurface. In fact, subsurface O_2 fields might increase in concentration due to the attenuation of nitrification. Therefore, the niches of denitrifying bacteria might be reduced and alter the negative feedback between N_2-fixation and denitrification. However, this tentative conclusion is tied to the O_2 fields from a single model analysis. Unfortunately, PISCES is a high oxygenated model and changes in the volume of OMZ might have been overlooked in the model experiments.

- By the same token, the underestimation of CEX by contemporary ocean biogeochemical models, i.e., PISCES and the ocean biogeochemical components of the CMIP5 model ensemble, suggests that changes in nitrification could be even

larger than those which have been projected in this work. That would imply an even larger attenuation of N_2O production in the ocean interior and a significant change in the role of the ocean as source of N_2O and its contribution to the global GHG budget.

7.2. Perspectives

The work developed in this thesis shows the path to further improvements needed in analysing the marine N-cycle. Strengths and weaknesses were identified in the CMIP5 model suite as well as in the particular case of PISCES. Interannual variability of N_2O and further analysis of changes on other N-cycle processes due to anthropogenic activities complete this final section of the thesis.

7.2.1. N-cycle processes in OGCBMs

Various caveats have been observed when ocean biogeochemical models deal with available N_2O parameterizations. The O_2 dependency is of paramount importance, particularly when OGCBMs are not yet mature enough to provide reliable O_2 fields (Steinacher et al., 2009, Cocco et al., 2012, Bopp et al., 2013).

Models such as PISCES provide nitrification and denitrification as explicit variables. A ratio of mol of N_2O produced per mol of NH_4 or NO_3 consumed could be developed using the model nitrification and denitrification variables alone without relying largely on proxy variables such as O_2. Despite the variety of existing values for N_2O production rates from these pathways, this feature shows the path to obtain mechanistic parameterizations based on such production rates. However, laboratory experiments still lack a more precise description of N_2O production during nitrification and denitrification processes. Other potential N_2O production pathways such as annammox remain unknown and must be taken into account in laboratory and model experiments to obtain an accurate estimate of the occurrence and N_2O production rate of this formation mechanism.

Multimodel analysis and fully coupled ocean-atmosphere-land scenarios would shed light into global climate feedbacks of N_2O emissions. The use of multiple models would help to narrow down the uncertainties derived from the different O_2 fields, as well as to explore different high- to low-O_2 N_2O production pathways ratios beyond the 75/25 ratio used in PISCES. Fully coupled models might provide additional information on the potential compensation between land and oceanic N_2O emissions and how these changes modulate atmospheric N_2O,

the contribution to radiative forcing and O_3 depletion.

Ocean biogeochemical models have to improve the process description in the mesopelagic region (Vogt et al., *in prep*), where export of organic matter occurs and so does nitrification. An improved representation of changes in the ballast effect, for instance, might have consequences in nitrification in subsurface layers (Gehlen et al., 2011). Variable stoichiometry in models, as reported by Riebesell et al. (2007) and Tagliabue et al. (2011), would significantly improve many processes such as the effect of changes in C:N ratio in CEX or the response of the OMZs volumes to ocean acidification. This additional processes could contribute to the picture of the response of the marine N-cycle to future stressors.

7.2.2. Living compartments in OGCBMs

The model analysis has been based on a single model with two phytoplankton groups, none of them being *diazotrophs*. In addition, the model version that has been used does not include bacteria as an explicit compartment. All the population dynamics derived from changes in the nutrient pool, the expansion of N_2-fixation occurrence or changes in the volume of OMZ and hence on the niches of nitrifying and denitrifying bacteria have been therefore addressed only in part.

Despite the fact that including more PFTs might not improve the representation of N_2-fixation process, a broader spectrum of groups might help to better understand the resource competition between diazotrophs and non-diazotrophs. Swings in the population of both subgroups and the role of nutrient supply in the new arenas N_2-fixers are expected to occupy could be addressed with more complex models. As any other phytoplankton group, the efforts of projects such as MAREDAT (Buitenhuis et al., 2012) seem crucial to validate the representation of several phytoplankton groups in ocean biogeochemical models. Larger datasets of N_2-fixation biomass and rates are needed. Based on the lack of a valid reference, it is difficult to discard any of the different approaches shown by the CMIP5 model output and there is also a lack of theoretical grounds about which are the most relevant environmental variables of N_2-fixation. The problem of including additional phytoplankton groups can be transferred to species among phytoplankton families. Different diazotrophs species have different responses to higher levels of CO_2. The implementation of heterogeneous diazotrophs population in models would also refine the analysis shown in this thesis and quite likely show a smoother response of global N_2-fixation to ocean acidification.

The N_2O experiments have assumed ubiquitous bacteria in the ocean as well as a uniform metabolic response to increasing temperatures or changes in any other environmental variables. Explicit representation of bateria within the model would help to determine their

response to global warming as well as changes in their efficiency producing N_2O. Ultimately, adding gene records and the growing databases in this field are the pivotal and essential challenge in ocean biogeochemical models as today.

7.2.3. Interannual N_2O emissions from the ocean

Interannual variability of N_2O has not been considered in this model analysis, neither in the CMIP5 offline estimates nor in the transient PISCES analysis, forced by monthly means from NEMO ocean circulation model but producing yearly model output to optimize the existing computational resources for the experiments I have done. There are evidences, as shown by Thompson et al. (2013), that tropospheric N_2O is highly anticorrelated with the ENSO index (Figure 1). A higher resolution simulation in the temporal domain would allow us to study the mechanisms behind this anticorrelation. Intuitively, La Niña episodes would enhance the transport of subsurface N_2O to the sea-to-air interface and therefore facilitate gas exchange, contributing to the tropospheric N_2O concentration.

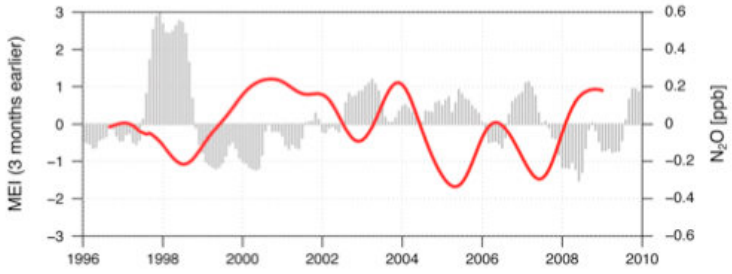

Figure 1: Anomalies in N_2O concentration in the troposphere (in red in ppb) compared to the El Nino index (in grey) from 1996 to 2010 (Thompson et al., 2013).

7.2.4. Combined effects on the N-cycle

The combined effect of global warming and ocean acidification simultaneously on N_2-fixation and nitrification has not been analyzed. In addition to the individual effects shown separately on N_2-fixation and nitrification, a detailed analysis on this extra model output available in terms of primary productivity, changes in the bioavailable nitrogen pool and on N_2O production would complete the picture that has been shown. Moreover, the sensitivity of denitrification to changes in dissolved CO_2 has not been included in the experiments. In addition to the previously mentioned changes in the C:N ratio in response to ocean acidification and therefore on the O_2 utilization, a more detailed description of denitrification

process would allow us to estimate changes in the global nitrogen budget. Analyzing simultaneous changes in N_2-fixation, nitrification and denitrification to multiple stressors would address fundamental questions as those formulated by McElroy (1983) and Gruber (2008) about the major forcings driving a potential imbalance of the N-cycle over long time periods.

These longer time periods could also reveal different aspects of the interactions that have been analyzed. The increasing N_2O reservoir that has been estimated in 2100 could be ventilated via the Southern Ocean. Moreover, the penetration at depth of higher concentrations of dissolved CO_2 could have a larger impact on nitrification below the subsurface. Changes in pH at depth over longer timescales must be explored, as they could become relevant for certain OMZs, particularly at shallow depths such as those in the ETP, Arabian Sea and Bay of Bengal.

7.2.5. External N input

Direct anthropogenic impact on the N-cycle via atmospheric nitrogen deposition and river nitrogen discharge have not been explored. Future atmospheric nitrogen deposition could equal the contribution of fixed nitrogen from N_2-fixation alone (Duce et al., 2008, Krishnamurthy et al., 2007). Experiments increasing the deposition of nitrogen compounds in coastal regions are not expected to change significantly neither primary production nor N_2O production (Suntharalingam et al., 2012). However, changes in the fixed nitrogen pool might have consequences for the groups composition in complex models with more PFTs, particularly when atmospheric nitrogen deposition and N_2-fixation are projected to increase within the next hundred years.

The extensive use of fertilizers will modify the amount of nitrogen compounds which are delivered to the ocean via riverine supply. The additional nutrient supply is expected to impact primary productivity at the same rate as future N_2-fixation does (DaCunha et al., 2007). Therefore, experiments combining additional river nitrogen supply in combination with N_2-fixation might lead to significant changes in primary production and hence on multiple biogeochemical markers. Future projections of river discharge are needed to evaluate its potential impact on contemporary ocean biogeochemical models.

Chapter 8

References

Assmann, K. M., Bentsen, M., Segschneider, J., and Heinze, C.: An isopycnic ocean carbon cycle model, Geoscientific Model Development, 3, 143-167, 2010.

Aumont, O., and Bopp, L.: Globalizing results from ocean in situ iron fertilization studies, Global Biogeochemical Cycles, 20, 10.1029/2005gb002591, 2006.

Badger, M. R., and Bek, E. J.: Multiple Rubisco forms in proteobacteria: their functional significance in relation to CO(2) acquisition by the CBB cycle, Journal of Experimental Botany, 59, 1525-1541, 10.1093/jxb/erm297, 2008.

Bange, H. W., Rixen, T., Johansen, A. M., Siefert, R. L., Ramesh, R., Ittekkot, V., Hoffmann, M. R., and Andreae, M. O.: A revised nitrogen budget for the Arabian Sea, Global Biogeochemical Cycles, 14, 1283-1297, 10.1029/1999gb001228, 2000.

Bange, H. W., Bell, T. G., Cornejo, M., Freing, A., Uher, G., Upstill-Goddard, R. C., and Zhang, G.: MEMENTO: a proposal to develop a database of marine nitrous oxide and methane measurements, Environmental Chemistry, 6, 195-197, 10.1071/en09033, 2009.

Barcelos e Ramos, J., Biswas, H., Schulz, K. G., LaRoche, J., and Riebesell, U.: Effect of rising atmospheric carbon dioxide on the marine nitrogen fixer Trichodesmium, Global Biogeochemical Cycles, 21, 10.1029/2006gb002898, 2007.

Behrenfeld, M. J., and Falkowski, P. G.: Photosynthetic rates derived from satellite-based chlorophyll concentration, Limnology and Oceanography, 42, 1-20, 1997.

Beman, J. M., Chow, C.-E., King, A. L., Feng, Y., Fuhrman, J. A., Andersson, A., Bates, N. R., Popp, B. N., and Hutchins, D. A.: Global declines in oceanic nitrification rates as a consequence of ocean acidification, Proceedings of the National Academy of Sciences of the United States of America, 108, 208-213, 10.1073/pnas.1011053108, 2011.

Berg, I. A., Kockelkorn, D., Buckel, W., and Fuchs, G.: A 3-hydroxypropionate/4-hydroxybutyrate autotrophic carbon dioxide assimilation pathway in archaea, Science, 318, 1782-1786, 10.1126/science.1149976, 2007.

Berman-Frank, I., Cullen, J. T., Shaked, Y., Sherrell, R. M., and Falkowski, P. G.: Iron availability, cellular iron quotas, and nitrogen fixation in Trichodesmium, Limnology and Oceanography, 46, 1249-1260, 2001.

Bianchi, D., Dunne, J. P., Sarmiento, J. L., and Galbraith, E. D.: Data-based estimates of suboxia, denitrification, and N2O production in the ocean and their sensitivities to dissolved O-2, Global Biogeochemical Cycles, 26, 10.1029/2011gb004209, 2012.

Bopp, L., Resplandy, L., Orr, J. C., Doney, S. C., Dunne, J. P., Gehlen, M., Halloran, P., Heinze, C., Ilyina, T., Seferian, R., Tjiputra, J., and Vichi, M.: Multiple stressors of ocean ecosystems in the 21st century: projections with CMIP5 models, Biogeosciences, 10, 6225-6245, 10.5194/bg-10-6225-2013, 2013.

Buitenhuis, E. T., Vogt, M., Moriarty, R., Bednaršek, N., Doney, S. C., Leblanc, K., ... and Swan, C.: MAREDAT: towards a world atlas of MARine Ecosystem DATa. Earth System Science Data, *5*(2), 227-239, 2013.

Butler, J. H., Elkins, J. W., Thompson, T. M., and Egan, K. B.: Tropospheric and dissolved N_2O of the west pacific and east-indian oceans during the el-niño southern oscillation event of 1987, Journal of Geophysical Research-Atmospheres, 94, 14865-14877, 10.1029/JD094iD12p14865, 1989.

Capone, D. G., Zehr, J. P., Paerl, H. W., Bergman, B., and Carpenter, E. J.: Trichodesmium, a globally significant marine cyanobacterium, Science, 276, 1221-1229, 10.1126/science.276.5316.1221, 1997.

Carpenter E. J. and Capone D. G.: Nitrogen Fixation in the Marine Environment. In: Capone D. G., Bronk D. A., Mulholland M. R., and Carpenter E., editors, Nitrogen in the Marine Environment, pages 141–198. Academic Press, San Diego, 2nd edition, 2008.

Carpenter E. J. Nitrogen fixation by marine *Oscillatoria* (Trichodesmium) in the World's oceans. In: Carpenter E. J. and Capone D. G., editors, Nitrogen in the marine environment, pages 65–103. Academic Press, San Diego, Calif., 1983.

Chen, Y. B., Zehr, J. P., and Mellon, M.: Growth and nitrogen fixation of the diazotrophic filamentous nonheterocystous cyanobacterium Trichodesmium sp IMS 101 in defined media: Evidence for a circadian rhythm, Journal of Phycology, 32, 916-923, 10.1111/j.0022-3646.1996.00916.x, 1996.

Ciais, P., Sabine, C., Bala, G., Bopp, L., Brovkin, V., Canadell, J., Chhabra, A., DeFries, R., Galloway, J., Heimann, M., Jones, C., Le Quéré, C., Myneni, RB., Piao, S. and Thornton, P.: Carbon and Other Biogeochemical Cycles. In: Climate Change 2013: The Physical Science Basis. Contribution of Working Group I to the Fifth Assessment Report of the Intergovernmental Panel on Climate Change, 2013.

Cocco, V., Joos, F., Steinacher, M., Froelicher, T. L., Bopp, L., Dunne, J., Gehlen, M., Heinze, C., Orr, J., Oschlies, A., Schneider, B., Segschneider, J., and Tjiputra, J.: Oxygen

and indicators of stress for marine life in multi-model global warming projections, Biogeosciences, 10, 1849-1868, 10.5194/bg-10-1849-2013, 2013.

Cohen, Y., and Gordon, L. I.: Nitrous-oxide in oxygen minimum of eastern tropical north pacific - evidence for its consumption during denitrification and possible mechanisms for its production, Deep-Sea Research, 25, 509-524, 10.1016/0146-6291(78)90640-9, 1978.

Cornejo, M., and Farías, L.: Following the N2O consumption in the oxygen minimum zone of the eastern South Pacific. Biogeosciences, 9(8), 3205-3212, 2012.

Crutzen, P. J.: Influence of nitrogen oxides on atmospheric ozone content, Quarterly Journal of the Royal Meteorological Society, 96, 320-&, 10.1002/qj.49709640815, 1970.

da Cunha, L. C., Buitenhuis, E. T., Le Quere, C., Giraud, X., and Ludwig, W.: Potential impact of changes in river nutrient supply on global ocean biogeochemistry, Global Biogeochemical Cycles, 21, 10.1029/2006gb002718, 2007.

de Wilde, H. P. J., and de Bie, M. J. M.: Nitrous oxide in the Schelde estuary: production by nitrification and emission to the atmosphere, Marine Chemistry, 69, 203-216, 10.1016/s0304-4203(99)00106-1, 2000.

Dentener, F., Drevet, J., Lamarque, J. F., Bey, I., Eickhout, B., Fiore, A. M., Hauglustaine, D., Horowitz, L. W., Krol, M., Kulshrestha, U. C., Lawrence, M., Galy-Lacaux, C., Rast, S., Shindell, D., Stevenson, D., Van Noije, T., Atherton, C., Bell, N., Bergman, D., Butler, T., Cofala, J., Collins, B., Doherty, R., Ellingsen, K., Galloway, J., Gauss, M., Montanaro, V., Mueller, J. F., Pitari, G., Rodriguez, J., Sanderson, M., Solmon, F., Strahan, S., Schultz, M., Sudo, K., Szopa, S., and Wild, O.: Nitrogen and sulfur deposition on regional and global scales: A multimodel evaluation, Global Biogeochemical Cycles, 20, 10.1029/2005gb002672, 2006.

Deutsch, C., Sarmiento, J. L., Sigman, D. M., Gruber, N., and Dunne, J. P.: Spatial coupling of nitrogen inputs and losses in the ocean, Nature, 445, 163-167, 10.1038/nature05392, 2007.

Devol A. H.: Denitrification including Anammox. In: Capone D. G., Bronk D. A., Mulholland M. R., and Carpenter E., editors, Nitrogen in the Marine Environment, pages 263–302. Academic Press, San Diego, 2nd edition, 2008.

Duce, R. A., LaRoche, J., Altieri, K., Arrigo, K. R., Baker, A. R., Capone, D. G., Cornell, S., Dentener, F., Galloway, J., Ganeshram, R. S., Geider, R. J., Jickells, T., Kuypers, M. M., Langlois, R., Liss, P. S., Liu, S. M., Middelburg, J. J., Moore, C. M., Nickovic, S., Oschlies, A., Pedersen, T., Prospero, J., Schlitzer, R., Seitzinger, S., Sorensen, L. L., Uematsu, M.,

Ulloa, O., Voss, M., Ward, B., and Zamora, L.: Impacts of atmospheric anthropogenic nitrogen on the open ocean, Science, 320, 893-897, 10.1126/science.1150369, 2008.

Dufresne, J. L., Foujols, M. A., Denvil, S., Caubel, A., Marti, O., Aumont, O., Balkanski, Y., Bekki, S., Bellenger, H., Benshila, R., Bony, S., Bopp, L., Braconnot, P., Brockmann, P., Cadule, P., Cheruy, F., Codron, F., Cozic, A., Cugnet, D., de Noblet, N., Duvel, J. P., Ethe, C., Fairhead, L., Fichefet, T., Flavoni, S., Friedlingstein, P., Grandpeix, J. Y., Guez, L., Guilyardi, E., Hauglustaine, D., Hourdin, F., Idelkadi, A., Ghattas, J., Joussaume, S., Kageyama, M., Krinner, G., Labetoulle, S., Lahellec, A., Lefebvre, M. P., Lefevre, F., Levy, C., Li, Z. X., Lloyd, J., Lott, F., Madec, G., Mancip, M., Marchand, M., Masson, S., Meurdesoif, Y., Mignot, J., Musat, I., Parouty, S., Polcher, J., Rio, C., Schulz, M., Swingedouw, D., Szopa, S., Talandier, C., Terray, P., Viovy, N., and Vuichard, N.: Climate change projections using the IPSL-CM5 Earth System Model: from CMIP3 to CMIP5, Climate Dynamics, 40, 2123-2165, 10.1007/s00382-012-1636-1, 2013.

Dunne, J. P., Armstrong, R. A., Gnanadesikan, A., and Sarmiento, J. L.: Empirical and mechanistic models for the particle export ratio, Global Biogeochemical Cycles, 19, 10.1029/2004gb002390, 2005.

Dunne, J. P., Sarmiento, J. L., and Gnanadesikan, A.: A synthesis of global particle export from the surface ocean and cycling through the ocean interior and on the seafloor, Global Biogeochemical Cycles, 21, 10.1029/2006gb002907, 2007.

Dunne, J. P., John, J. G., Shevliakova, E., Stouffer, R. J., Krasting, J. P., Malyshev, S. L., Milly, P. C. D., Sentman, L. T., Adcroft, A. J., Cooke, W., Dunne, K. A., Griffies, S. M., Hallberg, R. W., Harrison, M. J., Levy, H., Wittenberg, A. T., Phillips, P. J., and Zadeh, N.: GFDL's ESM2 Global Coupled Climate-Carbon Earth System Models. Part II: Carbon System Formulation and Baseline Simulation Characteristics, Journal of Climate, 26, 2247-2267, 10.1175/jcli-d-12-00150.1, 2013.

Dutkiewicz, S., Ward, B. A., Monteiro, F., and Follows, M. J.: Interconnection of nitrogen fixers and iron in the Pacific Ocean: Theory and numerical simulations, Global Biogeochemical Cycles, 26, 10.1029/2011gb004039, 2012.

Elkins, J. W., Wofsy, S. C., McElroy, M. B., Kolb, C. E., and Kaplan, W. A.: Aquatic sources and sinks for nitrous-oxide, Nature, 275, 602-606, 10.1038/275602a0, 1978.

Eugster, O., Gruber, N., Flueckiger, J., and Giraud, X.: Was the inventory of the marine fixed nitrogen twice as large at the LGM compared to the Holocene?, Geochimica Et Cosmochimica Acta, 73, A343-A343, 2009.

Eugster, O., and Gruber, N.: A probabilistic estimate of global marine N-fixation and denitrification, Global Biogeochemical Cycles, 26, 10.1029/2012gb004300, 2012.

Eugster, O., PhD thesis, Constraining the pre-industrial and deglacial marine nitrogen cycle by combining models and observations, ETH Zuerich, 2013.

Falkowski, P. G.: Evolution of the nitrogen cycle and its influence on the biological sequestration of CO2 in the ocean, Nature, 387, 272-275, 10.1038/387272a0, 1997.

Fennel, K., Spitz, Y. H., Letelier, R. M., Abbott, M. R., and Karl, D. M.: A deterministic model for N-2 fixation at stn. ALOHA in the subtropical North Pacific Ocean, Deep-Sea Research Part Ii-Topical Studies in Oceanography, 49, 149-174, 2002.

Fluckiger, J., et al.: N2O and CH4 variations during the last glacial epoch: Insight into global processes, Global Biogeochemical Cycles, 18(1), 2004.

Follows, M. J., Dutkiewicz, S., Grant, S., and Chisholm, S. W.: Emergent biogeography of microbial communities in a model ocean, Science, 315, 1843-1846, 10.1126/science.1138544, 2007.

Frame, C. H., and Casciotti, K. L.: Biogeochemical controls and isotopic signatures of nitrous oxide production by a marine ammonia-oxidizing bacterium, Biogeosciences, 7, 2695-2709, 10.5194/bg-7-2695-2010, 2010.

Freing, A., Wallace, D. W. R., and Bange, H. W.: Global oceanic production of nitrous oxide, Philosophical Transactions of the Royal Society B-Biological Sciences, 367, 1245-1255, 10.1098/rstb.2011.0360, 2012.

Fu, F.-X., Yu, E., Garcia, N. S., Gale, J., Luo, Y., Webb, E. A., and Hutchins, D. A.: Differing responses of marine N-2 fixers to warming and consequences for future diazotroph community structure, Aquatic Microbial Ecology, 72, 33-46, 10.3354/ame01683, 2014.

Galloway, J. N., Dentener, F. J., Capone, D. G., Boyer, E. W., Howarth, R. W., Seitzinger, S. P., Asner, G. P., Cleveland, C. C., Green, P. A., Holland, E. A., Karl, D. M., Michaels, A. F., Porter, J. H., Townsend, A. R., and Vorosmarty, C. J.: Nitrogen cycles: past, present, and future, Biogeochemistry, 70, 153-226, 10.1007/s10533-004-0370-0, 2004.

Garcia, H. E., R. A. Locarnini, T. P. Boyer, J. I. Antonov, O. K. Baranova, M. M. Zweng, and D. R. Johnson: World Ocean Atlas 2009, Volume 3: Dissolved Oxygen, Apparent Oxygen Utilization, and Oxygen Saturation. S. Levitus, Ed. NOAA Atlas NESDIS 70, U.S. Government Printing Office, Washington, D.C., 344 pp., 2010a.

Garcia, H. E., R. A. Locarnini, T. P. Boyer, J. I. Antonov, M. M. Zweng, O. K. Baranova, and D. R. Johnson, World Ocean Atlas 2009, Volume 4: Nutrients (phosphate, nitrate,

silicate). S. Levitus, Ed. NOAA Atlas NESDIS 71, U.S. Government Printing Office, Washington, D.C., 398 pp. 2010b.

Gehlen, M., Gruber, N., Gangstø, R., Bopp, L., and Oschlies, A.: Biogeochemical consequences of ocean acidification and feedbacks to the earth system. Ocean acidification: 230-248, 2011.

Goreau, T. J., Kaplan, W. A., Wofsy, S. C., McElroy, M. B., Valois, F. W., and Watson, S. W.: Production of NO_2^- and N_2O by nitrifying bacteria at reduced concentrations of oxygen, Applied and Environmental Microbiology, 40, 526-532, 1980.

Grosskopf, T., Mohr, W., Baustian, T., Schunck, H., Gill, D., Kuypers, M. M. M., Lavik, G., Schmitz, R. A., Wallace, D. W. R., and LaRoche, J.: Doubling of marine dinitrogen-fixation rates based on direct measurements, Nature, 488, 361-364, 10.1038/nature11338, 2012.

Gruber, N.: The marine nitrogen cycle: Overview of distributions and processes. In: Nitrogen in the marine environment, 2nd edition, 1-50, 2008.

Gruber, N.: The dynamics of the marine nitrogen cycle and its influence on atmospheric CO_2 variations, in The ocean carbon cycle and climate, edited by M. Follows, and T. Oguz, pp. 97-148, Kluwer Academic Publishers, 2004.

Gruber, N., and Galloway, J. N.: An Earth-system perspective of the global nitrogen cycle, Nature, 451, 293-296, 10.1038/nature06592, 2008.

Gruber, N.: Warming up, turning sour, losing breath: ocean biogeochemistry under global change, Philosophical Transactions of the Royal Society a-Mathematical Physical and Engineering Sciences, 369, 1980-1996, 10.1098/rsta.2011.0003, 2011.

Gutknecht, E., Dadou, I., Le Vu, B., Cambon, G., Sudre, J., Garcon, V., Machu, E., Rixen, T., Kock, A., Flohr, A., Paulmier, A., and Lavik, G.: Coupled physical/biogeochemical modeling including O-2-dependent processes in the Eastern Boundary Upwelling Systems: application in the Benguela, Biogeosciences, 10, 3559-3591, 10.5194/bg-10-3559-2013, 2013.

Hahn, J., Nitrous oxide in the oceans, in Denitrification, Nitrification and Atmospheric Nitrous Oxide, edited by C. C. Delwiche, pp. 191 – 240, John Wiley, New York, 1981.

Hauglustaine, D. A., Lathiere, J., Szopa, S., and Folberth, G. A.: Future tropospheric ozone simulated with a climate-chemistry-biosphere model, Geophysical Research Letters, 32, 10.1029/2005gl024031, 2005.

Holl, C. M., and Montoya, J. P.: Interactions between nitrate uptake and nitrogen fixation in continuous cultures of the marine diazotroph Trichodesmium (Cyanobacteria), Journal of Phycology, 41, 1178-1183, 10.1111/j.1529-8817.2005.00146.x, 2005.

Hood, R. R., Bates, N. R., Capone, D. G., and Olson, D. B.: Modeling the effect of nitrogen fixation on carbon and nitrogen fluxes at BATS, Deep-Sea Research Part Ii-Topical Studies in Oceanography, 48, 1609-1648, 10.1016/s0967-0645(00)00160-0, 2001.

Horrigan, S. G., Carlucci, A. F., and Williams, P. M.: Light inhibition of nitrification in sea-surface films, Journal of Marine Research, 39, 557-565, 1981.

Hourdin, F., Musat, I., Bony, S., Braconnot, P., Codron, F., Dufresne, J.-L., Fairhead, L., Filiberti, M.-A., Friedlingstein, P., Grandpeix, J.-Y., Krinner, G., LeVan, P., Li, Z.-X., and Lott, F.: The LMDZ4 general circulation model: climate performance and sensitivity to parametrized physics with emphasis on tropical convection, Climate Dynamics, 27, 787-813, 10.1007/s00382-006-0158-0, 2006.

Huesemann, M. H., Skillman, A. D., and Crecelius, E. A.: The inhibition of marine nitrification by ocean disposal of carbon dioxide, Marine Pollution Bulletin, 44, 142-148, 10.1016/s0025-326x(01)00194-1, 2002.

Hutchins, D. A., Fu, F. X., Zhang, Y., Warner, M. E., Feng, Y., Portune, K., Bernhardt, P. W., and Mulholland, M. R.: CO2 control of Trichodesmium N-2 fixation, photosynthesis, growth rates, and elemental ratios: Implications for past, present, and future ocean biogeochemistry, Limnology and Oceanography, 52, 1293-1304, 10.4319/lo.2007.52.4.1293, 2007.

Hutchins, D. A., Fu, F.-X., Webb, E. A., Walworth, N., and Tagliabue, A.: Taxon-specific response of marine nitrogen fixers to elevated carbon dioxide concentrations, Nature Geoscience, 6, 790-795, 10.1038/ngeo1858, 2013.

Jansen, E., et al.: Paleoclimate, in Climate Change 2007: The Physical Science Basis. Contribution of Working Group I to the Fourth Assessment Report of the Intergovernmental Panel on Climate Change, Cambridge University Press, Cambridge, United Kingdom and New York, NY, USA, 2007.

Jin, X., and Gruber, N.: Offsetting the radiative benefit of ocean iron fertilization by enhancing N2O emissions, Geophysical Research Letters, 30, 10.1029/2003gl018458, 2003.

Johnston, H.: Reduction of stratospheric ozone by nitrogen oxide catalysts from supersonic transport exhaust, Science, 173, 517-&, 10.1126/science.173.3996.517, 1971.

Karl, D., Michaels, A., Bergman, B., Capone, D., Carpenter, E., Letelier, R., Lipschultz, F., Paerl, H., Sigman, D., and Stal, L.: Dinitrogen fixation in the world's oceans, Biogeochemistry, 57, 47-+, 10.1023/a:1015798105851, 2002.

Klaas, C., and Archer, D. E.: Association of sinking organic matter with various types of mineral ballast in the deep sea: Implications for the rain ratio, Global Biogeochemical Cycles, 16, 10.1029/2001gb001765, 2002.

Krishnamurthy, A., Moore, J. K., Zender, C. S., and Luo, C.: Effects of atmospheric inorganic nitrogen deposition on ocean biogeochemistry, Journal of Geophysical Research-Biogeosciences, 112, 10.1029/2006jg000334, 2007.

Kuypers, M. M. M., Lavik, G., Woebken, D., Schmid, M., Fuchs, B. M., Amann, R., Jorgensen, B. B., and Jetten, M. S. M.: Massive nitrogen loss from the Benguela upwelling system through anaerobic ammonium oxidation, Proceedings of the National Academy of Sciences of the United States of America, 102, 6478-6483, 10.1073/pnas.0502088102, 2005.

Lam, P., Lavik, G., Jensen, M. M., van de Vossenberg, J., Schmid, M., Woebken, D., Gutierrez, D., Amann, R., Jetten, M. S. M., and Kuypers, M. M. M.: Revising the nitrogen cycle in the Peruvian oxygen minimum zone, Proceedings of the National Academy of Sciences of the United States of America, 106, 4752-4757, 10.1073/pnas.0812444106, 2009.

Law, C. S., and Owens, N. J. P.: Significant flux of atmospheric nitrous-oxide from the northwest indian-ocean, Nature, 346, 826-828, 10.1038/346826a0, 1990.

Laws, E. A., Falkowski, P. G., Smith, W. O., Ducklow, H., and McCarthy, J. J.: Temperature effects on export production in the open ocean, Global Biogeochemical Cycles, 14, 1231-1246, 10.1029/1999gb001229, 2000.

Lenes, J. M., Darrow, B. A., Walsh, J. J., Prospero, J. M., He, R., Weisberg, R. H., Vargo, G. A., and Heil, C. A.: Saharan dust and phosphatic fidelity: A three-dimensional biogeochemical model of Trichodesmium as a nutrient source for red tides on the West Florida Shelf, Continental Shelf Research, 28, 1091-1115, 10.1016/j.csr.2008.02.009, 2008.

Levitus, S. (Ed.). World ocean atlas 2009, 2010.

Liu, B., Morkved, P. T., Frostegard, A., and Bakken, L. R.: Denitrification gene pools, transcription and kinetics of NO, N2O and N-2 production as affected by soil pH, Fems Microbiology Ecology, 72, 407-417, 10.1111/j.1574-6941.2010.00856.x, 2010.

Ludwig, W., Probst, J. L., and Kempe, S.: Predicting the oceanic input of organic carbon by continental erosion, Global Biogeochemical Cycles, 10, 23-41, 10.1029/95gb02925, 1996.

Luo, Y. W., Doney, S. C., Anderson, L. A., Benavides, M., Bode, A., Bonnet, S., ... & Zehr, J. P.: Database of diazotrophs in global ocean: abundances, biomass and nitrogen fixation rates. Earth System Science Data Discussions, *5*(1), 47-106, 2012.

Luo, Y. W., Lima, I. D., Karl, D. M., Deutsch, C. A., and Doney, S. C.: Data-based assessment of environmental controls on global marine nitrogen fixation, Biogeosciences, 11, 691-708, 10.5194/bg-11-691-2014, 2014.

Madec, G.: NEMO ocean engine. Note du Pole de modelisation, Institut Pierre- Simon Laplace (IPSL), France, No 27, ISSN No 1288-1619, 2008.

Maier-Reimer, E., Kriest, I., Segschneider, J., & Wetzel, P.: The Hamburg Ocean Carbon Cycle Model HAMOCC5. 1-Technical Description Release 1.1. Reports on earth system science, 14, 2005.

Mantoura, R. F. C., Law, C. S., Owens, N. J. P., Burkill, P. H., Woodward, E. M. S., Howland, R. J. M., and Llewellyn, C. A.: Nitrogen biogeochemical cycling in the northwestern indian-ocean, Deep-Sea Research Part Ii-Topical Studies in Oceanography, 40, 651-671, 1993.

Marti, O., Braconnot, P., Dufresne, J. L., Bellier, J., Benshila, R., Bony, S., Brockmann, P., Cadule, P., Caubel, A., Codron, F., de Noblet, N., Denvil, S., Fairhead, L., Fichefet, T., Foujols, M. A., Friedlingstein, P., Goosse, H., Grandpeix, J. Y., Guilyardi, E., Hourdin, F., Idelkadi, A., Kageyama, M., Krinner, G., Levy, C., Madec, G., Mignot, J., Musat, I., Swingedouw, D., and Talandier, C.: Key features of the IPSL ocean atmosphere model and its sensitivity to atmospheric resolution, Climate Dynamics, 34, 1-26, 10.1007/s00382-009-0640-6, 2010.

Martin, J. H., Knauer, G. A., Karl, D. M., and Broenkow, W. W.: Vertex - carbon cycling in the northeast pacific, Deep-Sea Research Part a-Oceanographic Research Papers, 34, 267-285, 10.1016/0198-0149(87)90086-0, 1987.

Mayorga, E., Seitzinger, S. P., Harrison, J. A., Dumont, E., Beusen, A. H. W., Bouwman, A. F., Fekete, B. M., Kroeze, C., and Van Drecht, G.: Global Nutrient Export from WaterSheds 2 (NEWS 2): Model development and implementation, Environmental Modelling & Software, 25, 837-853, 10.1016/j.envsoft.2010.01.007, 2010.

McElroy, M. B.: Marine biological-controls on atmospheric CO_2 and climate, Nature, 302, 328-329, 10.1038/302328a0, 1983.

Meinshausen, M., Smith, S. J., Calvin, K., Daniel, J. S., Kainuma, M. L. T., Lamarque, J. F., Matsumoto, K., Montzka, S. A., Raper, S. C. B., Riahi, K., Thomson, A., Velders, G. J. M., and van Vuuren, D. P. P.: The RCP greenhouse gas concentrations and their extensions from 1765 to 2300, Climatic Change, 109, 213-241, 10.1007/s10584-011-0156-z, 2011.

Middelburg, J. J., Soetaert, K., Herman, P. M. J., and Heip, C. H. R.: Denitrification in marine sediments: A model study, Global Biogeochemical Cycles, 10, 661-673, 10.1029/96gb02562, 1996.

Moore, J. K., Doney, S. C., and Lindsay, K.: Upper ocean ecosystem dynamics and iron cycling in a global three-dimensional model, Global Biogeochemical Cycles, 18, 10.1029/2004gb002220, 2004.

Morel, F. M. M., Rueter, J. G., and Price, N. M.: Iron nutrition of phytoplankton and its possible importance in the ecology of ocean regions with high nutrient and low biomass. Oceanography, 4(2), 56-61, 1991.

Myhre, G., Shindell, D., Bréon, F.-M., Collins, W., Fuglestvedt, J., Huang, J., Koch, D., Lamarque, J.-F., Lee, D., Mendoza, B., Nakajima, T., Robock, A., Stephens, G., Takemura, T. and Zhang, H.: Anthropogenic and Natural Radiative Forcing. In: Climate Change 2013: The Physical Science Basis. Contribution of Working Group I to the Fifth Assessment Report of the Intergovernmental Panel on Climate Change, 2013.

Naqvi, S. W. A., and Noronha, R. J.: Nitrous-oxide in the arabian sea, Deep-Sea Research Part a-Oceanographic Research Papers, 38, 871-890, 10.1016/0198-0149(91)90023-9, 1991.

Naqvi, S. W. A., Jayakumar, D. A., Narvekar, P. V., Naik, H., Sarma, V., D'Souza, W., Joseph, S., and George, M. D.: Increased marine production of N2O due to intensifying anoxia on the Indian continental shelf, Nature, 408, 346-349, 10.1038/35042551, 2000.

Nevison, C., Butler, J. H., and Elkins, J. W.: Global distribution of N2O and the Delta N2O-AOU yield in the subsurface ocean, Global Biogeochemical Cycles, 17, 10.1029/2003gb002068, 2003.

Nevison, C. D., Weiss, R. F., and Erickson, D. J.: Global oceanic emissions of nitrous-oxide, Journal of Geophysical Research-Oceans, 100, 15809-15820, 10.1029/95jc00684, 1995.

Nevison, C. D., Lueker, T. J., and Weiss, R. F.: Quantifying the nitrous oxide source from coastal upwelling, Global Biogeochemical Cycles, 18, 10.1029/2003gb002110, 2004.

Orcutt, K. M., Lipschultz, F., Gundersen, K., Arimoto, R., Michaels, A. F., Knap, A. H., and Gallon, J. R.: A seasonal study of the significance of N-2 fixation by Trichodesmium spp. at the Bermuda Atlantic Time-series Study (BATS) site, Deep-Sea Research Part Ii-Topical Studies in Oceanography, 48, 1583-1608, 10.1016/s0967-0645(00)00157-0, 2001.

Orr, J. C., Fabry, V. J., Aumont, O., Bopp, L., Doney, S. C., Feely, R. A., Gnanadesikan, A., Gruber, N., Ishida, A., Joos, F., Key, R. M., Lindsay, K., Maier-Reimer, E., Matear, R., Monfray, P., Mouchet, A., Najjar, R. G., Plattner, G. K., Rodgers, K. B., Sabine, C. L., Sarmiento, J. L., Schlitzer, R., Slater, R. D., Totterdell, I. J., Weirig, M. F., Yamanaka, Y.,

and Yool, A.: Anthropogenic ocean acidification over the twenty-first century and its impact on calcifying organisms, Nature, 437, 681-686, 10.1038/nature04095, 2005.

Oudot, C., Andrie, C., and Montel, Y.: Nitrous-oxide production in the tropical atlantic-ocean, Deep-Sea Research Part a-Oceanographic Research Papers, 37, 183-202, 10.1016/0198-0149(90)90123-d, 1990.

Palmer, J. R., and Totterdell, I. J.: Production and export in a global ocean ecosystem model, Deep-Sea Research Part I-Oceanographic Research Papers, 48, 1169-1198, 10.1016/s0967-0637(00)00080-7, 2001.

Paulmier, A., and Ruiz-Pino, D.: Oxygen minimum zones (OMZs) in the modern ocean, Progress in Oceanography, 80, 113-128, 10.1016/j.pocean.2008.08.001, 2009.

Pichevin, L., et al.: Evidence of ventilation changes in the Arabian Sea during the late Quaternary: Implication for denitrification and nitrous oxide emission, Global Biogeochemical Cycles, 21, 2007.

Prather, M. J., Holmes, C. D., and Hsu, J.: Reactive greenhouse gas scenarios: Systematic exploration of uncertainties and the role of atmospheric chemistry, Geophysical Research Letters, 39, 10.1029/2012gl051440, 2012.

Punshon, S., and Moore, R. M.: Nitrous oxide production and consumption in a eutrophic coastal embayment, Marine Chemistry, 91, 37-51, 10.1016/j.marchem.2004.04.003, 2004.

Ravishankara, A. R., Daniel, J. S., and Portmann, R. W.: Nitrous Oxide (N2O): The Dominant Ozone-Depleting Substance Emitted in the 21st Century, Science, 326, 123-125, 10.1126/science.1176985, 2009.

Resplandy, L., Levy, M., Bopp, L., Echevin, V., Pous, S., Sarma, V. V. S. S., and Kumar, D.: Controlling factors of the oxygen balance in the Arabian Sea's OMZ, Biogeosciences, 9, 5095-5109, 10.5194/bg-9-5095-2012, 2012.

Riebesell, U.: Effects of CO(2) enrichment on marine phytoplankton, Journal of Oceanography, 60, 719-729, 10.1007/s10872-004-5764-z, 2004.

Riebesell, U., Schulz, K. G., Bellerby, R. G. J., Botros, M., Fritsche, P., Meyerhoefer, M., Neill, C., Nondal, G., Oschlies, A., Wohlers, J., and Zoellner, E.: Enhanced biological carbon consumption in a high CO2 ocean, Nature, 450, 545-U510, 10.1038/nature06267, 2007.

Riley, G. A.: Factors controlling phytoplankton populations on georges bank, Journal of Marine Research, 6, 54-73, 1946.

Riley, G. A., Stommel, H. M., and Bumpus, D. F.: Quantitative ecology of the plankton of the western North Atlantic. Bingham Oceanographic Laboratory, 1949.

Rudd, J. W. M., Kelly, C. A., Schindler, D. W., and Turner, M. A.: Disruption of the nitrogen cycle in acidified lakes. Science, 240(4858), 1515-1517, 1988.

Sañudo-Wilhelmy, S. A., Kustka, A. B., Gobler, C. J., Hutchins, D. A., Yang, M., Lwiza, K., Burns, J., Capone, D. G., Raven, J. A., and Carpenter, E. J.: Phosphorus limitation of nitrogen fixation by Trichodesmium in the central Atlantic Ocean, Nature, 411, 66-69, 10.1038/35075041, 2001.

Sarmiento, J. L., Slater, R., Barber, R., Bopp, L., Doney, S. C., Hirst, A. C., Kleypas, J., Matear, R., Mikolajewicz, U., Monfray, P., Soldatov, V., Spall, S. A., and Stouffer, R.: Response of ocean ecosystems to climate warming, Global Biogeochemical Cycles, 18, 10.1029/2003gb002134, 2004.

Schlitzer, R.: Export production in the equatorial and North Pacific derived from dissolved oxygen, nutrient and carbon data, Journal of Oceanography, 60, 53-62, 10.1023/B:JOCE.0000038318.38916.e6, 2004.

Shi, D., Kranz, S. A., Kim, J. M. and Morel, F. M.: Ocean acidification slows nitrogen fixation and growth in the dominant diazotroph Trichodesmium under low-iron conditions. Proceedings of the National Academy of Sciences, 109.45, E3094-E3100, 2012.

Somes, C. J., Schmittner, A., Galbraith, E. D., Lehmann, M. F., Altabet, M. A., Montoya, J. P., Letelier, R. M., Mix, A. C., Bourbonnais, A., and Eby, M.: Simulating the global distribution of nitrogen isotopes in the ocean, Global Biogeochemical Cycles, 24, 10.1029/2009gb003767, 2010.

Sonntag, S., and Hense, I.: Phytoplankton behavior affects ocean mixed layer dynamics through biological-physical feedback mechanisms, Geophysical Research Letters, 38, 10.1029/2011gl048205, 2011.

Steinacher, M., Joos, F., Frolicher, T. L., Bopp, L., Cadule, P., Cocco, V., Doney, S. C., Gehlen, M., Lindsay, K., Moore, J. K., Schneider, B., and Segschneider, J.: Projected 21st century decrease in marine productivity: a multi-model analysis, Biogeosciences, 7, 979-1005, 2010.

Stendardo, I., Gruber, N., and Körtzinger, A.: CARINA oxygen data in the Atlantic Ocean. Earth System Science Data, *1*, 87-109, 2009.

Stewart, W. D. P., and Pearson, H. W.: Effects of aerobic and anaerobic conditions on growth and metabolism of blue-green algae, Proceedings of the Royal Society Series B-Biological Sciences, 175, 293-+, 10.1098/rspb.1970.0024, 1970.

Stocker, B. D., Roth, R., Joos, F., Spahni, R., Steinacher, M., Zaehle, S., Bouwman, L., Xu, R., and Prentice, I. C.: Multiple greenhouse-gas feedbacks from the land biosphere under

future climate change scenarios, Nature Climate Change, 3, 666-672, 10.1038/nclimate1864, 2013.

Stramma, L., Johnson, G. C., Sprintall, J., and Mohrholz, V.: Expanding oxygen-minimum zones in the tropical oceans, Science, 320, 655–658, doi:10.1126/science.1153847, 2008.

Stramma, L., Oschlies, A., and Schmidtko, S.: Anticorrelated observed and modeled trends in dissolved oceanic oxygen over the last 50 years, Biogeosciences Discuss., 9, 4595–4626, doi:10.5194/bgd-9-4595-2012, 2012.

Suntharalingam, P., and Sarmiento, J. L.: Factors governing the oceanic nitrous oxide distribution: Simulations with an ocean general circulation model, Global Biogeochemical Cycles, 14, 429-454, 10.1029/1999gb900032, 2000.

Suntharalingam, P., Sarmiento, J. L., and Toggweiler, J. R.: Global significance of nitrous-oxide production and transport from oceanic low-oxygen zones: A modeling study, Global Biogeochemical Cycles, 14, 1353-1370, 10.1029/1999gb900100, 2000.

Suntharalingam, P., Buitenhuis, E., Le Quere, C., Dentener, F., Nevison, C., Butler, J. H., Bange, H. W., and Forster, G.: Quantifying the impact of anthropogenic nitrogen deposition on oceanic nitrous oxide, Geophysical Research Letters, 39, 10.1029/2011gl050778, 2012.

Suthhof, A., et al.: Millennial-scale oscillation of denitrification intensity in the Arabian Sea during the late Quaternary and its potential influence on atmospheric N2O and global climate, Global Biogeochemical Cycles, 15(3), 637-649, 2001.

Takahashi, T., Broecker, W. S., and Langer, S.: Redfield ratio based on chemical-data from isopycnal surfaces, Journal of Geophysical Research-Oceans, 90, 6907-6924, 10.1029/JC090iC04p06907, 1985.

Taylor, K. E., Stouffer, R. J., and Meehl, G. A.: An overview of cmip5 and the experiment design, Bulletin of the American Meteorological Society, 93, 485-498, 10.1175/bams-d-11-00094.1, 2012.

Thamdrup, B., and Dalsgaard, T.: Production of N-2 through anaerobic ammonium oxidation coupled to nitrate reduction in marine sediments, Applied and Environmental Microbiology, 68, 1312-1318, 10.1128/aem.68.3.1312-1318.2002, 2002.

Thompson, R. L., Dlugokencky, E., Chevallier, F., Ciais, P., Dutton, G., Elkins, J. W., Langenfelds, R. L., Prinn, R. G., Weiss, R. F., Tohjima, Y., O'Doherty, S., Krummel, P. B., Fraser, P., and Steele, L. P.: Interannual variability in tropospheric nitrous oxide, Geophysical Research Letters, 40, 4426-4431, 10.1002/grl.50721, 2013.

Tiedje, J.M.: Ecology of denitrification and dissimilatory nitrate reduction to ammonium. Biology of anaerobic microorganisms, 179–244, 1988.

Vichi, M., Pinardi, N., and Masina, S.: A generalized model of pelagic biogeochemistry.for the global ocean ecosystem. Part I: Theory, Journal of Marine Systems, 64, 89-109, 10.1016/j.jmarsys.2006.03.006, 2007.

Watanabe, S., Hajima, T., Sudo, K., Nagashima, T., Takemura, T., Okajima, H., Nozawa, T., Kawase, H., Abe, M., Yokohata, T., Ise, T., Sato, H., Kato, E., Takata, K., Emori, S., and Kawamiya, M.: MIROC-ESM 2010: model description and basic results of CMIP5-20c3m experiments, Geoscientific Model Development, 4, 845-872, 10.5194/gmd-4-845-2011, 2011.

Weiss, R. F., and Price, B. A.: Nitrous-oxide solubility in water and seawater, Marine Chemistry, 8, 347-359, 10.1016/0304-4203(80)90024-9, 1980.

Wolff, E. W.: Greenhouse gases in the Earth system: a palaeoclimate perspective, Philosophical Transactions of the Royal Society a-Mathematical Physical and Engineering Sciences, 369, 2133-2147, 10.1098/rsta.2010.0225, 2011.

Wu, J. F., Sunda, W., Boyle, E. A., and Karl, D. M.: Phosphate depletion in the western North Atlantic Ocean, Science, 289, 759-762, 10.1126/science.289.5480.759, 2000.

Ye, Y., Volker, C., Bracher, A., Taylor, B., and Wolf-Gladrow, D. A.: Environmental controls on N-2 fixation by Trichodesmium in the tropical eastern North Atlantic Ocean-A model-based study, Deep-Sea Research Part I-Oceanographic Research Papers, 64, 104-117, 10.1016/j.dsr.2012.01.004, 2012.

Yool, A., Martin, A. P., Fernandez, C., and Clark, D. R.: The significance of nitrification for oceanic new production, Nature, 447, 999-1002, 10.1038/nature05885, 2007.

Yoshida, N., Morimoto, H., Hirano, M., Koike, I., Matsuo, S., Wada, E., Saino, T., and Hattori, A.: nitrification rates and N-15 abundances of N_2O and NO-3 in the western north pacific, Nature, 342, 895-897, 10.1038/342895a0, 1989.

Yoshinari, T.: Nitrous oxide in the sea, Ph.D. Thesis, DalhousieUniv., Halifax, N.S., 1973.

Yoshioka, T., and Saijo, Y.: Photoinhibition and recovery of NH-4+-oxidizing bacteria and NO-2-oxidizing bacteria, Journal of General and Applied Microbiology, 30, 151-166, 10.2323/jgam.30.151, 1984.

Yukimoto, S., Adachi, Y., Hosaka, M., Sakami, T., Yoshimura, H., Hirabara, M., Tanaka, T. Y., Shindo, E., Tsujino, H., Deushi, M., Mizuta, R., Yabu, S., Obata, A., Nakano, H., Koshiro, T., Ose, T., and Kitoh, A.: A New Global Climate Model of the Meteorological

Research Institute: MRI-CGCM3-Model Description and Basic Performance, Journal of the Meteorological Society of Japan, 90A, 23-64, 10.2151/jmsj.2012-A02, 2012.

Zahariev, K., Christian, J. R., and Denman, K. L.: Preindustrial, historical, and fertilization simulations using a global ocean carbon model with new parameterizations of iron limitation, calcification, and N-2 fixation, Progress in Oceanography, 77, 56-82, 10.1016/j.pocean.2008.01.007, 2008.

Zamora, L. M., Oschlies, A., Bange, H. W., Huebert, K. B., Craig, J. D., Kock, A., and Loescher, C. R.: Nitrous oxide dynamics in low oxygen regions of the Pacific: insights from the MEMENTO database, Biogeosciences, 9, 5007-5022, 10.5194/bg-9-5007-2012, 2012.

Zamora, L. M., and Oschlies, A.: Surface nitrification: A major uncertainty in marine N2O emissions, Geophysical Research Letters, 41, 4247-4253, 10.1002/2014gl060556, 2014.

Zehr, J. P., and Ward, B. B.: Nitrogen cycling in the ocean: New perspectives on processes and paradigms, Applied and Environmental Microbiology, 68, 1015-1024, 10.1128/aem.68.3.1015-1024.2002, 2002.